HYBRID METHOD FOR THE SEISMIC VULNERABILITY ASSESSMENT OF HISTORIC MASONRY CITY CENTRES

by

Viviana Iris Novelli

Submitted to the Department of Civil, Environmental and Geomatic Engineering in partial fulfilment of the requirements for the degree of

Doctor of Philosophy in Earthquake Engineering

at

UNIVERSITY COLLEGE LONDON

February 2017

I, Viviana Iris Novelli confirm that the work presented in this thesis is my own. Where information has been derived from other sources, I confirm that this has been indicated in the thesis.

ACKNOWLEDGEMENTS

I acknowledge my supervisor Dr. D'Ayala, for her precious guidance and sharp technical insight, which have so much contributed to the development of this research project.

I also wish to acknowledge the FP7-PERPETUATE project, which was not only my main sources of funding, but also an inspirational environment that nurtured and challenged me as a researcher.

Ai miei genitori.

HYBRID METHOD FOR THE SEISMIC VULNERABILITY ASSESSMENT OF HISTORIC MASONRY CITY CENTRES

by
Viviana Iris Novelli

Submitted to the Department of Civil, Environmental and Geomatic Engineering in partial fulfilment of the requirements for the degree of Doctor of Philosophy in Earthquake Engineering

ABSTRACT

Buildings in historical city centres are particularly vulnerable to seismic events, as observed from past earthquakes in Bhuj (India, 2001), Bam (Iran, 2003), Sichuan (China 2008), L'Aquila (Italy 2009), Gorkha (Nepal 2015), and most recently in Amatrice (Italy 2016). To reduce damage and loss in historic city centres, seismic vulnerability of buildings should be assessed on site with approaches that take into account how parameters related to geometric/structural features, deficiencies and seismic damage impact on seismic failure modes. Currently, an approach that investigates all these parameters in only one consistent procedure for the identification of failure modes is not available, although, there are numerous methods developed to evaluate the seismic vulnerability. This dissertation aims to tackle such a gap by developing a hybrid approach that investigates causes of failure modes through an analytical method and effects of failure modes through a visual inspection tool. The analytical method proposed in the hybrid approach is FaMIVE (Failure Mechanism Identification and Vulnerability Evaluation method), mechanical method that estimates failure modes, capacity and fragility curves by taking into account geometric/structural features and deficiencies of buildings. The second method is LOG-IDEAH (LOGic trees for Identification of Damage due to Earthquakes for Architectural Heritage) web knowledge based system that complements FaMIVE by estimating failure modes through engineering judgements codified in rules developed to interpret seismic damage observed on buildings. The hybrid approach is validated on the city centres of L'Aquila (Italy) damaged by the earthquake in 2009, characterised by typical historic masonry houses. Through the application, the thesis provides a validation approach that is used to refine the framework of the proposed hybrid method and to provide guidance for those facing the challenge of assessing the seismic vulnerability of historic city centres.

Thesis Supervisor: Prof. Dina D'Ayala

CONTENTS

LIST OF FIGURES

Page

LIST OF TABLES

1 INTRODUCTION

1.1 Assessment of historic city centres in seismic prone areas

The “Great Lisbon Earthquake”, also known as “the Disaster at Lisbon”, occurred on Saturday, 1 November 1755. The city of Lisbon was destroyed and approximately 10,000 people lost their lives (Pereira, 2009).

Figure 1-1: "The Earthquake at Lisbon in 1755", (1887) In Hartwig, G. L., "Volcanoes and Earthquakes: A popular Description in the Movements in the Earth's Crust", from The subterranean world, London: Longmans, Green, and Co. - Image by © Bettmann/CORBIS. https://nisee.berkeley.edu/elibrary/Image/KZ103)

The painting in Figure 1-1 documents the despair and sense of helplessness of a population who is losing the link with its historic city through the loss of its houses

destroyed by the irreversible and unconditional effects of a catastrophic earthquake. The fear, and the dismay that an earthquake is capable to reduce buildings to ruins within fractions of minutes, clearly represented in the painting, underlines the need of protecting traditional densely built city centres, to avoid/reduce their damage and to defend their historic identity.

The preservation of historic city centres is not an easy task and careful measures such as seismic assessment of building performance are among the current means, which can be employed so that the seismic vulnerability can be estimated to mitigate the damage and the heritage loss.

The word vulnerability was coined in early 17th century and comes from the Latin word “vulnus” that means "wound". The Oxford dictionary defines with vulnerability “the quality or state of being exposed to the possibility of being attacked or harmed, […]”.

In the seismic engineering field, vulnerability describes the *probability of a building to be damaged or to collapse in an earthquake of a given intensity (*Coburn, et al., 1994). The continuous research of methods to estimate the seismic vulnerability of buildings points out an urgent need to identify the suitable method that best predicts the performance of buildings and their possible physical damage under seismic events.

This thesis offers a contribution in such a sense; it tries to address the gaps in the existing approaches for the assessment of seismic vulnerability of densely built up historic city centres. In particular, in this work, the attention is paid to those approaches developed to assess the vulnerability of historic city centres characterised by masonry buildings, since these types of constructions have demonstrated to be very vulnerable to earthquakes as the ones occurred in Northridge (California, 1994), Bhuj (India, 2001), Bam (Iran, 2003), L’Aquila (Italy, 2009), Christchurch (New Zealand, 2011), Gorkha (Nepal, 2015) and most recently in Amatrice (Italy, 2016).

Why is it difficult to find an approach capable to assess the seismic response of historic masonry buildings? What is the minimum data required to assess heritage building performance under seismic events? How data should be recorded at territorial scale? What are the optimal requirements for a method suitable to assess the seismic vulnerability of historic city centres? What are the expected outputs for these approaches?

These questions gave the impetus to the research described in the following pages.

1.2 Aims and objectives

Studies and approaches aimed at developing vulnerability assessment methods for buildings in historic city centres are available in literature since the 1980s. Among these approaches, the procedures based on rapid inspections of buildings and simplified methods of analysis for the evaluation of the seismic vulnerability at territorial scale, rather than sophisticated methods suited for the assessment of single building, are the ones that should be used to assess the building performance of historic city centres (D'Ayala and Novelli, 2013).

Moreover, suitable approaches for the estimation of the vulnerability of masonry constructions should be specifically developed to assess historic buildings and their seismic performance by taking into account the causes and the effects of their different ways of failing, since this aids to predict reliable probability of seismic damage.

The causes and the effects of a given failure mode, whereby masonry buildings collapse under an earthquake, are very different, as observed in Turkey (1999), Taiwan (1999), China (2008), Haiti (2010), Nepal (2015), Ecuador (2016). The causes can be related, for instance, to a low quality of the construction materials, or poor structural details, or irregularity in plan and in elevation, while the effects can be investigated by observing the types of cracks and severity of the damage.

Among the existing approaches, a method capable to correlate structural features and deficiencies together with seismic damage in a consistent procedure for the investigation of the failure modes of buildings to assess the vulnerability at territorial scale is not available.

This research focuses on introducing a suitable procedure for the assessment of the seismic vulnerability of historic buildings in city centres. This work started within the FP7 research grant PERPETUATE project, (Grant Agreement No 244229, http://www.peprtuate.eu), aimed at the development of guidelines to preserve cultural heritages in seismic prone regions of Europe and the Mediterranean Countries. The PERPETUATE project, where the author was responsible to propose a performance–

based approach for the vulnerability assessment at territorial scale, has given the prospective in this research, to propose a new robust method for the vulnerability assessment of historic city centres.

In light of this, a hybrid methodology, only applicable to buildings already damaged by earthquakes, is a procedure to investigate causes (structural/geometric features, deficiencies) and effects (seismic damage) generating failure modes and to provide a starting point tool for vulnerability reduction based on strategies that can be identified, known the failure modes to which buildings are most vulnerable.

Currently, the proposed hybrid methodology in this research, consisting of two different methods suitable to assess failure modes of buildings, is only a post-earthquake assessment procedure aimed at establishing the mentioned correlation between causes/effects and failure modes and becoming a tool for seismic vulnerability assessment for future development.

The first method included in the hybrid approach is FaMIVE (Failure Mechanism Identification and Vulnerability Evaluation method) originally developed by D'Ayala and Speranza (2003) and presented for this work in a new version, developed by the author, to assess the failure modes of masonry buildings with irregular opening layouts.

Within the hybrid approach, FaMIVE is used both to estimate the building performances by way of an analytical method based on mechanical approaches and to estimate the damage level probability distribution. The choice of proposing this method derives from the need of adopting a tool capable to assess failure modes of masonry constructions by a simplified numerical method that takes into account the structural features and deficiencies of buildings.

The second method in the proposed hybrid approach is the entirely novel LOG-IDEAH (LOGic trees for Identification of Damage due to Earthquakes for Architectural Heritage), developed by the author to provide a visual inspection tool for the assessment of failure modes of buildings through the observation and the interpretation of seismic damage recorded on site (Novelli and D'Ayala, 2015).

During the development of LOG-IDEAH, it has become apparent that the existing guidelines and approaches for the seismic evaluation of buildings only offer a little support to the users wishing to investigate, by using only visual inspection, the failure

modes whereby masonry buildings collapse under seismic events. Furthermore, the thesis also shows how the assessment based on observation of buildings is strongly affected by experience and judgement of inspectors and points out how this knowledge in assessing buildings can be captured and implemented in an expert system (LOG-IDEAH) to reduce the uncertainties deriving from the subjective interpretation.

The union of both approaches mentioned above is conceived as a flexible hybrid method, which can be enlarged to the estimation of the failure modes of different building samples characterised by a variety of construction materials and structural features. Specifically, this approach is presented to be applied to residential masonry buildings, with regular/irregular plans, with or without courtyard, regular irregular opening layout distribution, where most of the seismic capacity of the buildings is concentrated on the external facades.

The present method aspires to provide an example towards the development of new efficient hybrid solutions based on the integrations and different methods developed for the seismic evaluation of building performances that are capable to capture different aspects and modality of building failures.

1.3 Content of thesis

Besides this first introductory chapter, the thesis consists of five chapters, plus a chapter of conclusions and further works, and a list of references.

Chapter 2, after a relevant definition of seismic vulnerability in this context, presents and reviews the existing approaches for the seismic vulnerability assessment of historic city centres characterised by masonry constructions. In particular, the chapter discusses advantages and limitations of the methods based on empirical, analytical or hybrid approaches, as reported in the literature, and identifies the essential requirements for an approach suitable for the seismic vulnerability assessment of a historic city centres.

In particular, this chapter points out the importance of relying on approaches for the vulnerability assessment that estimate the building performance by taking into account

the different possibility of failure modes to which buildings are most vulnerable under seismic events.

In light of this initial states, in Chapter 3, it is discussed that the most reliable proof of how buildings perform and fail during seismic events, can be found on site by inspecting buildings in the aftermath of a damaging earthquake. Therefore, a further review of the existing methods suitable to investigate seismic behaviours of buildings and their possible failure modes through visual inspection is carried out to propose the methodology adopted in the research project.

The proposed methodology is presented with the aid of a flowchart that illustrates the fundamental steps of the framework proposed to identify those failure modes required to understand the building performance and developed (or improved existing) methods that provide vulnerability of historic buildings by taking into account their possible failure modes under earthquakes.

This methodology illustrates the data collection protocols, and discusses the analysis, the post processing and the issues related to the interpretation of the results derived from the joint application of FaMIVE and LOG-IDEAH. Finally, the chapter also outlines the approach adopted to assess the capacity of the methods to predict the building responses.

Chapter 4 overviews a new version of the existing approach FaMIVE (Speranza and D'Ayala, 2003) developed to assess the failure modes and the seismic vulnerability of historic city centres. In particular, since FaMIVE in its original version was only developed to assess the vulnerability of regular constructions, in its new implementation, presented in a flowchart, it is enriched with mechanical models capable to assess the failure modes of irregular masonry constructions.

A further development of FaMIVE (D'Ayala 2005) limited to the determination of capacity curves is also presented by illustrating an iterative procedures developed to derive damage probability at territorial scales by intersections between fragility curves and performance targets estimated for building types with reference to N2 method (Fajfar, 2000).

Chapter 5 focuses on the development of LOG-IDEAH implemented as a web-knowledge based tool for the estimation of failure modes of buildings through the

interpretation of damage recorded on site by visual inspection. The tool is firstly presented by first describing the approach adopted to assess the seismic damage and then illustrating knowledge and judgments to interpret the collected damage adopted by surveyors. Defined such a logical process for the interpretation of the damage, the logic process for the interpretation of the damage is outlined systematically with logic trees that through a succession of YES/NO answers illustrate the overall architecture of LOG-IDEAH. The coding of the logic trees in an automatic and interactive tool is carried out within the computational environment of Answer Set Programming (Gelfond and Lifschitz 1988; Gelfond and Lifschitz 1991).

The outcome of the chapters 3, 4 and 5 feeds into the application presented in chapter 6, where the entire methodology is applied to the historic centre of L'Aquila in Italy, badly affected by an earthquake in 2009. L'Aquila earthquake represents a watershed in the attention paid to this problem at European and global level and therefore it was selected as a suitable case study to validate the capacity of the proposed hybrid approach for the vulnerability assessment of historic city centres.

The main achievements, further challenges and possible improvements of the research conclude the thesis.

2 REVIEW OF EXISTING APPROACHES FOR THE ESTIMATION OF THE SEISMIC VULNERABILITY OF HISTORIC CENTRES

2.1 Introduction

Seismic vulnerability, exposure and hazard are the fundamental parameters to estimate the seismic risk of seismic prone areas. In this chapter, after a general definition of the concept of seismic risk, the seismic vulnerability of buildings is discussed in the context of historic city centres. This is followed by a review of the existing methods developed for the vulnerability assessment. The review of the vulnerability assessment approaches commonly applied in this context is discussed within the following classification: 1) empirical methods, 2) analytical methods and 3) hybrid methods, defined in the following sections. Using this review, the approaches are compared, their effectiveness in assessing historic city centres is highlighted, and their drawbacks are pointed out in order to identify the approach that best predicts the seismic vulnerability and specific needs for developing a novel method, if required.

2.2 Seismic risk and seismic vulnerability: definitions

The concept of seismic risk was introduced during the international convention in 1979 organised by the Office of United Nations Disaster Relief Coordinator (UNDRO, 1980). By the word risk, the expected losses of an element from a given hazard over a specified future period was defined by three essential components: hazard, exposure, and vulnerability, (Coburn, et al., 1994; CSSC, 1999; Chandler and Nelson, 2001, Bendimerad, 2001), shown in Figure 2-1.

Hazard

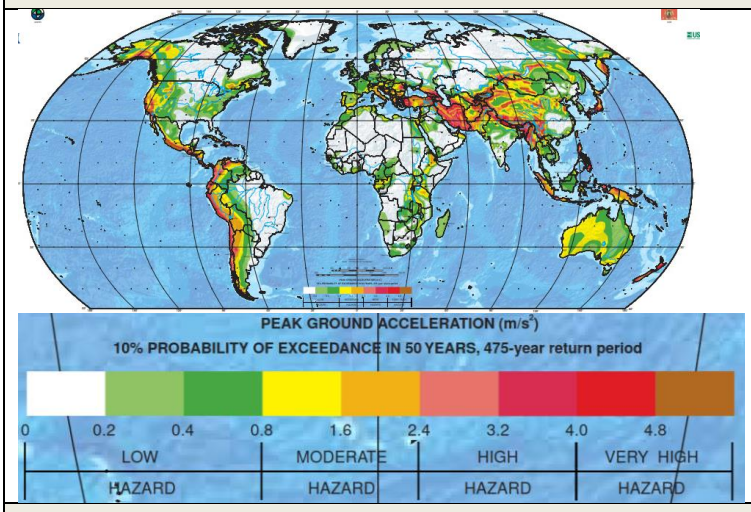

The Global Seismic Hazard Map depicts the seismic hazard as Peak Ground Acceleration (PGA) with 10% probability of exceedance in 50 years, corresponding to a return period of 475 years.
(Giardini, et al., 1999)

Exposure

Building types according to structural and geometric features from onsite inspections, and available database

Use, and occupancy from census data

£

Building cost

Vulnerability

Observed damage
Source: Damage Identification based on observation, Amatrice (EERI). Giuseppe Bellini / Getty Images (2016)

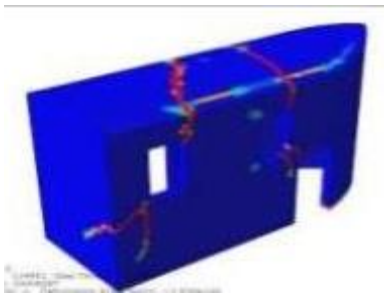

Estimated damage

Damage identification taken from numerical models.

(from finite element dynamic analysis in Abaqus of a historical masonry by Nasiri (2012))

Figure 2-1: Seismic risk framework

In this work, the definitions of these three components are provided by extending the existing definitions of Coburn et al. (1994) to historic city centres, relevant topic of this thesis, as discussed in the following three bullet points:

1. ***Hazard***: the likelihood in a historic city centre or location, characterised by historic houses to experience seismic events. Since the historic locations are inhabited for several centuries, there might be a good record of historic seismic events.
2. ***Exposure of buildings at risk in a historic urban context:*** building distribution of a historic urban context, where buildings can be classified by:
    - Type: according to structural/geometric features and historic value. This information can be collected from onsite inspections, or available databases with data collected from past seismic events;
    - Occupancy and use. This information can be collected from census data and costs for new constructions;
    - Cost for repair and cost for conservation. This information can be estimated by taking into account the cost of the new constructions that are determined on the local economy of the region under consideration.
3. ***Vulnerability of historic buildings at risk***: susceptibility of historic buildings to be damaged, when these experience a hazard. This propensity can be evaluated on site through observation or estimated through numerical models which are taken into account that historic buildings damaged from past earthquakes or modified over the time might have a different performance from the one targeted in the original design.

The vulnerability has a determinant effect on the seismic risk, since this is one of the few potential aspects, where engineering research can intervene (Vicente et al., 2014). The seismic vulnerability can be expressed for building types and can be measured by using fragility functions (see Figure 2-2); statistical tool representing the Probability (P) of exceeding a given damage state (from ds1 to dsn). If damage states are associated with repair/replacement costs, fragility curves together with economic functions allow the estimation of economic losses due to an earthquake.

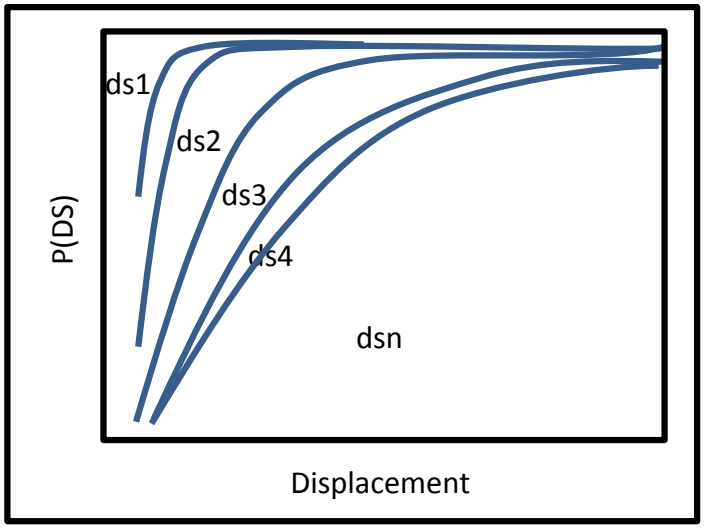

Figure 2-2: Example of fragility curves for different damage states

The capacity of the fragility curves, to predict the damage probability distribution correctly, depends on the level of details of the collected data, since detailed data on a building type generates numerical models that best simulate the building behaviours. This underlines the need of defining damage levels for seismic hazard by taking into account the variability in building types through probabilistic distributions of the damage levels for each building types recognised in an area of study (D'Ayala et al., 2014). In particular, when fragility curves are derived for historic buildings, the damage levels require to be defined not only to characterise the structural features in relation to their safety but also in relation to the conservation requirement, as this allows determining the probability of occurrence of structural damage and heritage losses (D'Ayala and Lagomarsino, 2015).

In the next section, the existing methods developed for the assessment of the seismic vulnerability are presented and discussed.

2.3 Seismic vulnerability assessment methods for historic centres

The existing methods for the assessment of the seismic vulnerability can be grouped in two major classes: empirical and analytical approaches (Lang 2002).

Empirical methods are based on post-earthquake surveys and observation of damage. They are generally developed and tested on a specific geographic location, and therefore they might be not adequate if applied to assess the vulnerability in a region where the building stock has different structural and architectural characteristics from the ones considered in the region, whereby the methods were originally developed, as seismic response of buildings and associated heritage losses might be very different, if located in different regions (D'Ayala and Novelli, 2013).

Expert judgements (Knowledge Guided Decision, see Figure 2-3) can be adopted to extend the validity of these methods to different regions, further concerns arise since the reliability of these methods becomes questionable due to their dependency on the ability, experience and interpretation of the surveyor who does the building assessment (Pitilakis et al., 2014).

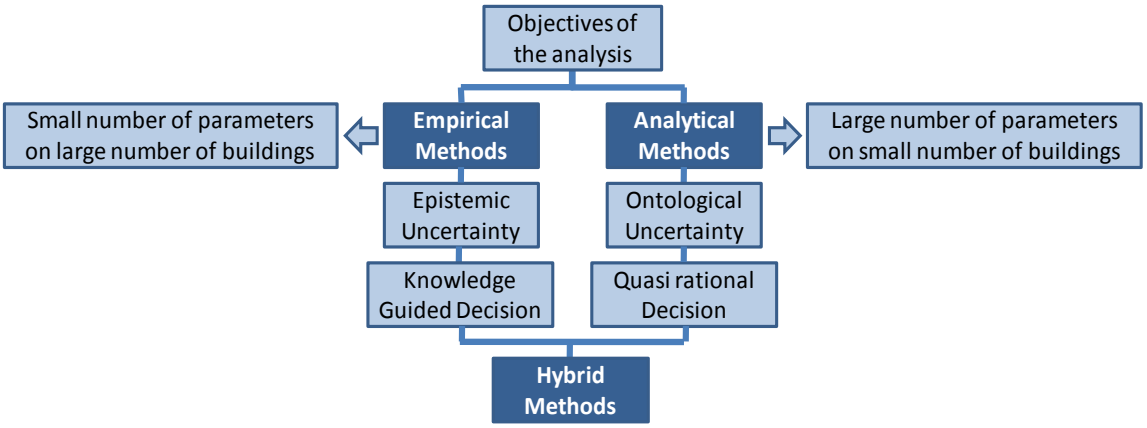

Figure 2-3: Empirical, analytical, and hybrid methods for the seismic vulnerability assessment at territorial scale

The input data required by empirical methods to classify buildings in types, whereby the vulnerability is estimated, consists of few structural parameters that are observed and recorded on site. These parameters are selected with the scope at characterising the variability of the factors that have the greatest effect on the building performance under seismic events. Therefore, since only few parameters are needed for the goal of these methods, detailed surveys on the single building are not carried out, as they are not required.

However, since the empirical approaches tend to overlook peculiarity, defects, and structural lacks that can be identified even in buildings belonging to the same type, these methods estimate a seismic vulnerability with an epistemic uncertainty due to a limited knowledge (information) of the buildings under consideration (Figure 2-3). In particular, this type of uncertainty becomes distress, when these approaches are applied to assess the seismic vulnerability of historic buildings, characterised by strong irregularity deriving from alterations or deteriorations due to lack of maintenance or aging.

The second group of available approaches for the estimation of the seismic vulnerability, as mentioned above, includes the analytical methods aimed at using numerical (analytical) models (or quasi-rational decision, see Figure 2-3) to achieve accurate estimation of the building performance. Due to their high accuracy and capability to simulate the response of buildings under seismic events, that improve by increasing the level of knowledge of the building under inspection, these methods are becoming more attractive than the empirical methods.

The analytical models are commonly adopted to assess the performance of historic buildings, whereby extensive data is available. Input data required for these approaches can be collected on site, by visual inspection and measurements. In some cases, experimental tests are also needed to investigate mechanical properties of the construction materials. Structural features, such as details of connections, roof/floor and foundation types also need to be investigated, and therefore destructive investigation techniques might be also required.

Most of the existing numerical models adopted in the analytical vulnerability assessment methods are calibrated on single buildings and implemented to assess the performance of specific buildings under question. Therefore, their applicability at territorial scale or even to a single building characterised by geometric/structural/architectural features different from the ones used in the initial calibration might be limited. Therefore these approaches are characterised by an ontological uncertainty, type of uncertainty that underlines the inadequacy of a model calibrated on a specific building to be applied to various buildings.

However, there is also a further issue derived from the lack of feasibility of carrying out detailed inspections of a large number of buildings, due to the extensive time required to complete the survey for a single one.

The combination of an empirical and an analytical method is given by the hybrid approaches, which aim at compensating drawbacks of single seismic vulnerability approaches. Generally, these hybrid procedures are composed of an empirical and analytical method, both considered adequate to investigate the seismic vulnerability of the case studies under consideration. However, not all approaches of a hybrid method are necessary adopted to assess the seismic vulnerability of a case study. Indeed, the choice of favouring the use of an empirical or analytical method in a hybrid approach to assess the vulnerability depends on the level of details and information available for the buildings. This underlines that hybrid approaches are specifically introduced to overcome issues related to lack of data or incomplete surveys.

Most importantly, since the hybrid methods are composed of more approaches, in which the seismic vulnerability could be computed with parameters that are not comparable, these methods need a procedure that allows joining results.

These three classes of methods are extensively adopted to estimate the seismic vulnerability of historic city centres (D'Ayala and Novelli, 2013). However, many of these approaches were not originally developed for estimating the vulnerability of historic city centres, but to assess frame structures and successively readapted to assess masonry houses, or masonry with more regular layout than the ones that can be observed in historic houses. Therefore, some aspects and factors impacting on the historic building performance are overlooked. Moreover, in some of the existing vulnerability assessment methods, another common issue is that the capacity of historic buildings is estimated by using codes, although existing codes have limited reference to historic buildings.

In the next section, the existing methods for the vulnerability are described and discussed in relation to their applications in historic city centres in order to identify their suitability to estimate building performance at territorial scale.

2.4 Empirical vulnerability assessment methods

At the beginning of the ‘70s, the empirical vulnerability assessment methods were introduced for the first time. The empirical methods can be grouped in the three categories:

- **Damage Probability Matrix Methods.** They express, in a discrete form, the conditional probability of a damage level due to a ground motion corresponding to a given macro intensity grade. The methods are based on existing data of damage for a given site exposed to a specific level of shaking. The damage probability matrices are mainly used for probabilistic prediction of damage levels on buildings. These methods are developed and calibrated for specific regions, therefore, they are valid only for the areas and building types whereby they are defined for;
- **Vulnerability Index Methods.** They are continuous functions that are used to express the probability of exceeding a given damage level, given an earthquake with a specific macro seismic intensity or PGA. These methods are derived by associating a number of building types characteristics to a corresponding expected level of damage given a shaking intensity. These methods are developed and calibrated for specific regions, therefore, they are valid only for the areas and building types whereby they are defined for;
- **Continuous Vulnerability Curves.** They are continuous functions, that are used to express the probability of exceeding a given damage state. These curves are based on observed damage of buildings collected from past earthquakes and derive vulnerability functions by Medvedev–Sponheuer–Karnik (MSK) damage scale through the use of Parameterless Scale of Intensity (PSI).
-

2.4.1 *Damage Probability Matrix (DPM)*

The Damage Probability Matrix (DPM) method is the most common approach for the seismic vulnerability assessment. Based on site observations, it expresses in a

discrete form the conditional probability of obtaining a damage level Dj, due to a ground motion of macro intensity Ii, P=[D=Dj\Ii].

The method relies on the wealth of available data of damage observed from past earthquakes and their correlation, on the one hand, with assigned shaking macroseismic intensity at the site of observation and, on the other, with construction materials and methods in different geographical and seismic regions. Notwithstanding its popularity, the DPM has major limitations: they have a discrete definition of damage levels/states and limited applicability due to the high dependence on the specific seismic and architectural context, for which the damage levels/states are defined. Hence, it may not be applicable to different geographic locations, in the absence of direct damage data (D'Ayala and Novelli 2013).

The first DPM was developed by Whitman in 1973 and applied in S. Fernando Valley, near Sylmar, (California) after being damaged in 1971 by S. Fernando earthquake of magnitude 6.6. This approach relies on the hypothesis that, buildings, located in the same region, has the same structural features and the same seismic response, and consequently they statistically have the same probability of damage. This implies that, if the geographic context changes, the DPM needs to be re-tested on the new case study to verify its suitability to assess the vulnerability. The matrix defined for damage for not recorded intensity shaking is obtained by using a binomial distribution.

Moreover, if the regions are very heterogeneous, and characterised by very different building types, these approaches, even if re-calibrated, might estimate a seismic vulnerability with a high epistemic uncertainty due to limited capability of capturing the variety of the geometric/structural features that impact on the building performance.

This method has been applied to masonry structures in different applications, such as in Irpinia region after the earthquake of 1980 (Braga et al., 1982), in Friuli after the earthquake in 1974 (De Natale et al., 1987) and in Potenza after the earthquake in 1990 (Dolce et al., 2003 and Di Pasquale, 2005). Nowadays, the DPM is still widely used to assess the seismic vulnerability in developing countries and regions with extensive historic seismicity records (Askan and Yucemen, 2010; Zobin et al., 2010).

However, although numerous versions of DPMs methods have been developed and a more realistic vulnerability can be estimated, compared to the one originally developed by Whitman (1973), the existing seismic databases still do not cover all seismic prone areas. This underlines the constant need of collecting not only new data but also of re-calibrating this approach for each seismic area, whereby the DPM has not been applied before.

2.4.2 *Vulnerability Index Methods (VIMs)*

The Vulnerability Index Methods (VIMs) were introduced by Benedetti and Petrini (1984), and applied for the first time by Benedetti et al., (1988) at urban scale in various Italian historic districts such as Gemona del Friuli and Gubbio. In 1993, the GNDT (National Group for Earthquake Protection: http://emidius.mi.ingv.it/GNDT/) adopted the VIM as the institutional method for the estimation of the seismic vulnerability at national level in Italy. This approach consists of estimating the seismic vulnerability of historic buildings by calculating a vulnerability index (I_v) as the weighted sum of specific parameters that most affect the seismic response of a building type. In the original version of this approach (Benedetti and Petrini, 1984) the I_v is estimated by scoring the following parameters: 1) resisting system type, 2) resisting system quality, 3) conventional seismic strength, 4) location and soil condition 5) horizontal structures, 6) plan shape, 7) regularity in elevation, 8) maximum distance between walls, 9) roof, 10) non-structural elements, and 11) preservation state. In order to rank the effect of these parameters on the building response under seismic events, a weight, defined by using expert judgement, is associated to each of these parameters.

The required input data characterising these parameters is recorded on site, while seismic damage data is recorded on site, if possible, or taken from seismic damage databases from past earthquakes.

The most substantial improvement of the VIMs over the DPM methods consist of providing continuous vulnerability functions, against the latter that provides discrete vulnerability classes of expected damage for building types. This implies that if it is required to quantify the effect of a strengthening intervention to shift the vulnerability level of structural types to a lower level, while the VIMs are already arranged for this,

the DPM methods need to adopt specific functions capable to evaluate how seismic performance of retrofitted buildings improves (D'Ayala and Novelli 2013).

The VIMs have been also adopted by Giovinazzi and Lagomarsino (2001), Giovinazzi and Lagomarsino (2002) and Giovinazzi and Lagomarsino (2004) in a wider framework, where VIM together DPM are presented in one approach that associates vulnerability index to the damage levels computed for a given macroseismic intensity. This approach has been applied to assess the seismic vulnerability of the historic centre of Faro (Oliveira et al., 2004), Lisbon (Oliveira et al., 2005), and Barcelona (Barbat et al., 2008). The major advantage of proposing VIM and DPM in only one method for the seismic vulnerability assessment consists in providing the possibility of choosing the most suitable approach according to the type of data and level of information that are available for the region of study. In particular, for case studies with limited information on a given building typology, this approach proposes to compute the I_vs as the mean values of the I_vs computed for the building types that have been fully inspected and for which data is available. These mean values of I_vs, before being applied to a building type, are also weighted with modifiers, introduced to rank the structural features and their effect on the seismic response of the building types identified in the area of study.

However, since different approximations are introduced to overcome the lacks of data, this approach also proposes recording the level of knowledge (level of information) of buildings under inspection, and considering this in the results in order to provide an indicator of the level of accuracy of the estimated vulnerability.

This approach was adopted by Bernardini and Lagomarsino (2008) to estimate the seismic vulnerability in the historic centre of Imperia (Italy) with the scope at providing an emergency management and a retrofitting intervention plan and reducing the seismic risk of this Italian city. For this application, only data for parameters that most affect the performance of the buildings in the Province of Imperia was collected. Vulnerability curves were derived from a statistical analysis of damage observed from past Italian earthquakes, or, in case of lack of data, were derived from a fuzzy version of the DPM by using all available information collected on homogeneous group of buildings (Bernardini et al., 2007).

Lourenco and Roque (2005) were the first to propose a further development of VIM of Benedetti and Petrini (1984) that take into account the heterogeneity between adjacent historic buildings by introducing three new parameters to characterise the total height, the openings layout, and the interaction between buildings. This new version of VIM was applied for the first time to assess the seismic vulnerability of 58 churches (Lourenço, and Roque, 2006) and the city of Coimbra in Portugal (Vicente et al., 2011).

Recently, Formisano et al., (2010a, b) have also proposed an extention to the version of Lourenco and Roque (2005) by adding new parameters introduced to characterise the position in plan of buildings in an aggregate, the number of staggered floors, and the heterogeneity in plan and in elevation for taking into account possible pounding between buildings due to earthquakes.

These new parameters are calibrated on parametric analyses on typical masonry buildings of Torre del Greco, town in the province of Naples, (Italy). These analytical models are performed in the finite element software TREMURI (Lagomarsino et al., 2013) (see section 2.5.2). The methodology has been recently applied in the historic centre of Poggio Picenze (AQ) (Formisano et al., 2015).

2.4.3 *Continuous Vulnerability Curves*

Continuous fragility curves describe the probability that a structure exceeds a specific damage state given a continuous range of ground motion intensities. In the 1990s most fragility functions were expressed in terms of the discrete intensity levels of macroseismic intensity scales such as Modified Mercalli Intensity (MMI) scale or Medvedev Sponheuer Karnik (MSK) scale , and later European Macroseismic Scale (EMS), and hence their measure of vulnerability, also discrete and inherently dependent on the definition of the macro seismic intensity grades of the scale used. A first attempt at deriving continuous fragility curves using a Parameter-less Scale of Intensity (PSI) was made by Spence et al., (1992), who adopted this approach to provide vulnerability curves for different building types and to quantify the building performance with and without strengthening interventions.

The fragility functions are derived by assuming a constant value of dispersion for all damage states given a building class. This approach assumes that the levels of damage for a class are correlated to each other, and therefore once a median value of fragility is defined for one of the levels in the damage scale, the other levels can be correlated to it by shifting the median fragility left or right with respect to the horizontal axis. Generally, the fragility curves in this approach are derived by starting from damage level D3 (structural damage).This approach makes damage grades and fragility curves independent of the macro seismic intensity scales, thereby overcoming the main limitation of the seismic vulnerability functions in the DPMs.

The lack of data or partial information on a case study limits the applicability of this method that is considered robust only if there is an extensive database that can be used to calibrate fragility curves, and to correlate the observed damage with the expected damage.

Orsini (1999) has also used the PSI to assess the value of the seismic excitation in 41 municipalities in Italy after the 1980 Irpinia earthquake. This study performed by Orsini (1999) was developed to correlate the PSI to the PGA by empirical correlation functions (Calvi et al., 2006).

Further seismic vulnerability functions with PSI for Italian building types were also presented by Sabetta et al., (1998) and Rota et al., (2006) who applied this method by assuming a suit of several artificial accelerograms randomly generated. The seismic damage data collected for different Italian regions were classified according to the damage states of the MSK scale (Medvedev et al., 1964) for six different structural classes, and the empirical fragility curves with binomial distribution were derived as a function of the PGA, Arias Intensity and effective peak acceleration.

The applications described above, where the vulnerability curves are expressed by Parameterless Scale of Intensity, are mainly derived by empirical data randomly generated assuming a large sample size. Given the specificity of structural features and corresponding response in the building stock of historic city centres, where buildings are fairly uniform in original construction characteristics but might have been altered or strengthened through the ages, the corresponding vulnerability function is usually highly influenced by these conditions. Hence, an assumption of random

distribution of vulnerability and damage might not be correct. Therefore, these types of approaches are not favoured to predict the seismic vulnerability of historic city centres.

2.5 Analytical Vulnerability Assessment Methods

Analytical methods have the advantage, compared to the empirical ones, of framing the problem of seismic vulnerability of masonry constructions in structural engineering terms through algorithms with meaning directly connected to the structural behaviour of buildings.

Furthermore, the continuous development of attenuation equations for the derivation of seismic hazard maps in terms of spectral ordinates for specific regions, as opposed to macroseismic intensity or PGA maps, have also given a major impetus to develop analytical methods (D'Ayala and Novelli 2013), as these allow estimating vulnerability functions directly affected by the seismicity of the region under consideration.

In the development of analytical fragility functions for masonry structures, two approaches can be identified, which correlate:

- vulnerability index to damage levels; such as the mechanical approaches VULNUS (Bernardini el at., 1990) and FaMIVE (D'Ayala and Speranza, 2003) and
- acceleration/displacement capacity curves to spectral demand curves, following the HAZUS-MH (FEMA, 1999) or N2 method (Fajfar, 2000), or Non Linear Time History Analyses (NLTHAS) such as Jalayer and Cornell, (2009), Vamvatsikos and Cornell (2004).

In these procedures, the fragility curves and damage levels are directly linked to the demand parameters, which are expressed in terms of displacement or drift. Fragility curves by referring to engineering demand parameters (drift, for instance) to the ground motion intensity parameters for a given building type. The demand parameters are derived from capacity curves defined with the scope of identifying the building response in terms of capacity and ductility estimated with reference to discrete damage states. Once the capacity curves are defined, then the range of behaviour and variability of

fragility within a building type can be analysed, providing important insight for retrofitting (D'Ayala, 2005).

Analytical approaches to define seismic vulnerability of masonry buildings are becoming more and more popular, as the engineering knowledge on the behaviour of masonry structures improves the confidence on the reliability of such models.

2.5.1 *Methods based on the correlation between damage index and damage thresholds*

Among analytical methods available for masonry buildings, the mechanical methods VULNUS (Bernardini el at., 1990) and FaMIVE (D'Ayala and Speranza, 2003) are the ones that estimate the vulnerability indices that are ranked in a scale directly correlated to the expected damage levels for a given intensity of shaking, expressed in terms of PGA. The vulnerability indices are estimated by using mechanical approaches based on the application of kinematics models, which identify collapse load factor multipliers of a given configuration of macro-elements and loads, by imposing kinetic energy equations. These methods present the advantage of requiring few input parameters to determine the building features, to estimate collapse load factor multipliers and to identify the occurrence of possible failure modes. The failure mode that has the highest level of vulnerability (and therefore the highest possibility of occurrence) in an inspected building is the one that has the lowest collapse load factor multiplier.

VULNUS (Bernardini el at., 1990) is the first mechanical vulnerability index method purposely developed for masonry structures using the fuzzy-set theory and the definition of collapse multipliers. The data collection of the geometrical and mechanical properties, required as input for this approach, is performed on site. The output of this method consists of three indexes. The first index is, I1, for in-plane behaviour given by the ratio between the shear strength of the systems of walls, floors and total weight of the building. The second index is, I2, for the out-of-plane behaviour and is defined by the ratio of flexural strength of the most critical external walls and the total weight the most critical wall, evaluated by summing the resistance of the vertical and horizontal strips. A third index, I3, is calculated as weighted sum of seven factors related to plan,

height, connections among buildings, homogeneity between adjacent buildings in terms of class and interaction with soil, use and damage (Benedetti & Petrini 1984). This approach is particularly suitable to assess the seismic vulnerability of small and regular masonry buildings. The major limitation of this method consists in considering only a limited number of failure modes, one in-plane and one out-of-plane failure mode, as simple rigid body overturning.

D'Ayala et al., (1997) also proposed a mechanical approach that included a larger number of possible failure modes with the scope of capturing the typical in-plane and out-of-plane failure modes of masonry buildings. Each failure mode, defined as a possible kinematic of a masonry building, is representative of different constraint conditions between façades and the rest of the structure.

This method was applied for the first time to 200 buildings in Lisbon with the key aim of defining collapse load factors for each surveyed building and identifying failure mode with highest vulnerability level. The results led to the development of vulnerability functions, which were validated against vulnerability functions derived from statistical analysis on the observed damage recorded after the Lisbon earthquake in 1755. The method was also used to predict how the vulnerability reduces by introducing low-cost strengthening techniques, such as tie-rods, used to connect façade walls to floors.

This approach was further developed by D'Ayala and Speranza (2003) with the mechanical approach FaMIVE, by extending the range of failure modes considered and defining a better correlation between damage and vulnerability. Differently from other mechanical approaches, in FaMIVE, the highest vulnerability is linked to the failure mode, which shows the lowest value of the collapse load factor multiplier, and to the greatest extent of façade involved in the collapse. This approach is implemented in Visual Basic in an open format, which allows easy modifications of the programme to adapt it to new applications, for instance when new failure modes or building characteristics are identified.

This method was validated for the first time in the historic centres of the Umbria-Marche region, in Italy, hit by the 1997 earthquake sequence. The results obtained from this application demonstrated the good capacity of FaMIVE in estimating the seismic vulnerability, and differing the vulnerability levels for each inspected building by

taking into account its geometric and structural features, type of connections, presence of retrofitting interventions.

2.5.2 *Methods based on the correlation between acceleration/displacement capacity curves and spectral demand curves*

The Capacity Spectrum Based Methods (CSBM) estimate the seismic performance of structures by comparing seismic capacity and seismic demand in terms of spectral coordinates. This comparison is carried out by using acceleration–displacement response spectra, adequately reduced to consider the inelastic behaviour of the structures.

The HAZUS (Hazards U.S.) framework proposed by Kircher et al., (1997) is classified as a CSBM and identifies the damage probability by providing fragility curves developed assuming lognormal distributions of data available from seismic damage observed from past earthquakes. For this approach, high level of details of the input data is not necessarily required, since fragility curves are derived from simplified analytical models that use few parameters to simulate the seismic response of building types, as described in the HAZUS Technical Manual (NIBS,1997). In HAZUS 99, thirty-three occupancy classes are defined to distinguish among residential, commercial, industrial, or other buildings; and 36-model building types are used to classify buildings within the overall categories of wood, steel, concrete, masonry, or mobile homes. For each of these building categories, which are classified according to the design code in force of the time of construction and level of rise, four levels of damage for structural and non-structural elements are identified and used to derive related fragility curves. Pushover curves and related-capacity curves are derived from assumptions and methods found in the NEHRP (National Earthquake Hazards Reduction Program) Guidelines for the Seismic Rehabilitation of Buildings (FEMA 273, 1997), and in Seismic Evaluation and Retrofit of Concrete Buildings (ATC and SSC, 1996), known as ATC-40. Potential problems of this methodology are related to the fact that the capacity and fragility curves provided by HAZUS 99 (Kircher et al., 1997) are only valid for buildings located in the United States, therefore they require to be recalibrated, if they are used in a different geographical area.

An example of HAZUS 99 approach (Kircher et al., 1997) applied for constructions, which are not located in the US, is provided by Erdik et al. (2003, 2008) who adopted HAZUS 99 to derive modified capacity and fragility curves for seismic loss estimation of the masonry buildings in Turkey by using the ELER (Earthquake Loss Estimation Routine) platform (Hancilar et al., 2010).

The HAZUS 99 framework has been also applied in the city of Basel in Switzerland, where the seismic damage from past earthquakes is not available (Lang and Bachmann, 2004). In order to overcome the lack of data to qualify the building response in this region, simplified methods for the estimation of the capacity curves have been proposed. These methods are based on a nonlinear static approach acknowledging the importance of the nonlinear deformation capacity of the buildings subjected to seismic actions. The inelastic displacement demand is identified, known that the elastic spectral displacement is a function of the natural period, the participating mass and the ductility demand. In order to obtain capacity curves for masonry buildings, floors are assumed as rigid diaphragms and the capacity is obtained by considering only the in-plane capacity of walls laying parallel to the direction of application of the acceleration. The vulnerability functions are expressed in terms of the damage scale defined by EMS'98 (Grünthal, 1998), although the correlation between them is not clearly explained by Lang and Bachmann (2004). This approach could be applied only to buildings with rigid diaphragm and in-plane response, so that the methods cannot be applied to determine the capacity of the structure associated with out-of-plane failure modes.

A more recent CSBM procedure is SP-BELA, aimed at defining analytical vulnerability functions for masonry structures in urban context (Borzi et al., 2008). This method was originally developed to assess the seismic vulnerability of reinforced concrete buildings, and then extended to unreinforced masonry buildings. This probabilistic framework generates vulnerability curves by simplified methods based on pushover analyses of a non-linear Single Degree of Freedom (SDOF) system, simulating an entire building. The building performance is derived by comparing 1) the displacement capacity of the SDOF expressed in terms of limit states with 2) the displacement demand obtained from the median displacement demand and the logarithmic standard deviation at a given period.

The seismic vulnerability of masonry buildings can also be estimated by using more sophisticated CSBM, based on finite element models, such as TREMURI (Lagomarsino et al., 2013), or DIANA finite elements (Ramos et al., 2004), Etabs (Computers and Structures, Inc. produce), Abaqus (www.simulia.com), ANSYS (www.ansys.com), Autodesk Simulation Multiphysics 2013 (www.autodesk.com).

These methodologies require a computational burden heavily, than the computational burden required for the approaches previously described. Hence, they are suitable for the analysis of single buildings rather than large samples at territorial level. Furthermore, the modelling assumptions make them only suitable to investigate the seismic performance of buildings with good connections and characterised by rigid diaphragms, because the out-of-plane failure modes, which are common failure modes in masonry buildings, are completely disregarded.

Lagomarsino et al., (2010) also proposed a CSBM based on a mechanical model for masonry buildings, which derives the capacity curves by using three parameters: yield acceleration of resistant walls; fundamental period of an equivalent SDOF; the ultimate displacement capacity, derived from the drift limit associated to the failure modes of the masonry panels. In this approach, in order to take into account possible irregularities in buildings, corrective factors are also provided. This method can be easily applied to a large amount of masonry buildings, since it only requires few parameters to estimate the capacity of buildings. Its limitation, like the previous methods, consists in being only adequate to compute the performance of buildings characterised by good connections between orthogonal walls, but excludes that façades can fail for overturning.

The MeBaSe approach for unreinforced masonry buildings proposed by Restrepo-Velez et al., (2004) is a mechanical model classified as CSBM capable to estimate in-plane and out-of-plane failure modes. Limit states for overturning are defined, based on the works developed by Doherty et al., (2002) and Griffith et al., (2003) which assume a tri-linear model for the nonlinear behaviour of the masonry walls. The limit states are classified in relation to drift limits, depending on the type and quality of masonry. However, the approach is only limited to determine the collapse condition, while it does not consider intermediate levels of damage.

The FaMIVE approach has been further developed from its original version of D'Ayala and Speranza (2003) to allow computation of both spectral acceleration and spectral displacement through the integration of the original mechanism approach with the capacity spectrum method (D'Ayala, 2005). Capacity curves are defined for the single façade of a building, which is analysed as an equivalent non-linear SDOF system. The maximum strength capacity of the single façade is directly correlated with the collapse load factor multiplier, which identifies the failure modes with the highest vulnerability (D'Ayala and Speranza, 2003).

The elastic limit displacement at the top of each façade is calculated as a function of the elastic stiffness and the mass of the façade, involved in the activated failure mechanism. The ultimate displacement is defined as the displacement that determines the geometric instability of the façade and hence its collapse. The reliability of the results depends on the data level of reliability, which is explicitly recorded during the on site data collection.

This version of the FaMIVE has been applied to a study of the seismic vulnerability of the Fener-Balat district of Istanbul, with the aim at deriving fragility curves for the Turkish building typologies and estimating cumulative damage (D'Ayala 2005). Since its development, this approach has been also applied to several historic sites in Italy, India, Spain, Iran, and Nepal, showing flexibility of application to different construction contexts and capacity to include a large variety of failure modes, both in-plane and out of plane. The application to different locations has consistently shown good agreement between, the computed vulnerability, the damage, and the seismic damage observed in each site under scrutiny.

The Non Linear Time History Analyses (NLTHA) is considered a very accurate methodology for predicting building response to earthquake ground motion. As with CSBM, the first step in NLTHA analysis is to create a computer model of the building that captures the nonlinear post-elastic behaviour of a building's structural elements that undergo damage. A large number of historical (where available) or simulated ground motion records of varying intensities are loaded into the software to perform a time-history (dynamic) analysis. Essentially, the virtual building is shaken (rather than pushed) using the recorded ground motions in the same way that it would be shaken

by an actual earthquake. NLTHA allows higher modes of vibration to be captured as well as different failure modes.

Moreover, the use of time-history analysis allows an explicit consideration of the effects of the duration of the earthquake shaking on the cumulative damage of building components. In each analysis, the forces and deformations occurring in all structural members of the model are calculated and used to evaluate the global response measures such as maximum peak inter-story drifts and forces, roof displacement, and peak story accelerations. More specifically, the peak inter-story drift is the highest lateral displacement between two consecutive floors, normalised by the inter-story height. The maximum peak inter-story drift is the maximum drift among all stories that is observed over the entire duration of the earthquake. The peak floor acceleration (PFA) is the highest acceleration of a particular floor in response to ground shaking. Similarly, the maximum peak floor acceleration is the highest PFA found along the entire height of the building. This quantity is well correlated with damage to acceleration-sensitive non-structural components (e.g. suspended ceilings), and to contents. As in the CSBM approach, these parameters can be related to the damage suffered by all types of components and, therefore, to the repair strategies that are expected due to the predicted damage. The use of ground motions from multiple earthquakes allows the model to obtain not only an estimate of the mean response given a certain level of ground shaking, but also allows it to account for the variability in the buildings' nonlinear response generated by different records of the same intensity (e.g. Jalayer and Cornell, 2009; Vamvatsikos and Cornell, 2004). NLTHA directly provides, without any limiting assumptions, the force imposed on a building by ground motion. Deformation levels (or storey acceleration levels, when necessary) are then used to determine component damage and the associated repair strategy. The monetary loss for the entire building is estimated by combining component repair costs.

Similar to NLTHA, FRACAS (FRAgility through CApacity Spectrum assessment) allows the use of suites of scaled and/or unscaled ground motion records and delivers the immediate seismic response of the considered structure. Moreover, FRACAS does not rely on reduction factors or indices to determine the inelastic spectrum from the elastic one. Instead, for each target ductility and period, it carries out a simplified dynamic analysis on the idealised nonlinear Single Degree of Freedom (SDoF) model

corresponding to the capacity curve. This process proves to be more time-consuming than the commonly-used static approaches (e.g. the CSBM and its variations) but it is more robust and remains faster than performing full NLTHA on finite element models. This feature also has the advantage of permitting the use of various ground motion records that generate unsmoothed spectra as opposed to standardised design spectra. Therefore, the record-to-record variability can be directly introduced and the resulting cloud of performance points leads to seismic responses that account for the natural variability in the seismic demand. Previous studies (e.g. Rossetto et al. 2014) have shown that FRACAS procedure outperforms CSBM and its variants, particularly for the cases of low- and mid-rise RC regular frames of various vulnerability classes. This method is recommended in the recently published GEM Guidelines for Analytical Vulnerability Estimation (D'Ayala et al. 2014); further details on the FRACAS methodology are also provided in Gehl et al. (2014). Examples of FRACAS implementation on RC buildings, representative of European and Mediterranean/Italian stock can be found in Rossetto et al. (2014) and Minas et al. (2014).

2.6 Hybrid Vulnerability Assessment Methods

The existing hybrid methodologies are based on estimating the seismic vulnerability by using different methods, from simplified to more sophisticated ones that are characterised by features borrowed from either empirical or analytical approaches. This implies that the hybrid approaches, by relying on more than one method to estimate the seismic vulnerability, are generally very adaptable to heterogeneous data, since they allow choosing, according to the available information on a case study, the method that best estimates the building performance under seismic events. Therefore, if the level of information on a building is detailed, the most advanced method in the hybrid approach is favoured; otherwise, a simplified approach is adopted, if the level of information on a building is not accurate.

The first hybrid approach was developed by Kappos et al., (1998), who proposed a method involving elements from both empirical and theoretical methods. A model for correlating analytically calculated structural damage indices to loss (in monetary terms) is also proposed and calibrated against available statistical data. Probability damage

matrices (Whitman et al., 1973) derived using this methodology are incorporated into a cost-benefit model tailored to the problem of estimating the feasibility of seismic interventions in existing building stocks.

This approach was applied, in the city of Thessaloniki (Kappos et al., 1998) and Volos (Kappos et al., 2002) in Greece on a large number of building types, representing most of the common building typologies in South Europe. The vulnerability curves for the selected case studies were estimated as mentioned above and by referring to the mean spectrum of the Microzonation of Thessaloniki. The approach has been also adopted to estimate the seismic risk in Thessaloniki, where capacity curves were derived from pushover analyses and reduced to standard capacity curves, and then used together with fragility curves for the derivation of damage probability (Kappos et al., 2006, 2008, 2010).

Although this hybrid approach proposes the use of different methods to overcome lack of data, the applications in Greece show that such procedure estimates reliable seismic performance of buildings only if these are inspected in details and data is accurately recorded.

A further hybrid method was also developed by Barbat et al., (1996). This approach was applied to assess the vulnerability of masonry building types in Spain, damaged by Barcelona earthquake in 1995 with intensity of VII on the MSK scale. For this specific case study, structural and non-structural damage was collected on site and correlated to the vulnerability indexes, calculated as proposed by Benedetti and Petrini (1984) for the Italian regions. Vulnerability functions for buildings hit by the earthquake of intensity of VII on MSK scale were derived on data collected on site after Barcellona earthquake while vulnerability functions for earthquake of intensities different from the ones in Barcelonese were derived through Monte Carlo (random) simulations. The random simulations were also carried out to derive the typical features for sixty different hypothetic Spanish building types, whereby the capacity curves were determined by using simplified analytical models, as the ones proposed by Abrams (1992), although these models are not always suitable to simulate the complexity and variability in the building features and building performance.

Within the framework of Risk-UE project (www.risk-ue.net) another hybrid approach was introduced by Lagomarsino & Giovinazzi, (2006) to link the use of different approaches to the levels of knowledge and quality of data available for a specific study. In this context, three levels of knowledge are considered and defined with reference to the level of detail pursued in the data collection. These three levels are defined as follows: Level 0: based on rapid assessment of a single building, Level 1: based on rapid survey of a small building sample, Level 2: based on detailed survey of the single building (Lagomarsino, 2006). Empirical approaches based on macroseismic models are adopted to analyses data of both Level 0 and Level 1, while a mechanical model is used for data of Level 2. The major drawback of this approach consists of a lack of a specific procedure to compare the results obtained from the different methods that are not directly linked to each other.

The approach proposed by Giovinazzi (2005) is also classified as a hybrid one, and is adopted to calculate the effective-cost of loss with the aid of simplified bilinear capacity spectra, defined according to seismic codes. By using this simplified method, the stiffness, capacity and ductility are derived with reference to design codes although those do not have any specifications for historic buildings.

Most recently, Maio et al., 2015 proposed a hybrid approach based on the integration of TREMURI software (Lagomarsino et al., 2013) with the VIM by Vicente et al.(2011) and Formisano (2012). This approach was applied on the urban block of San Pio delle Camere in Abruzzo (Italy) damaged by the earthquake in 2009 with epicentre in L'Aquila. The main limitation of this method consists of the fact that by using TREMURI software, as discussed in section 2.5.2 the out-of-plane failure modes in masonry buildings is neglected.

The hybrid methods proposed by Aldemir et al., (2013) differ from the others mentioned above, as this approach is not based on the use of empirical method and analytical method but only on the use of two different analytical procedures: the finite-element approach ANSYS and equivalent-frame approach SAP.

The finite-element approach ANSYS (http://www.ansys.com/) is used to model single masonry macroelement for estimating local effects, while the equivalent-frame approaches SAP (https://www.csiamerica.com/products/sap2000) is used to model

entire structure for estimating global effects. The approach has been applied to assess existing brick masonry buildings, damaged during Dinar earthquake in 1995. This method also overlooks possible out-of-plane failures, and it is more adequate to estimate the vulnerability of individual buildings rather than at territorial scale.

2.7 Final remarks and gaps

The methods discussed in this chapter are classified according to the criteria introduced in D'Ayala and Novelli (2013) and summarised in Table 2-1 to identify the most suitable method for the assessment of the seismic vulnerability at territorial scale. The criteria adopted to select the method that best suits the research project are the following:

- Method class: the approaches are classified as Empirical, Analytical or Hybrid method by following the classification introduced in sections 2.4, 2.5 and 2.6;
- Data collection approach: the methods are classified according to how the data is collected (for instance: by using visual inspections, or detailed surveys, or databases with data collected from past earthquakes, etc.);
- Input data: This is the list of the fundamental parameters required by each method to assess the seismic vulnerability;
- Demand input data: this is the list of data/factors/parameters such as drift, or displacement, required to verify the building performance by each method;
- Assessment type: the methods are classified according to how input data is processed and analysed (for instance: by mechanical approaches, statistical methods, etc.)
- Output: this is the list of output parameters provided by each method to assess the seismic vulnerability (for instance: drift capacity, failure mode, etc.).

Among the existing approaches in Table 2-1 , the most suitable methods to estimate the seismic vulnerability at territorial scale are the ones based on simple models of analyses developed by using data that can be collected on site by rapid visual inspections. These methods are favoured as they allow collecting data in a relatively short time for a large number of buildings. According to these criteria, the following methods emerge from the literature as possible choices: DPM (Whitman et al., 1973), VIM (Benbedetti and Petrini, 1984), HAZUS 99 (Kircher et al., 1997); FAMIVE (D'Ayala and Speranza, 2003) Vulnus (Benardini et al., 1990), Kappos et al., (2010, 2008), Barbat et al., (2008, 1996).

Most of these approaches need, as input, information related to building geometry, structural details, and mechanical properties. Information related to the geometry can be easily collected by visual inspection, while data related to quality of the materials and structural detailing, might require accurate inspections or laboratory tests. Analytical approaches are the ones that rely on models built up on data collected from rapid surveys for more exhaustive surveys of buildings, while empirical approaches are the ones that can provide reliable vulnerability assessment by using data collected on site. However, although the empirical approaches are apparently the most suitable for the vulnerability assessment at territorial scale, these methods have a limited applicability. Since these methods characterise the performance of buildings by only using few selected parameters, these approaches might be not adequate to assess the vulnerability of building types located in different regions. So according to this, DPM and VIM, implemented and tested on building types located in a specific region, excluded, in order to favour analytical approaches that best take into account peculiarities and defects of specific buildings.

However, not all analytical approaches are adequate for the assessment of the vulnerability at territorial scale, as the ones considered suitable, as discussed before, should not rely on refined numerical models but on simplified approaches based on data collected rapidly. This is the reason why NLTHA and models built by using finite element software such as TREMURI (Lagomarsino et al., 2013) Diana (Ramos et al., 2004) Etabs (Computers and Structures, Inc. produce), Abaqus (www.simulia.com), ANSYS (www.ansys.com), Autodesk Simulation Multiphysics 2013 (www.autodesk.com) are excluded, as they provide an accurate results, only if

numerical models are built on data collected by detailed surveys and/or laboratory tests. Moreover, as discussed in section 2.5, TREMURI (Lagomarsino et al., 2013) has also another limitation, which consists of providing only the response of masonry buildings characterised by good connections between their bearing walls and between their bearing walls and floors/roof. Therefore, these analytical approaches are not applicable and excluded at large scale first because it is not feasible to develop accurate models for a large number of buildings, and second because they are not capable of simulating out-of-plane failure modes.

The analytical method SP-BELA (Borzi et al., 2008) is also excluded because it only simulates in-plane failure modes. This limitation, as reported in section 2.5.2, is because this approach was originally developed to model reinforced concrete buildings as frames and then adapted to masonry constructions.

Among the analytical approaches, methods based on predefined capacity curves such as HAZUS 99 (Kircher et al., 1997) are considered possible methods that can be adopted to estimate the vulnerability at territorial scale, only if these are applied in the regions where they have been developed, see section 2.5.2. This implies that their applicability is limited. Among the approaches for vulnerability assessment considered most flexible and applicable at territorial scale are the hybrid methods (Kappos et al., 2010, 2008, Barbat et al., 2008, 1996), since they are based on using different type of approaches according to the reliability and level of details of the available data. However, as discussed in section 2.6, their major limitation consists of using approaches that provide output which are difficult to be compared.

The previous considerations leave the mechanical approaches by Benardini et al., (1990), D'Ayala and Speranza (2003), Restrepo-Vélez and Magenes (2004) as the only methods based on analytical simplified models, capable to provide vulnerability functions by taking into account both in-plane and out-of-plane failure modes.

Table 2-1: Summary of procedures for the seismic vulnerability assessment of masonry structure

Name Method	Reference	Method class	Data collection approach	Input Data	Demand Input data	Analysis approach	Output
DPM	Whitman et al., 1973; Braga et al., 1982; De Natale et al., 1987; 1990; Dolce et al., 2003; and Di Pasquale 2005.	Damage probability matrix	Expert Judgements and On-site observation, Exposure database	Typological description	Macro-seismic Intensity	Empirical basis	Phenomenological Damage scale
VIM	Benedetti and Petrini 1984; Benedetti et al., 1988; Giovinazzi and Lagomarsino 2001, 2002, and 2004; Oliveira et al., 2004, and 2005; Barbat et al., 2008; Lourenco and Roque 2005; Bernardini and Lagomarsino 2008; Bernardini et al., 2007; Lourenco and Roque 2005; Vicente et al., 2010; Formisano et al., 2010a, b, and 2015.	Vulnerability Index Method	On-site observation, Exposure database	Typological description	Macro-seismic Intensity,PGA	Empirical basis	Phenomenological Damage scale
PSI	Spence et al., 1992; Orsini 1999; Sabetta et al., 1998; Rota et al., 2006.	Damage probability function	Exposure database	Typological description	Macro-seismic Intensity	Empirical Statistic basis I	Phenomenological Damage scale
VULNUS	Bernardini et al., 1990.	Mechanism Method	On-site observation or Systematic survey	Geometry, Material parameters, structural details	PGA, response spectrum	Analytical basis (Mechanical method))	Lateral Force, Lateral Drift, vulnerability index

FaMIVE	D'Ayala et al., 2003 and 2005.	Capacity spectrum-based Method,	On-site observation or Systematic survey	Geometry, Material parameters, structural details	PGA, response spectrum	Analytical basis (Mechanical method)	Lateral Force Lateral Drift, damage scale, vulnerability index
HAZUS 99	Kircher et al., 1997.	Capacity Spectrum Based Methods	On-site observation, Exposure database, Random generation	Typological description, structural details	PGA, response spectrum	Empirical basis	Damage scale, Lateral forces
SP-BELA	Borzi et al., 2008.	Capacity Spectrum Based Methods	Random generation	Structural description	PGA, response spectrum	Analytical basis (Pushover based)	Lateral Force, Lateral Drift
TREMURI	Lagomarsino et al., 2013.	Capacity Spectrum Based Methods	On-site observation	Geometry, Material parameters, structural details	PGA, response spectrum	Analytical basis (finite element method)	Lateral Force, Lateral Drift
Diana	Ramos et al., 2004.	Capacity spectrum-based Method	On-site observation	Geometry, Material parameters, structural details	PGA, response spectrum	Analytical basis (finite element method)	Lateral Force, Lateral Drift
MeBaSe	Restrepo-Velez et al., 2004.	Capacity spectrum-based Method	On-site observation or Systematic survey	Geometry, Material parameters, structural details	PGA, response spectrum	Analytical basis (mechanical method)	Lateral Force Lateral Drift, damage scale, vulnerability index
Risk-UE	Lagomarsino & Giovinazzi, (2006) Giovinazzi, 2005; Lagomarsino, 2006.	Capacity spectrum-based method	Systematic survey and random generation	Structural description	PGA, response spectrum	Empirical/Analytical, Statistical basis	Lateral Force, Lateral Drift
Hybrid Methods	Kappos et al., 1998, 2002, 2006, 2008, 2010; Barbat et al., 1996 Maio et al., 2015.	Hybrid Methods	On-site observation	Structural description	Macro-seismic Intensity, PGA	Empirical/Analytical, Statistical basis	Damage scale, Lateral forces

Among these, FaMIVE is the method that has the capacity to capture the highest number of possible failure modes, which can occur on regular masonry constructions. Moreover, FaMIVE has also the advantage of being characterised by a flexible framework that can be updated with new mechanisms, and in the latest version (D'Ayala, 2005) it also integrates the mechanism approach with the capacity spectrum method, which allows to frame a new procedure for seismic vulnerability assessment of historic buildings in terms of seismic performance based assessment (Lagomarsino et al., 2010).

However, in order to update FaMIVE to new building types, it is important to be aware the typical failure modes of the building in question, so that an appropriate mechanical model can be developed to simulate the expected building response. The most reliable proof of how a building type performs during seismic events, can be found on site by inspecting buildings in the aftermath of a damaging earthquake.

How these buildings should be assessed on site? What type of data should be collected to understand the failure modes occurring to a building? Is there an approach capable to assess failure modes by only using visual inspection?

These questions gave the impetus to the research rationale described in Chapter 3 to introduce a new methodology for vulnerability assessment at territorial scale and applicable in historic city centre.

3 RESEARCH RATIONALE FOR THE DEVELOPMENT OF A NEW METHODOLOGY FOR THE SEISMIC VULNERABILITY ASSESSMENT OF HISTORIC CITY CENTRES

3.1 Introduction

The ability of any existing analytical vulnerability assessment method to estimate the seismic performance of masonry constructions, as discussed in the previous chapter, is dependent on a robust knowledge of the seismic behaviour of a construction class and the possibility of developing a mechanical model able to simulate the expected performance. The review highlighted that the FaMIVE procedure has the required flexibility to adapt to the construction characteristics of different building practices, across the world, as proven by its several applications in Europe, Africa and Middle East.

However, so far, its results could only be validated in locations where an earthquake had occurred and seismic damage of the assessed building stock is available. Hence, to make the method more universally applicable it would be also important to identify the data that can be collected onsite, which can be used to reliably predict failure modes from existing crack pattern or specific construction details, and how to consistently include such information in the analytical approach.

To this end, the chapter 3, first presents in section 3.2, a review of the existing visual inspection methods for the seismic vulnerability assessment of masonry buildings to investigate if these approaches can be adopted to identify and classify the causes of specific seismic response and failure modes.

During the review, attention is paid to pre-earthquake Rapid Visual Screening methods, simplified Visual Assessment methods, part of Tiered assessment

procedures and post-earthquake visual screening, used for safety tagging and assessment of need for repairs.

The assumption postulated here is that these methods, to varying extent, are useful to quickly determine the essential seismic behaviour of historic masonry buildings, and hence they are applicable within a strategy aimed at identifying their most probable failure modes, simply on the basis of observation. This assumption is put to the test in section 3.3, by applying it to three Nepalese masonry houses damaged by the earthquake in 25th April 2015 (Gorkha earthquake) in order to validate their capability in assessing their seismic response.

These tests on the Nepalese houses show that correct interpretation of observed behaviour needs to be based on expertise or intuition of the individual engineer.

Therefore, the discussion of the advantages and shortcomings of the existing approaches highlights the need for a purposely-developed method. The fundamental requirements and characteristics of such a method are introduced and the essential elements of the procedure named LOG-IDEAH (LOGic trees for Identification of Damage due to Earthquakes for Architectural Heritage) are presented, emphasising the need of complementarity with the analytical method.

Finally, in section 3.4 the joint use of FaMIVE and LOG-IDEAH is proposed in a methodology presented to provide a hybrid approach to assess a seismic vulnerability of historic city centres through an analytical method and a visual inspection tool.

The major motivation for presenting a methodology based on the use of both methods is the current lack of approaches able to correlate in a robust way:

1. seismic damage observed on site to specific construction features and/or defects;
2. crack patterns observed on site to failure modes;
3. failure modes to simple or more complex analytical models used to determine the lateral capacity of wall assemblies.

This methodology is presented in steps that are introduced to describe the approaches adopted by both methods for data collection, and data analysis. Moreover,

in order to validate the capacity of prediction of FaMIVE and LOG-IDEAH and demonstrate that their joint application provides results that best predict the observed vulnerability, a validation approach based on statistical parameters is also introduced.

3.2 Review of the existing visual inspection methods for the assessment of masonry buildings at territorial scale

The existing visual inspection code based methods presented in this section are often included in national or international standards for seismic vulnerability assessment, and hence, their use is often mandatory. These approaches can be classified in two main groups.

The first one consists in methods used to assess buildings currently undamaged to determine their seismic vulnerability and seismic risk to damage. These methods can be further classified in two different subgroups: Rapid Visual Screening (RVS) methods and Qualitative Assessment methods included as the lower Tier of a more complete assessment procedure, which include also for instance, on site data collection, testing and analytical assessment. These of methods are usually employed to identify the need for strengthening and associated required resources.

The second class of visual inspection approaches are methods used in post-earthquake assessment. These are used to survey building conditions after an earthquake in order to determine, through the assessment of damage severity, if buildings can still be used, to which extent these buildings need to be repaired, or if these should be demolished as considered unsafe.

Both classes of approaches are described in this section and then applied to three Nepalese houses damaged by the Gorkha earthquake (2015) in the next section, to identify an approach based on the existing visual inspection tools that overcomes the gap between the understanding of the building behaviours under seismic events and the actual deficiencies causing the seismic damage (types and severity) observed on buildings.

In particular, the first class of methods (pre-seismic events) are introduced to describe how these approaches can be used to investigate the seismic deficiencies in

existing buildings, and how these deficiencies, once identified, can be adopted to include or exclude the possibility of occurrence of specific failure modes. In relation to the second group of approaches (post-seimsc events) these are mainly proposed in the present section to overview the existing damage scales included in these methods to classify the severity of damage and how these damage scales are necessary to assess the severity of the failure modes occurring on buildings.

Among the first class of methods, FEMA P-154 (2015), ATC 21-1 (1998), NRCC (1993), JBDPA, (2001), Angeletti et al., (1988); ING-GNDT (2001) are widely used. These approaches are typically adopted to assess the seismic adequacy of large number of buildings by the aid of systematic surveys. In order to evaluate the building seismic adequacy, the RVS methods proposes the use of a score system that consists in computing a score (Final score) given by a Basic Score modified by several parameters, estimated during on the site observation.

The Basic Score is determined taking into account to the lateral load resisting structural system, the seismic performance of the inspected building and the seismic hazard intensity of the region where the inspected building is located.

The other parameters defined as Modifiers of the Basic Score take into account the year of construction, the irregularity in plan and in elevation, and the soil conditions of the inspected building. These modifiers assume positive or negative values and increase or decrease to the Basic Score to give the Final Score. Once the Final Score is computed, this is compared with a Cut-off Score that defines the probability (or chance) that the inspected building collapses if an earthquake occurs.

The Cut-off Score is a recommended value. For instance, in FEMA P-54 (2015), the Cut-off Score is set at 2 and it means that if a building has a Final Score of 2 or less than 2, the building has a chance of 1 in 10^2, or 1 in 100 of collapsing if a ground motion occurs. (Additional information about the basis of the RVS scoring system is provided in FEMA P-154).

The RVS methods are not developed to identify the building performance but only to perform for a first screening and classify buildings in two categories: those that are expected to have acceptable seismic performance, and those that may be seismically unsafe and should be studied further. This implies that to investigate the building

performance, the RVS methods require to be used together with other methods that aim at investigating buildings with detailed inspections and more analytical approaches.

The major limitation of the RVS methods is highlighted when these are adopted to inspect unreinforced masonry buildings. This is because the Basic Score associated to this class has already a value that is lower than 2. This implies that if the Cut-off Score is equal to the value recommended in the RVS, most of the investigated unreinforced masonry buildings are automatically considered as buildings with an inadequate seismic provisions that need to be further investigated with Tiered assessment methods.

ASCE 41-13 (2013); NRCC 1993; NBIA (1996); CEN (1996, 2005); GNDT (2001) UNDP/UNIDO (1985) are classified as Tiered assessment approaches. They are basically developed for the assessment of individual buildings, therefore they are based on procedures of inspections that are more detailed, compared to those proposed in the RVS methods.

The existing approaches such as FEMA P-154 (2015), ASCE 41-13 (2013), and ATC 21-1 (1988) for USA, NRCC (1993) for Canada, NBIA (1996) for New Zealand and SERC (2002) for India, are specifically developed and mostly suitable to assess the deficiencies of buildings in the country where the code-based methods are defined.

These approaches propose an assessment for individual buildings based on three levels: Tier 1, preliminary assessment; Tier 2, evaluation of the building performance by preliminary calculations and some invasive inspections; and Tier 3, design of retrofitting interventions. Within the Tiered approaches, Tier 2 and Tier 3 are the ones that require numerical analyses to assess the seismic performance of buildings. These procedures are not described here, since this section only focuses on approaches that provide vulnerability assessment of buildings based on visual inspection.

Tier 1 is the only level of assessment where buildings are assessed by visual investigations. This assessment is carried out with inspection forms provided as a support to identify flows and vulnerabilities in the inspected buildings. The inspection form adopted during the investigation is selected according to the building class and seismicity of the region, where the inspected buildings are located. The inspection forms are organised in two different parts, the first one is for the investigation of the

structural deficiencies while the second part is for the investigation of the non-structural deficiencies.

The Tier 1 (ASCE 41-13, 2013) form developed to assess masonry constructions is very detailed, as it includes numerous checklists, useful to identify those defects that need attention from a seismic viewpoint. The form is organised in different sections developed to investigate building system, building configuration, geologic site hazards, foundations and diaphragms.

This inspection form also requires several checks on the level of connection between walls and floors that are used to identify if walls are vulnerable to overturn under seismic events. Not all checks included in these forms can be easily investigated only by observation, as many of those require opening up of walls or floor, removal of plaster/stucco or experimental tests.

In particular, for masonry buildings, where the materials can be classified by visual inspection according to type of masonry (i.e. bricks, stones, earth, etc.), type of mortar (i.e. lime, mud, cement, etc.), description of the friability and regularity of the mortar courses, etc., Tier 1 only requires a characterisation of the construction materials through the characterisation of their mechanical properties.

As mentioned above, the second class of procedures based on visual inspection are the ones developed to assess the structural conditions of buildings of their damage severity after an earthquake with the scope at assessing their safety.

In the US, P-E approaches (ATC20, 1989 and ATC20i, 2003) are mainly based on screening and tagging procedures to ascertain if buildings require to be written off (red tag), or inspected more accurately (yellow tag) or used straightaway (green tag).

In Italy, the AeDES approach (Baggio et al. 2009) is the national codified P-E assessment tool aimed at assessing usability of buildings after a seismic event and identifying prompt interventions, if required. This approach was applied, for the first time, in the region Umbria-Marche in 1997 and standardised in Italy by both the Italian National Civil Protection and the National Seismic Survey (SSN) in 2002 (Goretti A., Di Pasquale G., 2002). In the following years several versions of AeDES have been developed and the last revision, approved in 2006 (D.P.C.M. 23 February 2006, G.U.

7.3.2006, n. 55) was used for the post-earthquake assessment of L'Aquila in 2009 (O.P.C.M n. 3753, Gazzetta Ufficiale, 7th April 2009, n. 81. (2)).

AeDES consists of an inspection form, developed to assess masonry buildings. The form is filled on site by using expert judgements. The form allows collecting general information related to year of construction, plan, elevation, type of horizontal (floors/roof) and vertical (walls) elements. In the form, specific sections are included to describe the damage type and the damage severity observed on site. The damage is recorded by indicating the type of element such as roof, walls, stairs and etc., that is damaged. The type of damage observed on site that refers to i.e. loss of parapets and cornice, detachments of stucco, collapse of chimney, is recorded with the scope at identifying the most suitable prompt intervention to prevent further damage or building losses.

In the form, there is no reference to the type of failure modes occurring on the inspected buildings, therefore the prompt intervention and the judgements on the usability of the inspected buildings are provided by only taking into account which element is damaged, and which level of damage severity is observed.

The severity of the observed damage in AeDES inspection form is recorded by referring to the EMS' 98 (Grunthal, 1998), the most common damage scales adopted for classifying the damage of masonry buildings (Figure 3-1a).

According to the EMS-98 scale, 5 degrees of damage are considered:

- Degree 1: Negligible to slight damage (no structural and slight non-structural damage).
- Degree 2: Moderate damage (slight structural and moderate non-structural damage).
- Degree 3: Substantial to heavy damage (moderate structural and heavy non-structural damage).
- Degree 4: Very heavy damage (heavy structural and very heavy non-structural damage).
- Degree 5: Destruction (very heavy structural damage).

The EMS-98 is also proposed to classify buildings according to a Vulnerability Table reproduced in Figure 3-1b where for each building type, a circle shows the most likely vulnerability class(es), and also the probable range (indicated as a dashed line where this is uncertain). The position within the range of a specific building type has to be found by taking into account factors related to the state of disrepair, quality of construction, irregularity of building shape, level of the earthquake resistant design and so on.

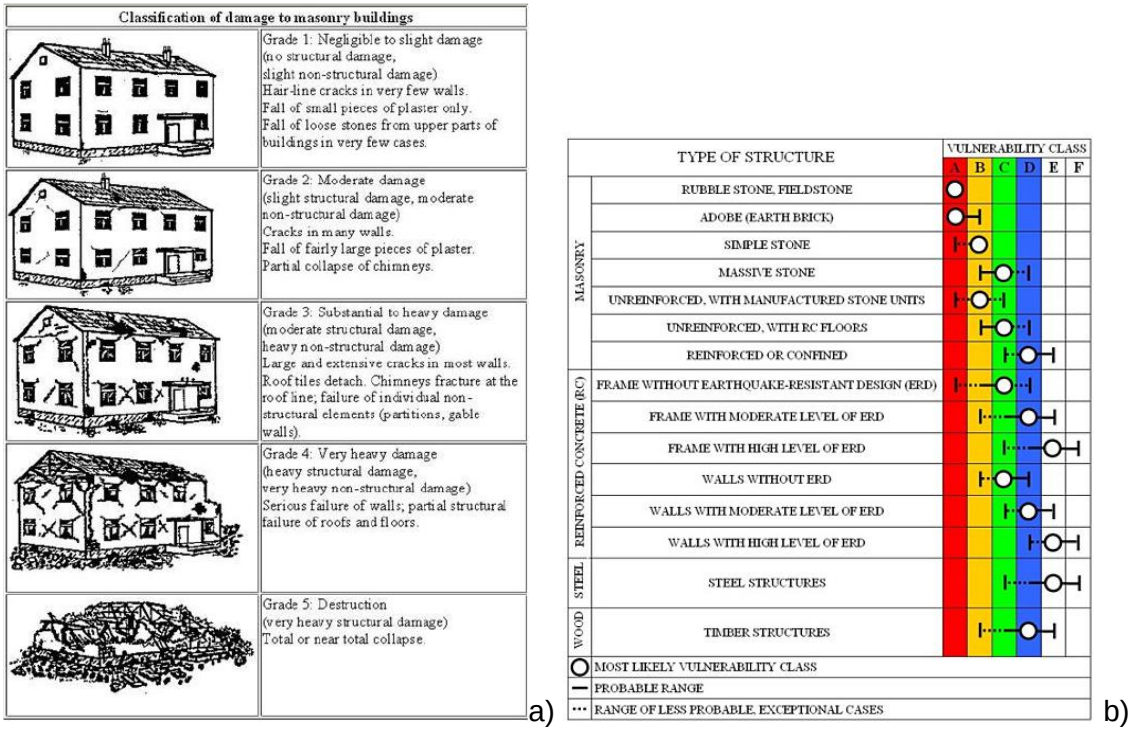

Figure 3-1: European Macroseismic Scale (1998) (EMS'98) a) Damage scales and b) Vulnerability Table (Grunthal, 1998)

In the next section, in order to investigate the capacity to assess the seismic performance of the existing approaches based on visual inspection, Tier 1 method of ASCE 41-13 (2013) is applied to assess three Nepalese houses, damaged by Gorkha earthquake on 2015. The approach is applied in order to identify the seismic deficiencies that have caused the damage observed on site. Since Tier 1 method does not allow recording the damage levels, the damage severity observed on site is described and classified by using the EMS'98 scale (Grunthal, 1998).

This test on the Nepalese houses is presented to validate if the deficiencies and damage severity identified with the selected visual inspection approaches are sufficient data to identify the failure modes observed on site by expert judgement, or whether further or different data is required to achieve this aim.

3.3 Application of Tier 1 approach (ASCI 41-13) and EMS'98 scale for the identification of the failure modes of masonry buildings

The Mw 7.8, Gorkha earthquake of 25th April 2015 resulted in the deaths of more than 7,500 people and caused widespread damage to buildings and infrastructure. The earthquake is particularly notable for the suffering that it caused to remote mountain communities due to, landslides and rock-fall. The earthquake also caused significant damage to unreinforced masonry buildings, and historic structures and temples.

In Figure 3-2, three typical Nepalese buildings are reported, as these were assessed after the Gorkha earthquake in June 2015 by the author during the Earthquake Engineering Field Investigation Team (EEFIT) mission (for more details on the mission refer to the following link: https://www.istructe.org/events/hq/2015/the-mw-7-8-gorkha-(nepal)-earthquake-of-25th-april).

The seismic capacity and defects of these three buildings are investigated by using the Tier 1 of the ASCE 41-13 (2013). Only structural deficiencies, identified by the structural Tier 1 checklists, reported in Appendix A, are discussed in this sections, while deficiencies on non-structural elements are out of scope of this application. Moreover, since the Tier 1 checklists do not allow classifying the damage severity and the vulnerability classes, these are introduced with reference to the European Macroseismic Scale EMS'98 (Grunthal, 1998).

The buildings are in fired brickworks with lime mortar. They belong to the class of unreinforced masonry constructions according to ASCE 41-13 (2013). Their floors are made of a single level of timber planks; therefore, they are classified as buildings with flexible diaphragms.

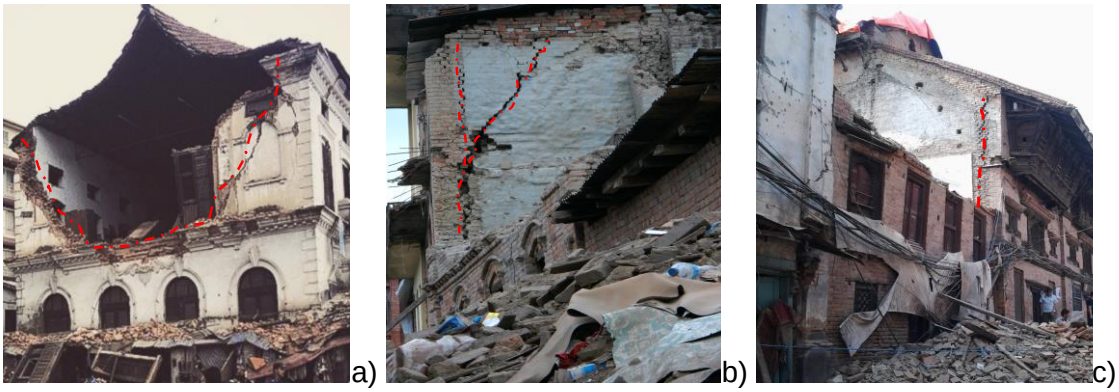

Figure 3-2: Identification of failure modes of the masonry constructions, surveyed in Nepal after the earthquake in 2015 by using visual inspections.

The Tier 1 inspection form includes specific checks on the diaphragms that require controls on the efficiency of wood lodgers, anchors, ties, beams, and girders. These are checked in order to verify if there are any deficiencies due to the lack of connection between diaphragms and walls. Some of these checks can be performed by visual inspections, while others require invasive investigations, in particular if there is no possibility to inspect roofs, where these structural elements are generally exposed. In the buildings in question, the checklists related to the diaphragms provide a verdict of no compliance, since no restrained elements are identified during the on site inspection.

Figure 3-3: Masonry buildings in bricks and mud mortar with timber floors, assessed in the city of Kathmandu in Nepal after the earthquake in 2015. a) The building is characterised by good quality of material and good connections between walls and between walls and floor. b) The building is characterised by poor quality of material and poor connections between walls and top floor

The Tier 1 inspection form also includes specific checklists related to wall anchorages, that are required to ascertain the presence of anchors or reinforcing dowels or straps to ensure the connections between walls. The buildings, in Figure 3-2a, Figure 3-2b, and Figure 3-2c do not comply with these checks, considering that strengthening devises are not identified.

These checklists on diaphragms and walls that assume unreinforced masonry buildings to have good connections if these are restrained by strengthening devices highlight a lack of confidence in this type of constructions and in particular in their construction materials.

This limited expectation from the unreinforced masonry constructions is confirmed, as discussed in the previous section, by the absence of checks on constructional materials in Tier 1 method that intrinsically excludes that an unreinforced masonry building is properly constructed and therefore seismic resistant.

The importance of qualifying the constructional materials is underlined by the houses in Figure 3-3 where the different type of mortar determines the different seismic response that is difficult to be forecasted by the data collected by Tier 1 method.

Buildings in Figure 3-2b and Figure 3-2c are also significant examples of constructions where the deficiencies related to the constructional materials are the causes of the observed failure modes triggered by the low capacity of binding in the mortar.

As introduced at the beginning of this section, by referring to EMS'98 (Grünthal, 1998) and Figure 3-1a, these buildings belong to the class of unreinforced masonry constructions with manufactured stone units. This class has a most likely vulnerability class in B with probable range between A and C. The damage severity refers to Figure 3-1b. The observed damage on the main façade of the building in Figure 3-2a is classified as D4, since the gable is completely collapsed. The damage observed on the rear façade of Figure 3-2b is classified as heavy damage therefore it is classified as D3, while the damage observed on the rear façade of Figure 3-2c is classified as very heavy damage and typified as D4.

Once data related to deficiencies, damage levels and related vulnerability classes is collected, it is required to understand how this data can be used to capture the building responses and if this data is sufficient for identifying their behaviour under seismic events.

By starting from the building in Figure 3-2a, the lack of restraining devices at the roof level underlines the possibility of overturning of the top level. However, only by observing the arch shape of the crack pattern on the top floor, it is possible to evaluate the consequence of the hammering effect of the purlins on the main façade.

Similarly, in Figure 3-2b only by the diagonal and vertical cracks along the edge of the side façade it is possible to deduct that the top corner of the façade is overturning due to a low friction capacity of the masonry observed on site.

The need of investigating the crack pattern to understand the building behaviour is underlined by the building in Figure 3-2c that, although it is characterised by weak mortar, and therefore it has the same deficiency identified for the building in Figure 3-2b, has a completely different damage. In Figure 3-2c the building has a vertical crack along the side façade that clearly points out an overturning of the main façade. Moreover, the arch crack pattern on the rear façade also points out an overturning in the gable, similarly to the one observed in Figure 3-2a, caused by lack of connection between the roof and the façade.

The highest damage levels assigned to the cracks are adopted to identify the severity of the identified failure modes. Generally, the severity of a failure mode corresponds, as it is for these buildings in Figure 3-2, to the worst damage levels observed on the buildings.

These examples answer to the question on how building performance should be investigated with visual inspection by underlining that deficiencies, damage levels and crack pattern are needed to understand the response of buildings.

This is because the identified deficiencies include or exclude the possibility of occurrence of some specific failure modes, while crack pattern together with damage levels are essential to capture the extent of the building’s failure, modality of failures and related severity.

However, it is not always straightforward interpreting the observed damage by using only information related to deficiencies and damage severity, in particular if buildings have several deficiencies and their crack patterns point out occurrence of different failure modes that can be identified only through the direct observation and expert judgements.

In order to overcome this, the knowledge based system LOG-IDEAH has been developed by the author as a knowledge based tool to predict failure modes through the interpretation of damage observed on site during post-earthquake surveys, by using a set of codified rules, capturing the reasoning which underlies expert judgement, on which failure diagnostic of masonry buildings is based. An explicit treatment of the uncertainties that accompany each stage of the diagnostic process, ensures the robustness of the outcome.

The development of LOG-IDEAH as a web platform, based on Answer Set Programming (Gelfond and Lifschitz 1988; Gelfond and Lifschitz 1991), is discussed in Chapter 5 of this dissertation. This tool allows recording damage location, damage types and damage severity at the level of the structural elements (local level), and determining the failure modes at the level of the buildings (at global level) by correlating position and extent of the observed cracks with crack patterns expected for the typical failure modes for masonry buildings.

However, although LOG-IDEAH is proposed to overcome the lack of an approach for the estimation of the failure modes by using visual inspection of crack patterns, its limitation lies in characterising buildings only for their geometry in plan and elevation, presence of constraints and seismic damage. This implies that LOG-IDEAH excludes the possibility of occurrence for some failure modes, since deficiencies related to types of materials, or types of floor and roof, or pre-existing damage cannot be always inspected during a post-earthquake survey due to reasons of safety.

In order to overcome this lack, in this research, LOG-IDEAH is proposed to assess the failure modes through visual inspection and interpretation of seismic damage, and FaMIVE to assess the failure mods by taking into account mechanical properties and structural deficiencies.

The joint use of both methods is presented in a hybrid approach relying on real condition assessment, well-established modelling procedures, flexible enough to include local traditional construction details and strengthening.

This hybrid approach is included in a methodology for the vulnerability assessment of historic city centres, based on the hypothesis that the joint use of FaMIVE and LOG-IDEAH provides results in terms of failure modes from the single method that can be jointed for better understanding the building performance.

This is further discussed in the next section.

3.4 Proposed methodology for the vulnerability assessment at territorial scale of masonry buildings

The methodology proposed in this section is based on numerous on site observations carried out by the author on residential buildings with regular/irregular plan and elevation, with or without courtyard made as unreinforced masonry constructions. Most of the observed buildings are located in Europe, Middle East, Africa and South America, and severe earthquakes damaged them.

The proposed methodology is based on a hybrid approach consisting of two methods: FaMIVE and LOG-IDEAH, which investigate, respectively, the causes of the failure modes through an analytical approach and effects of the failure modes through a visual inspection tool. The causes of a failure mode, represented by structural and mechanical properties of buildings, can be identified before a seismic event occur, while the effects of a failure mode, represented by the seismic damage on buildings can only be seen after an earthquake. This implies that since this hybrid approach seeks to cross validate both procedures and to provide a better estimation of the failure modes than the ones derived from the single method, this methodology can only be applied as a post-earthquake assessment approach.

Since the common output of both methods are the failure modes, these are used for validation by comparing those with failure modes observed on site and provided by experts who are capable with their knowledge and experience to capture causes and effects of the earthquake on buildings.

The flowchart in Figure 3-4 outlines this methodology consisting of the fundamental steps of both methods from data collection to analysis, and from processing of the results to their validation and integration.

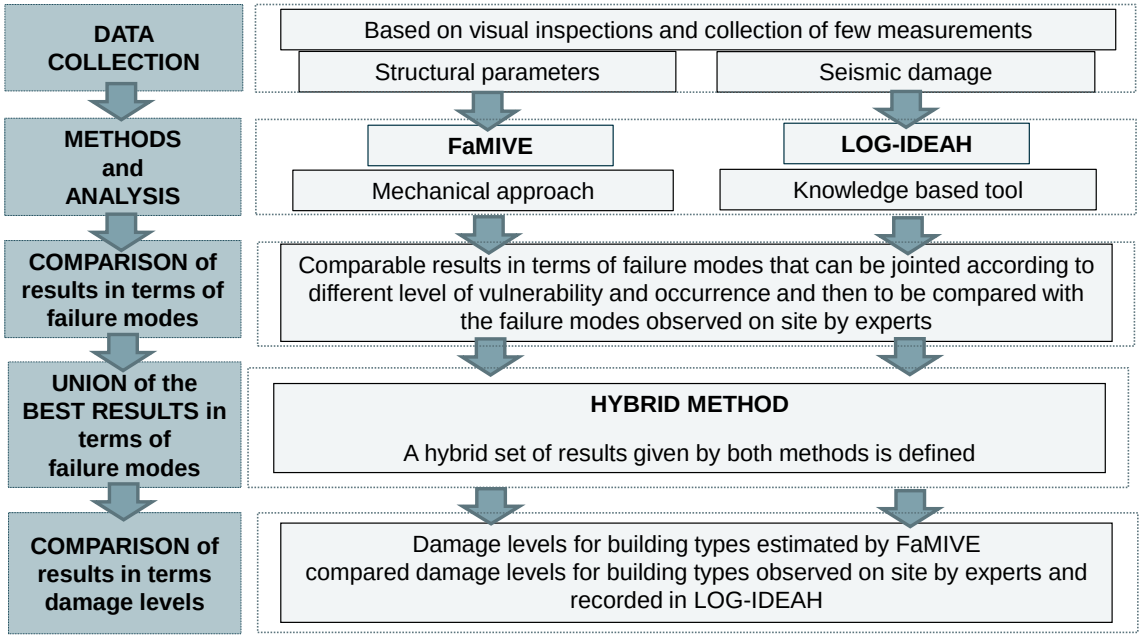

Figure 3-4: Proposed methodology for the seismic vulnerability assessment of historic centres

The steps are listed and illustrated as follows:

- **Preliminary assessment, selection of the urban blocks, data collection and building classifications**

The area of study is first assessed by rapid investigations to identify the constructions that are most representative of the urban context and the parameters that most affect the seismic vulnerability observed on site.

Once the typical and recurrent construction details have been identified, more detailed inspections are carried out on chosen urban blocks where there is a high concentration of such typical constructions to best characterise the sample.

This implies that data collection is confined to a selected number of urban blocks, whereby meeting the first objective of this methodology, i.e. developing an approach to assess the seismic vulnerability for the typical building classes of the area of study.

The inspections of the selected urban blocks are performed systematically by quick surveys to record the input data needed for both FaMIVE and LOG-IDEAH through an inspection form and a website tool, respectively. Input data with reference to the geometry and structural features are collected for FaMIVE, while data related to the seismic damage is compiled for LOG-IDEAH.

The data collected to characterise the building performance by FaMIVE and LOG-IDEAH focuses on identifying on one hand, the causes and on the other hand, the effects of seismic events on historic buildings. Details on the data protocols adopted by FaMIVE and LOG-IDEAH are discussed in chapter 4 and 5, respectively.

During the preliminary assessment carried out on site for the data collection, experts who had participated to the data collection can also record data in terms of failure modes identified by using their own expert judgements, knowledge and expertise.

The observed failure modes are only recorded with the scope at validating the proposed hybrid approach proposed in this methodology, therefore data in terms of observed failure modes is independent of the data used as in put in LOG-IDEAH or in FaMIVE to predict the possible failure modes on the inspected buildings.

- **Analyses of the input data by using FaMIVE and LOG-IDEAH and discussion of the output**

The analysis of the data collected on site is performed by using the analytical method FaMIVE (D'Ayala and Speranza 2003, D'Ayala 2005) and the visual inspection method LOG-IDEAH (Novelli and D'Ayala 2015). Both methods of analyses and related output in terms of failure modes and damage levels are described in detail in chapter 4 and chapter 5 respectively.

- **Validation of the output of FaMIVE, LOG-IDEAH and the Hybrid method**

FaMIVE and LOG-IDEAH provide results in terms of failure modes and damage severity.

FaMIVE estimates failure modes at the level of each inspected façade that has been surveyed on site and classified according to geometric and structural features. LOG-IDEAH provides failure modes at the level of the inspected building by taking into account the crack patterns on the inspected façades and assuming the crack pattern on the uneven façades.

The validation is carried out:

- on inspected façade. By comparing results from FaMIVE and LOG-IDEAH with the failure modes observed on site, provided from experts;
- on not inspected façades. By comparing results from LOG-IDEAH (capable to estimate failure modes on unware facades by taking into account the data on the inspected facades, for more detalts refer to chapter 5) with the failure modes observed on site, provided from experts, who are also capable to estimate failure modes on façades that have been not invastigated, as discussed by the example in section 3.3.

The cross validation and the union of results is carried out, by using two measures; Precision and Recall, defined with reference to the confusion matrix (Maimon et al, 2015, Abhari et al., 2011, Han et al., 2012) designated for the P (positive) and N (negative) outcomes, as indicated in Table 3-1 where:

- **True Positive (TP):** estimated failure modes correctly identified,
- **True Negative (TN):** NOT estimated failure modes correctly identified,
- **False Positive (FP):** estimated failure modes NOT correctly identified,
- **False Negative (FN)**: NOT estimated failure modes NOT correctly identified.

Table 3-1: Confusion matrix

	Observed	Not Observed
Estimated	True Positive (TP)	False positive (FP)
Not estimated	False Negative (FN)	True Negative (TN)

The Precision is defined as the proportion of predicted positives, which are actual (true) positive while the Recall is the proportion of actual (true) positives, which are predicted positive. Their definitions are given as follow:

$$Precision = \frac{TP}{TP + FP};\ \ Recall = \frac{TP}{TP + FN}$$

These measures are calculated on the results obtained from the individual methods, according to the level of occurrence of the identified failure modes.

To provide a single measure for comparing the capacity of FaMIVE and LOG-IDEAH to predict the failure modes observed on site, the F-1 score, which combines Precision and Recall scores in one formula, is introduced as follow:

$$F_1 = 2\frac{Precision * Recall}{Precision + Recall}$$

The same validation approach is also adopted to assess the performance of the proposed hybrid method obtained by joining the failure modes predicted by FaMIVE and LOG-IDEAH.

In order to assess the power of the proposed methods to identify the correct failure modes the results of FaMIVE, LOG-IDEAH and hybrid method are also compared against two random methods. The random methods aim at casually associating one or

more possible failure modes to an inspected façade. The first method assigns, to all possible failure modes, the same probability of being associated to a façade, while the second assigns, to all possible failure modes, a probability of being associated to a façade that depends on the occurrence of each failure mode in the buildings' sample observed on site.

Each random method generates 10000 predictions. The capacity of prediction of the random methods is estimated by computing Recall, Prediction and F1-Score measures the performances of the random methods are compared with the ones calculated for FaMIVE, LOG-IDEAH and the hybrid method in order to confirm that the methods proposed by the author have a much better capacity of prediction than the random approaches.

The validation is also carried out by comparing damage levels estimated by FaMIVE with the ones recorded in LOG-IDEAH.

According to the chapter 4, in FaMIVE the damage levels are estimated and expressed as damage probability while in LOG-IDEAH, as reported in chapter 5, the recorded damage levels coincide with the ones observed on site by experts.

The damage levels are estimated for building classes defined in relation to criteria specifically selected for the area of study.

The building classification that best predicts the failure modes observed on site, determines the classification that should be used to estimate the damage levels and performance of buildings in historic city centres.

3.5 Final remarks

In this chapter, the methodology based on the joint application of the methods FaMIVE and LOG-IDEAH is proposed to overcome the shortcomings of the existing methods for the vulnerability assessment at territorial scale.

In particular, FaMIVE is proposed to estimate the seismic vulnerability of historic masonry buildings with an analytical method using a mechanism based approach.

FaMIVE, resulted as the most suitable method for the problem at hands from the review conducted in Chapter 2.

For LOG-IDEAH, this is introduced in details in chapter 5, to provide a tool capable to estimate the vulnerability by visual inspection, in order to overcome a lack of an approach for the evaluation of the seismic performance of buildings by investigating damage observed on site.

The data collection and analyses of both methods are described in chapter 4 and 5 respectively, while in the methodology a robust approach is provided to validate the capacity of prediction of FaMIVE, and LOG-IDEAH and the capacity of prediction of the union of both methods.

The validation of the proposed methods consists in using statistical parameters and random methods introduced to assess the capacity of the methods and identify the criteria required to select the results from FaMIVE, and LOG-IDEAH that best predict the observations.

The validation is performed by comparing the estimated failure modes and damage levels with the observed failure modes and damage levels for the inspected façades.

In the next two chapters, FaMIVE and LOG-IDEAH are explained in details, and in chapter 6 the entire methodology is applied and discussed.

4 FaMIVE: ANALYTICAL APPROACH TO ESTIMATE FAILURE MODES AND TO ASSESS SEISMIC VULNERABILITY OF BUILDINGS IN HISTORIC CITY CENTRES

4.1 Introduction

In this chapter, the analytical method for the assessment of the seismic vulnerability of historic city centres adopted in the hybrid approach presented in chapter 3 is presented and its application outlined.

From the literature review conducted in Chapter 2, FaMIVE emerged as the suitable approach to include in the proposed methodology of chapter 3, given its reliability proven by previous applications and its flexibility to be adapted for the analysis of different building classes.

In this chapter, FaMIVE is presented in a new version in a framework of Figure 4-1 in five steps, defined to present the numerical models adopted in FaMIVE for the estimation of the failure modes and damage probability level of historic city centres.

The five steps are briefly introduced here, while specific sections are devoted to them for presenting their details later in the chapter.

- **STEP 1. On site inspection of the area of study**

  The first step consists of assessing the historic city centre through visual investigations that are carried out to identify the most representative building classes in the urban context under scrutiny. Building classes are defined according to the features presented in section 4.2.1 that most affect the seismic response of a building. Buildings can also be classified according to their

typical failure modes, if the area of study has been hit by a seismic event and damage can be observed, as described in section 4.2.2.

Once building classes are identified, data, used as input for FaMIVE, is only collected in urban blocks where the concentration of the identified building classes is higher. The data collection is designed to be carried out from the street with minimum need for entering the buildings (Speranza and D'ayala 2003). Pictures are used to add and verify the data recorded by using inspection forms connected to an electronic database purposely developed.

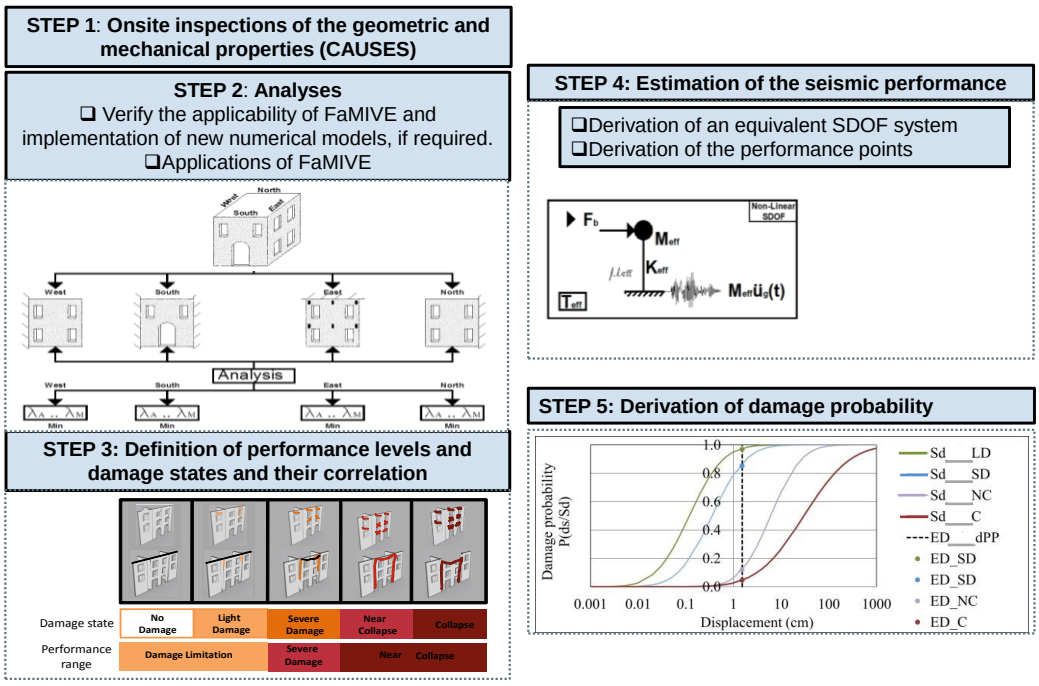

Figure 4-1: **Rationale for the analytical vulnerabiliy assessment by using FaMIVE**

Given the high variability of vernacular and historic constructions through the seismic prone regions of Europe and beyond, the computational procedure, and hence the inspection form, might need to be modified to include specific construction details that might enhance or reduce the vulnerability of a specific building class. The Excel + Visual Basic platform, on which FaMIVE is

developed allows with ease such modifications, without altering the overall structure of the algorithms and underpinned FaMIVE.

- **STEP 2. Methods of Analysis**

The second step, discussed in details in section 4.2.2, focuses on describing the approach adopted by FaMIVE to process the input data. This approach consists in mechanical models that simulate the performance of buildings by taking into account their typical geometric and mechanical parameters observed on site.

The scope of these analyses is to compute the load factor multiplier that identifies the failure modes to which the inspected building is most vulnerable.

If in the first step during on site inspections of historic city centres, it is observed that the seismic response of buildings is affected by parameters that are not taken into account in the current version of FaMIVE, one or more new mechanical models might be needed and integrated in FaMIVE to simulate the failure modes observed on site.

This is exemplified in section 4.3.2 where the formulation of a new mechanical model is presented and a new data collection protocol sets out, in order to provide a version of FaMIVE capable to assess the seismic vulnerability of masonry façades with irregular openings. The applicability and relevance of this new formulation is tested in section 4.4 by means of parametric analysis.

- **STEP 3. Correlation of building's performance levels and damage states.**

In this step, presented in section 4.5, seismic performance levels for historic masonry constructions are defined. The performance levels are introduced by extending the definitions included in EC8 (CEN, 2005) with reference to the observed masonry-building performance in historic city centre, the typical

damage and the level of intervention required to restore the pre-earthquake condition in a building.

This step also consists in defining the damage levels adopted in this approach, that are introduced by extending the current definitions included in EMS'98 (Grünthal, 1998) with the definition of the damage associated to the expected types of failure modes to which historic masonry buildings are most vulnerable.

Finally, a correlation between performance levels and damage states is proposed by referring to on site experience of the author.

- **STEP 4. Estimation of the seismic performance**

This step described in section 4.6 consists in the following:

- Derivation of capacity curve of equivalent non-linear SDOF systems. In order to describe the evolution of the building performance under seismic events from an initial state, when the building is not damaged, up to a final state when the building is collapsed, idealised capacity curves are derived.

  Capacity curves are defined for equivalent non-linear SDOF systems directly defined using the load factor multiplier. The numerical expressions adopted to derive the idealised capacity curves (D'Ayala, 2013) are re-proposed in details in section 4.6.1.

- Estimation of the non-linear demand and derivation of the performance points.

  The performance points are computed by following the N2 method (Fajfar, 2000) through the intersection between the capacity curves for an equivalent non-linear SDOF system and the nonlinear spectrum, as discussed in section 4.6.2.

  Once the performance point is identified on the capacity curves, the damage state and performance level of the building class is automatically derived according to the correlation defined in section 4.5

➢ **STEP 5. Derivation of fragility functions and probability of damage**

In this last step, fragility curves are derived for the building classes identified in the area of study as the lognormal distribution of the median and standard deviation of the damage thresholds (as discussed in details in D'Ayala, 2013 and GEM guidelines for the analytical vulnerability assessment (D'Ayala et al. 2014).

The probability of damage for building classes is calculated by intersecting performance point and fragility curves. An iterative procedure for the estimation of the damage probability is developed and integrated to the existing FaMIVE method. The development of this iterative procedure is presented and discussed in section 4.7.

The author's contribution on this approach focuses on the development of the following steps:

- Step 2, by developing specific mechanical models to take into account the typical failure modes that can occur in buildings characterised by irregular opening layout
- Step 3, by defining specific performance ranges and damage levels for hitoric constructions and setting their correlations and
- Step 5, by developing the iterative procedure for the estimation of the performance points of masonry constructions.

4.2 STEP 1: On site inspections

As discussed in the previous sections, historic buildings, in particular if these are characterised by irregularity in plan and elevations due to alterations carried out over the time, need to be inspected on site, since their typical features and parameters that have the highest effect on building performance under seismic events can be identified only by direct observation.

Currently, the Italian National Building Code (Normativa Tecnica delle Costruzioni,: NTC 2008) also underlines the need to assess existing historic buildings by visual inspections, although there is not a clear description of the approach that should be adopted for this scope.

International documentations such as (Charter A., 1931, Charter V., 1964; ICOMOS ISCARSAH Recommendations, 2005) have introduced specific recommendations for the evaluation of the seismic performance of historic and monumental buildings. These recommendations introduce approaches for the assessment of the seismic vulnerability and approaches for the evaluation of the retrofitting interventions proposed to preserve not only the structural functions of historic buildings but also their architectural features from future earthquakes in agreement with the building conservation philosophy.

The remarks reported in the next sub-sections are observations on typical geometric features and typical failure modes derived from past seismic inspections carried out by the author in Emilia Region and L' Aquila (Italy), Algiers (Algeria), Lima, Ica and Cusco (Peru'), Ljubljana and Bovec (Slovenia) and Kathmandu (Nepal).

4.2.1 *Typical structural features observed on site in historic buildings*

The Italian standard and seismic classification for the national territory OPCM 3274 (2003), modified in OPCM 3431 (2005) defines as historic urban centres agglomerates of buildings forming one or more building clusters defined as blocks of heterogeneous constructions connected with each other by structural links that interact with dynamic actions.

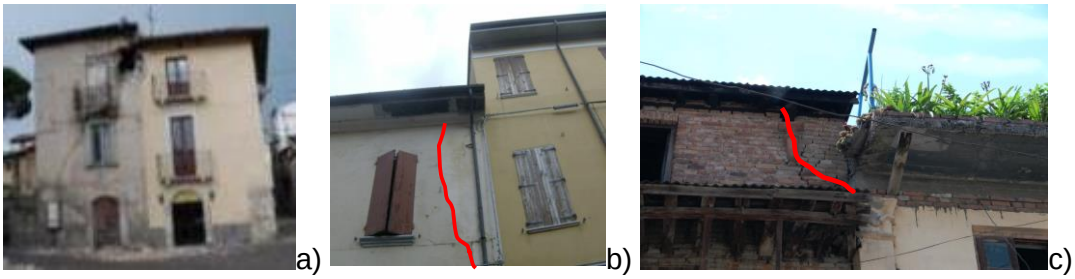

Figure 4-2: Pounding damage. Examples of buildings in the historic centre of a) L'Aquila in Italy b) Emilia in Italy and c) Kathmandu in Nepal

This definition highlights that in an historic centre it might be possible that buildings in the same urban setting are characterised by different geometry and mechanical features. This is particularly evident in historic urban clusters of buildings built in different periods and with different constructional techniques that are not always suitable in seismic prone areas.

Buildings in cluster properly constructed and seismically adequate are considered the ones that share party walls that are properly connected with floors by anchors, ring beams, lodger and trusses, adopted to prevent overturning of the façades and collapse of horizontal structures. However, buildings in adjacency, in particular if these have horizontal floors at different heights and different overall height, might not be properly connected, and, as shown in Figure 4-2 hammering between buildings of different height and stiffness can result in damage at the interface. This underlines the need of taking into account the interactions between buildings, by considering and storing information related to their relative position and height in the urban block.

The seismic performance of single buildings in a cluster is also strongly affected by irregularities in their geometric plan and vertical elevations. These irregularities, commonly observed on site, are mainly a consequence of alterations, made to adapt existing buildings to new uses, or to new householders' needs. Such alterations usually consist in adding new appendix or new storeys to the existing buildings.


a)

b)

Figure 4-3: Additional floors. a) The original building is an unreinforced masonry construction, while the last floor is unlikely to be of the same class of the original building, due to the presence of the column connected to the roof. b) The opening layout, materials, and height between the additional floor and the original building are differnt. Examples of buildings in the historic centre of L'Aquila. Earthquake 2009

The materials used to construct these alterations may be different from the original construction material (Figure 4-3). Most common materials used in recent times to modify or extend walls made of bricks or stones are hollow brick masonry or concrete blocks, while reinforced concrete slabs are used to construct new floors or to substitute original floors in timber or masonry vaults. These reinforced concrete slabs have typically greater in-plane stiffness than the original timber floor.

Buildings with irregular opening layouts (see Figure 4-4) also require a particular attention, as their performance is strongly affected by the uneven distribution of the stiffness resulting from the uneven distribution of openings that might create weak storeys or weakness in a single pier or a single spandrel.

In the existing codes such as NTC (2008), and EC8 (CEN 2005) state that masonry buildings can be assessed by neglecting any types of irregularity related to their opening layout.

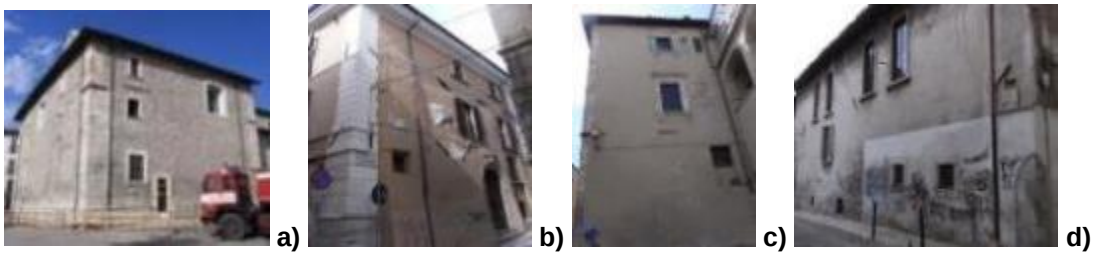

Figure 4-4: Irregular openings. Examples of buildings in the historic centre of L'Aquila. Earthquake 2009

Although existing codes stress to simplify the numerical models for the evaluation of the performance of masonry buildings, on the other hand past experimental tests (Paquette and Bruneau 2003; Yi et al., 2006; Bothara et al., 2010) have demonstrated that irregularities in the opening layout increase the seismic vulnerability in buildings as they generate a concentration of damage that leads to global failure of buildings.

This concerns about the irregularity in the masonry constructions has brought different researchers to focus on the development of procedures, such as the RAN Method by Parisi and Augenti (2013), the SAM method (Magenes and Calvi, 1996), or TREMURI (Lagomarsino et al., 2013), to analyse the effect of the openings on the capacity of masonry buildings.

In the next section, the typical seismic performance of historic buildings is described by taking into account their geometric and structural features and how their irregularity in plan and in elevation affects their seismic response.

4.2.2 *Typical failure modes of historic buildings observed on site*

In the next subsections, the typical failure modes that can be observed on historic buildings damaged by seismic events are classified according the following three classes:

1. Out-of-plane failure modes (OOP)
2. In-plane failure modes (IP)
3. Combined failure modes (COMB)

These three classes are described and shown through examples of buildings assessed on site in Europe, Africa and South Asia. The causes of these failure modes and their typical crack patterns are illustrated and discussed in relation to the typical structural and geometrical deficiencies observed on site.

The failure modes discussed in the following subsections are regrouped as OOP, IP, and COMB and are resumed in Appendix B.

Before illustrating the differences of the classes mentioned above, it is important to mention that these failure modes represent kinematics that describe a "*global*" behaviour of buildings and involve the collapse of at least one entire floor of a facade. This is particularly pointed out in the following subsections, since all typical failure modes identified for masonry buildings are only detected on facades, where most of the capacity of a building is concentrated. This underlines the need of clarifying that crack on a single structural element (e.g. pier, spandrels, internal column, beam) is only representative of a "*local*" damage, that affect the building performance but not necessarily trigger a global failure mode.

4.2.2.1 Out-of-plane failure modes (OOP)

Direct observations of seismic damage underline that most of the masonry constructions fail for overturning of their façades (D'Ayala, 1999), (D'Ayala, 2003), (Karantoni and Bouckovalas, 1997), (Tomazevic, 1999), (Carocci, 2001), (Borri and Castori 2004). This failure mode is caused by lack of connections between walls (Giuffre', 1993a, b).

The typical crack pattern for this type of failure mode is generally characterised by vertical cracks along the edges of an entire or part of a façade, and underlines a complete disconnections between façades, as it is illustrated in Figure 4-5a. The OOP failure mode is associated not only to complete overturning of façades, but also to the overturning of a portion of a façade.

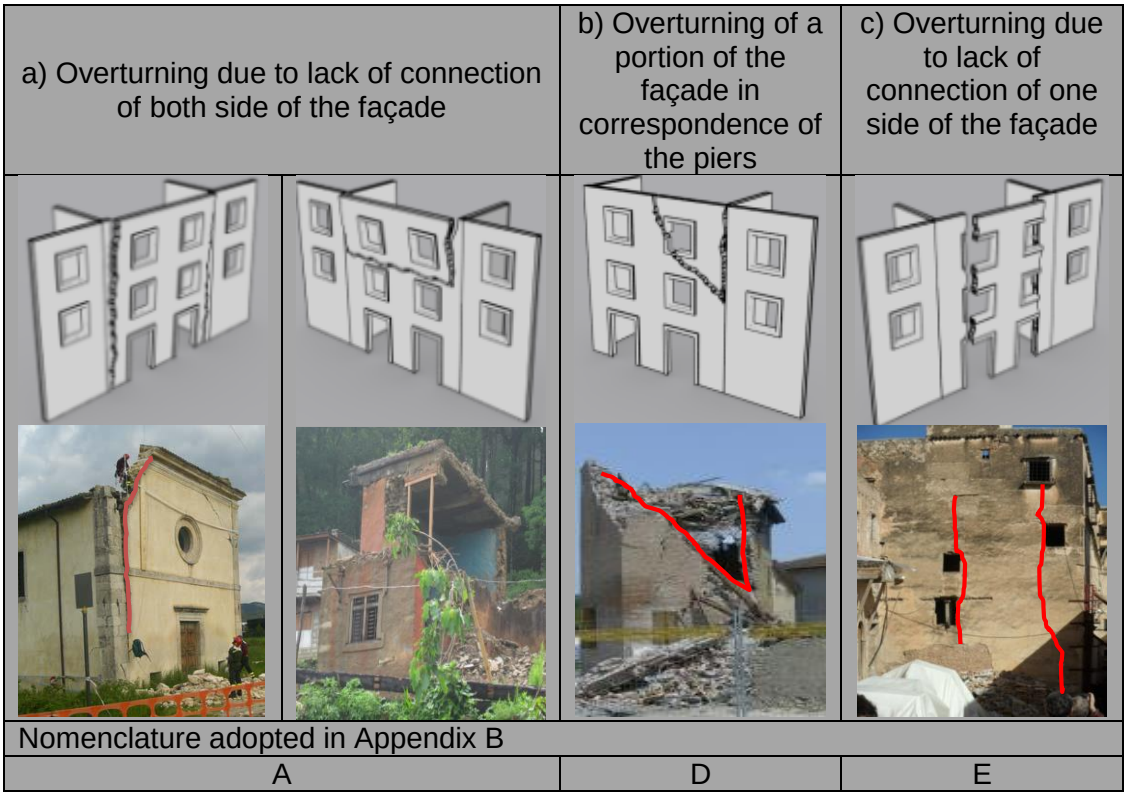

Figure 4-5: Out-of-plane of a single façade .Examples of buildings in the historic centre of a) L'Aquila in Itlay on the left and Gorka in Nepal on the right , b) Gorka in Nepal and c) Algiers in Algeria

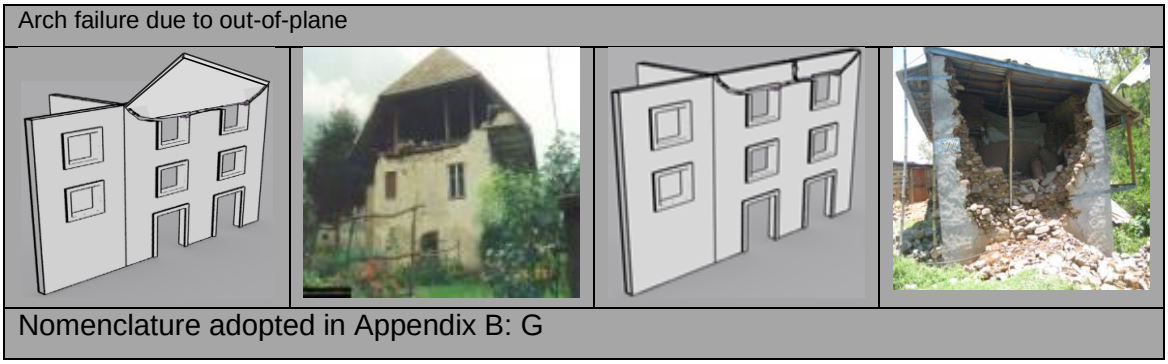

Figure 4-6: Overturning of the upper horizontal spandrel. Examples of buildings in the historic centre of Bovec in Slovenia (left), and Gorka in Nepal (right)

Figure 4-5b shows the typical OOP of a portion of a façade, highlighted by a diagonal and vertical crack. The top corner of the façade is failing in overturning due to its lack of connection with its adjacent façade.

Another failure mode, also classified as an OOP, is the one that occurs within the same façade where a strip, underlined by vertical cracks along piers, see in Figure 4-5c, overturns under seismic events. This type of failure modes has a high probability of occurrence in buildings characterised by regular opening layout.

Figure 4-6 is also another example of failure modes classified as OOP. This failure mode is introduced to represent the overturning of a gable or arch failure mode, not properly anchored to the roof. The arch crack pattern that characterised this type of failure mode is caused by the hammering of the roof on the façade located in the transverse roof span direction.

4.2.2.2 In-plane failure modes (IP)

This failure mode occurs in buildings characterised by strong connections among façades and floors able to transmit the horizontal forces to shear walls. These buildings generally have a “box” behaviour under seismic events, in particular if they are characterised by rigid floors.

In-plane failure modes are classified as 1) local failure modes when the cracks (with diagonal or X shape) are localised only on a few structural elements (piers and

spandrels) or 2) as global failure modes when the cracks cause the failure of a whole façade or the failure of at least one entire floor.

If the in-plane failure mode is caused by flexure, the seismic action generates rocking in the pier, and the damage is characterised by horizontal tensile flexural cracks at the bottom of the structural element (Figure 4-1a).

On the other hand, the seismic action causes crushing of the pier and the crack pattern is widespread and characterised by vertical cracks oriented towards the compressed corners of the piers, see Figure 4-1a.

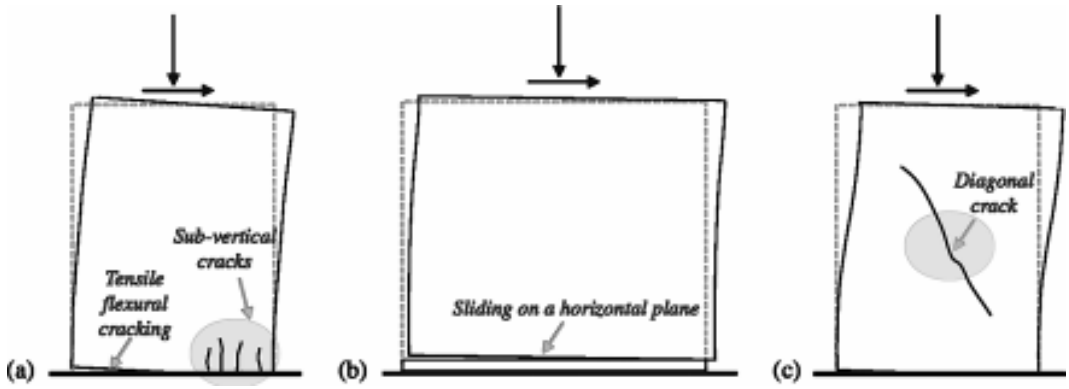

Figure 4-7: Typical failure modes of masonry piers due to horizontal loads: (a) rocking, (b) sliding shear failure, and (c) diagonal cracks (Calderini et al., 2009)

As for the local in-plane failure mode due to shear, this also involves two different classes of cracks. The first one (Figure 4-1b) is characterised by horizontal cracks, due to the sliding of a pier along its bed joint mortar located at the bottom corner, and the second one (Figure 4-1c) is characterised by diagonal cracks, which start from the centre and then go to the corner of the pier (Calderini et al., 2009).

This type of cracks pass through mortar joints and bricks (Calderini et al., 2009) and it is the most common local failure mode in masonry buildings with numerous windows and regular opening layout. These X or diagonal cracks on piers and spandrel, see Figure 4-8a and Figure 4-8b, although they might have a very damage level, do not necessary cause the failure mode in a building.

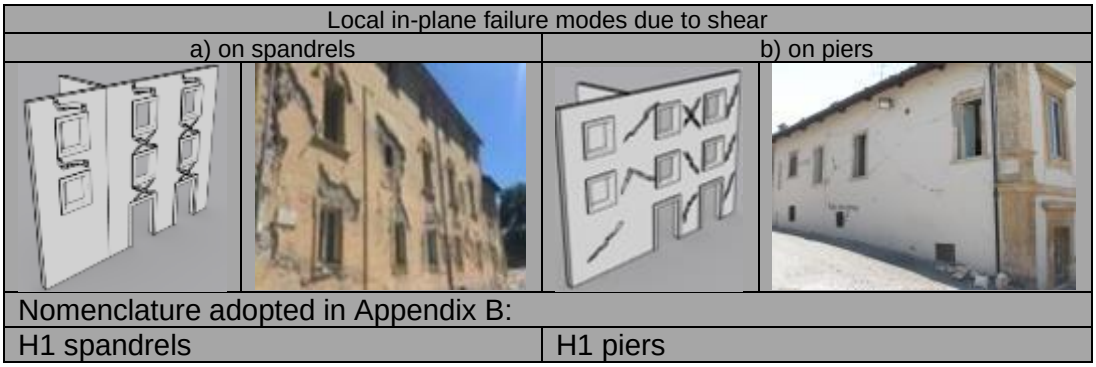

Figure 4-8: Local In-plane failure mode. Examples of buildings in the historic centre of Amatrice in Italy (left), and in the historic centre of L'Aquila in Italy (right)

Figure 4-9: Global In-plane failure mode. Examples of buildings in the historic centre of Gorka in Nepal (left) and Bovec in Slovenia (right)

As for the global in-plane failure modes, this is characterised by a full crack pattern that involves the entire façade, see Figure 4-9. This class of failure mainly occurs on masonry buildings with very slender façades or irregular opening layout that leads to uneven distribution of stiffness and shear capacity among piers and spandrels, therefore some structural elements might be more vulnerable than others might. Furthermore, piers might be failing in a combination of bending and shear, rather than just shear (Casapulla and D'Ayala, 2006).

The typical crack pattern for this class of in-plane failure is characterised by diagonal cracks that follow a specific pattern that creates a triangular macrolement completely unstable, leading to collapse (Casapulla and D'Ayala 2006, Parisi and Augenti 2013). This class of failure mainly occurs on buildings with irregular opening layout (see Figure 4-9).

4.2.2.3 Combined failure modes (COMB)

Combined failure modes represent the typical failure modes of buildings characterised by good connections between intersecting façades and poor connections between intersecting façades and floors. The occurrence of a COMB failure mode also depends on the opening layout the spanning direction of the horizontal structures, and the presence of internal load bearing walls.

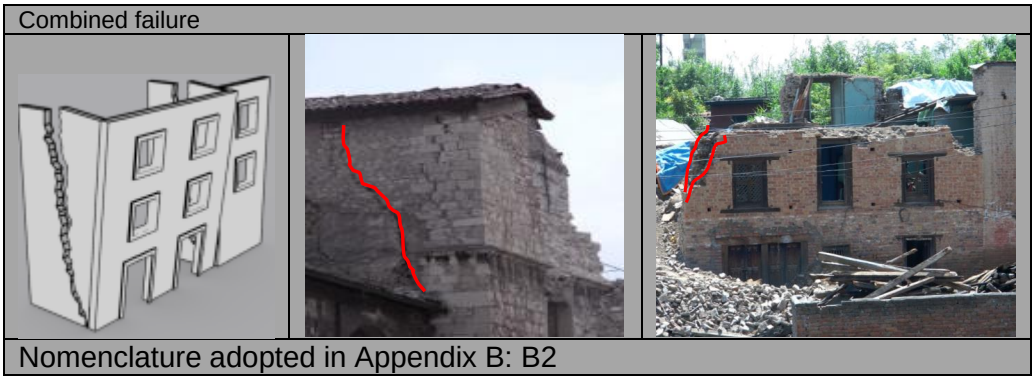

Figure 4-10: Combined failure modes due to good connections between adjecent façades and lack of connections between adjecent façades and walls. Examples of buildings in the historic centre of L'Aquila in Italy (left), Kathmandu in Nepal (right)

This failure mode is associated to a kinematic that involves the collapse of two or three intersecting façades. The typical crack patterns of these failure modes induce overturning of a façade, which is orthogonal to the span floor direction, and sliding of one or two portion of walls parallel to the span floor direction, as illustrated in Figure 4-10.

The overturning of the top corner of buildings of Figure 4-11 is also classified as a COMB failure mode. This specific failure mode is caused by a flexible floor that hits the façades by causing diagonal cracks that indicate an overturning of a portion of two adjacent walls.

If the connections between walls and floor are strengthened by ring beams or ties, the typical COMB failure modes that occur are illustrated in Figure 4-12.

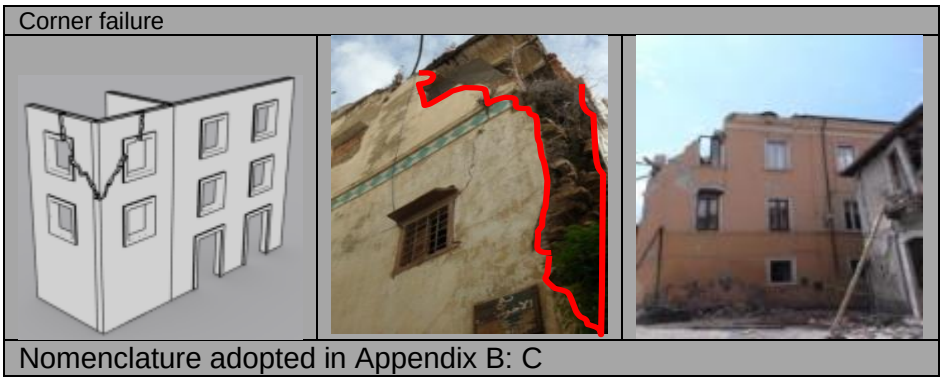

Figure 4-11: Corner failure due to flexible floors. Examples of buildings in the historic centre of Algiers in Algeria (left) and L'Aquila in Italy (right)

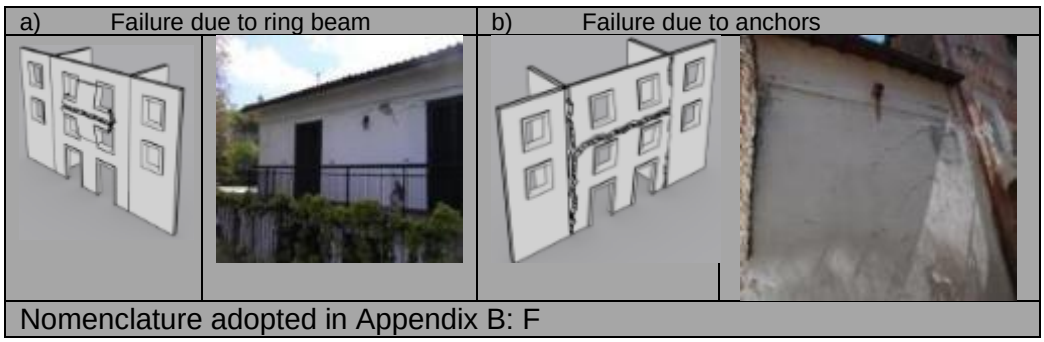

Figure 4-12: Combined failure modes due to strengtehned interventions. Examples of buildings in the historic centre of L'Aquila in Itay

4.3 STEP 2: Methods of analysis

FaMIVE estimates the seismic vulnerability of historic city centres by using mechanical models developed to simulate the seismic performance of historic buildings presented in this chapter through the description of their typical features, and failure modes as discussed in section 4.2.1 and 4.2.2 respectively.

These mechanical models are based on the assumption that buildings behave as an assemblage of macroelements held together by compressive forces, liable to crack as soon the tensile stresses begin to develop. In these models, the earthquake action is simulated as a horizontal static force, proportional to the masses.

In order to identify the failure modes that has the highest vulnerability level, the mechanical models of FaMIVE estimate the collapse load multipliers (λ), representing the maximum spectral acceleration of the site (with reference to the maximum pga experienced in the site), for all possible failure modes, described in section 4.2.2, and reported in a table in Appendix B.

Once λ are estimated, the Vulnerability Index that expresses the propensity of the façade of being damaged respect to all failure modes of Appendix B, is computed as $I_{Vuln}= (1/\lambda)\rho$, where ρ takes into account the damaging consequences of each failure modes defined in Appendix B and varies from 0 to 1 from the less to most damaging failure mode, as discussed in Speranza and D'Ayala, 2003.

Then, these I_{Vuln} are classified in four Vulnerability ranges, defined in Figure 4-1, as functions of $I_{Vuln,max}$, the I_{Vuln} with maximum value among the ones computed for the failure modes in Appendix B.

The failure mode with the highest vulnerability level is selected by multiplying each estimated $I_{Vuln(s)}$ for the Damage extent (De) that represents the percentage of mobilised façade and floor structure (defined as macroelemt Table 4-1) participating in each failure mode. The ranges of De defined in Table 4-1 corresponds to the Damage Levels that are defined in Figure 4-24.

Once these are calculated, the resultant values are binned into 4 classes of vulnerability: Minor, Moderate, Significant and Severe, as introduced in the matrix of Table 4-1. Ranked the failure modes, FaMIVE selects the failure modes with the most significant level of vulnerability as the ones with highest probability of occurrence.

In order to apply the FaMIVE to assess the vulnerability of historic city centres it is required to verify if the exiting numerical models in FAMIVE are adequate to take into account the parameters, which most affect the building performance observed on site.

As discussed in sections 4.2, historic masonry buildings are often characterised by strong irregularity in their construction materials, geometric plan and elevations and floor classes. In particular, irregularities in walls given by different number of

openings per floor or lack of their alignment in vertical and or horizontal direction are commonly observed in historic buildings.

Table 4-1: Vulnerability ranking estiamted by FaMIVE (D'Ayala and Speranza 2003)

Damage extent (De)	Vulnerability Range			
	$I_{Vuln,max}/6 < I_{Vuln} <= I_{Vuln,max}$	$I_{Vuln,max}/4 <= I_{Vuln} < I_{Vuln,max}/6$	$I_{Vuln,max}/2 <= I_{Vuln} < I_{Vuln,max}/4$	$0 = I_{Vuln} < I_{Vuln,max}/2$
De > 80% of the macroelement (from Near Collapse to Collapse)	**VERY HIGH**	**HIGH**	**MEDIUM**	**MEDIUM**
40% of the macroelement < De <=80% of the macroelement (from Severe to Near Collapse)	**VERY HIGH**	**HIGH**	**MEDIUM**	**LOW**
40% of macroelement <De<= No damage (from No Damage to Severe)	**HIGH**	**MEDIUM**	**LOW**	**LOW**

The current version of FaMIVE by D'Ayala and Speranza (2003) and by Casapulla and D'Ayala (2006) is developed to assess the vulnerability of regular constructions.

In section 4.3.1, a new version of FaMIVE is introduced able to handle the data necessary to represent the geometry of façades with irregular layout and to simulate their behaviour. A new electronic inspection form is a by-product needed to input and store the data. Section 4.3.2, presents the analytical working of the specific mechanism developed to deal with irregular opening layouts and implemented in this new version of FaMIVE.

4.3.1 *Input electronic form for irregular historic buildings*

The new electronic form for storing data for irregular constructions is presented in Figure 4-13 and an enlargement of it is reported in Appendix C Although data needed to describe the irregularity in a buildings are more detailed than the once for

regular constructions, the time required for the data collection are not changed significantly, as the new information required in the new version of FaMIVE can still be collected by observations only or by taking few measurements.

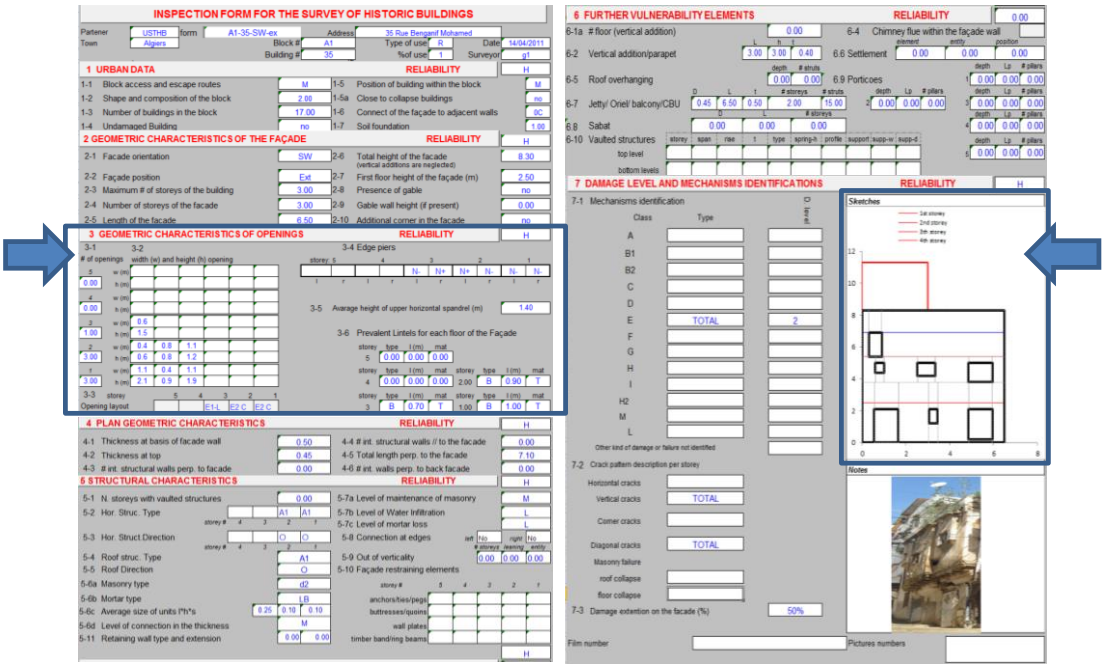

Figure 4-13: New Inspection form developed in the approach FaMIVE to collect data of irregular buidings. Refer to Appendix C for more detailts of the inspection form

Major changes to the electronic data-input form have been made to section 3, highlighted in Figure 4-13, modified to accommodate all input data required to characterise an irregular opening layout.

Specific nomenclature introduced in Figure 4-14a, and Figure 4-14b are introduced and adopted as a reference to define the opening layout and the width of the edge piers for each storey of the inspected façade. Given the increased complexity of the façade geometry, to check if input data has been stored correctly, the new electronic inspection form provides also a sketch of the inspect façade built on the stored data and to be compared with the real façade on site or its reference picture (see Figure 4-13 and 4-19).

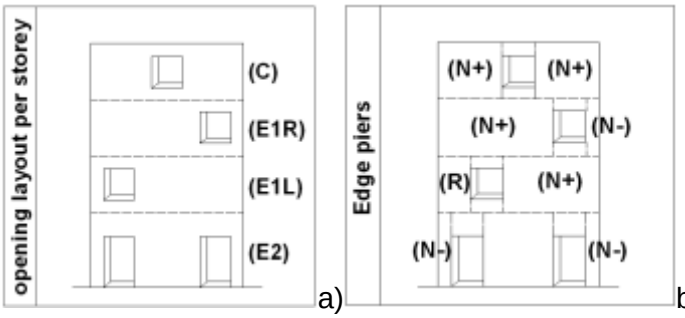

Figure 4-14: a)Nomenclature adopted to define the opening layout per floor: C: opening in the centre of the façade; E1R: opening on the right edge of the façade; E1L: opening on the left edge of the façade; E2: openings on the both edges of the façade. b) Nomenclature adopted to assign the width of the pier on the edge of the façade: N+: the width of the pier is larger than the width of the adjacent opening; N- the width of the pier is smaller than the width of the adjacent opening; R: the width of the pier is equal to width of the adjacent opening

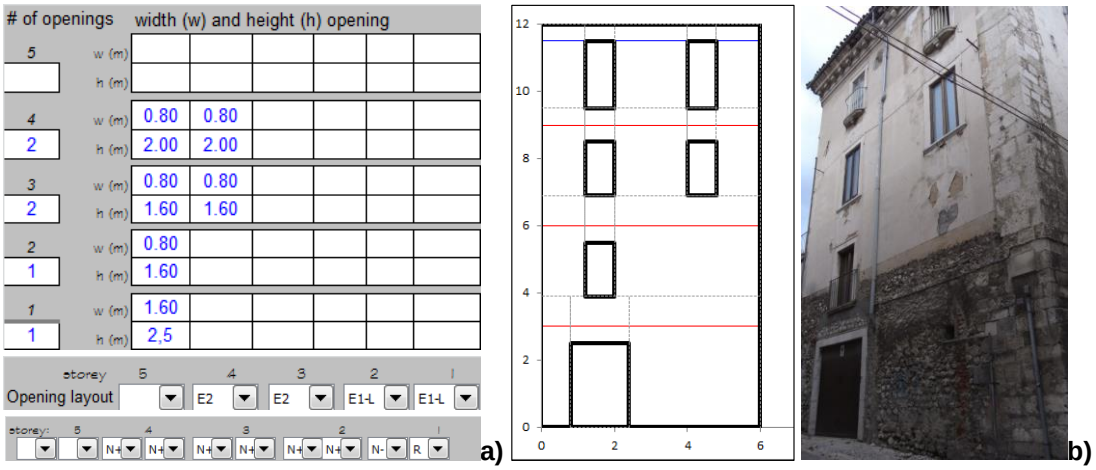

Figure 4-15: a): Input data for the definition of the opening dimension (w: width, h: height), opening layout (defined in Figure 4-14a), piers dimension at the edges of the elevation (defined in Figure 4-14b), b): sketch related to the input data on the left, which has been collected on site for the façade on the right.

4.3.2 *Mechanical models for irregular historic buildings*

In sections 4.2.2.2 it has been discussed that the opening layout incisively affect the in-plane failure modes. In particular, the strong irregularity in the opening

distribution is the main cause of the global in-plane failure mode represented by a global collapse of an entire façade.

In the current version of FaMIVE, the in-plane failure approach is developed for masonry buildings with regular opening layout (Casapulla and D'Ayala, 2006). This model is based on a macroelement approach based on the hypothesis that walls are constructed of brick orblock masonry with a frictional behaviour and that they fail under seismic loading by the occurrence of a diagonal crack that divides the wall into two macroelements. With reference to Figure4-20, the first macroelement can be identified with the bottom-left portion of the wall that does not participate to the failure, while the second is the upper-right portion of the wall that fails in sliding or overturning or for a combination of the two (Figure 4-16). Two different conditions of equilibrium can occur when the inspected walls fails, and these conditions depend on the value of the crack angle, defined as α_c in Figure 4-16.

By defining α_p: the shape factor of the cracked portion of the wall (H/L), and α_b: the shape factor of the masonry unit (*s*/*h*; where *s* is the overlap of the masonry units, *h* is the height of one unit), the two conditions (see Figure 4-16) are given as follows:

1) $\alpha_p \geq \alpha_c$
2) $\alpha_b \geq \alpha_c \geq \alpha_p$

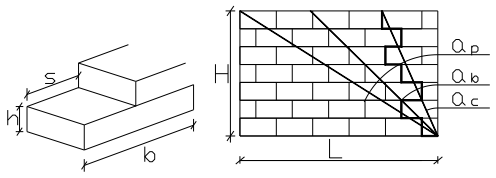

Figure 4-16: Block dimensions and variable angle of crack in a pier

If the distribution of openings on a façade is regular, the height of the piers is the same for each floor and the values of α_p and α_c are constant. This implies that a simplified model with a prevalent rigid spandrel or rigid piers behaviour, which determines the relative stiffness and the lateral capacity of piers and spandrel, allows defining the global lateral capacity.

However when the opening layout is substantially irregular, as shown in Figure 4-17 , the division of the façade into pier and spandrels becomes blurred and the crack pattern generating the failure can follow a number of different paths. Hence, an optimisation routine is needed to determine the path of least resistance within the façade, i.e. the one that will yield the minimum collapse load factor.

The geometric quantities used in the virtual work equations for the computation of the load factor multiplier for the in-plane mechanism are shown in Figure 4 21: l_{si} and l_{pi} are the spandrel and pier width respectively; h_{fi} and h_{si} are the interstorey and spandrel height respectively, while h_{pi} is the height of the pier over which a crack will develop and H_{gi} is the distance between the centre of gravity of the pier and the point where the cylindrical hinge forms, which coincides with the crack initiation point; q_{fi} (or q_r) is the i^{th}floor (or roof) load resultant, taken from the horizontal structures acting upon the portion of wall involved in the mechanism.

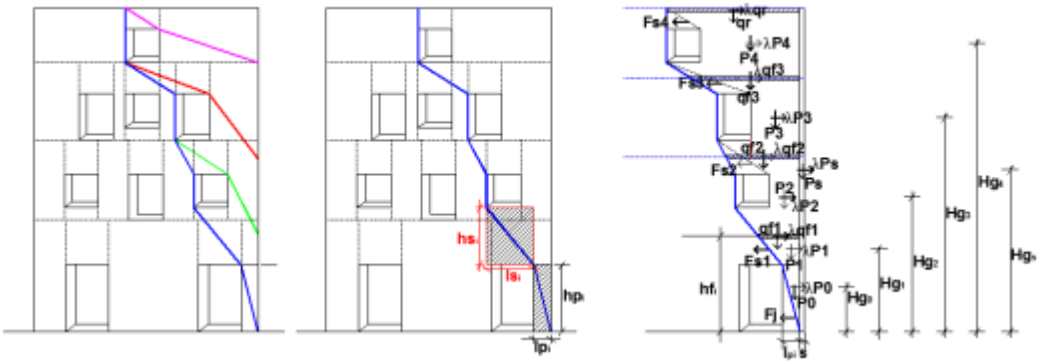

Figure 4-17: Geometric variables, crack initiation points and forces involved in a façade with irregular opening layout where αb≥αc ≥αf. (Novelli et al., 2015)

The friction present along the crack provides a frictional restraint to the horizontal sliding in both pier and spandrels. This is however uneven given the uneven load paths that develop for the vertical load to the ground, given the non-uniform geometry. The frictional forces along the crack in the pier, F_j can be calculated by using Eq. 1 for $\alpha_p \geq \alpha_c$, independent from the crack angle, and Eq. 2 for $\alpha_b \geq \alpha_c \geq \alpha_p$; where γ is the density of the masonry units and t_m is the thickness of the façade.

$$F_{j1} = \left[q_{fi} h_{pi} tan\ \alpha_b + \frac{(h_{pi}\ tan\ \alpha_b + s) h_{pi}}{2} \gamma \right] t_m f \quad (1)$$

$$F_{j2} = \left[tan\ \alpha_b \left(q_{fi} + h_{pi} \gamma \right) + \frac{\gamma}{2} \left(\frac{l_{pi} tan\ \alpha_b}{tan\ \alpha_c} - s \right) \right] \frac{l_{pi}}{tan\ \alpha_c} t_m f \quad (2)$$

The angle of the crack in the spandrel is taken as $\alpha_c \leq \alpha_s$, where α_s is the shape ratio of the spandrel. The inter-storey heights, h_{fi}, are taken as a constant for each storey, except for the first storey, for which a different height can be input, in agreement with onsite observation. The spandrel heights are calculated using the inter-storey height and opening geometry. The restraint force generated in the spandrel to equilibrate the lateral load is computed by:

$$F_s = \left[q_{fi} h_{si}\ tan\ \alpha_b + \frac{(h_{si}\ tan\ a_b + s) h_{si}}{2} \gamma \right] t_m f \quad (3)$$

The basic virtual work equation can be written from each floor from the top to the bottom, by taking into account the cracks might be concentrated only in one floor (partial collapse mechanism) or on the entire façade (total collapse mechanism).

The basic virtual work equation for any crack developed from the *ist* floor *upwards* can be written as:

$$\lambda_1 \sum_i^n q_i\, h_{pi} n + \lambda_1 \sum_i^n P_i H_{gi} + P_s H_{gs} = \sum_i^n q_i \left(\frac{h_{pi}\ tan\ \beta + s}{2} \right) + \sum_i^n P_i \left(\frac{h_{pi}\ tan\ \beta + s}{3} \right) + P_s \frac{s}{2} + F_j \frac{h_{pi}}{3} + \sum_i^n F_{si} \left(h_{fi} - \frac{h_{si}}{6} \right) \quad (4)$$

In the virtual work equations, β indicates the angle of the straight line between the crack initiation point and the point at which the crack meets the far edge of the pier accounting for the overlap *s* of the first masonry unit. Crack angles greater than α_b are unlikely to form under the assumed conditions (Casapulla and D'Ayala, 2006). F_{si} in Eq. 4 is the restraining force due to friction in the spandrels. In the next section, parametric analyses are carried out with the scope at validating the new version of FaMIVE and its capacity of predicting in-plane failure modes in façades with irregular opening layout.

4.4 Parametric analyses for assessing the effect of the irregularity in masonry buildings on their vulnerability by using the new version of FaMIVE

These parametric analyses are performed on the façade in blue of the building reported in Figure 4-18. The house is made of brickworks with lime mortar, and horizontal structures of timber joist with screed and planks. The friction fiction is set at 0.6 in order to ensure that in pane failure modes have the highest probability od occurrence.

.

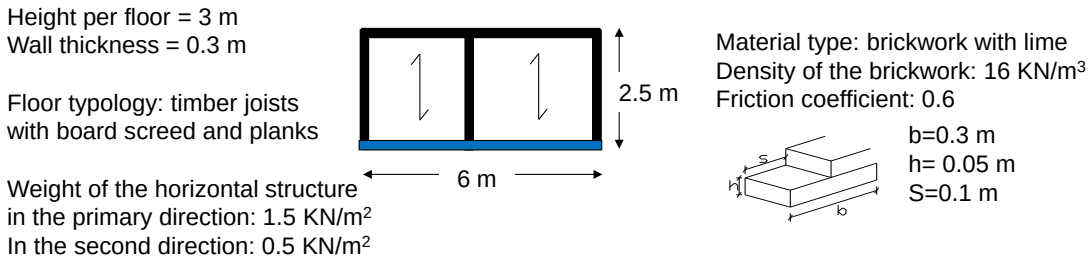

Figure 4-18: Geometric features of the masonry building adopted for the parametric analyses

In order to investigate the impact of the opening layouts on the building response under seismic events, it is assumed that the house has good materials, good connections among walls and good connections among walls and floors. This has been assumed in order to prevent failures modes belonging to OOP, and

ensuring triggering of either COMB or IP failure modes, which are mostly effected by the opening layouts, as discussed in section 4.2

The parametric analysis is performed first on a house of two and then a house of three storeys with the structural features described above. In order to represent the variability of openings' size within a storey and their layout the following parameters are varied:

- Three openings of different aspect ratio are assumed, initially with very small size with respect to the façade size, then increased proportionally, up to leave an edge pier of the size of the unit. By way of example, the Initial (I) and Final (F) configuration is shown in Figure 4-19. The relative position of the opening does not change.
- The location of the opening on a different storey is considered
- Both conditions of openings at only one storey and at both storeys are considered, varying the opening size only at one storey at a time, while considering three different size of opening for the other storey
- The above variations are repeated for a three storey façade, assuming that the first storey only contains a door

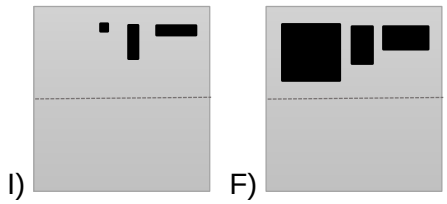

Figure 4-19: Initial (I) and Final (F) configuration used in the parametric analyses

The results from the analyses are expressed in terms of the value of the load factor multiplier λ as a function of the ratio of the opening surface in respect to the façade surface.

The choice of introducing the opening surface derives from the need of defining a parameter that allows investigating not only the effect of the slenderness of the piers, but also the effect of the entire opening distribution on the building performance.

The failure mode associated with the collapse load factor multiplier and the number of storeys involved in the failure modes are also discussed to underline how the position of a given opening layout at different storeys can affect the building performance.

Therefore, in the following plots, the values of λ refer to the entire façades or to the single storey depending on where the identified failure mode with highest level of vulnerability is concentrated, as mentioned in section 4.3.2.

This parametric analysis, although not exhaustive of all possible configuration provides a good range of variability of sizes and layout, which allow highlighting the importance of considering irregular distributions, when they are present.

4.4.1 *Irregular opening layout on a two-storey building*

The opening layouts considered for a two-storey façade are shown in Figure 4-21. These configurations introduce two different irregularities. The first one is an irregularity between the first and the second storey, since one of the two storeys does not have openings, while the second irregularity is among the openings of the same level, since they have different size.

Figure 4-20a is the results of the parametric analyses carried out by varying the volume of the openings of the first level of the two storey façade from configuration I) to configuration F). As expected, since the openings are only at the bottom storey, the façade fails for failure modes that involve only the collapse of the bottom level. Therefore the increment of the opening sizes located at the first storey determine the failure of the facades for an in-plane failure mode for λ*1=0.24, associated to Vol*1, volume of the openings at bottom level, when the first storey starts failing for in-plane failure mode.

In Figure 4-20b, where the parametric analyses is carried out by varying the volume of the openings of the first level from configurations I) and F), the façade fails for failure mode that only involves the first level, where the openings are located. The increment of the openings of the top level does not affect the facade performance until the opening configuration destabilises the top storey with a significant reduction of the capacity of the entire façade, underlined by the drop in λ (λ^*_2=0.13) associated to

Vol*2, volume of the openings at top level when the façade starts failing for in-plane failure mode.

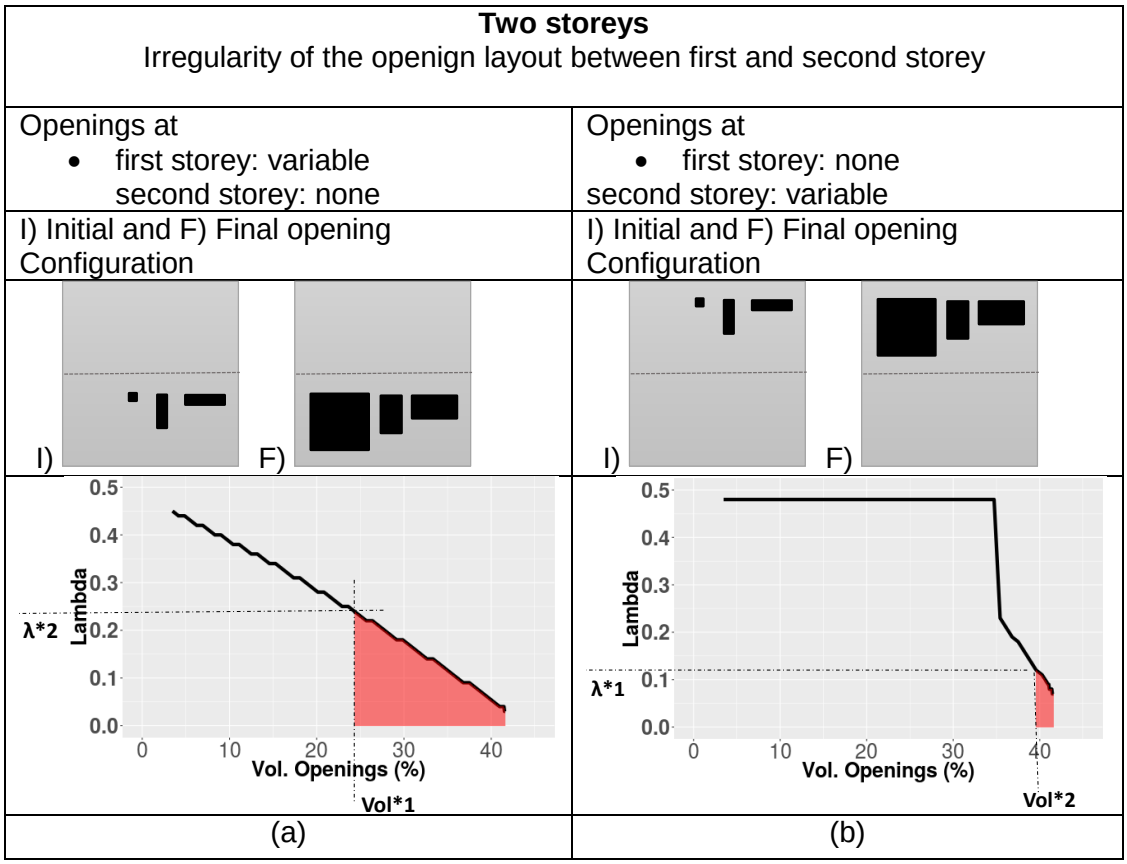

Figure 4-20: Parametric analyses on the two storey buildigns carried out to estimate the effect of the opening layout distrubution of the single level on the building performance. The openings are only at the bottom storey in a) and only at the top storey in b). The façade starts to fail for in-plane failure mode for λ <= λ*1 in a) and λ<= λ*2 in b)

Identified from the analyses above, the opening volume (Vol*1 and Vol*2) whereby the façades start failing for in-plane failure modes the following analyses are performed as indicated in Figure 4-21.

During the parametric analysis in (a) the opening layout of the second storey and in (b) the opening layout of the first storey vary, and in (a) the opening layout of the first storey and in (b) the opening layout of the second storey are fixed. The fixed openings in (a) and in (b) are set at three different volume, 1) < 2) = and 3) > Vol*1, 2 identified in Figure 4-21a and Figure 4-21b.

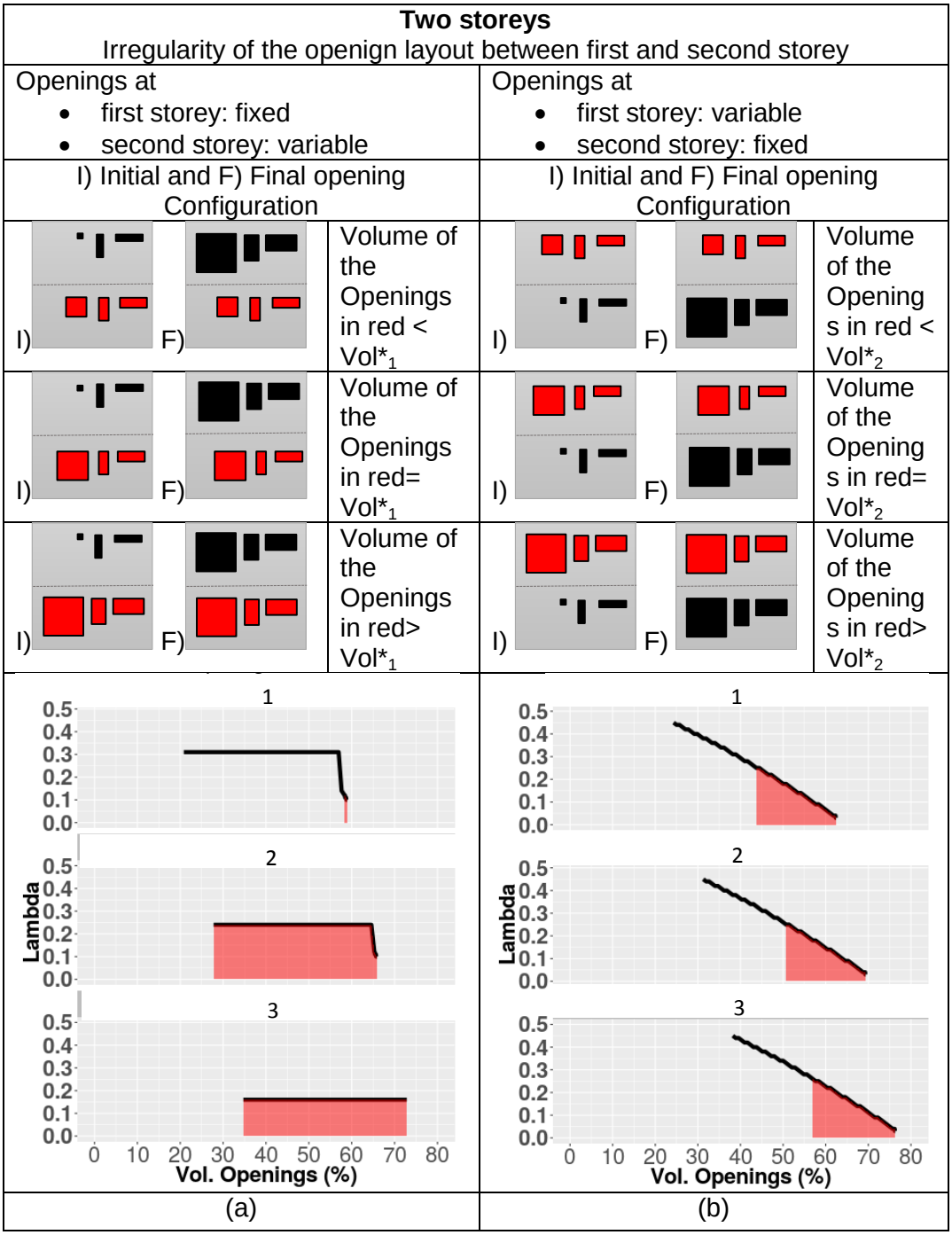

Figure 4-21: a) two storey façade with three irregular openings at the second storey that vary from I) to F) and three irregular opening at the first storey that are fixed and have opening volume 1) <Vol*1 ; 2) =Vol*1 and 3) >Vol*1 identified in Figure 4-20, b) two storey façade with three irregular openings at the first storey that vary from I) to F) and three irregular opening at the second storey that are fixed and have opening volume 1) <Vol*2 ; 2) =Vol*2 and 3) >Vol*2 identified in Figure 4-20

In Figure 4-21a1, by maintaining fixed the opening size at the first storey and starting to increase the opening volume at the top storey, the entire façade fails for a failure mode that is different from the in-plane failure mode. Indeed, only when the opening size at the top storey is particularly large, the failure of the entire façade is due to an in-plane failure mode of the top storey.

The fact that the failure mode of the façade is determined by the collapse of the top storey is confirmed by the value of λ (=λ *1=0.13) identified when the façade starts failing for in-plane failure mode in Figure 4-20b.

In Figure 4-21a2 and Figure 4-21a3, the façade fails only for in-plane failure mode. This is because the volume at the bottom storey is already critical (=, > Vol*1) and already causes an in-plane failure mode to the façade, as observed in Figure 4-19a. Furthermore, these analyses underline that if the bottom storey has already a critical configuration to an in-plane failure mode, the increment of the openings at the top level has only a minimum effect on the performance of the entire façade.

Therefore, Figure 4-21a2 shows for most of the analyses λ= λ*2=0.24, value identified in Figure 4-20a for the façade with only opening at the bottom, failing for in-plane failure modes. Then when the top level also starts failing for in-plane failure modes (for large opening size) there is a decrement of the capacity of the entire façade underlined by the drop in λ that became equal to λ= 0.13 (=λ*1).

In Figure 4-21a3, it can be observed that since the size of the openings at the bottom are already very large, by incrementing the opening size at the top, the entire façade fails for a in-plane failure modes with a constant value of λ= 0.16 that is smaller than both λ*1, and λ*2, by underlining that the both storeys are involved in the identified failure modes.

In Figure 4-21b, the results are strongly affected by the variation of the opening volume on the bottom storey, as confirmed by the linear trend of λ that reflects the linear trend of λ observed in Figure 4-20a. During these analyses the façades fail for in-plane failure mode for λ= 0.24 (=λ*2), value identified in Figure 4-20a, by underlining that façade starts failing for in-plane failure mode only when the bottom level starts failing for in-plane failure mode.

In conclusion, it can be stated that the façade is mainly affected by the change of the opening volume of the bottom level as observed for Figure 4-20, where the effect of change of the opening at the top level provides a constant value of λ for most of the analyses.

4.4.2 *Irregular opening layout on a three-storey building*

The analyses presented in Figure 4-22 and Figure 4-23 are carried out in order to investigate the performance of a three-storey building with an irregular opening layout. The structural features considered for the following analyses are reported in Figure 4-18.

Since from the previous analyses, results pointed out that by varying the opening volume at the bottom storey, the building performance changes consistently, the following analyses on the three-storey building are performed by only varying the opening layout of the first and second storey.

In particular, in Figure 4-22a, the three-storey building has different openings on the first storey, no opening at the second storey and two different openings at the top level. The analysis in Figure 4-22a is computed by increasing the number of the openings at the first storey from I) to F). At the beginning of the parametric analyses, the entire façade (all three storeys) does not fail for in-plane failure modes, since only when λ= λ*3 = 0.21 (associated to Vol*3, opening volume when the façade starts failing for in-plane failure mode) the façade fails because the first storey starts failing for in-plane failure modes.

In Figure 4-22b, the three-storey building has no openings on the first storey, and openings at the second and third level. The analysis in Figure 4-22b is computed by increasing the number of the openings at the second storey from I) to F). At the beginning of the parametric analyses, the entire façade (all three storeys) does not fail for in-plane failure modes, and λ is not consistently affected by the increment of the opening volume. The significant reduction of the capacity of the façade is underlined by the drop in λ (=λ^*_4=0.15) associated to Vol*4, opening volume when the façade starts failing for in-plane failure mode.

Identified from the analyses above, the opening volume (Vol*3 and Vol*4) whereby the façades start failing for in-plane failure modes the following analyses are performed as indicated in Figure 4-23.

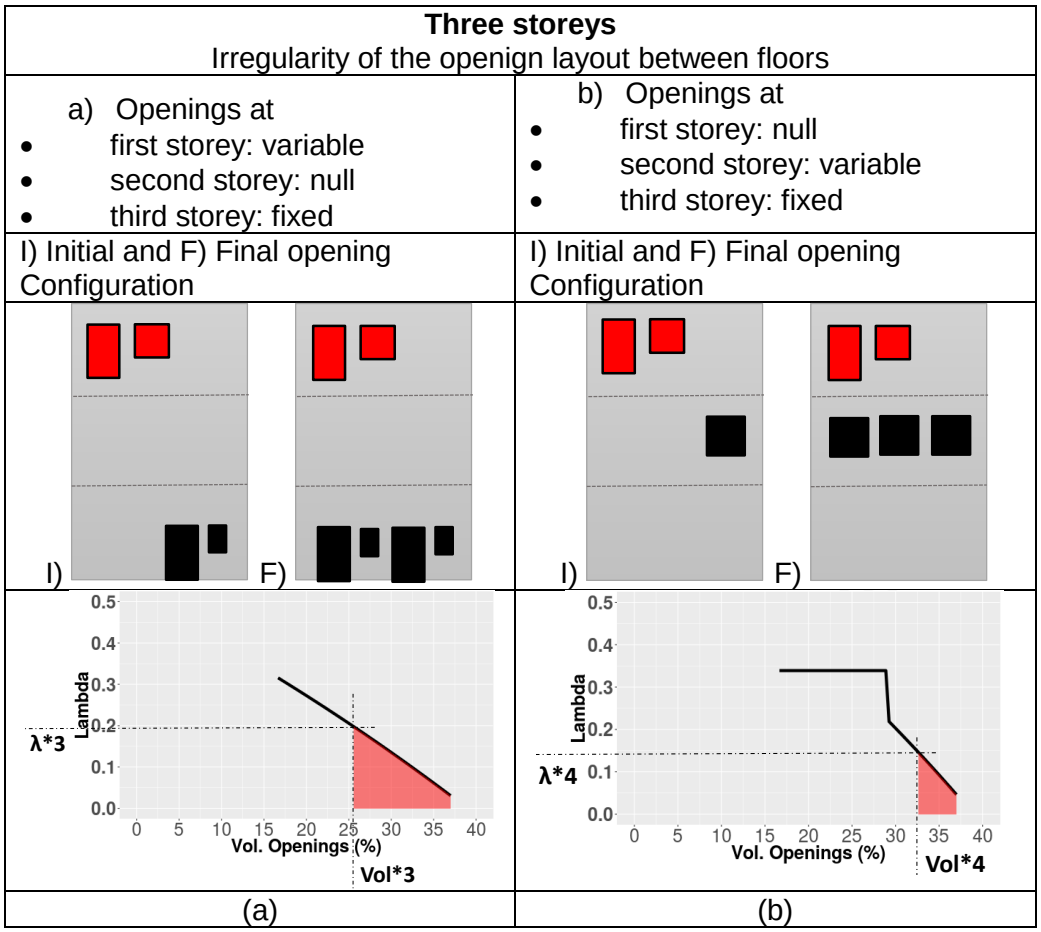

Figure 4-22: Three storey façade with a) openings at the first storey that vary, no openings at the second storey and openigs at the third storey that are fixed b) no openings at the first storey, openings at the second storey that vary and openigs at the third storey that are fixed

During the parametric analysis in (a) the opening layout of the first storey and in (b) the opening layout of the second storey vary, and in (a) the opening layout of the second and third storey and in (b) the opening layout of the first and third storey are fixed. The fixed openings in (a) and in (b) are set at, 1) < 2) = Vol*3, 4 identified in Figure 4-22a and Figure 4-22b.

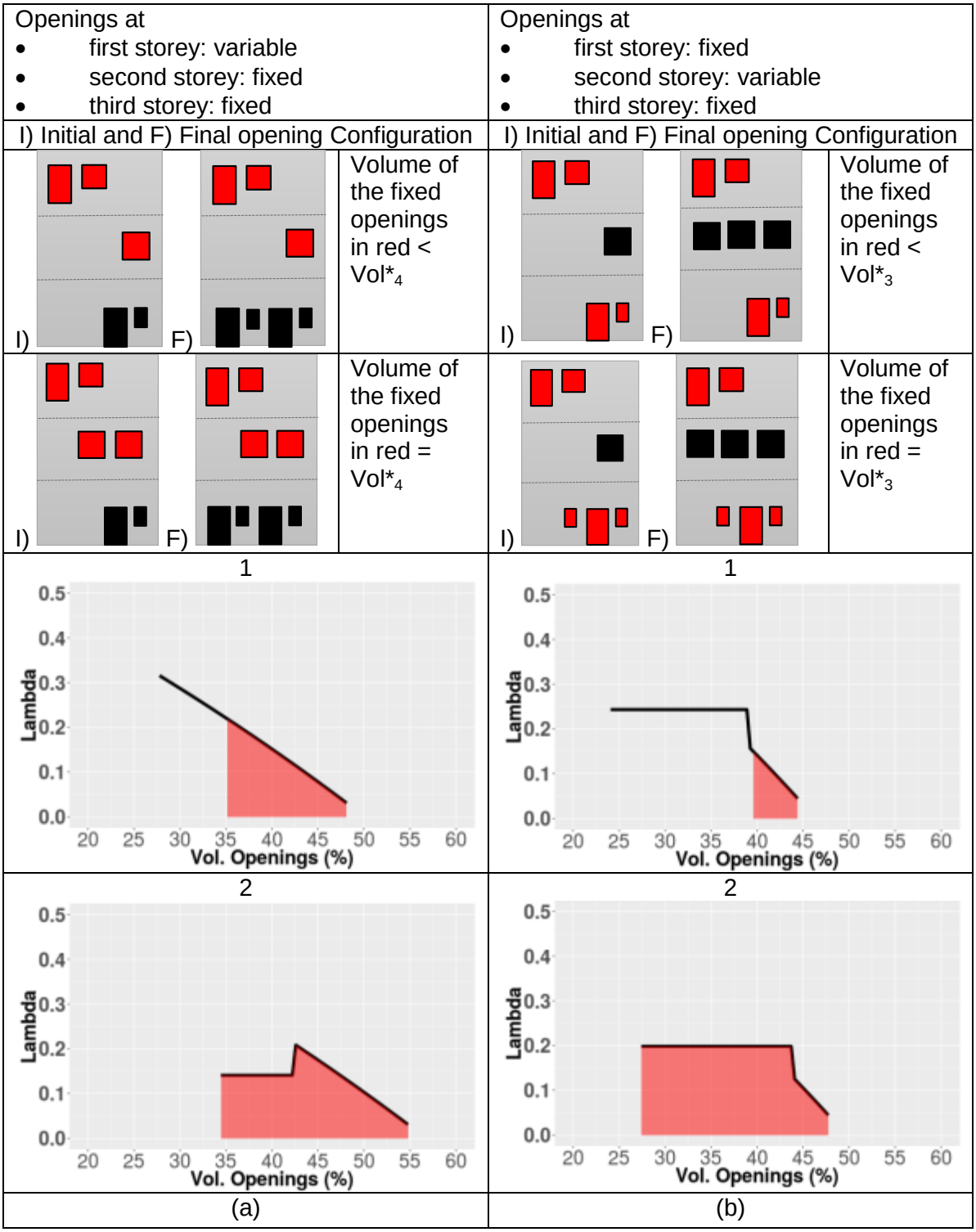

Figure 4-23: Three storey façade with openings in red that are fixed and openings in black that vary in volume. in a) the sum of the fixed opening volume is set at <,= Vol*3 in b) and the sum of the fixed opening volume is set at <,= Vol*4

In Figure 4-23a1, by maintaining fixed the opening size at the second and third storey and starting to increase the opening volume at the first level, the entire façade fails for a failure mode that is different from the in-plane failure mode. Indeed, only when the opening at the first storey are particularly large and the opening size of the entire façade from ~35% to ~48%, the failure of the façade is due to an in-plane failure mode of the first storey.

The fact that the failure mode of the façade is determined by the collapse of the first storey is confirmed by the value of λ (=λ*4=0.21) identified when the façade starts failing for in-plane failure mode in Figure 4-22a.

In Figure 4-23a2, the façade fails only for in-plane failure mode. This is because the volume at the second and third storey is already critical (= Vol*4) and already causes an in-plane failure mode to the façade, as observed in Figure 4-22.

Furthermore, these analyses underlines that if the second and third storey have already a critical configuration to an in-plane failure mode, the increment of the openings at the bottom level has effect on the performance of the entire façade when the facade has an opening volume of 45%. On the other hand, when the openings layout is regular the façade has a better performance t, underlined by the peak in λ at 0.21. After this peak λ decreases linearly with the increment of the opening volume of the second storey

In Figure 4-23b1, the results are strongly affected by the variation of the opening volume on the second storey, as confirmed by the value of λ= λ*4=0.15 whereby the façade start failing for in-plane. In Figure 4-23b2, the effect of the increment of the opening volume in the second is particularly evident when λ drops at λ*4=0.15. During this analysis the façade fails only for in-plane failure mode occurring on the first two storey.

4.4.3 *Concluding remarks on the parametric analyses*

As observed in section 4.2, buildings with strong connections between façades and between façades and floor/roof have high probability of failing for in-plane failure modes. By taking into account this, the analyses above have been carried out by setting good connections in the façade and a high value of the friction

coefficient (at 0.6), since the section aims at assessing how different opening layouts effect the façade capacity and consequently the value of the load factor multiplier λ associated to the identified failure mode.

The analyses have shown that the value of λ is strongly affected not only by the opening layout of the entire façade but particularly by the distribution of the openings in each single storey. This is underlined by the fact that, in most of the parametric analyses, the in-plane failure modes occur because one specific storey is failing for in-plane failure mode.

Moreover, the parametric studies have also highlighted the importance of analysing buildings with their real opening distribution since it was possible to observe that consistent drops in the capacity of the façade can also occur for a slight change in the opening distribution, in particular if these changes are concentrated at the top levels of a façade.

4.5 STEP 3: Definition of the building performance levels and damage states

The concept of performance targets was introduced in 1992 by FEMA within the framework of the ATC-33 (1995) project funded for the development of guidelines for the seismic assessment and retrofit of buildings. Successively, SEAOC Vision 2000, (OES, 1995) and latterly FEMA 273 (BSSC, NEHRP 1997) and FEMA 274 (ATC, 1997) developed performance based approaches for the rehabilitation of existing buildings. These approaches provide methodologies to design retrofitting interventions for buildings that do not achieve the expected performance target. According to these procedures, the definition of each performance target for a given building is determined by taking into account building importance, class, and seismic hazard.

Nowadays performance-based approaches are commonly adopted by different international and national codes such as EC8 (CEN 2005), NTC (2008), IBC (2003), ASCE 41-13 (2013), ATC-20 (1989), CBC (2010), ASCE 7-05.(ASCE 2005).

They provide the definition of the performance targets, procedures for the evaluation of the building performance for a given seismic hazard, and criteria to verify the fulfilment or otherwise of the performance target by the seismic response of a given structure. In these codes, the performance ranges are defined on the basis of the socio-economic consequences of historic buildings failing for a given performance target, such as

- safety of the building's occupants during and after a seismic event,
- costs and feasibility of restore buildings to their pre-earthquake condition,
- length of time needed to be removed buildings from their service, to complete repairs and to re-establish their economic, architectural and historic value.

As it is clear from the above definitions, the performance target is directly related to the extent of damage that would be sustained by buildings during seismic events. This implies that once performance levels are introduced, building damage states need to be correlated to them, and criteria provided to check the fulfilment of the defined performance target, require to be introduced.

In this work, the performance levels are set following the performance levels provided by EC8 (CEN, 2005), and they are adapted to describe the global response of masonry buildings. Three different performance levels to describe the extent of damage, the safety, and the level of interventions required for restoring the pre-earthquake conditions in masonry buildings are presented, as follows:

- Damage Limitation (DL): The entire historic building is between no damage to light damage. Structural, non-structural and architectural components may have light cracks. The building does not require to be removed from its service, as the building is considered safe. Quick interventions may be required to restore the pre-earthquake condition of the building.
- Significant Damage (SD): The entire historic building is severely damaged. Some structural, non-structural and architectural components have significant cracks, which underline the occurrence of failure modes,

while others may have light cracks. The historic building requires to be removed from its service, as it is considered unsafe. The building requires to be propped immediately in order to prevent collapse and preserve their architectural value. Repair and retrofitting interventions according to conservation philosophy are required to restore the pre-earthquake condition of the building.

- Near Collapse (NC): The entire historic building is heavily damaged. Some of the structural, non-structural, and architectural components have completely crushed, while others may have severe cracks, which underline a collapse in the building due to the occurrence of partial/total failure modes. The building may not survive from future aftershocks. The historic building is considered completely unsafe. Only in a few cases, these buildings are immediately removed or rebuilt, by against any conservation philosophy. Most commonly, these buildings are immediately shored, to prevent further damage or loss of the building itself or loss of the adjacent buildings and access is denied for safety.

Given such definitions of the performance levels that are directly related to the damage severity observed on buildings, the damage states can also be introduced.

In this work, the damage scale of the EMS'98 (Grünthal, 1998) is presented in a modified version that describes the damage states for masonry buildings through pictures, and sketches that take into account the possible failure modes. Five-damage grades are defined and reported in Figure 4-24.

Once performance levels and damage states have been defined from a conceptual viewpoint, it is possible to correlate them with the performance ranges in Figure 4-25.

The damage states from No Damage to Light Damage are associated to first performance range (Damage Limitation) then the Severe Damage state is associated to second performance range (Severe Damage), while the last ranges from Near Collapse to Collapse Damage is associated to the third performance range (Near Collapse).

Damage State	Description	In-plane failure	Overturning failure
No damage (ND)	Hair-line cracks in very few walls, detachment or fall of small pieces of stucco only. Fall of loose stones or bricks from upper parts of buildings		
Light damage (LD)	Slight cracks in few walls. Detachment or fall of large pieces of stucco. Partial collapse of chimneys, and detachment of few roof tiles		
Severe damage (SD)	Large and extensive cracks in external façades, and in gable walls, partial detachment between façades and between internal walls and façades, failure of chimneys; fall of roof tiles.		
Near collapse (NC)	Serious failure in external façades, and gable walls complete detachment between façades and between internal walls and façades, partial structural failure of roof and floors		
Collapse (C)	Total or near total (more than 50%) failure or crush of external façades, and gable walls, total structural failure of roof and floors		

Figure 4-24: Damage states for masonry buildings

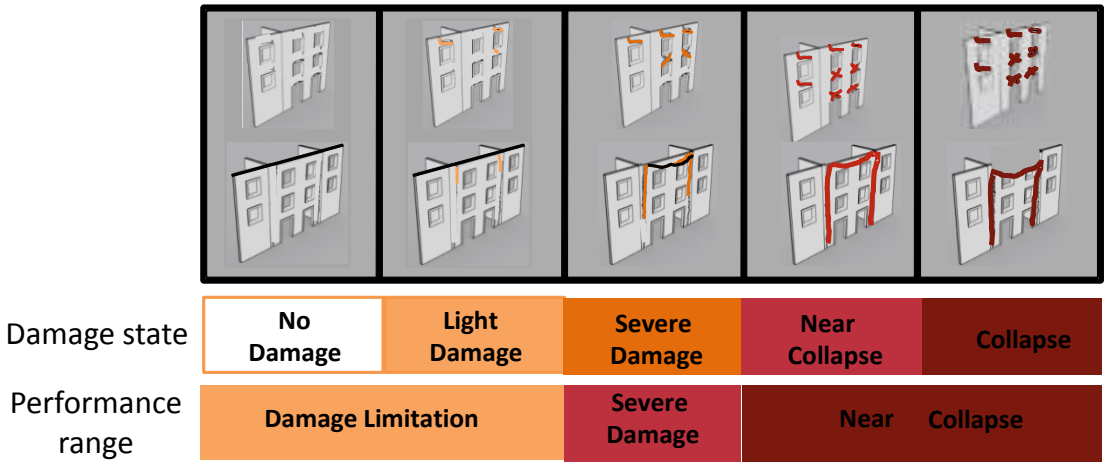

Figure 4-25: Correlation between damage states and performance ranges

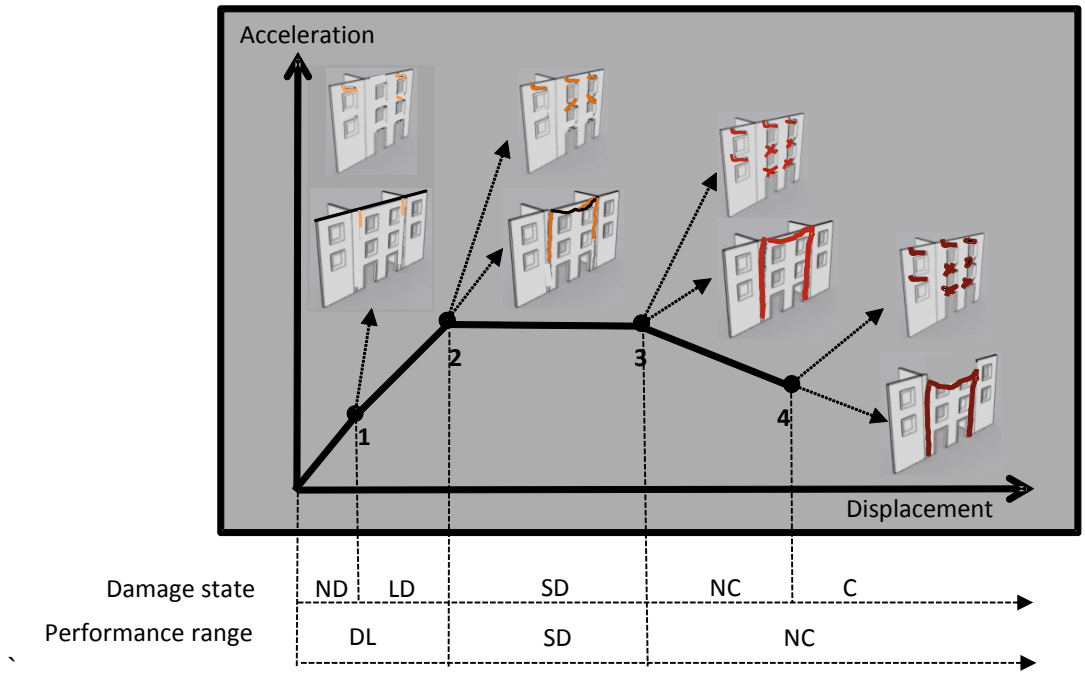

Figure 4-26: Association of the damage states to the conventional points of the capacity curves

The correlation between performance ranges and damage thresholds can also be visualised by means of a capacity curve, idealised as succession of straight segments over which the damage states and performance ranges are reported. The intersection between the straight segments are the performance or damage thresholds. This capacity curve, represented qualitatively in Figure 4-26 quantifies the building seismic

performance through a relationship between the lateral acceleration and the corresponding horizontal displacement. In the next section, the thresholds are defined numerically.

4.6 STEP 4: Estimation of the seismic performance of masonry buildings

Several codes, such as Displacement Coefficient Method (DSM): FEMA-356 (2000) and FEMA-440 (2005), Capacity Spectrum Method (CSM): ATC-40 (1996), N2 method (Fajfar, 2000), EC8 (CEN, 2005) and IBC (2000, 2003), can be adopted to convert a real structure to a nonlinear single degree of freedom.

These approaches aim at estimating the building performance by 1) idealizing a Multi Degree Of Freedom (MDOF) system into an equivalent elasto-plastic Single Degree Of Freedom (SDOF) system and 2) transforming the elastic demand in inelastic demand by increasing structural damping, or alternatively global ductility.

In this work, a similar approach is proposed with reference to the GEM guidelines (D'Ayala et al., 2014), whereby a capacity curve is derived by idealising the inspected façade into SDOF oscillators, and assuming that the kinematic chain is formed when the failure mode is activated in the inspected façade, as discussed in section 4.6.1.

Estimated the capacity curves, these are intersected with the inalestic spectra acceleration in order to estimate the actual performance of the inspected façades. This approach is presented as an iterative approach, integrated to the new version of FaMIVE presented in section 4.2.2. Details of the iterative approach are illustrated in section 4.6.2.

4.6.1 *Transformation of the inspected façade into an equivalent SDOF system and derivation of capacity curves*

The approach adopted to represent the Capacity Curves (CC) is detailed in D'Ayala and Novelli (2013) and summarised in this paragraph to provide a complete reference for the whole process adopted in this work.

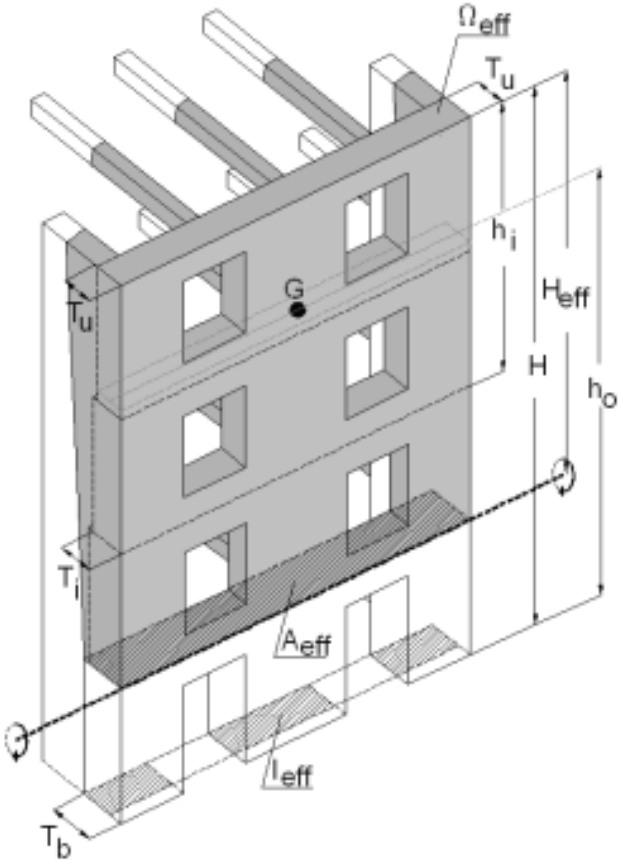

Figure 4-27: Schematic meanings of the parameters used in the calculation of the effective stiffness and effective mass for the equivalent degree of freedom

This approach is adopted to define capacity curves for SDOF oscillators that are derived by idealising the façades inspected and analysed with FaMIVE into equivalent nonlinear SDOF systems. The effective stiffness, effective mass and period of the SDOF system is estimated by taking into account the property of the inspected façade. Therefore the SDOF system is derived by taking into account plan geometry of the building to which the façade belongs to, its openings' layout, constraints of the inspected façades with their adjacent walls, and floors and their mass participating to the critical failure mode computed with FaMIVE.

With reference to Figure 4-27 for the meaning of the symbols, equation (5) is used for the calculation of the lateral effective stiffness:

$$K_{eff} = k_1 \frac{E_t I_{eff}}{H_{eff}^3} + k_2 \frac{E_t A_{eff}}{H_{eff}} \qquad (5)$$

where, H_{eff} is the height of the portion involved in the critical failure mode, E_t is the initial elasticity modulus of the masonry, derived from literature or experimental data. The terms I_{eff} and A_{eff} are the second moment of area and the cross sectional area respectively, calculated by taking into account the dimension of the openings and variation of thickness over the height of the inspected façade.

The constants k_1 and k_2 assume different values depending on edge constraints and on whether shear and/or flexural stiffness are relevant for the elastic performance of the façade given a mode of failure.

The effective participating mass Ω_{eff} is calculated in equation (6) and it is given by the mass of the portion of façade activated by the failure mode plus the mass of the horizontal structures (f: floors and r: roof) involved in the mechanism (shown in grey in Figure 4-27, for a mechanism involving only the upper 3 storeys of the front façade):

$$\Omega_{eff} = V_{eff}\delta_m + \Omega_f + \Omega_r \qquad (6)$$

where V_{eff} is the solid volume of the portion of façade and side-walls involved in the mechanism, δ_m is the density of the masonry; Ω_f, and Ω_r are the masses of the horizontal structures involved in the mechanism.

Using the effective mass and stiffness of equations (5) and (6), the natural period T_{eff} of the equivalent SDOF system in computed as:

$$T_{eff} = 2\pi\sqrt{\frac{\Omega_{eff}}{K_{eff}}} \qquad (7)$$

Once the effective stiffness, mass and period of the equivalent SDOF oscillator are identified, the related capacity curve is defined through the load factor multiplier λ calculated on the single inspected façade with FaMIVE,.

The capacity curve derived for the equivalent SDOF oscillator is defined with reference to the four damage limitation threshold defined Figure 4-26.

The first point of the capacity curve is represented by the “damage limitation threshold” and defined by the transition from the “no damage” state to the “light

damage" state. Hence, this point represents the first appearance of cracking in the macroelement, which will essentially depend on the overall geometry of the wall (out-of-plane) or most exerted piers (in-plane).

If the macroelement fails for out-of-plane mechanisms, the mass is applied at the height of the centre of gravity of the collapsing portion with respect to the ground. The lateral acceleration A_y is the acceleration that will provide the combination of lateral and gravitational load that will cause a triangular distribution of compression stresses at the base of the overturning portion, just before the onset of cracking:

$$A_1 = A_y = \frac{t_{top} + t_{base}}{2h_0} \text{ with corresponding displacement } D_1 = D_y = \frac{A_y}{4\pi^2} T_{eff} \quad (8)$$

where, t_{top} and t_{base} are the effective thickness of the wall at the top and base of the overturning portion, h_o is the height from the ground to the centre of mass of the overturning portion, and T_{eff} the natural period of the equivalent single degree of freedom (SDOF) oscillator, as defined in (7).

When the macroelement fails for an in-plane mechanism, the lateral acceleration is provided by the following equation:

$$A_1 = A_y = \min\left(\frac{L_{ps}}{n s h_{s0}}\right) \text{ for s} = 1 \text{ to } n_s$$
$$\text{with corresponding displacement } D_1 = D_y = \frac{A_y}{4\pi^2} T_{eff} \quad (9)$$

where L_{ps} is the length of the façade without the openings at each storey, n_s is the number of piers at storey s, assuming they all have the same width at a given storey, h_s is the storey height. For irregular façades with irregular piers, equation (9) will search for the pier with the minimum ratio of width to height of pier. The second and the third point of the capacity curve in Figure 4-26 determine the thresholds between the "light damage" and "Severe damage" states and between the latter and the "Near Collapse" state, respectively. As it is assumed that the "severe damage" state, is characterised by a perfectly plastic behaviour, the ultimate acceleration capacity A_u of the SDOF system, is computed as follows:

$$A_{2,3} = A_u = \frac{\lambda_c}{\alpha_1} \qquad (10)$$

where λ_c is the critical collapse load factor computed by FaMIVE, and α_1 is the proportion of total mass participating to the critical mechanism. This is calculated as the ratio of the mass of the façade and sides or internal walls and floor involved in the mechanism Ω_{eff} to the total mass of the involved macroelements (walls, floors, and roof).

The displacement D_2 corresponding to the "Severe damage" threshold is defined by the following:

$$3D_y \leq D_2 \leq 6D_y \qquad (11)$$

as suggested by Tomazevic et al., (2007). The range in Equation (11) is useful to characterize masonry fabric of variable regularity and its integrity at ultimate conditions, with the lower bound better describing the behaviour of adobe, rubble stone, and brickwork in mud mortar, while the upper bound can be used for massive stone, brickwork set in lime or cement mortar and concrete block work.

The displacement corresponding to the "Near collapse" state is defined by the following:

$$D_{3(bending)} = D_{u(bending)} = t_{base}/3 \quad or \quad D_{3(shear)} = D_{u(shear)} = \min(s/2; t_{pier}/3) \qquad (12)$$

where *s* is the staggering as it is shown in Figure 4-16.

The fourth point of the capacity curve in Figure 4-26 is defined by the threshold to the collapse state, where the displacement of the SDOF oscillator is identified by the condition of loss of vertical equilibrium due to overturning or in-plane failure mode. These conditions are expressed by different formulas as follows:

$$D_{4\,(overturning)} = D_{c\,(overtuning)} = tana * l * \frac{1}{\sqrt{2}} * \frac{2}{3} + \frac{t_{base}}{2};\ or$$
$$D_{4\,(shear)} = D_{c\,(shear)} = \max(s; \frac{t_{pier}}{2}) \qquad (13)$$

where in the formula for the overturning t_{base} is the thickness at the base of the overturning portion, *l* is the typical length of units forming the wall and *α* is the crack angle of the façade caused by its overturning. In the case of in-plane mechanism the geometric parameter used for the estimation of the displacement related to the collapse is the maximum value between the staggering ratio *s* and half of the thickness of the pier of the macroelement.

As for the acceleration capacity related to the collapse state it is assumed that its value is equal to 80% of the ultimate acceleration capacity computed in equation (10).

4.6.2 *Computation of the non-linear demand*

The approach adopted in this work for the estimation of the building performance and damage analyses is based on the N2 method, originally implemented by Fajfar and Fischinger (1989), and lately modified, and gradually developed into a more mature version by Fajfar and Gašpersič (1996).

Currently, this method is part of EC8 and IBC (Fajfar, 2000) as the performance based approach adopted for the design of new buildings and rehabilitation of existing ones.

This approach can be applied for the estimation of the seismic performance of simple and regular structures of even for buildings with irregularity in plan and with accidental eccentricities (Fajfar, 2006; De Stefano and Pintucchi, 2008; Magliulo et al., 2008).

The basic idea of this approach came from Q-model, developed by Saiidi and Sozen (1981), who presented the N2 method in an acceleration-displacement format (Fajfar, 1999) according to an idea proposed by Bertero's, (Bertero's 1995) and Reinhorn (Reinhorn 1997).

The N2 method has the same advantage introduced in the CSM (Freeman et al. 1975, Freeman 1998) of representing the building performance as the intersection between the building capacity and the inelastic spectra in a Cartesian plane.

However, the N2 method reduces the elastic spectrum by increasing the global ductility of a structure while the CSM, proposes the use of fictitious damping to identify the inelastic response of the structure. The introduction of the concept of ductility in N2 method derives from a lack of physical evidence in the relationship between hysteretic energy and equivalent viscous damping, (Chopra and Goel, 1999; Miranda and Akkar, 2002).

The N2 method, where N stands for non-linear seismic analysis and 2 for two-dimensional structural model, proposes to estimate the non-linearity of buildings by developing numerical models of buildings and carrying out static pushover analyses for the estimation of the Capacity Curve (CC), and deriving equivalent bilinear curve for an equivalent SDOF. In this work, the derivation of CC for an equivalent SDOF, follows the procedure outlined in section 4.6.1, while the definition of the μR-T relationship proposed by Fajfar et al. (2000) is used for the computation of the inelastic spectra.

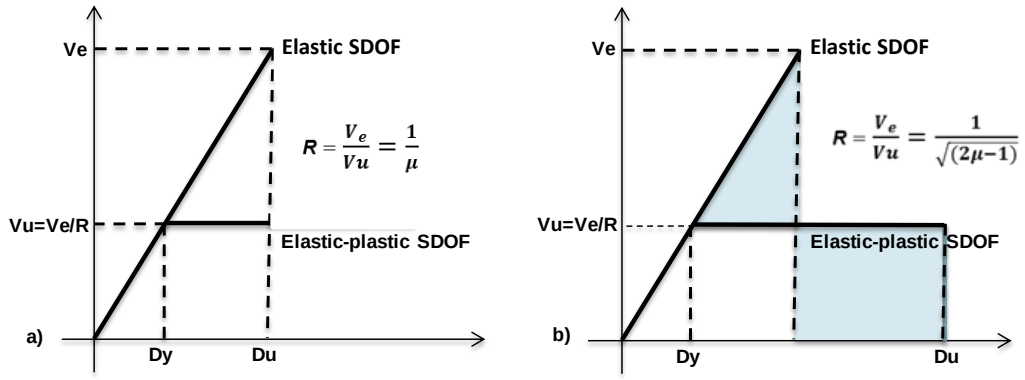

Figure 4-28: Performance identified with N2 method by a) Equal Displacement Principle and b) Equal Energy Principle

The nonlinear spectrum can be derived by using two different values of ductility μ computed by either of the following principles: the Equal Displacement (ED) Rule adopted for structures with long period and Equal Energy Rule (EE) adopted for structures with short period, represented graphically in Figure 4-28.

The ED rule is given by a geometric equation, illustrated in Figure 4-28a, and expressed by the following:

$$\mu = \frac{R^2 + 1}{2}; V_u = \frac{V_e}{R}; D_u = \frac{D_e}{R} \qquad (14)$$

where V_u and D_u are the ultimate base shear and displacement of the elasto-plastic system and V_e and D_e the ultimate base shear and displacement of the corresponding elastic system. This approach is based on the assumption that the maximum displacement of an inelastic system is equal to the maximum displacement of an elastic system, characterised by the same mass and initial stiffness.

The EE rule is given by the equivalence between the area of the triangle and the area of the parallelogram, illustrated in Figure 4-28b, and it is expressed by the following:

$$\mu = \frac{R^2 + 1}{2}; V_u = \frac{V_e}{R}; D_u = \frac{1 + A_y^2}{2A_y} De \qquad (15)$$

where A_y is the yielding displacement as defined in section 4.6.1.

In this work, by referring to the GEM guidelines for the Analytical vulnerability assessment (D'Ayala et al.2014) the performance point are calculated by uing the ED rules

4.6.3 *Determination of the performance points*

The relationship between μ and R for the identification of the performance point (in term of ultimate displacement) with reference to the ED rule, defined in section 4.6.2, needs interactions in order to identify a value of the ductility μ (ratio between Du and Dy) that matches the value R, whereby the LSA: Linear Spectrum is reduced in NLSA: Non-linear Linear Spectrum (Fajfar et al., 2000).

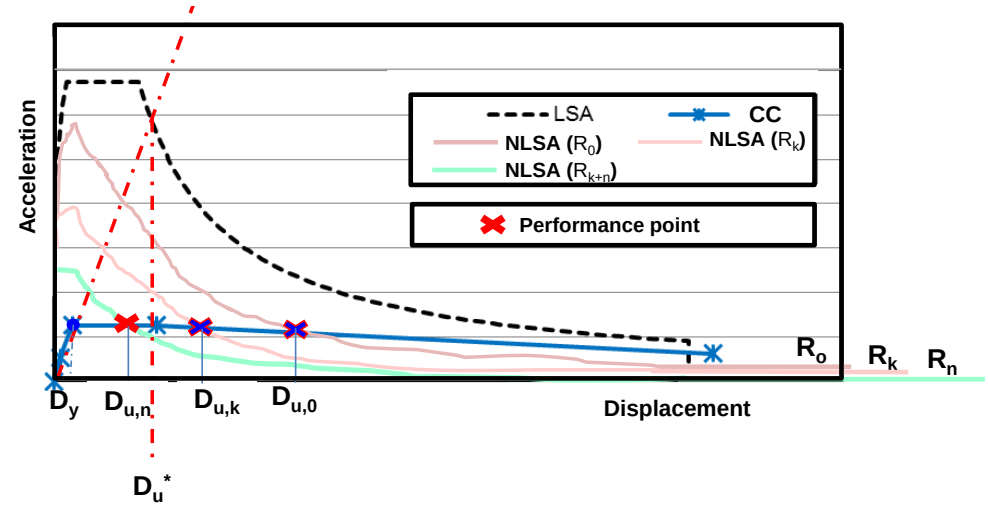

Figure 4-29: Iterative procedure for the identification of μ and R

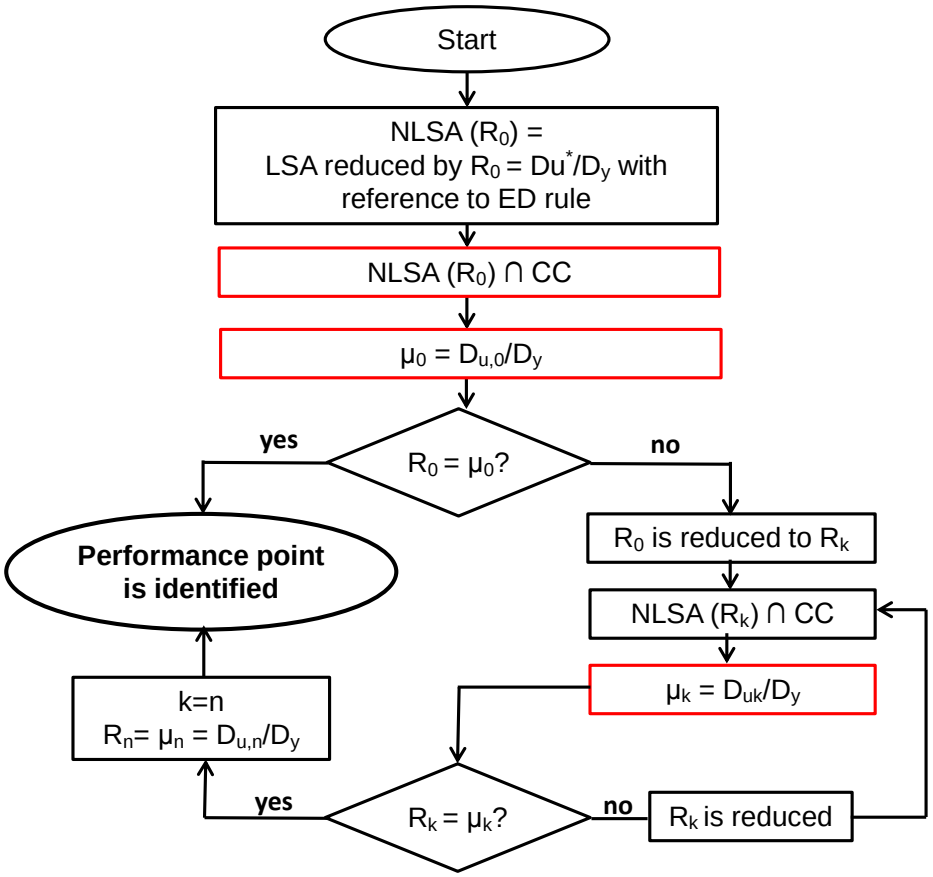

Figure 4-30: Iterative procedure for the identification of μ and R

This iteration is illustrated by Figure 4-29 and the flowchart in Figure 4-30, where LSA is first reduced by R_0 (reduction factor identified by the ED rule) in NLSA(R_0) and then intersected with CC: capacity curve, identified as discussed in section 4.6.1.Their intersection provides $\mu_0=D_{u,0}/D_y$ that identifies the performance point only if μ_0 is equal to R_0. In case this is not verified, the LSA is reduced up to identifying a value of the R_n that is equal to μ_n given by the intersection between the CC and NLSA(μ_n).

This iterative procedure for the estimation of the performance points is implemented in Visual Basic and integrated in the existing tool of FaMIVE. The performance point can be derived by a measured record of the LSA, if this is available, or the LSA can be estimated by referring to part 3 of the EC8 (CEN, 2005).

4.7 STEP 5: Derivation of the damage probability

In the literature, different methods for the derivation of the fragility curves are proposed to estimate the probability of damage of building classes, by taking into account the territorial distribution of the buildings classes, and related hazard intensity parameters in terms of peak ground acceleration or Macroseismic intensity (Porter et al., 2012).

Among the exiting approaches for the derivation of the fragility curves, the well-known HAZUS-MH (FEMA 2003) and N2 methods (Fajfar 2000) can be identified. These are the most commonly used in existing seismic loss estimation tools, such as SELENA (Molina et al., 2010), or ELER V3.0 (Erdik et al., 2010). In these approaches, the fragility curve is associated to a specific structural class adopted to characterise the global response of buildings. While HAZUS and ELER relay on predetermined sets of fragility curves, SELENA provides with the possibility of accommodating new fragility, if required.

Substantial work has been developed within the framework of the European projects PERPETUATE (D'Ayala and Lagomarsino 2015; Lagomarsino and Cattari 2015) and SYNER-G (Pitilakis et al., 2014) to develop robust fragility functions for masonry structures in historic centres using a performance point based approach.

Recently, an international, multi-institutional project sponsored by the Global Earthquake Model (http://www.globalquakemodel.org/) has developed complementary guidelines to derive vulnerability and fragility functions by empirical approaches (Rossetto et al., 2014), analytical approaches (D'Ayala et al., 2014), or by using experts' judgment (Jaiswal and Wald, 2013). The increasing research on both ground motion prediction and performance based assessment of existing structures, together with increasing availability of exposure data, has considerably improved the reliability of analytical approaches for the derivation of fragility curves.

Within this work, in agreement with N2 method (Fajfar, 2000), fragility curves for different limit states, as defined in GEM guidelines (D'Ayala et al. 2015), are obtained by computing the median and standard deviation of the thresholds defined for the damage states of sections 4.6.1.

The median and standard deviation are used to derive equivalent lognormal distributions. To this end, the median displacement for each damage limit states can be calculated as:

$$\hat{S}_{ds_i} = e^{\bar{\mu}_i} \qquad \text{with} \qquad \bar{\mu}_i = \frac{1}{n}\sum_{j=1}^{n} ln\, S_{ds_i}^{j} \qquad (16)$$

and the corresponding standard deviation as:

$$\beta_{ds_i} = e^{\bar{\mu}_i + \frac{1}{2}\sigma_i^2}\sqrt{e^{\sigma_i^2} - 1} \qquad \text{with} \qquad \sigma_i = \sqrt{\frac{\sum_{j=1}^{n}(ln\, S_{ds_i}^{j} - ln\, \bar{S}_{ds_i}^{j})^2}{n}} \qquad (17)$$

If only one index building is available, a random sample can be generated by considering the typical range values of the parameters assessed on site (i.e. Lower and Upper bounds) and assuming a normal distribution for each of the identified parameters. FaMIVE can also be run on the defined random sample, and once the performance thresholds are defined for the building sample in terms of mean values capacity and fragility curves can be derived for each building index of the random sample.

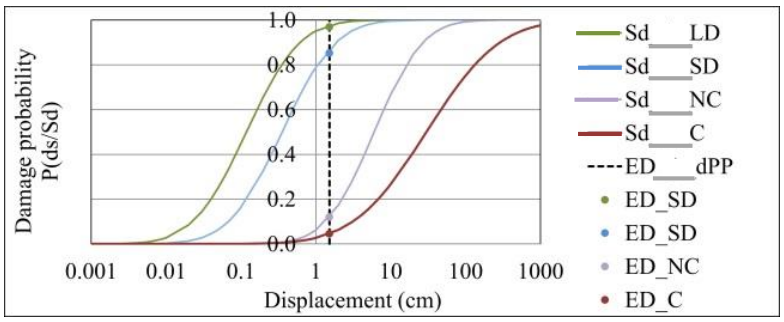

Figure 4-31: Damage probability plots derived from the iterative approach integrated in the new version of FaMIVE

If the sample of buildings has been surveyed on site, a real cumulative distribution can be produced and compared with an equivalent lognormal distribution, having calculated a median and standard derivation of the performance thresholds. As building response can be sampled by construction characteristics, class of mechanisms or level of vulnerability, the dispersion associated with building variability and modelling can be explicitly computed for each of these classes.

In order to quantify the probability that, given a performance point computed as in section 0, a specific building class or set of buildings, is in a damage states, an procedure in Visual basic has been developed and added to FaMIVE to automatise the calculation.

This procedure consists in the following steps:

- Derivation of the fragility curves for each damage states of section 4.5, by using the equation (16) and (17)
- Intersection between the fragility curves and the ED__dPP, representing the displacement of the performance point derived as discussed in section 0
- Quantification of the damage probability given by the intersection between the fragility curves and the ED__dPP.
- Graphical representations of the intersections between the fragility curves and ED__dPP for the derivation of the damage probability.

4.8 Final remarks

In this chapter, FaMIVE is presented as the method adopted in the hybrid approach of chapter 3 to estimate the analytical vulnerability of historic city centres.

FaMIVE is introduced in a new version, capable to assess the performance of irregular masonry constructions, by using new mechanical models developed to simulate the typical failure modes observed in buildings with irregular opening layout.

The parametric analysis carried out to investigate the capacity of the new version of FaMIVE has underlined the importance of assessing buildings by taking into account their real geometry in elevations and irregularity, since these affect the building performance and their failure modes under seismic events.

These results reflect what can be observed on site where buildings with irregular opening distribution and consequently an uneven strength distribution per storeys fail for failure modes that are partial failure modes since they are located in only one storey, are assessed as the prevalent and most vulnerable failure mode of the entire inspected façades.

Another important improvement of the existing FaMIVE approach consists in the development of the iterative procedure for the estimation of the performance points implemented to simplify the derivation of the damage probability.

5 LOG-IDEAH: VISUAL INSPECTION APPROACH TO ESTIMATE FAILURE MODES OF BUILDINGS IN HISTORIC CITY CENTRES

5.1 Introduction

This chapter focuses on describing the knowledge-based system LOG-IDEAH, developed to estimate the failure modes of historic city centres, and introduced in the hybrid approach of chapter 3 as the method adopted to estimate failure modes of masonry houses by the only use of observation and interpretation of seismic damage.

Before introducing the framework of LOG-IDEAH, in section 5.2 the existing remote sensing tools are reviewed with the scope at proposing these methods as possible approaches to estimate failure modes of historic city centres due to their robust capacity to record and to process large amount of data collected by visual inspection.

However, since the major limitation of these approaches consist of a lack of ability to identify the seismic damage in buildings that are not severely cracked, this shortcoming is overcome through the use a procedure based on situ observations that allow to collect cracks with different damage severity.

This procedure, proposed in section 5.3, consists of collecting damage in terms of class (e.g. diagonal crack, vertical crack etc.) and severity (e.g. light, moderate, etc.) at the scale of the single structural element (e.g. pier; column, etc.) and analysing this information to determine the failure modes at the level of the overall building.

Such a procedure requires that data is organised in a database with a hierarchical structure, which mirrors the urban structure of historic city centres, where urban blocks can be theoretically deconstructed into buildings, then buildings into macroelements, and finally macroelements into structural elements and artistic assets. This deconstruction, presented in section 5.4, underpins the procedure, introduced in section 5.5, used for recording the seismic damage.

The approach adopted for the interpretation of the seismic damage is discussed in section 5.6, where LOG-IDEAH, developed by the author, is introduced as the web based knowledge expert system capable to predict failure modes through rules defined for the assessment of the seismic damage. The framework of LOG-IDEAH is illustrated in section 5.7, and its developments are described in four stages.

The first stage introduces the logic trees and related rules, defined in section 5.8 and 5.9 respectively, for describing the logic adopted in LOG-IDEAH to interpret the seismic damage and to capture the failure modes. The logic tress and rules consist of a sequence of YES/NO logic gates that allow matching the recorded cracks with the crack patterns that describe the most typical failure modes of masonry houses, described in section 4.2 of chapter 4 and resumed in Appendix B. In section 5.9.2, rules that take into account the reliability of the collected data are also defined and these are adopted to identify not only the type of failure modes but also their level of probability of occurrence.

The second stage, presented in section 5.10 and developed in collaboration with the Department of Computer Science of the University of Bath, focuses on describing the ontology required to provide a formal representation of the terminology and the concepts underlined in the logic trees and related rules. This ontology is implemented within a Resource Description Framework (RDF) (Antoniou & van Harmelen, 2004), a standard model for data interchange on Web.

The third stage, presented in section 5.11, describes the code developed to implement the rule set in the logic trees. The coding of these rules is carried out by using the Answer Set Programming, a declarative computing language (Gelfond and Lifschitz 1988; Gelfond and Lifschitz 1991) suitable to code the declarative statements of the logic trees.

The last stage, presented in section 5.12, consists of illustrating the architecture of LOG-IDEAH, including the functions related to storing, processing, and sharing data among devices with internet access.

LOG-IDEAH is available online at (http://perpetuate.cs.bath.ac.uk/perpetuate-testing/) and it is optimised for Android, and MacOS operating systems. The current version of the web based expert system LOG-IDEAH has been applied by the author in Italy, and by other operators in Slovenia and Algeria in the framework of the FP7 PERPETUATE

project, funded by the European Union to develop guidelines for the vulnerability assessment and the risk reduction of historic assets in Mediterranean countries (http://www.perpetuate.eu/). Recently, LOG-IDEAH has been also used during the EEFIT mission to assess the failure modes of the masonry houses in Amatrice, in Italy, damaged by the earthquake in August 2016.

In section 5.13 the capacity of LOG-IDEAH to predict the failure modes is illustrated through an application of the tool on a building surveyed in L'Aquila after the earthquake in 2009.

The main achievements and final remarks conclude the chapter with section 5.14.

5.2 Seismic damage assessment of existing buildings by using remote sensing tools

Remote Sensing (RS) tools have long been adopted by several industry such as World Bank Group (http://www.worldbank.org/), Google (https://www.google.co.uk/) The Rochester Institute of Technology (http://www.rit.edu/), Image Cat (http://www.imagecatinc.com/) to perform damage building assessments, as pointed out by the several studies carried out with both airborne and space borne imagery (e.g., Kerle et al., 2008; Metternicht et al., 2005; Voigt et al., 2007; Zhang and Kerle, 2008). The RS tools have the advantage of acquiring and processing data within hours from an earthquake, therefore these technologies play an important role for initiating effective emergency response actions (Brunner et al., 2010). The results of the data analysis are typically presented in Geographic Information Systems (GIS) platforms or printed maps, which can be provided to rescue teams on the ground. The airborne and space borne images are taken from a quasi-vertical perspective, and hence efficiently detect severe damage due to total or partial failure of buildings or collapse of roof structures. However, damage that occurs on building façades cannot be easily identified by either airborne or space borne image (Kerle, 2010; Hassanzadeha et al., 2012; Wielanda et al., 2012, Maruyama et al., 2014, Galarreta F. et al., 2015).

A promising data source that can be collected by using RS techniques and delivers an improved level of damage details, is the one obtained from the airborne oblique imageries. These provide better resolution than vertical airborne data but they are difficult to integrate with other spatial information (Gerke and Kerle, 2011). More

recently, developments have been achieved by the use of pictometry data (Gerke and Kerle, 2011) that includes views from five directions (four oblique views from orthogonal directions, and a vertical image), and positional information that simplify the process of location and restitution.

However, although these tools allow the observation of damage on building façades, the literature review on this topic makes very clear that the class of damage which can be observed by these technologies requires being very severe. Therefore, with reference to EMS' 98 scale (Grünthal 1998), introduced in section 3.2, these tools are only capable to assess damage in class D4 (very heavy damage) and D5 (total or near-total collapse) since the differentiation between classes D1 to D3 is only possible through field investigations (Gerke and Kerle, 2011).

However, although currently the use of drones or omnidirectional cameras has improved the detection of the damage, the human eyes associated to the human judgements are still the best tool to capture damage of different severity that requires to be taken into consideration to identify all possible failure modes that can occur on buildings.

5.3 Seismic damage assessment of existing buildings through field inspections

Starting from the conclusions of the previous section, advantages and shortcomings of methods based on site inspection for the estimation of failure modes are discussed as follows.

One of the major benefits of collecting data by field surveys, instead of using satellite imagery or aerial pictures, consists of the possibility of better characterising buildings, which can be categorised according to their geometric features and deficiencies. Therefore, while satellite imageries and aerial pictures allow classifying buildings only by taking into account their structural resistance systems, by on site inspections more details of the constructions can be observed and more data can be collected to define building classes and their possible response and failure modes.

However, although there are several advantages in collecting data through field inspection, it is also important to take into account that only limited data can be

collected on site for a large number of buildings, since it is not possible to carry out detailed inspections at large scale, as discussed in chapter 2.

Therefore, while RS tools have the high capacity to collect extensive data in short time, tools based on situ observation necessarily need to adopt approaches that require only few parameters to estimate failure modes of buildings. This underlines the need of using methods for the data collection that clearly define the types of information required for the failure modes, and how this information can be observed and stored in order to overcome possible issues related to the lack and heterogeneity of input data, while preserving efficiency.

In section 3.3, through the examples taken from the on site inspections of the Nepalese houses, the essential information to assess the building performance by using visual inspection were discussed and defined as the minimum requirements to investigate the failure modes on buildings.

However, still another important issue needs to be discussed. This consists of proposing a suitable approach that can be adopted to store the observed damage by recording class, position and severity of cracks (minimum input required for the identification of failure modes).

As discussed in section 3.2, the existing guidelines for the post-earthquake assessments do not provide a systematic procedure to record the damage, as these standards only provide guidance to define deficiencies and damage severity by the use of general description of the causes of damage.

In the literature, Vatan and Arun (2010) propose the only example of approach that defines a systematic method to record the seismic damage. This method, based on visual inspection, proposes to record the seismic damage of a structural element through a reference axial system defined in the geometric base plan of a building. Letters in the horizontal direction and numbers in the vertical direction label this axial system, given by axial lines along the structural elements identified in the building plan. This grid is used for storing the position of damaged structural elements. The major limitation of the present method consists in requiring detailed internal inspections, which might be difficult to perform in highly damaged buildings, thereby highlighting the need to propose a visual inspection method that estimates failure modes by only using data collected from external inspections of buildings.

However, it is important to mention that the use of a visual inspection approach that provides failure modes by using data collected from street is an acceptable approximation, by taking into account that the typical failure modes of masonry buildings, as presented in section 4.2, are generally characterised by cracks that occur on structural elements of the building façades.

The above considerations inform the data collection protocol for the storage of the seismic damage required to estimate the failure modes, proposed and tested in the remainder of the chapter.

5.4 Seismic damage assessment through field inspections based on a hierarchical approach

The approach proposed in this section to store class, severity and position of damage requires the introduction of a hierarchical model, which allows deconstructing urban blocks into architectonic assets, architectonic assets into their macroelements and macroelements into their structural elements and artistic assets. This deconstruction sets out membership links defined through the hierarchical model, initially presented for individual historic buildings by the author within the PERPETUATE Framework (in the Deliverable 5 by D'Ayala and Novelli 2010; Deliverable 30 D'ayala et al. 2012; and Novelli and D'Ayala, 2015) and later extended to include also the relationship between buildings in urban blocks, by providing the framework for taking into account their interaction.

Such a model, pictured with the pyramid in Figure 5-1 is composed of the following levels:

- **Urban Blocks (UBs):** the Urban Blocks can be composed by isolated building or by building clusters defined as an agglomerate of adjacent and connected constructions (see section 4.2.)

- **Architectural Asset (AA):** according to the classification devised in the PERPETUATE project (www.perpetuate.eu), the AA classes cover seven different classes of assets according to their architectural morphology and use. Of these seven classes, the approach proposed here is adequate to assess 1) isolated buildings of both class A: palaces, castles, religious

houses, caravansaries, collective buildings; and class B: churches, mosques, baptisteries, mausoleums, hammam, modern theatres, markets and bazaars, industrial buildings and 2) building clusters of class G: aggregate of residential buildings. For more details on the architectural assets classification see Deliverable 4 of PERPETUATE project (Abbas et al., 2010).

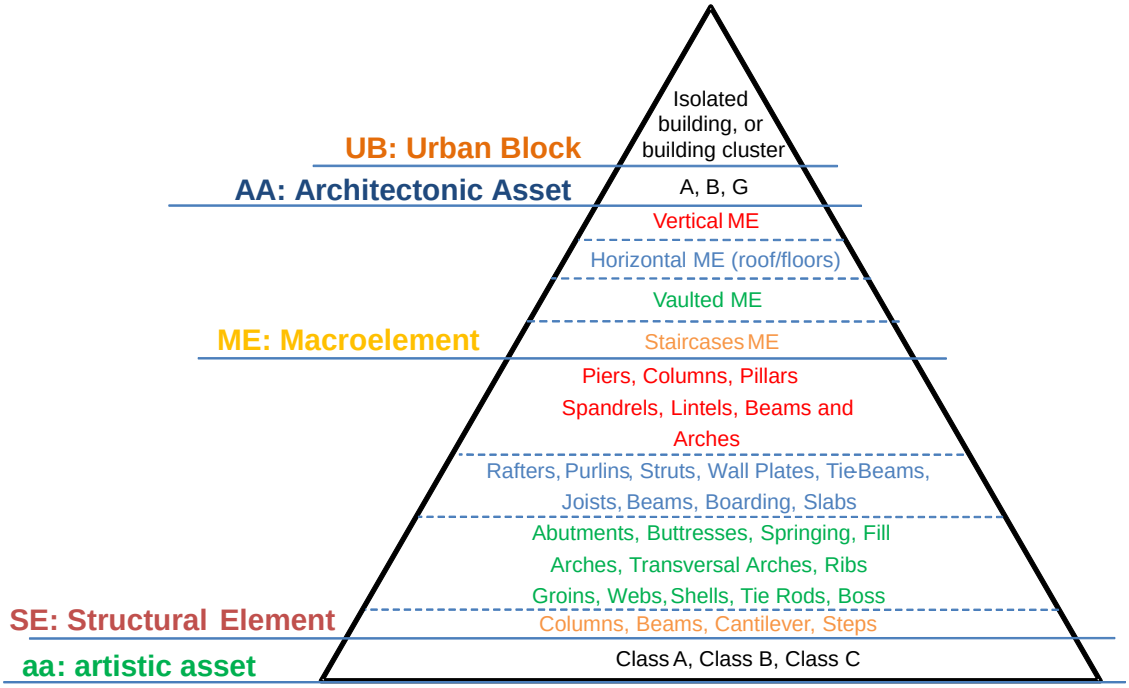

Figure 5-1: Hierarchical model for Architectural Assets

- **Macro-Elements (ME):** this level covers four classes: Vertical ME (VeME), Horizontal ME (HoME), Vaulted ME (VaME) and Staircases ME (StME). More detail on this classification and their interactions presented in section 5.4.2.

- **Structural Element (SE):** this level covers four classes. For each class of ME, defined above, the elements composing them with distinct structural role are identified and classified. More detail about this deconstruction and classification is provided in section 5.4.3.

- **artistic asset (aa)**: the artistic assets are classified depending on their relationship with the structural elements. Three classes are considered: class A, structural elements with artistic value; class B, artistic assets, which are strictly connected to structural elements but do not have a structural function; and class C, artistic assets, which are not strictly connected to structural elements and do not have a structural function. The aas in class A (e.g.: carved stone columns) have structural functions and play a structural role in a building, while the aas connected to SEs in Class B (e.g.: frescos, stuccos, cornices), and or jutted out from SEs in Class C (e.g. pinnacles) have only artistic value.

These three classes are also subdivided in three subgroups, which specify the class of SE to which the aa is connected to. These subgroups are defined as follows:

1) artistic assets on vertical structural elements,
2) artistic assets on horizontal structural elements,
3) artistic assets on vaulted structural elements.

By means of example, Appendix D shows some typical aas that can be identified on vertical SEs (Piers, Columns and Pillars), horizontal SEs (Spandrels, Lintels, and Beams) and Arches, by following the classifications provided above. More details on the artistic asset classification can be found in the Deliverable 4 of the PERPETUATE project (Abbas et al., 2010).

5.4.1 *Hierarchical approach applied to building aggregates in historic centres*

As discussed in the previous section, the hierarchical model in Figure 5-1 can be applied to isolated buildings of Class A and B or to building aggregates of class G. However, since the aim of this work is to assess the seismic vulnerability at territorial scale, this section focuses on illustrating how the model is applied to historic city centres (class G) damaged by earthquakes.

In order to apply this model, the city centre under examination needs to be deconstructed in UBs, classified by to their layout according to their geometric plan and the number of buildings pertaining to them, as this allows recording how the buildings are laid out and connected to each other in the UBs. The buildings (AA) are then

classified according to whether they are still standing, damaged or collapsed. Once this has been recorded, inspections are carried out only on buildings that have damage. Surveys, as discussed previously, are performed on site, but, being mindful of safety conditions in the aftermath of an earthquake, the survey is conducted without entering the building.

This implies that data can only be consistently collected on VEMEs (façades). Therefore in the remainder of this work the hierarchical model of Figure 5-1 is applied only to deconstruct 1) UBs in AAs 2) AAs in VEMEs, 3) VEMEs into vertical SEs (piers, columns, pillars) and horizontal SEs (spandrels, lintels, arches and beams) and 4) SEs in aas.

This implies that specific considerations and judgments on ME such as floors and roof that have been not inspected are made at a later stage, as discussed in section 5.9.

In the next sections, the pyramidal relationship between each level of the hierarchical approach is univocally set out by creating taxonomic strings that allow creating the same hierarchical links pictured in the model of Figure 5-1.

5.4.2 *Relationships between urban blocks and architectonic assets and between architectonic assets and vertical macroelements*

In order to create membership links between Urban Blocks and Architectonic Assets and between Architectonic Assets and Vertical Macroelements, located in the first three levels of the pyramid in Figure 5-1, a taxonomic string is defined.

The first label of the taxonomic string is given by a label that is generally a distinctive number or distinctive letter associated to each UB identified in the historic city centre. Another label, corresponding to the second label of the string, is associated to all AAs identified in the UBs.

The third label of the string is a label related to the VeMEs. A distinctive number is associated to each VeME. This numbering is given in an anticlockwise direction. The orientation of the VeMEs, preceded by the number associated to the façade, is also part of the third label of the string. If some VeMEs in a building have been not inspected, the label associated to them corresponds to digit ‘zero’. The total length of this taxonomic string varies according to the number of the façades. The format of the

string that creates the hierarchical links between an UB, its AAs and their VeMEs is called [UB number.AA number] and it is defined as follows:

$$[UB\ number.AA\ number] = \sum_{k}^{tot\ number\ of\ VeMEs} \begin{bmatrix} UB\ number.AA\ number.VeME\ number_{\ k} \\ orientation \end{bmatrix} \quad (18)$$

where *UB number* is the label associated to the urban block, *AA number* is the label associated to the building, *VeME number* is the number associated to the façade, and orientation is the orientation of the façade.

The symbol Σ points out that the string stores information at the level of the entire AA by providing record for all VEMEs, even if these have not been inspected. This implies that missing information for any one of these elements is also part of the record stored in the string, which is also used to estimate the probability of occurrence of the identified failure modes, as discussed in section 5.9.

5.4.3 *Relationships between vertical macroelements and structural elements*

In order to create the membership link between VeMEs and SEs, the third and fourth levels of the pyramid in Figure 5-1, VeMEs are deconstructed into horizontal SEs and vertical SEs, as shown in Figure 5-2.

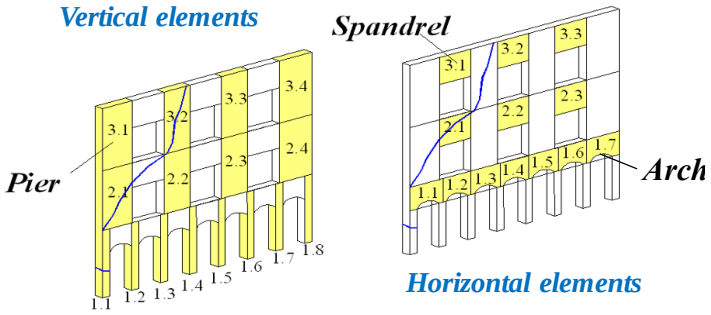

Figure 5-2: Naming of the structural elements of a VeME. Two numbers are associated to each vertical and horizontal element, where nf (storey number) identifies the number of the floor and i (position) the position of the element at each floor (e.g. the pier located at the second position of the third floor has label P3.2)

This deconstruction allows associating, to each single SE, a label given by two digits representing the storey number (nf) and the position (i) of the SE at its storey number (nf). By associating this label to each SE, the position and class of each

structural element is univocally identified within two different grids in the VeME, one defined for the horizontal SEs (piers, pillars or columns) and the other defined for the vertical SEs (spandrels, beams or arches) as illustrated in Figure 5-2.

[P (or S)nf.i] is the taxonomic string introduced to record the position of the single P: pier, pillar or column ; or S: spandrel, beam or arch in a specific VeME. This is defined as follows:

$$[P\ (or\ S)nf.i\ ] = \quad (19)$$

$$= [UB\ number; UB\ number.AA\ number;$$

$$UB\ number.AA\ number.VeME\ number_{orientation};$$

$$nf; i]$$

This string allows creating the membership links between VeMEs and their SEs, while maintaining the membership links between UB, AAs and VeMEs set in the previous section and in the pyramidal structure illustrated in Figure 5-1.

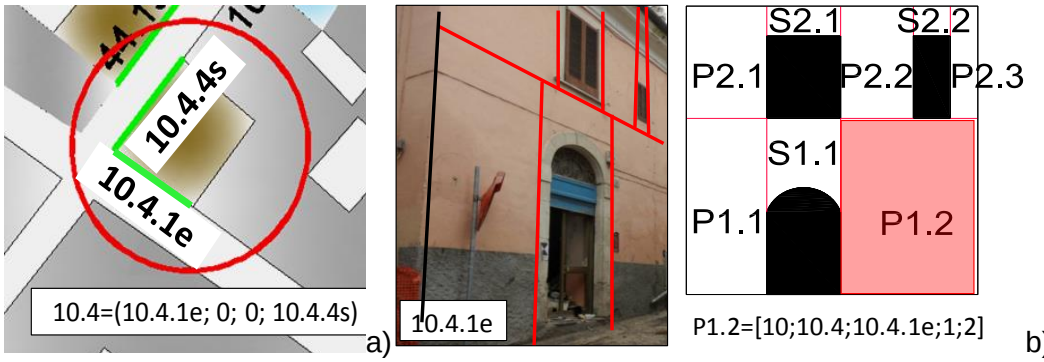

Figure 5-3: a) to correlate AA and its VeMEs; b) on the left: deconstruction of the VeME [10.4.1e] in SEs; on the right: string for correlation a SE to a specific VeME in an inspected AA

The format of this taxonomic string is illustrated, by means of an example, a building inspected in L'Aquila (Italy) after the earthquake in 2009, shown in Figure 5-3.

Before defining the string, a label has been associated to the UB, to its AAs and VeMEs. The building selected for this example, reported in Figure 5-3a, is the AA [4] located in the UB [10]. This building has four VeMEs. Only the VeME [1] and VeME [4]

with east and south orientation, respectively, are inspected. VeME [2] and VeME [3] are not accessible from the street, since these are party walls between the AA under inspection and its adjacent buildings. The taxonomic string that link UB, AA, and the VeMEs of this building is defined as follows with reference to the expression (18)

$$[10.4] = [10.4.1e, 0, 0, 10.4.1s]$$

On the left of Figure 5-3b, VeME [10.4.1e] is deconstructed in its SEs through a grid that highlights piers and spandrels, while on the right of Figure 5-3b, the same façade is reported in a sketch that simplifies the identification of the SEs. In the sketch, the (horizontal and vertical) SEs are highlighted by labels that indicate the class and position of the single identified SE.

The next taxonomic string is defined for the pier, highlighted in red, located at the storey [1] in position [2]. The string has the following format, and it is defined with reference to the expression (19)

$$[P1.2] = [10;10.4;10.4.1e;1;2]$$

5.4.4 *Relationships between structural elements and artistic assets*

This section creates the membership link between aas and SEs, positioned in the forth and the fifth levels of the pyramid in Figure 5-1.

Before setting these relationships, the aas are first classified according to:

- the type of SE, to which the aa is connected (see section 5.4.1 and in Appendix D) and
- how the aa is connected to the SE (ex. aa is SE; or jeting from a SE, or directely connected to a SE, referring to the grid defined for the SEs in section 5.4.3

[aaA,1(or B,or C,or 2,or 3); P (or S) nf.i] is the taxonomic string introduced to record class and position of an aa identified on a P (piers, pillars or columns) or S (spandrels, beams or arches) of a specific VeME. This string is defined as follows:

[aaA,1(or B,orC,or 2,or 3); P (or S) nf.i] = (20)
[UB number;UB number.AA number; UB number.AA number.VeME number orientation; nf;i,aa class]

where (*nf. i*) is the position of the identified aa on a pier (P) or a spandrel (S), defined by referring to the label associated to the SEs in section 5.4.3, and *aa class* refers to the class associated to the identified aa, defined according to Appendix D.

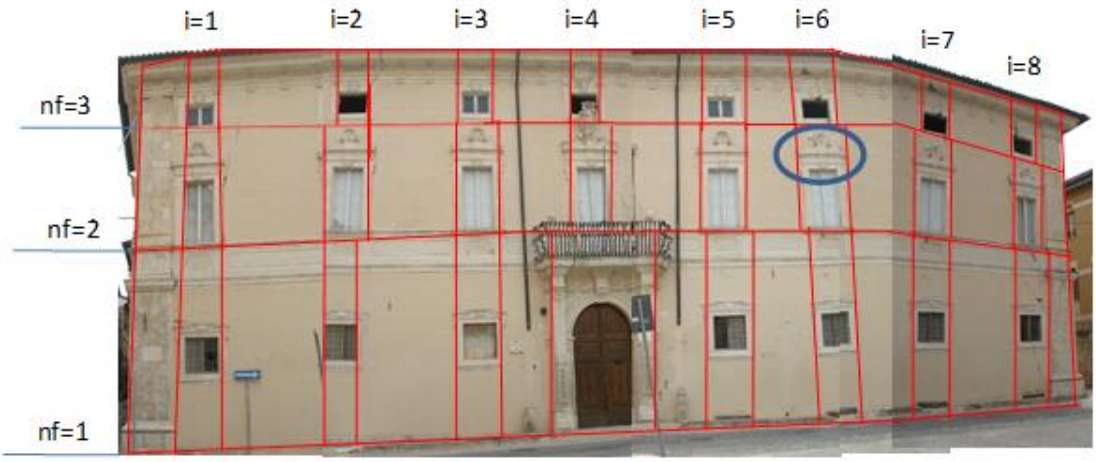

Figure 5-4: Deconstruction of the VeME [7.4.3e] in SEs; taxonomy for aa (highlighted in blue) is given by UB number; AA number; VeME number + orientation; position of the SE = (nf; i); aaclass]

This string allows creating the membership links between aas and their SEs, while maintaining the membership links between UB, AAs, VeMEs and SEs set in the previous sections and in the pyramidal structure illustrated in Figure 5-1.

The format of this taxonomic string is illustrated by means of an example, a building inspected in L'Aquila after the earthquake in 2009, shown in Figure 5-4.

Before defining this string, labels are associated to the UB, to its AAs and VeMEs. The UB has a digit [7], the AA has a digit [4], and the façade under consideration is the VeME with digit [3] and east orientation.

The string (20) is specifically defined for the aa highlighted by the blue circle. The selected aa is a decorative stucco, cornice for the window, classified as a non-structural element, fully connected to the spandrel (S) at the storey [2] in position [6].

The taxonomic string for this element has the following format:

[aaB2; S2.6] = [7, 7.4; 7.4.3e; 2.6; B2]

5.5 Local damage type and local damage level

In the next sub-sections, the typical damage types and related damage severity that can be identified on SEs and aas are classified and specific taxonomic strings are introduced to set membership links between damage type and damage level as attributes of SEs and aas.

The damage type and damage scale follow the classification borrowed from Deliverable 5 of PERPETUATE project (D'Ayala and Novelli 2010).

5.5.1 *Damage recording for structural elements*

The majority of the damage that can be observed on SEs relate to cracking caused by tensile actions and can be classified according to its alignment as reported in Figure 5-5, where the most common damage types on SEs are listed as follow: V, Vertical crack; H, Horizontal crack; D1 and D2, Diagonal crack from left to right and from right to left, respectively; and X crack.

However, the cyclic nature of seismic loading can also cause loss of material due to high compression. This class of damage is classified in S: spalling or Cr: crushing, as reported in in Figure 5-5.

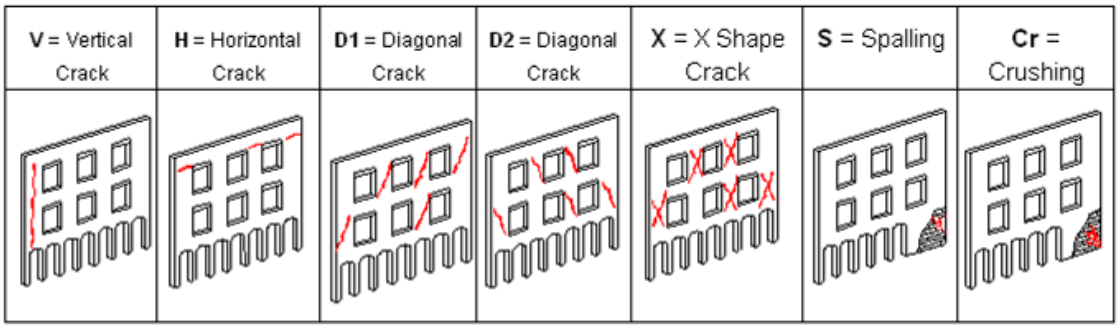

Figure 5-5: List of structural damage types identifiable on site

The damage severity is classified according to the four damage states defined in section 4.5, introduced as follows: (1) Light damage (LD); (2) Severe damage (SD); (3) Near collapse (NC); (4) Collapse (C).

In order to define the position of the damage on SEs, the same grid introduced in 5.4.2 to deconstruct the VeME in horizontal and vertical SEs is also adopted to define the position of damaged SEs and consequently to record the location of the identified damage.

[Pier (or Spandrel) $_{cracklocation}$*]* is the taxonomic string introduced to record the damage type, damage levels and location of damaged SEs. This string is defined as follows:

$$[Pier\ (or\ Spandrels)_{cracklocation}] = \\ = [UB\ number; UB\ number.AA\ number; \\ UB\ number.AA\ number.VeME\ number \\ orientation; nf; i; damage\ type; damage\ severity] \quad (21)$$

This string, as defined, contains all information required to store the seismic damage, with reference to the pyramidal structure defined in Figure 5-1 among UB, AAs, VeMEs, and SEs, so that the location and pertinence of any crack in space is defined with respect to the urban block.

The format of this taxonomic string is illustrated by means of an example in Figure 5-6. The attention is on the VeME [1], with east direction, of the AA [4] in the UB [10] introduced in Figure 5-3. The deconstruction of the VeME in piers and spandrels is shown in red, while its seismic damage is highlighted in blue.

Figure 5-6: Damage identification for VeME [10.41e]

Once the damage is identified on each SE, this is defined according to its type, level and position, as reported in Table 5-1, which summarises each single crack observed and recorded for this VeMe.

Table 5-1: List of the structural damage observed for VeME [10.4.1e]

UB	AA	VeME	Damaged SE class	Position of the damaged SE (nf; i)	Damage type	Damage level
10	10.4	10.4.1e	Pier	1.2	V	SD
				2.3	V	SD
				2.2	D1	SD
				2.2	D2	SD
			Spandrel	1.1	V	SD
				1.1	D2	SD

As reported in this table, some SEs have only one crack (i.e. piers in position 1.2 and 2.3), while others (i.e. pier in position 2.2 and spandrel in position 1.1) have more than one. The damage is classified as vertical or diagonal cracks. The damage severity is defined as SD (Significant Damage).

For the sake of illustration, this string is used to describe the damage on the pier in position [2] of the storey [1] damaged by a V crack with SD severity and the spandrel in position [1] of the storey [1] damaged by a V crack and D2 with both SD severity (highlighted in pale blue in Table 5-1). The strings for these two damaged SEs are defined as follows:

[Pier_cracklocation (1.2)]=[10;10.4;10.4.1e;1;2; V; SD];
[Spandrel_cracklocation (1.1)]=[10;10.4;10.4.1e;1;2; V; SD] +
[Spandrel_cracklocation (1.1)]=[10;10.4;10.4.1e;1;2; D2; SD].

5.5.2 *Damage recording for artistic asset*

Damage types and damage levels of the aas classified as SEs and belonging to class A in Appendix D, follow the classification reported for the SEs of section 5.5.1.

The aas damage types connected and jutting out from the SEs, and reported in class B and C of Appendix D, refer to the classification summarised in Table 5-2 and

Table 5-3 and set out in Deliverable 4 (Abass et al. 2010) and Deliverable 5 (D'Ayala and Novelli 2010) of PERPETUATE project.

Table 5-2: Local damage type for artistic asset of class B

d-Ba: detachment and loss of parts	**d-Bb:** spalling	**d-Bc:** cracks	**d-Bd:** irreversible deformations
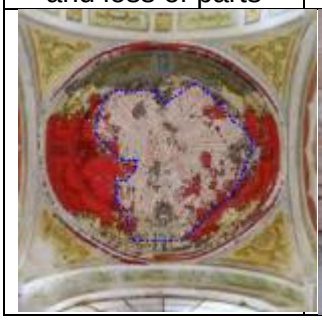			

Table 5-3: Local damage type for artistic asset of class C

d-Ca: dislocations	**d-Cb:** unthreading or failure of connections	**d-Cc:** overturning
		

In the same deliverables, damage levels for classes B and C are also defined, and they are introduced with reference to the movement level of the aas respect to the SEs to which the aas are attached. The definition of these damage levels derives from the need of monitoring the connection between the aas and SEs and preventing architectural and artistic losses with suitable interventions of restauration, if required.

The damage severity of the aas in class B and C are defined by five levels defined as follows:

- LM: Little Movement (micron, integrity is not compromised),
- EM: Evident Movement (crack appearance or spalling, integrity is locally compromised),

- TM: Total Movements (major loss of integrity, loss of substantial portions),
- C: Collapse.

In order to set the membership link between damage position, damage type and damage level of aas, and to maintain the pyramidal structure defined in Figure 5-1, the strings *[ArtisticPier_cracklocation (or ArtisticSpandrel_cracklocation)]* are introduced, as follows:

ArtisticPier_cracklocation (or ArtisticSpandrel_cracklocation) = [UB number;UB number.AA number; UB number.AA number.VeME number orientation; nf;i, aa class; damage types of the aa, damage level of the aa]. (22)

Figure 5-7: Damage identification for VeME [7.4.3e]

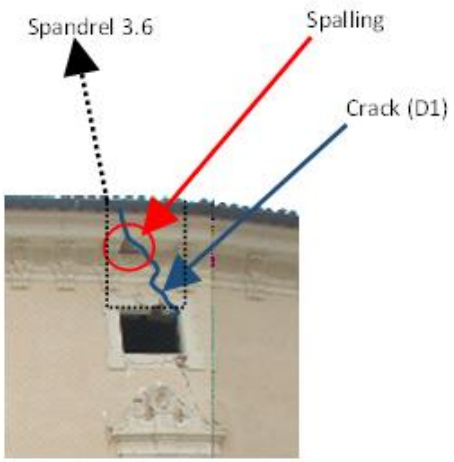

Figure 5-8: A close up photo of the specific damaged spandrel

The format of this taxonomic string is illustrated by means of an example in Figure 5-7. The AA [7.4] introduced in Figure 5-4 is also reported in this section in order to discuss its seismic damage and to illustrate how this damage can be recorded. In this example, the attention is focused on the VeME [3] on the east direction, where its seismic damage is highlighted in blue.

For the sake of illustration, this string is used to describe the damage on sculpted stone window frame, located at the spandrel in position [6] of the storey [3]. The spandrel is aa and it is classified as A2 (Carved or plastically decorated horizontal structural assets in Apeendix A), damaged by D1 (Diagonal) crack with SD (Severe Damage) while the sculpted stone window frame on the spandrel is classified as B2 (Assets connected to horizontal structural elements in Apeendix A) and it is spalling (d-Bb in Table 5-2). The cracks (d-Bc in Table 5-2) have a EM (Evident Movement). The close up of the observed damage is reported in Figure 5-8 and the related string is defined as follows:

[ArtisticSpandrel_cracklocation (3.6)]=[10;10.4;10.4.1e;3;6; A2, D1; SD]
[ArtisticSpandrel_cracklocation (3.6)]=[10;10.4;10.4.1e;3;6; B2, d-Bb; EM]
[ArtisticSpandrel_cracklocation (3.6)]=[10;10.4;10.4.1e;3;6; B2, d-Bc; EM]

5.6 Interpretation of the seismic damage collected by visual inspection

The seismic damage collected by using the hierarchical approach presented in the previous sections is interpreted by using a Knowledge-based Expert System (KBES).

The KBESs are commonly adopted to solve complex engineering problems without resorting to intensive investigations or extensive analysis but only using systems capable to emulate the decision-making ability of human experts (Watson, 1998, Berrais, 2005).

In particular, their high ability to acquire new knowledge as well as learning from existing information is a fundamental requirement for a visual inspection tool based knowledge system to predict failure modes in buildings, specifically if these have been only partially inspected after an earthquake.

Figure 5-9 illustrates this concept by way of example. Specifically the aim is to highlight the importance for a visual inspection tool to provide solutions by replicating

the thought process of a surveyor and by using engineering judgements to solve problems with incomplete data.

The building in Figure 5-9 was assessed in Algiers, having been damaged by the 2003 Bourmedes earthquake. The façades that have been inspected are the ones reported in the picture: façade 1, 2, 3, and 4 in Figure 5-9a. The other façades of the building have not been inspected since they were located on a street that was not accessible during the time of inspections.

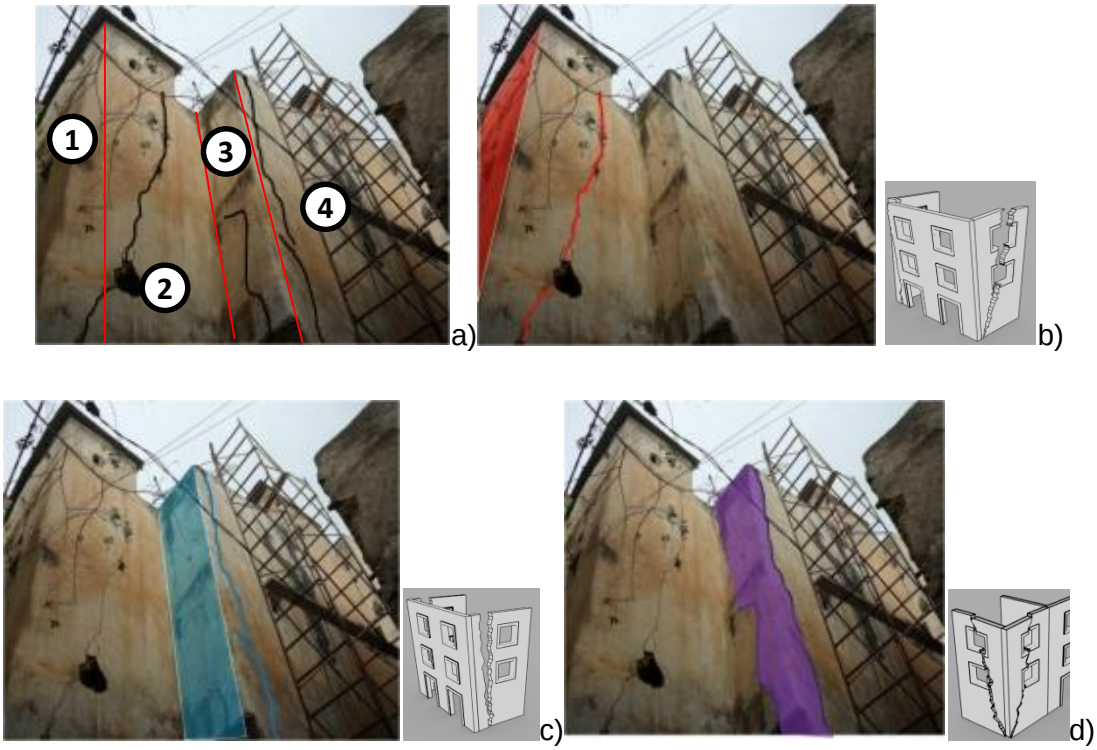

Figure 5-9: Visual inspection of a building in Algiers, and assessment of the damage caused by the Bourmedes earthquake in 2003 (Novelli et al., 2015b)

The seismic damage of the building is marked in black in Figure 5-9a. Several cracks are captured and due to their complex pattern, it is difficult to univocally identify the possible failure modes that are occurring on the building, if engineering judgement is not used.

In order to illustrate how a surveyor assesses a building, the highlighted cracks (in black) are differently grouped by using engineering judgement in Figure 5-9b, Figure 5-9c, and Figure 5-9d in order to illustrate the possible failure modes that the cracks

might be determining. The failure modes mentioned below need to be referred to Appendix B.

- The red diagonal crack on the façade 2, highlighted in Figure 5-9b, might point out the occurrence of the combined failure mode B1. This type of failure mode causes an overturning of the façade 1 and a rotation of the façade 2. However, this failure mode can be verified only if the façade opposite to the façade 2 is inspected.

- The blue vertical crack on the façade 4, highlighted in Figure 5-9c, might point out the occurrence of the out-of-plane failure mode A. This type of failure mode causes an overturning of the façade 3 for lack of connections with the adjacent façades. However, this failure mode can be only verified if the internal façade opposite to the façade 4 is inspected and it is verified that the two façades are detached from each other.

- The purple cracks on the façades 3 and 4, highlighted in Figure 5-9d, might point out the occurrence of the combined failure mode C. This type of failure mode causes an overturning of the corner of the building. However, in order to ensure that C is occurring, there should be evidence that façades and floors are well connected to each other.

The example reported in Figure 5-9 highlights that the visual inspection is not always straightforward, in particular when cracks observed on a building contribute to the occurrence of different types of failure modes, and experts' judgement or more data are required to assess the failure modes of a building.

This confirms that a visual inspection tool based on KBES should use the same logic adopted by surveyor in assessing buildings and in overcoming issues related to incomplete, inconsistent and defaulting data derived from limited observation.

Moreover, it is also important that the KBES is able to handle possible human errors, deriving from inaccurate hypothesis on behaviour of a specific building class.

This underlines that the KBES should be implemented with alert systems to avert possible errors and to mitigate their effects (Gomes et al., 2013) in order to provide a tool that can be confidently used by surveyors with limited experience in seismic engineering (Carreño et al., 2012).

The implementation of KBESs requires advanced programming skills and specific languages since these systems require a substantial knowledge of reasoning process adapted to model information (Gomes et al., 2013). Comprehensive reviews of KBESs used to solve specific problems in the field of civil engineering were carried out by Adeli (2001) and more recently by Lu et al., (2012).

Further consideration is also required to develop “on-line” KBES, i.e. web based expert systems (WBES), since the reasoning and information modelling programming need to be coupled with specific routines allowing to exchange data from any place and at any time (Nofal and Fouad, 2014).

The next subsection presents a review of existing applications of the KBES in the different fields related to civil/seismic engineering, afterwards the architecture of the visual inspection tool proposed for the present work will be introduced.

5.6.1 *Review of the existing Knowledge Expert Based System (KBES) in the civil/seismic engineering*

The traditional use of computers allows identifying finite number of solutions through algorithms and does not provide users with the possibility to contribute with their expertise and judgements into the research of solutions (Kuhn & Inan, 1989; and Areitio, 1990). One of the major advantages of the KEBS consists of offering to users this opportunity of interacting with their knowledge into the elaboration of solutions, since the KBESs is capable to transfer knowledge and expertise from humans to computer and to solve engineering problems, whereby numerical models are not available or suitable.

In the past, KBESs have been applied to solve civil-engineering problems by providing structural engineers with decision-making systems to support and to guide them in the design of new constructions, as discussed in the review presented by Berrais and Watson (1993) and Berrais (2005). Some examples of KBES used to design bridges and reinforced concrete buildings can be found in Edlund et al. 1994;

Kumar and Krishnamoorthy, 1996; Lehane and Moore, 1996; Berrais and Watson1993. KEBSs have been also proposed for engineering diagnosis of existing buildings of their performance with the scope at identifying retrofit interventions (Raphael and Smith, 1998 and Berrais, 2005). In the literature, there is also an example where a KBES is used to identify the damage in existing engineering facilities such as bridges, or airplanes by taking into account (dependent) forces and faults/defects that may occur and/or grow during the life times of the inspected facilities (Natke and Yao, 1993).

In the field of the seismic damage assessment of buildings, only few applications are specifically developed with KBES. Among these existing applications, the tool named DASE has been used to assess reinforced concrete buildings by Melchor-Lucero and Ferregut (1995) and the tool named SPERIL was used to assess reinforced concrete and steel buildings in an application of Ogawa and Fu (1981).

Another example of KBES is given by the tool IGOR (Cadei et al., 1990) developed to estimate the performance of masonry buildings by encoding expertise of engineers and architects in estimating the structural behaviour of masonry structures and evaluating the most suitable strengthening interventions. This approach requires a large number of input parameters, to estimate the possible critical scenarios for a building, and to compute the probability of occurrence of specific scenario of damage. However, since IGOR system is not always able to simulate all critical scenarios of damage, this tool proposes strengthening interventions for buildings based on economic considerations rather than structural considerations (Dovers, and Handmer, 1995).

Most recently, KBESs are also used to assess the performance-target ground acceleration of schools in Taiwan by a tool based on a system that integrates a support vector machine with a messy genetic algorithm, where the expert knowledge is adopted to identify solutions that can be extended to similar problems in the future (Chen et al. 2012).

KBESs were also adopted to evaluate seismic risk in an urban area (Cardona, 2004, Carreño et al,. 2007) and to measure performance and effectiveness of disaster risk management strategies at national, subnational, and local levels (Carreño et al., 2007b). This is an artificial neural network and fuzzy logic approach, which defines the safety level of buildings by computing a damage index as a function of the following three parameters: damage levels on structural and non-structural elements, soil

conditions and state of the buildings before the seismic event. Since this approach aims at providing the level of safety, the damage index is calibrated on the severity of damage rather than on the class of damage.

Most recent applications of KBES for seismic risk management are reported in Tesfamariam et al. 2010. This application is based on a multiple decision makers and fuzzy utilities proposed to select seismic retrofit implementation of existing buildings by taking into account not only engineering performance indicators but also uncertainties related to social factors such as life cycle costs, aesthetics, etc.. In particular, for the mentioned social uncertainties, heuristic hierarchical structure are proposed and tested on a three storey building in reinforced concrete. Another application of KBES used for the seismic risk management field is proposed by Vahdat et al. (2014) who developed a system capable of integrating various perspectives of seismic risk, conducting seismic risk assessment and handling uncertainty within risk assessment and supporting mitigation strategies.

Currently KEBS also finds a large application in the field of the seismic risk assessment, since decision-making systems are often jointed with GIS tools (Morandi et al 2014, Jaramillo et al. 2016) that are a good support in the representation of the seismic risk. The use of KBES in this filed is strongly recommended since the expert judgements are fundamental to evaluate how socioeconomic conditions effect on the physical damages (Salgado-Gálvez et al. 2016).

A number of KEBSs, in a web environment (WBES: Web Based Expert System) are also developed, although Web based applications are a complex challenge in multidimensional projects since scientists have recognized this complexity of and the need for referring to protocols in 1998, the year where Web Engineering was introduced in the Web applications (Ginge and Murugesan 2001). WBES and Web Engineering concerns and discussions have started almost simultaneously (i.e. around the second half of 1990's) within the scientific community, although there are still very few references on the Web engineering field (Dokas 2005).

In particular, in the field of the seismic engineering, as discussed above, the decision-making systems are adopted to estimate the social impacts on both risk assessment and risk management, and therefore they are not suitable to capture the knowledge and judgements used by engineers to investigate failure modes of buildings. Moreover, these are not developed as WBES.

In the next section, the architecture of LOG-IDEAH is presented in order to overcome the lack of the tools in a web environment that can be used to interpret seismic damage observed on site within WBES.

5.7 Architecture proposed for LOG-IDEAH

As underlined from the review in the previous section, existing applications of KEBS for the evaluation of the failure modes of masonry structures are not available, since these systems, even if they have been applied for the detection of the seismic damage are not specifically developed for the identification of the failure modes.

In this section, a tool for the estimation of the failure modes of historic city centres by visual inspection is proposed with the scope at providing a KBES within a web environment.

This tool is LOG-IDEAH: “LOGic trees for Identification of Damage due to Earthquakes for Architectural Heritage”, described in the following four stages, and detailed point by point in the next sections.

- **Knowledge acquisition and organisation of rules for the estimation of failure modes of buildings fully/partially inspected**

  The expertise of seismic engineers and post-earthquake surveyors is harnessed to define the engineering knowledge, through the facts and the rules that are adopted to interpret seismic damage collected by following the hierarchical approach described in the previous section and to determine possible failure modes. The thought process underlying this interpretation is visualised in logic trees, introduced in section 5.8. An example of these logic trees is presented and discussed in section 5.8.1. The complete set of logic trees is collated in Appendix E.

  In section 5.9, additional rules are also introduced to illustrate how failure modes are estimated on buildings that have been only partially inspected. Finally, in section 5.9.2, rules for the definition of the level of occurrence of the failure modes are defined.

- **Knowledge representation.**

  The domain knowledge is represented by describing the ontology introduced to define the terminology and the concepts contained in the logic trees. Since the logic trees process the data collected according to the hierarchical approach presented in section 5.4, the ontology introduces semantic definitions of each term used, which maintain the membership link introduced in the hierarchical approach.

  This ontology is implemented within a Resource Description Framework (RDF) presented in section 5.10.

- **Answer Set Programming (ASP)**

  An Answer Set Programming language (ASP) (Gelfond and Lifschitz 1988; Gelfond and Lifschitz 1991) is adopted to connect the terms defined in the ontology through the rules outlined in the logic trees. The features of this language are described and an example of ASP routine for LOG-IDEAH is provided in section 5.11.

- **Web-based interface**

  In section 5.12, a web interface is developed in order to provide a platform for data collection and data processing. Input data, collected by following the hierarchical approach of section 5.4, is recorded in XML format in the mentioned website, and the ASP, adopted to codify the logic trees in rules for the estimation of the failure modes, is used to analyse the stored data. The results produced by the ASP are also directly provided in xml format, added to the input script and immediately visualised on the web interface. An example of this process is shown at the end of section 5.13.

The third and fourth stage of this process, were implemented in collaboration with the Department of Computer Science of the University of Bath, who has supported the author in encoding the ASP and developing the website. Details of this process are also published in Novelli et al., (2012).

5.8 Knowledge acquisition and organisation of rules for the estimation of failure modes of fully inspected buildings ***(complete match between observed cracks and failure modes)***

The first stage, considered the most critical phase for the expert system development, consists in the knowledge acquisition and organisation (Leao and Rocha, 1990). The structure adopted to describe the domain knowledge highly influences the quality of the results provided by WBES, therefore a robust organisation and consistent acquisition process are required. The most common tools to acquire the knowledge domain for WBES are the logic trees, as these are the basis for the object oriented programming languages used to define objects containing data, attributes, code and rules (Nofal and Faud 2014).

In this work, the logic trees are introduced as a graphical breakdown of issues dissected into objects (or questions with yes/no answers presented) reported in a flowchart developed vertically from the top to the bottom with the scope at exploring issues and identifying solution. Therefore, by referring to this definition, the logic trees are adopted in this work to point out the issues and to summarise all questions (in steps or rules) that need to be answered to identify a solution to the identified issue.

In particular the use of the logic trees in LOG-IDEAH is proposed to identify failure modes of buildings through engineering knowledge that is dissected into questions requiring a yes/no answers to verify if the observed cracks correspond to a crack pattern defined as representative of a possible failure mode for a building.

The logic trees introduced in this section are presented to identify failure modes only on buildings that have been fully inspected and the cracks and damage seen on their facades in post-earthquake surveys match at least one of the possible failure modes, defined in chapter 4. As for buildings that have been only partially inspected, or their damage only corresponds to a partial development of the possible failure modes defined in chapter 4, specific rules based on the engineering knowledge are defined, as the one discussed in section 5.9.

Before introducing the logic trees and moving from the mechanical analytical model provided in chapter 4 to the synthetic acquisition tool developed here, the failure modes in chapter 4 need to be further classified and refined, taking into account the

localisation of the VeMEs involved in the failure modes, and localisation of the crack pattern on the facades as they are defined in section 5.4 and 5.5. Appendix F shows the expanded set of failure modes, obtained when considering such localisation.

In order to explain how the set of failure modes of Appendix B has been modified in the set of failure modes of Appendix F, Figure 5-10 shows the reclassification of failure mode B1 of Appendix B, into B1-Left and B1-Right of Appendix F. The failure mode B1 Figure 5-10a involves the failure mode of the front façade and its adjacent one that can be located on the left side (see Figure 5-10b) or the right (see Figure 5-10c), leading to the occurrence of B1-Left or B1-Right, respectively. This distinction is needed because the data collected for each façade is location specific and the failure mode is not given by a symmetric crack pattern on the side walls.

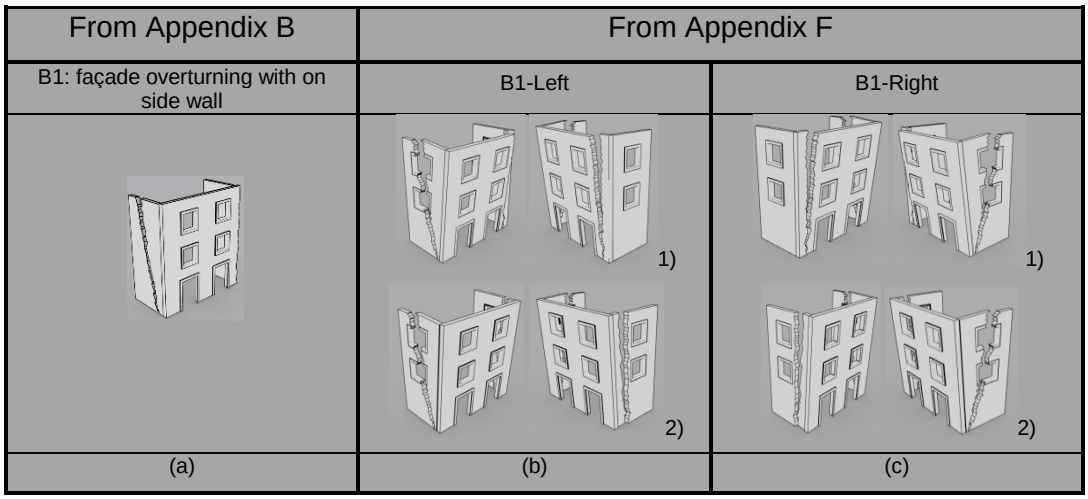

Figure 5-10: Comparison between the failure modes B1 in Appendix B and the failure modes B1-Left and B1 –Right of Appendix F

Furthermore, it should be noted that for each class B1-Left and B1-Right, defined I Appendix F, two different cases are considered, consistent of whether the crack pattern on the sidewalls is vertical or diagonal (see Figure 5-10a(1)), and whether the identified failure mode involves two or three façades (see Figure 5 10a(2)).

This should be compared with the fact that in the analytical model of Chapter 4 the inclination of the angle of the crack defining the mechanism B1 is one of the variables determined by the optimisation procedure, which minimises the collapse load factor, and hence encompasses all possible failure modes observed on site.

Similar considerations to take into account that the cracks collected as input for LOG-IDEAH are location specific also underpin the development of failure modes belonging to class C, D, and E that become failure modes C-left, C-rigth, D-left, D-right, E1 and E2 in Appendix F.

The logic trees are built up on the hierarchical deconstruction and reconstruction introduced for the UBs in section 5.4 and 5.5. Indeed, because data on damage is collected at the level of the single SE, but a single crack, even very severe, would not result in a failure mode, then each of the failure mode needs to be associated to a global crack pattern and each of those needs to be deconstructed in local crack identified on the single SEs. Once this hierarchical relationships from local to global level re set for each of the failure mode of Appendix F, the logic trees can sample all individual cracks recorded on the single SEs of a VeME or set of VeMEs, assemble the recorded cracks, determine the correspondence between the cracks and failure modes.

The logic trees for the recognition of failure modes A1, F and G and class D, E, H, and M are developed to interrogate, time by time, data stored on the single VeME, as these failure modes are associated to a crack pattern, fully contained within one VeME. For the other failure modes in Appendix F, such as A2 and classes B and C described by cracks pattern recorded on at least two VeMEs, the questions (or checks) in the logic trees are more complex as different sets of data need to be matched with crack pattern involving different adjacent VeMEs.

The logic trees also include rules for failure modes, which are in some cases mutually exclusive, and in some other cases possible alternatives. By doing so the number of possible association of crack patterns to failure modes can be condensed and the set of rules reduced to the essential.

By way of an example, the recognition of failure mode A1, which can only occur for lack of connections among VeMEs and presence of vertical cracks developed at the edges of a façade, automatically excludes the possibility of occurrence of A2, B or C, failure modes requiring good connection between adjacent VeMEs, or D or E, failure modes requiring presence of cracks within the façade and good connection on at least one edge of the façade.

Finally, in the logic trees, specific rules are also implemented in order to identify crack patterns corresponding to failure mode F of Appendix F, which occurs in presence of ties.

Once logic tree have been cross all input data, the process provides two possible outcomes: the operator can either accept or reject the outcome suggested by the logic tree. In the latter case, the operator is required to reconsider the collected data, either by re-checking the classification of the individual cracks, in terms of position, class and severity; or by reducing/expanding the set of data. The analysis can then be repeated, until a satisfactory outcome, which does not conflict with any of the predetermined sets of rules based on constraints and mechanical laws is obtained. This implies that once the data set is modified, this constitutes a new data set, which can be reprocessed and used to improve and to enrich the results.

5.8.1 *Example of logic tree: Identification of the failure mode A2*

The reasoning (questions with YES/NO answers) embedded in the logic trees can be illustrated by way of the example given in Figure 5-11 and Figure 5-12, which leads to the identification of failure mode A2. Figure 5-11a and Figure 5-12a show a graphic representation of the logic trees (LT)-Ar and (LT)-Al defined for the identification of the crack pattern on the left and right side of a facade. A set of explanatory notes of the two logic trees are included in Figure 5-11b, Figure 5-12b and Figure 5-12c.

The logic trees *(LT)-Ar* and *(LT)-Al* are developed to verify the crack pattern on VeME_R and VeME_L, façades on the right and on the left of the VeME, as reported in Figure 5-11 and Figure 5-12. The logic trees' questions progress from the top storey to the bottom storey of both façades VeME_R and VeME_L, by verifying at each level if the piers highlighted in yellow in Figure 5-11 and Figure 5-12 present a vertical crack.

If these cracks are identified, failure mode A2 is captured and this solution is considered one of the possible failure modes for the VeME. The occurrence of A2 excludes the possibility that other COMB failure modes of class B, C can occur and the OOP failure mode of class D caused by lack of connection can arise.

Logic tree A-r

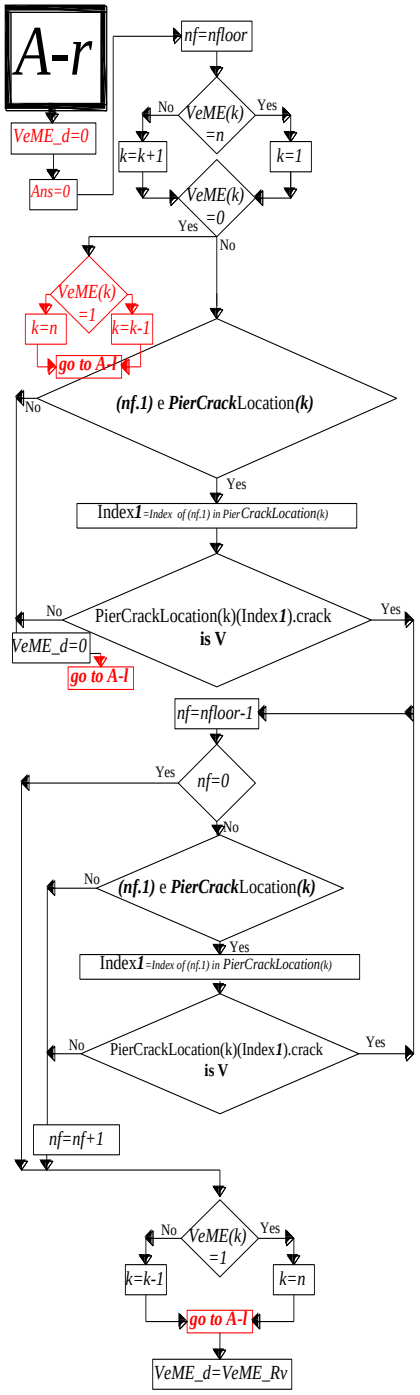

a)

Note: Logic Tree (*LT*) *A-r*

The *LT A-r* checks the damage on VeME_R, if two conditions are verified concurrently; a) no damage has been observed on the central VeME, (VeME_d=0 states that the total number of damaged VeMEs, identified by the system, is null) and b) data is available for this VeME_R. If the condition b) is not verified, go to *LT* A-I (Figure 5-12) for checking the state of damage of VeME_L.

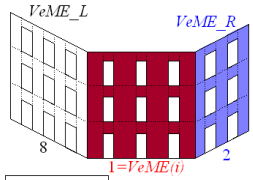

(0)

If a) and b) are verified (0), *LT A-r* checks if the vertical crack in red (1) has been recorded on the pier highlighted in yellow on the top storey.

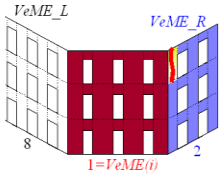

(1)

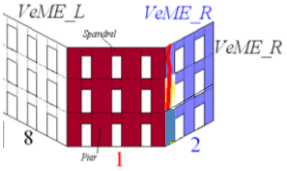

(2)

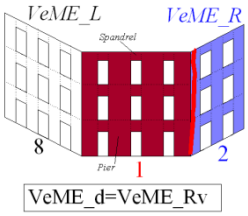

(3)

If the condition (1) is not verified go to the *LT A-I*.
If the condition (1) is verified, *LT A-r* checks if the vertical crack has been recorded on the pier highlighted in yellow on the second storey (2).
If the condition (2) is not verified go to the *LT A-I*.
If the condition (2) is verified, *LT A-r* checks if the vertical crack has been recorded on the pier highlighted in yellow on the ground storey (3).
If the condition (3) is not verified go to the *LT A-I*.
If one of the conditions (1), (2) or (3) is verified, before going to *LT A-I*, set VeME_d=VeME_Rv, which means: VeME_R is damaged with vertical cracks.
If none of the conditions (1), (2) or (3) is verified, go to *LT A-I* with VeME_d=0 which states that the total number of damaged VeMEs, identified by the system, is null, in relation to both VeME and VeME_R.

b)

Figure 5-11: a) Logic tree A-r for the interpretation of the vertical crack pattern on the VeME_R and b) explanatory notes

Logic tree A-I

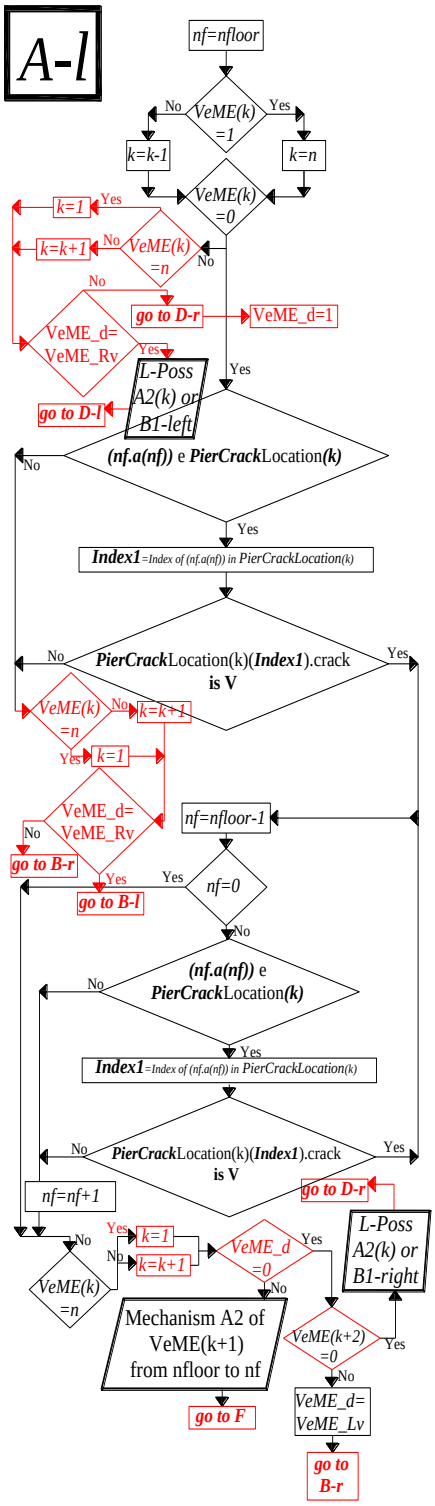

a)

Note: Logic Tree (*LT*) *A-I*

The *LT A-I* checks the damage on VeME_L, If the central VeME is not damaged, and one of the following conditions are verified: a) VeME_R is not damaged according to *LTA-I*(VeME_d=0) and b) VeME_R is damaged according to *LT A-r* (VeMe_d=VeME_Rv).

If VeME_d=0 and no data is available on VeME_L go to check if the mechanisms D-Right of Appendix F is occurring on VeME_L.

If VeMe_d=VeME_Rv and no data is available on VeME_L, go to check the level of possibility of occurrence of the mechanisms A2 and B1-left of Appendix F on the central VeME according to the criteria of section 5.9 and if D-Left of Appendix F occurring on VEME_R.

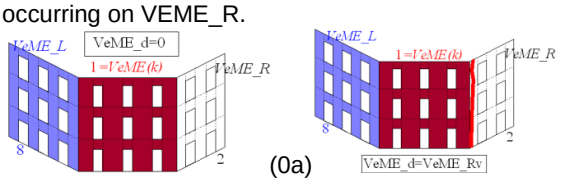

(0a)
(0b)

If data is available on VeME_L, *LT A-I* checks if the vertical crack in red has been recorded on the piers highlighted in yellow on the top storey in (1a) for VeME_d=0 and in (1b) for VeMe_d=VeME_Rv.

If the condition (1a) is not verified go to check if the mechanism B2 of Appendix F is verified on the central VeME.

If the condition (1b) is not verified go to check if the mechanism B1-left of Appendix F is occurring on the central VeME.

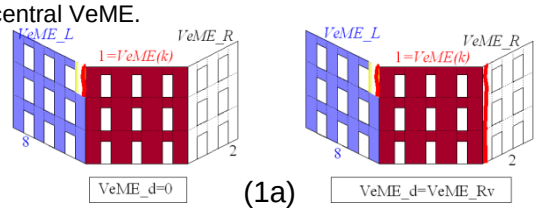

(1a)
(1b)

If the condition (1a) or (1b) is verified, *LT A-I* checks if the vertical crack has been recorded on the pier highlighted in yellow on the second top storey in (2a) for VeME_d=0 and in (2b) for VeMe_d=VeME_Rv.

If the condition (2a) is not verified go to check if the mechanism B1-Right of Appendix F is occurring.

If the condition (2b) is not verified go to check if the mechanism B1-Left of Appendix F is verified.

If condition (2a) or (2b) is verified, *LT A-I* checks if the vertical crack has been recorded on the piers highlighted in yellow on the top third storey in (3a) for VeME_d=0 and in (3b) for VeMe_d=VeME_Rv and so on for more storeys.

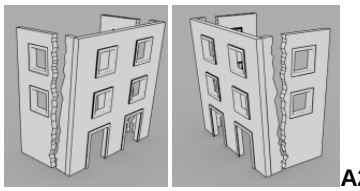

A2

b)

Note: Logic Tree (LT) A-I 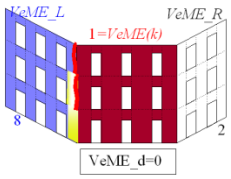 (2a) 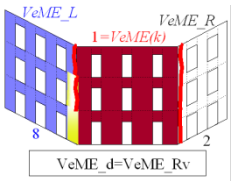 (2b) 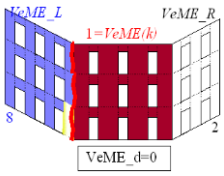 (3a) 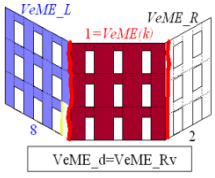 (3b)	If one of the conditions (1a) or (2a) or (3a) is verified, before going to check if the mechanism B1-Right of Appendix F is occurring on the central VeME, set VeME_d=VeME_Lv which states that VeME_L is damaged with vertical cracks. If the mechanism B1- Right is not verified, check if D-Right of Appendix F is occurring on VeME_L If D-Right it is not occurring, check the level of possibility of occurrence of the Mechanisms A2 or B1- Right on the central VeME according to the criteria of Sections 0. If one of the conditions (1b) or (2b) is verified, the Failure mode A2 is partial on the central VeME. If the condition (3b) is verified, the Failure mode A2 is identified and involves the entire VeME. Once Failure mode A2 is identified, check if the mechanism F of Appendix F is occurring on the central VeME.	c)

Figure 5-12: a) Logic tree A-I for the interpretation of the vertical crack pattern on the VeME_L and b) and c) explanatory notes

Once A2 is captured, *(LT)-AI* also checks (or questions) if the VeME has restraining elements, and in case of affirmative answer, *(LT)-AI* verifies if failure mode F (see Appendix F) occur. If a vertical crack pattern is identified only on the VeME_R or VeME_L, the next step in *(LT)-Ar* and *(LT)-Al*, respectively, is to check if mechanisms B1-Left or B1-Right occur.

If B1-Left or B1-Right are not occurring, therefore there is not a complete match between the observed crack and failure modes, hypothesis, discussed in Section 5.9, are made to interpret the available data and to identify the most plausible failure modes. If *(LT)-Ar* and *(LT)-Al* do not lead to the identification of A2, the logic trees B-l, B-r, B1-l and B1-r, collated in Appendix F, are used to verify if failure modes of class B are taking place.

5.9 Knowledge acquisition and organisation of rules for the estimation of failure modes of partially inspected buildings ***(partial match between observed cracks and failure modes)***

In case of partial inspection of buildings, the example of Figure 5-9 had already shown that it is worthwhile to identify failure modes by making hypotheses on the lack of information on both seismic damage and structural characteristics of the buildings.

This section focuses on organising the thought process needed to interpret the available data by using reasonable assumptions on AA that has been only partially inspected. In order to discuss the different situations, some examples of damaged buildings represented by simplified sketches are reported to underline the issues, and assumptions needed to estimate the type of failure modes and their level occurrence.

5.9.1 *Rules to estimate the uncertainty level of occurrence of the identified failure modes.*

The sketch in Figure 5-13 illustrates the case of a building that has been only partially inspected. Only VeMEs 1 and 2 of of the AA have been surveyed. VeME 1 has vertical cracks on all piers on its left edge, while VeME 2 has no damage. By submitting this information to the logic trees in Appendix F, the issue is to identify if the vertical cracks match one of the failure modes in Appendix F.

POSSIBLE FAILURE MODES					
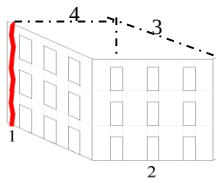	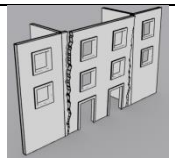	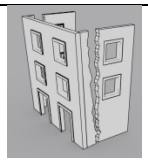	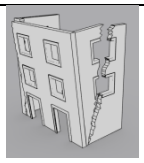	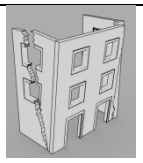	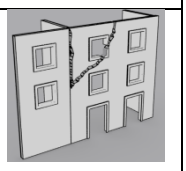
Vertical crack pattern	A1	A2	B1-right	B1-left	D-left
UNCERTAINTY level	M	H	M	H	M

Figure 5-13: Uncertainty levels of the failure modes identified for the vertical crack pattern on the VeME1

In Figure 5-13, it is possible to observe that although there is not a complete match between the reported cracks in red and any of the failure modes of Appendix F, the vertical cracks can be considered a partial development of five different failure modes, described as follows.

By starting from failure modes A1 and D-left, these can be identified only by inspecting one façade, since their crack pattern is contained in only one VeME. In this case, the VeME, required to identify these failure modes, has been inspected, and the observed cracks in red only partially match the crack patterns of A1 and D-left. Therefore:

- A1 and D-left are possible failure modes for VeME1, because the partial match is considered a possible partial development of the mantioned failure modes.

For failure modes A2, B1-right and B1-left, these can be identified only if three façades for the first failure mode and two façades for the other two are inspected. The observed vertical cracks also represent only a part of the crack pattern representative of mentioned failure modes. In particular:

- the occurrence of A2 is ensured only if VeME3 is inspected and has a vertical crack on its right side. Such a partial match, due to an incomplete survey, allows considering A2 as a possible failure mode for VeME4.
- the survey for B1-right is complete, and only a partial match between its crack pattern and the observed cracks is identified. Such a partial match allows considering B1-right as a possible failure mode for VeME1 due to a possible partial development of its crack pattern.
- the occurrence of B1-left is ensured only if VeME3 is inspected and has a diagonal crack on its right side. Such a partial match due to an incomplete survey allows considering B1-left is as a possible failure mode for VeME4.

This example underlines the need for introducing a parameter representing the level of investigation of the knowledge and the level of judgement made to recognise the possible failure modes. Such a parameter, representing the epistemic uncertainty associated with the whole process, derives from two sources: the level of

correspondence between the observed cracks and failure modes, and the level of investigation of the AA.

- A qualitative uncertainty scale with three grades can be set up as shown in Table 5-4: if the match between the observed cracks and the failure modes of Appendix F is complete, the each identified failure modes have a LOW level of uncertainty. When the cracks are derived from a complete survey only partially match one or more failure modes in Appendix F each identified failure mode has a MEDIUM level of uncertainty, (i.e. A1, D-Left and B1-Right, in Figure 5-13).

Table 5-4: Definition of the uncertainty levels

UNCERTAINTY level	**Match between failure modes of Appendix F and observed crack pattern**	**All VeMEs involved in the possible failure mode have been inspected**
L: LOW	Complete	Yes
M: MEDIUM	Partial	Yes
H: HIGH	Partial	NO

On the other hand, a failure mode has a HIGH uncertainty of occurrence, when the observed cracks only partially match one or more failure modes of Appendix F and not all façades involved in the identified failure modes have been surveyed (i.e. A2 and B1-Left, in Figure 5-13).

5.9.2 *Rules to estimate the possibility of occurrence of the identified failure modes*

In this section, the concept of possibility level of occurrence of a failure mode is introduced and a formal relationship is set out between this and the uncertainty level through Table 5-5.

The possibility level of occurrence, defined as HIGH in Table 5-5, is assigned, when there is a complete match between the observed cracks and the failure modes of Appendix F, by fulfilling the minimum condition that observed cracks match failure modes, according to the upper bound theorem of limit analysis (Munoz et al., 2008).

In all other cases, the possibility level of occurrence is defined through hypotheses set to define the deficiencies of the building and to derive the failure modes with the highest possibility of occurrence. These assumptions are explained in the next subsections.

Table 5-5: Definition of the uncertainty and possibility levels of the occurrence in a failure mode

UNCERTAINTY level	***missing crack***	***possibility level***
L: LOW	No cracks	H: HIGH
M: MEDIUM	Vertical	L: LOW
	Diagonal	M: MEDIUM
H: HIGH	Vertical	M: MEDIUM
	Diagonal	L: LOW

Rules for the identification of the level of possibility of occurrence for a failure mode with high observation uncertainty.

In this section, since these assumptions on the occurrence of cracks are made on façades that have been not inspected, there is a need to adopt a conservative approach, based on the assumption that failure modes associated with the lowest seismic performance of the AA has the highest possibility of occurrence.

This conservative approach also implies that it is assumed that uneven façades are always considered to be damaged according to the maximum level of severity of the damage observed on the other façades. Moreover, the assumptions are made not only on the severity of the damage but also on all possible crack pattern, required to match a failure mode.

In order to maintain a conservative approach, the cracks that should e on the uneven facades and are required to fulfil the match with a failure mode, are always assumed to exist on the uneven façades, even it is not known whether these cracks exist or not.

By way of example, Figure 5-14 reports the possible failure modes, and where these failure modes are located, by referring to the example given in Figure 5-13 of section 5.9.1, and the uncertainty levels and the possibility levels of occurrence of the identified failure modes by referring to Table 5-4 and Table 5-5.

The failure modes A2 and B1-left in the example of Figure 5-14 are used to explain the assumptions that are made to assess the possibility level of occurrence of failure mode with HIGH uncertainty level of occurrence.

n is the VeME with damage	***Failure mode***	***VeME***	***UNCERTAINTY level***	***POSSIBILITY level***
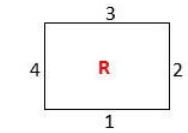 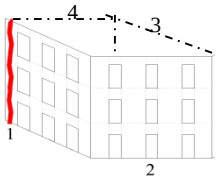 Vertical damage on the left edge of the VeME n=1	A1	n= VeME 1	M	L
	A2	n-1= VeME not defined. VeME 4	H	M
	B1-right	n= VeME 1	M	M
	B1-left	n-1= VeME not defined VeME 4	H	L
	D-LEFT	n= VeME 1	M	M

Figure 5-14: Possibility level of occurrence for the failure modes identified for the vertical cracks recorded on the left edge of the VeME 1.

For the conservative approach mentioned above and introduced to assume the type of damage on the uneven façades VeME3 and VeME4, it is assumed that VeME3 is damaged by vertical cracks to fulfil the crack pattern associated to the failure mode A2, while VeME4 is damaged by diagonal cracks to fulfil the crack pattern associated to the failure B1-left.

To distinguish the possible level of occurrence of these failure modes, assumptions on the type of deficiencies, underlined by the presence of the assumed cracks on the uneven façades are considered as follow.

Presence of vertical cracks on lateral piers of a façade reflects a lack of connections between this façade and its orthogonal sidewalls, while the presence of diagonal cracks on the sidewalls indicates a better connection than the previous one. Based on these considerations, the presence of vertical cracks on one side of a façade compared to the presence of diagonal cracks not only underlines a weaker structural condition for the building and reduces the possibility that the building (lack of connections) but also decreases the possibility of occurrence for the failure modes involving the presence of diagonal cracks.

These assumptions on failure modes with HIGH uncertainty of occurrence (due to an incomplete survey) allow setting the following criteria to estimate the level of possibility of occurrence:

- the failure mode has MEDIUM POSSIBILITY of occurrence, if the cracks required to fulfil the match between the observed crack pattern and a failure modes are VERTICAL on the uneven VeMEs, see Table 5-5;
- the failure mode has LOW POSSIBILITY of occurrence, if the cracks required fulfilling the match between the observed crack pattern and a failure modes are DIAGONAL on the uneven VeMEs, see Table 5-5.

Rules for the identification of the possibility level of occurrence for a failure with medium uncertainty of occurrence

To estimate the level of possibility of occurrence of a failure mode with input affected by a MEDIUM level of uncertainty (due to a partial match between observed cracks and failure modes in Appendix F, the assumptions are made not only on the observed cracks, but also on the possible sources of resilience that have limited the complete development of the identified failure mode. To this, it is also assumed that the absence of an expected crack on an inspected façade automatically reduces, but not excludes, the possibility of occurrence of a failure mode.

By way of example, the failure mode A1, B1-rigth and D-left in Figure 5-14 are used to explain the assumptions that are made to assess the possibility level of occurrence of failure mode with MEDIUM uncertainty level of occurrence. For the assumptions mentioned above and introduced to define the possibility level of occurrence, the

absence of vertical cracks on the right side of VeME1 and the absence of diagonal cracks on the left side of VeME2, required to match the crack pattern of A1 and B1-Rigth, respectively, highlight the possibility that VeME1 and VeME2 are well connected to each other, since no cracks have been identified on their common corner. Furthermore, the absence of a diagonal crack to match D-left on VeME1 reduces the possibility of its occurrence, since the triangular macroelement, which is supposed to be formed, does not appear according to the observed damage.

These examples underline the need of differing the levels of possibility of occurrence by taking into account the deficiencies or strength, which can be inferred by the presence or lack of cracks.

Therefore, in case of MEDIUM uncertainty, the absence of vertical cracks compared to the absence of diagonal cracks on an inspected façade, not only highlights a stronger structural condition by increasing the possibility that the AA has good connections between VeMEs but also decreases the possibility of occurrence of failure modes that are triggered by the presence of weak connections.

Hence, in the present conditions, the following criteria are set to estimate the level of possibility of occurrence of failure modes:

- the failure mode has MEDIUM POSSIBILITY of occurrence, if the cracks, required to fulfil the match between the observed cracks and a failure are DIAGONAL;
- the failure mode has LOW POSSIBILITY of occurrence, if the cracks, required to fulfil the match between the observed cracks and a failure are VERTICAL.

5.9.3 *Output: rules to estimate the failure modes with the highest probability of occurrence and related damage levels*

In order to rank all possible failure modes identified as solutions, five probability levels of occurrence are introduced in Table 5-6. These are defined from 1 to 5 (from VERY HIGH to VERY LOW probability of occurrence) and they are provided as a function of the uncertainty levels and the possibility levels of occurrence defined in the previous section.

The level of damage assigned to the identified failure modes are directly derived from the observation. The maximum severity of damage observed on cracks determines the severity of the identified failure mode.

Table 5-6: Probability level of occurrence

Uncertainty Level	Possibility Level	Probability level of Occurrence	
low	high	VERY HIGH	1
medium	medium	HIGH	2
high	medium	MEDIUM	3
medium	low	LOW	4
high	low	VERY LOW	5

5.10 Knowledge representation

This section focuses on the definition of a comprehensive ontology to capture and to define the domain concepts and relationships defined during the knowledge acquisition and organisation of section 5.8 and 5.9. Because the knowledge assimilated with logic trees is expressed in terms of the ontology presented in this section, an overview of the concepts and how these are defined within this ontology is presented.

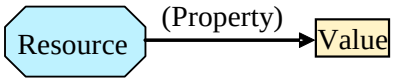

Figure 5-15: Graphic representations of RDF model

The ontology provides a shared and common understanding of the knowledge domain and sets a direct communication across earthquake engineers and expert system' developers, which is essential if the seismic engineering knowledge is to be embedded in the web based application. Fundamental publications covering various aspects of ontologies are represented by Uschold & Gruninger (1996), van Heijst et al. (1997), Gomez Perez & Benjamins, (1999).

In this work, the ontology is implemented with the Resource Description Framework (RDF), a framework adopted to represent the concepts of the knowledge domain (Antoniou & van Harmelen, 2004, Staab, and Studer, 2013). The RDF is based upon the idea of making statements in the form of subject (s) – predicate (p) – object (o). These expressions <s-p-o> are known as triples in RDF terminology, indicated graphically in Figure 5-15.

By the use of the defined triple, the members of the hierarchical approach of section 5.4, the types and severity levels of the seismic damage of section 5.5 and failure modes of Appendix F are represented in Figure 5-16, where each object is described by the predicate (is-a) to define its values. The formal representation of this ontology is developed in OWL (Web Ontology Language), and its graphic representation is shown in Figure 5-17. It should be noted that the ontology represents neither the logical links between attributes of a given entity, nor the causal logic defined in section 5.8 through the logic trees, which allows determining the development of specific failure modes. This is indeed set out in the HTML scripts introduced in section 5.11, by use of Answer Set Programming.

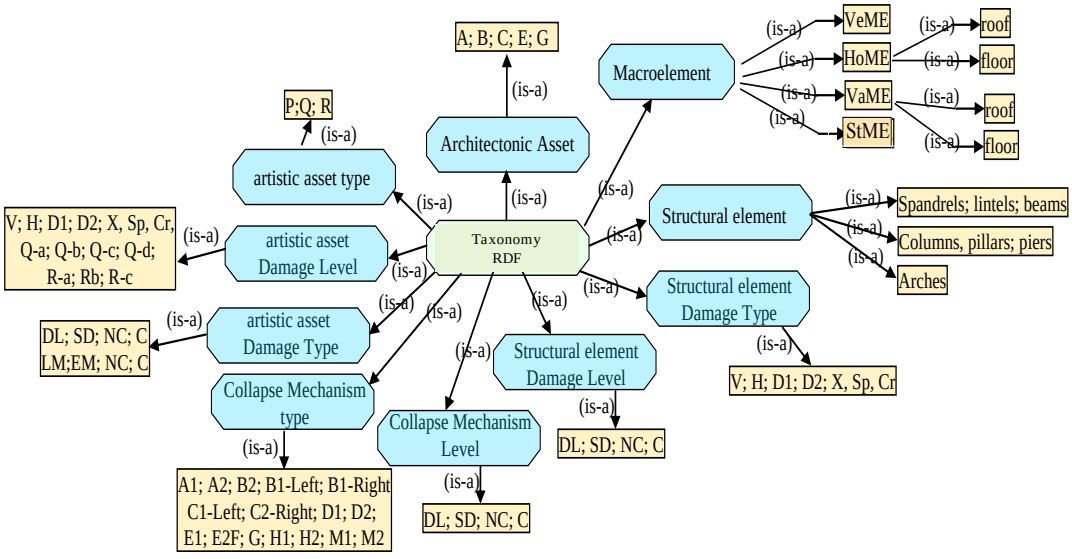

Figure 5-16: Ontology for the heirachical approach proposed for the Architectural Asset (AA) and for its damage identification, illustrated as requested for the RDF

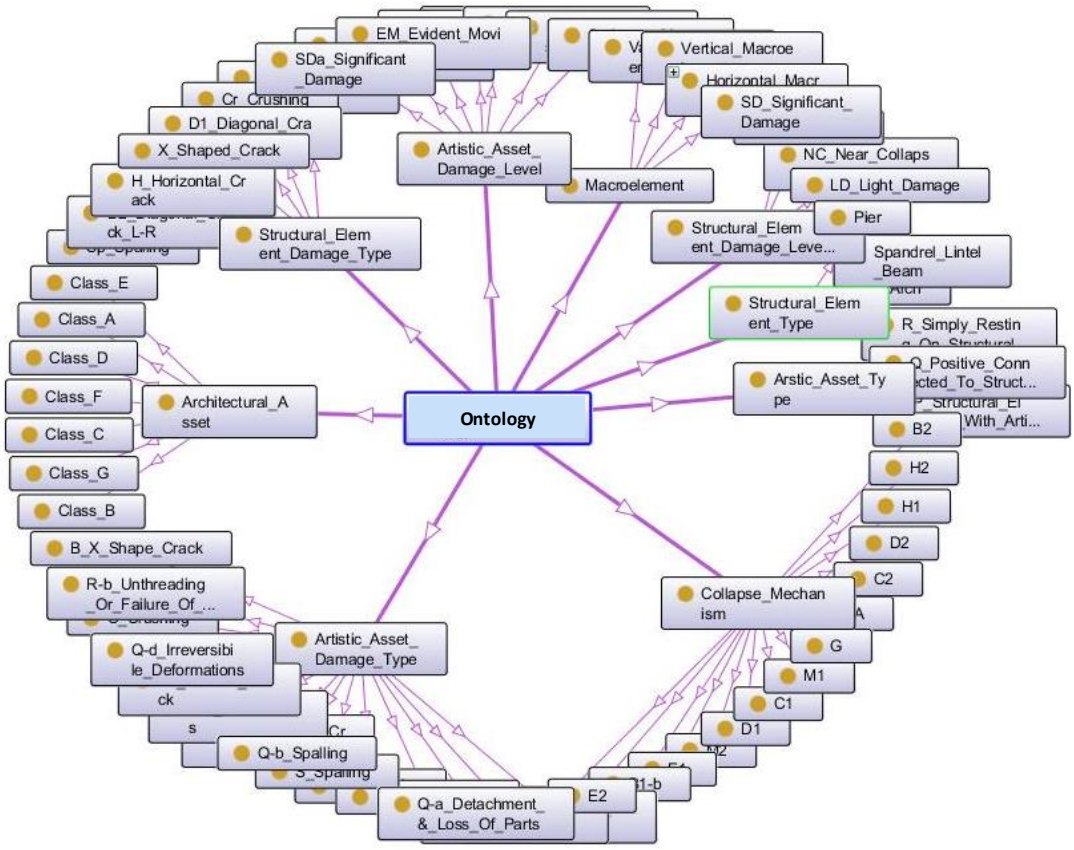

Figure 5-17: OWL representation of the ontology for the heirachical approach proposed for an Architectural Asset (AA) and for the damage identification

5.11 Answer Set Programming (ASP)

This section focuses on programming the rules defined in the logic trees of section 5.8 and section 5.9 on the ontology introduced in section 5.9.2. Given the intrinsically procedural nature of logic trees, a procedural programming approach could be considered as a possible method for the implementation. However, given the declarative description of the failure modes provided in the logic trees (e.g. vertical cracks on either sides of a façade cause mechanism A), a declarative paradigm would be more efficient.

For this reason, facts and rules defined for the description of the buildings and interpretation of the failure modes have been implemented by using Answer-set programming (ASP) (Gelfond and Lifschitz, 1988 and 1991), a declarative

programming paradigm in which logic programs are used to describe all requirements that must be fulfilled by the solutions of a certain problem.

AnsProlog (Baral 2003) is the implementation language of the ASP. Its basic components are atoms, elements that can be either true or false. An atom *a* can be negated using negation as failure. A literal is an atom *a* or a negated atom *not a*. An atom *not a* is true if an evidence supporting the truth of *a* is not found. Using atoms and literals, rules are created, and their general forms are represented as follows:

a: b1, … , bm, not c1, … , not cn.

where *a, bi,* and *cj* are atoms. Intuitively, this can be read as: if all atoms *bi* are known/true and no atom *cj* is known/true, then atom *a* must be known/true. The atom *a* is also defined as the *head* and *b1, … , bm, not c1, … , not cn* as the body of the rule.

A program is constituted by a consistent set of rules that determines the relationships between known/true and not-known/untrue atoms. This is also defined as the answer set needed to determine the predefined solution.

Algorithms and implementations for obtaining answer sets are referred to answer-set solvers. Among the most popular and widely used solvers, Clingo has been chosen for the purpose of this implementation (Gebser at al. 2007).

In order to facilitate the interpretation of the algorithms, the program fragments have been annotated with a description of the atoms that have been used. These annotations are made by using a subset of the annotation language Lana (De Vos et al., 2012). This language uses program comments plus semantic tags in the style of Javadoc to describe the various components of the program. For sake of simplicity only the @block tag, indicating the specific sets of rules, and the @atom tag, describing individual atoms and their attributes, have been used. In Figure 5-18, the rule to denote the various damage types and damage levels are reported to show how these have been encoded. This same approach has been followed to describe the other resources in the ontology defined in section 5.10.

```
% @block buildingconstants {
% provides the constants used in damage description of buildings
% @atom damageType(T)
% type of damage from vertical;horizontal;diagonal crack / ;
% diagonal crack \ ;
% x shape;spalling;crushing
% @atom damageLevel(L)
% severity of damage from damage limitation;significant damage;
% near collapse;collapse

damageType(v;h;d1;d2;x;s;cr).
damageLevel(ld;sd;nc;c).
```

Figure 5-18: Definition and annotation in LANA language of the parameter damage types and damage levels for structural elements (see section 5.10)

In a similar fashion, each failure mode of Appendix F is encoded in a separate file and LANA block for ease of testing, flexibility and readability. In this section, this process is presented for the failure mode A1. To demonstrate the ease of use of the ASP-encoding, the same code for the failure mode A1 is also extended to identify the failure mode A2, whose rules for occurrence and corresponding logic trees were presented in section 5.8.

Figure 5-19 shows the AnsProlog code defined to detect failure mode A1. Similarly, to what already seen in the logic tree's flow of decision gates, most encodings of failure modes, and the failure modes A1 is not exception, start from the top storey of a façade and try to identify a given crack pattern. If this is found at the storey under observation, lower storeys are considered until a storey is found which does not have this desired pattern or until all storeys have been checked. The system will then return the specific pattern with the range of storeys involved in the pattern. For the encoding, distinct parts of a sought crack pattern are tested separately (e.g. patternAr and patternAl) to support reuse for other failure modes using the same partial patterns. For each partial pattern, the lowest storey (e.g. lowpatternAl(Fa, Fl) and lowpatternAr(Fa, Fl)) up to which the partial patterns occurs, is determined and then the patterns combined to form the failure mode (e.g. collapseMechanism(outOfPlaneAt(Fa, FlT, Fr), patternAa)).

```
patternAl(Fa,Fl) :-
pierCrack(Fa,Fl,1,v,L1),topFloor(Fa,Fl),
floorNumber(Fa,Fl), facade(Fa),damageLevel(L1).
patternAr(Fa,Fl) :- rightPierFloor(Fa,Fl,R),
pierCrack(Fa,Fl,R,v,L2),topFloor(Fa,Fl),
facade(Fa), floorNumber(Fa,Fl), damageLevel(L2).
```

This rule determines whether the piers located at the edges of the facades on the top storey have a vertical crack. This part of code can be reused to identify the same partial crack patterns of other failure modes

```
patternAl(Fa,Fl) :-
pierCrack(Fa,Fl,1,v,L1), floorNumber(Fa,FlH),floorNumber(Fa,Fl),
patternAl(Fa,FlH), Fl = FlH - 1, facade(Fa),damageLevel(L1).
patternAr(Fa,lL) :-
pierCrack(Fa,Fl,R,v,L2), rightPierFloor(Fa,Fl,R),
floorNumber(Fa,FlH),floorNumber(Fa,Fl), ,damageLevel(L2)
patternAr(Fa,FlH), Fl = FlH - 1, facade(Fa)
```

If a vertical crack on the pier at the edges of the facades is determined on the top storey, the code checks if the same crack is also on the pier on the storeys below

```
lowpatternAl(Fa,Fl) :-
patternAl(Fa,Fl), not patternAl(Fa,Fll), Fl = Fll + 1,
floorNumber(Fa,Fl),floorNumber(Fa,Fll), facade(Fa).
lowpatternAr(Fa,Fl) :-
patternAr(Fa,Fl), not patternAr(Fa,Fll), Fl = Fll + 1,
floorNumber(Fa,Fl),floorNumber(Fa,Fll), facade(Fa).
```

This rule determines the lowest storey on which the vertical crack is determined

```
lowpatternAl(Fa,1) :- patternAl(Fa,1).
lowpatternAr(Fa,1) :- patternAr(Fa,1).
```

This part of the code sets the position of the lowest storey where a pier at the edges of the facades have a vertical cracks

```
lowpatternA(Fa) :-
lowpatternAl(Fa,Fl), lowpatternAr(Fa,Fll), facade(Fa),
floorNumber(Fa,Fl), floorNumber(Fa,Fll)
```

This rule establishes that the piers on both edges of the façade have a vertical cracks. This part of the code is used to exclude that other failure modes are occurring

```
collapseMechanism(outOfPlaneAt(Fa,FlT,Fr),patternA) :-
lowpatternAl(Fa,Fl), lowpatternAr(Fa,Fr), Fl < Fr, topFloor(Fa,FlT),
floorNumber(Fa,Fl), floorNumber(Fa,Flt), facade(Fa).
collapseMechanism(outOfPlaneAt(Fa,FlT,Fl),patternA) :-
lowpatternAl(Fa,Fl), lowpatternAr(Fa,Fr), Fl >= Fr, topFloor(Fa,FlT),
floorNumber(Fa,Fl), floorNumber(Fa,Flt), facade(Fa).
```

This part of the code underline that failure mode A is occurring from the top of the facade to the floor where there is vertical crack on both piers on the edges of the facade

Figure 5-19: Rules used to capture the failure mode A1. (Novelli et al., 2012)

The scenario described in the failure mode A1, where there are vertical cracks down both edges of the façade under scrutiny, leads to the overturning of the whole façade, if developed for all the storeys, but involves only the crack pattern of that single façade. Failure mode A2 instead, as seen in section 5.8.1 involves the analysis of crack patterns on at least two façades.

The failure mode A2 has much in common with the failure mode A1, in that there are vertical cracks on either side of the façade concerned, but those cracks are in the adjacent façades, and, as a consequence, the reasoning process must be applied not at the single ME level, but across the AA as a whole. The relative ease with which is it possible to extend the analysis illustrates the benefit of the hierarchical approach to the representation of the building and the declarative nature of the encoding. In the encoding (Figure 5-20), partial patterns for vertical cracks on the left and right side of a façade defined for A1 are reused for A2.

```
lowpatternAa(Fa) :-
lowpatternAl(FaR,Fl), lowpatternAr(FaL,Fll),
floorNumber(FaR,Fl),floorNumber(FaL,Fll),
rightFacade(Fa,FaR),leftFacade(Fa,FaL),facade(Fa;FaR;FaL).

collapseMechanism(
outOfPlanePortion(Fa,FlT,Fll),
patternAb) :- Uses atoms derived in scenarioA
lowpatternAl(FaR,Fl), lowpatternAr(FaL,Fll),Fl<Fll,
floorNumber(FaR,Fl),floorNumber(FaL,Fll),
floorNumber(FaL,FlT),
rightFacade(Fa,FaR),leftFacade(Fa,FaL),facade(Fa;FaR;FaL).

collapseMechanism(
outOfPlanePortion(Fa,FlT,Fl),
patternA2) :-
lowpatternAl(FaR,Fl), lowpatternAr(FaL,Fll),Fll<=Fl,
floorNumber(FaR,Fl),floorNumber(FaL,Fll),
floorNumber(FaL,FlT),
rightFacade(Fa,FaR),leftFacade(Fa,FaL),facade(Fa;FaR;FaL).
```

Uses atoms derived in scenario A1

Uses atoms derived in scenario A1

Figure 5-20: Rules used to capture the failure mode A2. (Novelli et al., 2012)

Figure 5-21 contains the data as it is generated from the website in a XML format, as discussed in the next section. The data refers to a generic AA. Only one façade of this AA has been inspected. This façade has three storeys and three openings per storey. The XML data reports that the VeME has vertical cracks on the piers at edges of each single storey.

By applying the encoding of the failure mode A1 of Figure 5-19, to the data in Figure 5-21, the result is the identification of an out-of-plane collapse across three floors, as expected.

The encodings in AnsProlog extends to the whole catalogue of failure modes of Appendix F.

The verification process was carried out by creating unit test cases for each failure modes. While initially created manually, they were later re-created through the web-site described in the next section. Determining the failure modes for an AA with 4 VeMEs of 6 storeys takes at most 1 or 2 seconds, which is significantly fast.

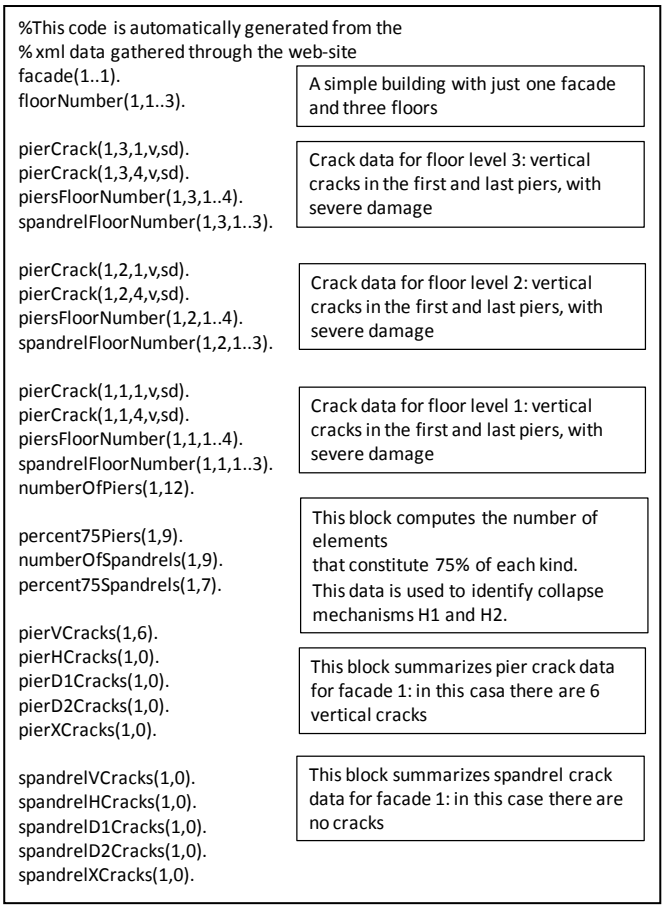

Figure 5-21: Encoding of the geometry and crack pattern of a single VeME (Novelli et al., 2012) gathered from the website introduced in section 5.12

5.12 Web-based interface of LOG-IDEAH

This section aims at presenting the user-friendly web-based interface of LOG-IDEAH, see Figure 5-22, created for collecting and storing the data, ensuring that collected data is correct, processing data in an online environment, and sharing information with other users.

The web site for LOG-IDEAH records seismic damage data at the UB level by maintaining the hierarchical approach of Figure 5-1.

The position of AA in an UB is recorded in the website through their address, directly linked to Google map, to produce a fully georeferenced database.

The inspected façades are defined in relation to their number of storeys, and opening layout through sketches that can be created directly on the web platform of LOG-IDEAH. Photos can also be stored, and if georeferenced, these are directly linked to the building position through the website. Direct links can also be established between the photos and location of the inspected façades, by referencing the taken pictures to the piers and spandrels.

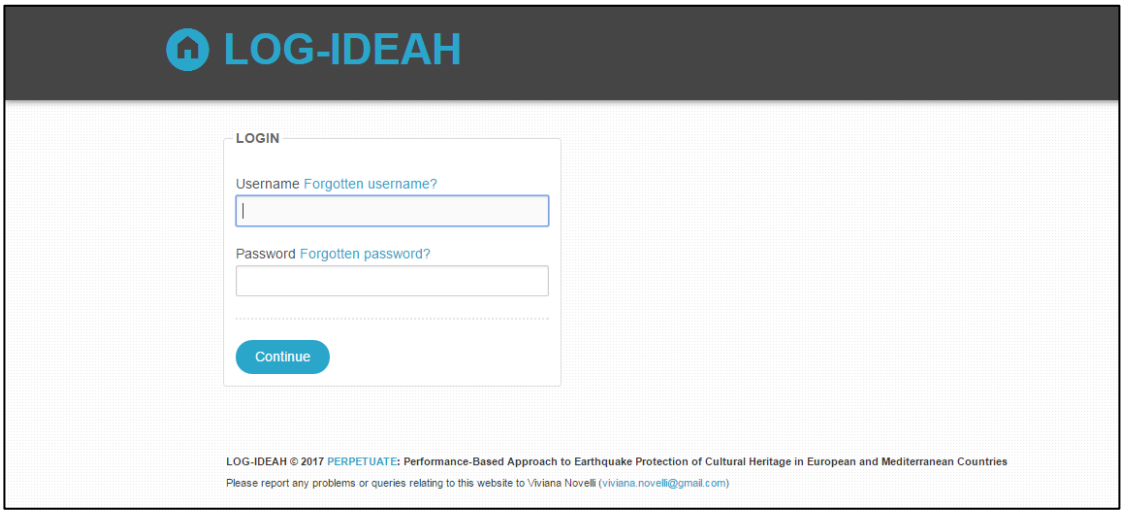

Figure 5-22: Homepage of LOG-IDEAH (http://perpetuate.cs.bath.ac.uk/perpetuate-testing/index.php)

The same sketches are also used to produce a graphic record of the class and severity of damage at both SE and aa levels, as required for the section 5.5. The website automatically stores the location of the damaged elements, as this information with the damage severity and damage type are required to determine the failure modes. The web app also allows the surveyor to record personal interpretation of the crack pattern observed on site in terms of failure mode.

The input data is stored in XML document format (Bray et al, 1998) consisting of a properly nested set of open and close tags, where each tag can have a number of attribute-value pairs. The XML documents are converted into AnsProlog code, (e.g see Figure 5-21), and then processed. The results computed by the ASP are stored in XML documents, displayed on the website.

As computed results and on site observations might not coincide, the procedure allows checking the input data, discarding or adding some cracks, considering only cracks of similar level of severity, for instance, create a new XML, pass it through the

AnsProlog code, and produce a new answer. The output might still not fully agree with the observations, but both the surveyor's judgement and the results procedure might be valid, plausible, possible answers. The next section shows an application of the procedure.

In Figure 5-23, a quick start guide of LOG-IDEAH is presented as a simple introductory guide to get users quickly accustomed to the basic operations of the web platform.

LOG-IDEAH web platform :

1. Log into the web platform at (http://perpetuate.cs.bath.ac.uk/perpetuate-testing/index.php)

For the inspected urban block
1. Provide a name to the urban block and identify its location on the GIS map in the web platform with the use of address of the inspected urban block
2. Define the shape of the urban block and number of buildings in the urban block

For the single inspected building:
1. Define plan geometry
2. Upload pictures of the inspected building, if possible

For the single inspected façade:
1. Create a sketch defining number of floors and number of opening for floors
2. Create facades with irregular opening layout and different structural and architectural features (e.g. facades with arches, or pillars; facades with different number of openings for floors, facades with irregular opening distribution vertically and horizontally, facades with alfresco, facades with jetting architectural elements), if required
3. Upload pictures of the single inspected façade, if possible

For the single damaged structural and architectural element:
1. Define damage type and damage severity
2. Upload pictures of the identified damage, if possible

Once data entry is completed,
1. Record the failure modes observed on site, if possible
2. Run the collected data (input data is processed by the rules defined in ASP)

Output of the web platform:
1. Failure modes and severity
2. Number of floors involved in the identified failure modes
3. Location of the facades involved in the identified failure modes

Compare the output of the web platform (failure modes identified with the ASP) with failure modes observed on site, if possible

Figure 5-23: Quick start guide for LOG-IDEAH web platform

5.13 Application of LOG-IDEAH for the identification of failure modes in an existing building

The UB in Figure 5-24 is located in L'Aquila, in Italy and was assessed on site after the earthquake in 2009 by visual inspection and by using LOG-IDEAH. The historic building has a corner position in the UB [22], as illustrated in Figure 5-24, therefore the seismic damage, as reported in Figure 5-25, has been collected only for the two corner façades, VeME [22.9.1e] and VeME [22.9.4s].

Since this example is presented with the scope at validating the ability of LOG-IDEAH of estimating failure modes, initially LOG-IDEAH is applied on VeME [22.9.1e] by assuming that data is only available for this façade, and then LOG-IDEAH is applied by taking into account that data is available for both facades. Therefore, results are first presented for this first case and then a second run of LOG-IDEAH is performed on data for both VeME [22.9.1e] and VeME [22.9.4s], in order to show how the results can change according to the extent of the input data.

VeME [22.9.1e] has diagonal cracks highlighted in yellow and violet, and a vertical crack highlighted in red, as reported in Figure 5-26. According to the observed cracks, the surveyor based on his expert judgements has identified D1-left (sse Figure 5-26) as a possible failure mode since the red and yellow cracks clearly show the formation of a hinge at the bottom of VeME [22.9.1e], underlining an overturning of the façade. VeME [22.9.4s] reported in Figure 5-26, has no damage.

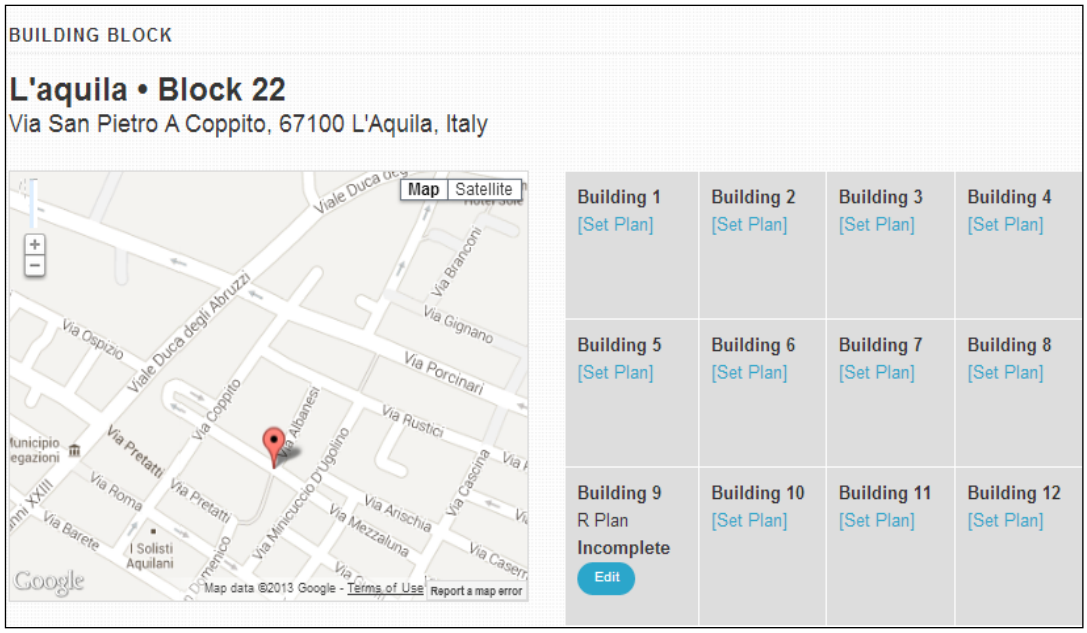

a)

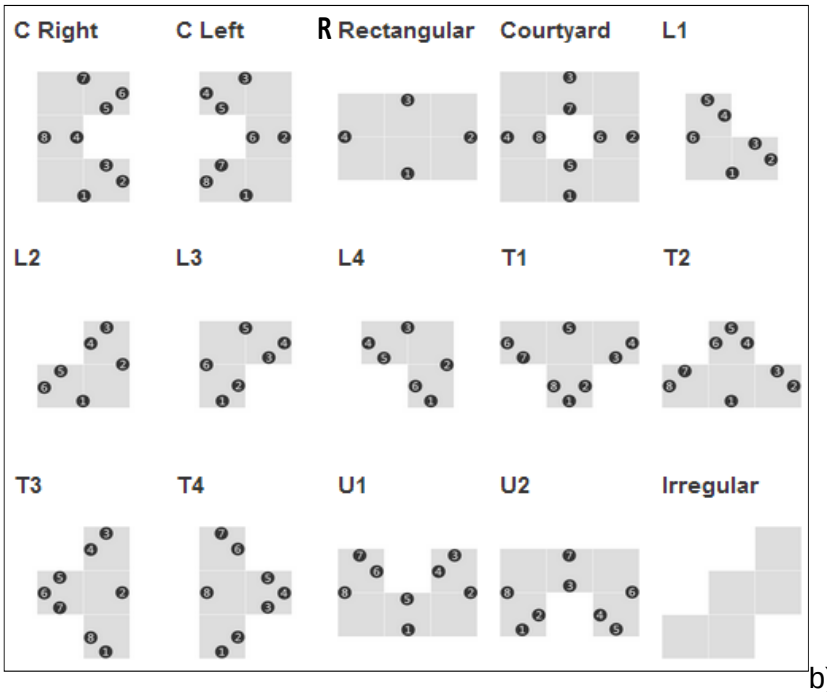

b)

Figure 5-24: Extract from the web-interface of LOG-IDEAH. a): location of the inspected urban block and definition of the number of buildings in the identified urban block; b): possible plan geometry of a building

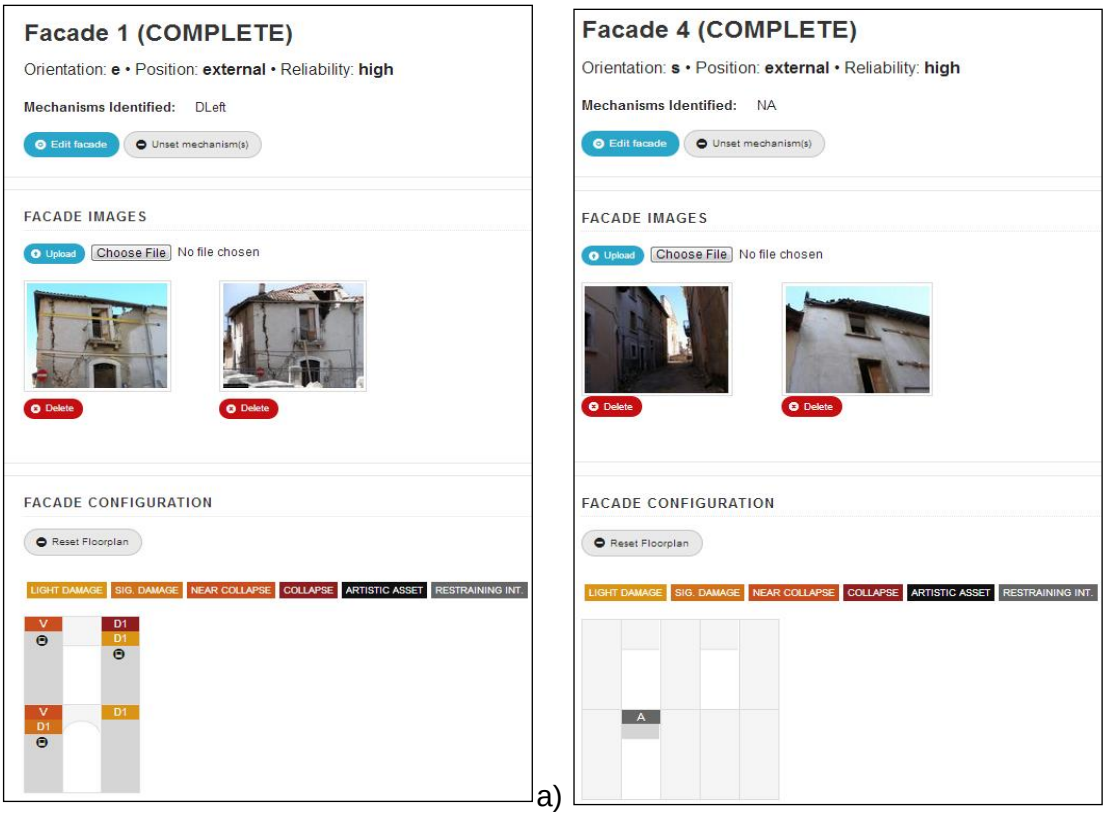

Figure 5-25: Extract from the web-interface of LOG-IDEAH. Simplified sketch and identification of the damage for a) VeME 22.9s and b) VeME 22.9s

As mentioned before, LOG-IDEAH is first run on the data reported in Figure 5-25a reporting the elevation, opening layout and damage of VeME [22.9.1e]. In this first run, only cracks with severity levels C, NC and SD are considered. With this input, LOG-IDEAH identifies D1-left as a possible failure mode, by confirming the on site diagnosis. However, LOG-IDEAH captures another possible failure mode H2 of Figure 5-26. Both failure modes identified by LOG-IDEAH have LOW uncertainties and HIGH possibility of occurrence, since the crack patterns required to identify both failure modes are contained on a single VeMEs and the observed cracks (yellow, violet and red in Figure 5-24) exactly match the identified failure modes D1-left and H2.

To consider the crack patterns of both VeMEs as input of LOG-IDEAH, the data available for VeME [22.9.4s] is added to pre-existing record. As mentioned before and from the data reported in Figure 5-25b, VeME [22.9.4s] is not damaged, therefore, only data related to number of floors and maximum number of openings per storey and opening layout is the only information of VeMEs [22.9.4s] added to the pre-existing record.

Based on the new set of data and considered only the most severe damage observed on the building, LOG-IDEAH captures not only the failure modes D1-Left and H2 for the VeME [22.9.1e] but also the failure mode B1-Right Figure 5-26 for the VeME [22.9.4s], which was not recognised during the on site inspection.

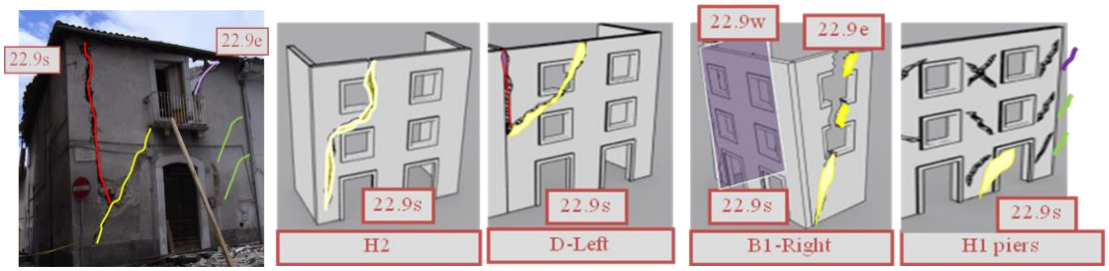

Figure 5-26: LOG-IDEAH output of VeME 22.9e and VeME 22.9s

The failure modes D1-Left and H2 occur with LOW uncertainty and HIGH possibility, as it was already captured in the previous run performed on only one façade. For B1-Right, this occurs with HIGH uncertainty, since only by inspecting VeME [22.9.3w], highlighted in Figure 5-26, the occurrence of this failure mode can be confirmed.

Moreover, due to the criteria defined in section 5.9, since VeME [22.9.3w] has not been inspected, LOG-IDEAH assumes that VeME [22.9.3w] and [22.9.4s] are not well connected, and therefore the identified B1-Right has a MEDIUM possibility level of occurrence.

If the analysis is repeated by considering all cracks observed on site, LOG-IDEAH adds the failure mode H1 (see Figure 5-26) to the previous identified failure modes. This failure is characterised by a LOW uncertainty level and HIGH possibility level of occurrence.

Since the levels of cracks involved in H1 have a severe damage level, H1 has also severe damage level. For the other failure modes, these have between Near Collapse to Collapse damage level depending on the highest damage levels observed on the cracks used by LOG-IDEAH to capture the identified failure modes.

5.14 Final remarks

In this chapter, the WBES LOG-IDEAH has been presented as the procedure in the hybrid methodology developed for the estimation of the failure modes by using on site inspection. As discussed in this chapter, LOG-IDEAH is the results of a process derived by the review and criticisms of the existing procedures for the assessment of the failure modes based on visual inspection.

The real innovation of this procedure consists in proposing the use of an expert system for the assessment of failure modes of buildings, and demonstrating its suitability to find solutions for problems requiring knowledge and experience of experts. Moreover, since LOG-IDEAH is developed in a Web environment, this tool has also the advantage of being available from any locations with internet access. Furthermore since LOG-IDEAH is developed in a web platform has also the benefit that does not require the installation of specific software or supports from any powerful machines since data and reasoning is all placed on an external server.

6. CASE STUDY: THE HISTORIC CENTRE OF L'AQUILA (ITALY)

6.1 Introduction

In this chapter, the methodology presented in section 3.4 is applied to a real case study, with the scope at validating the capability of the hybrid approach through the application of the methods FaMIVE and LOG-IDEAH, presented in chapter 4 and chapter 5.

This application addresses the capacity of both methods to predict the seismic performance of historic buildings and showing how the hybrid approach given by the joint application of FaMIVE and LOG-IDEAH provides a better output than the one that can be obtained if only one of the two methods is applied.

The selected case study for this application is the historical centre of L'Aquila, in Italy, damaged by the sequence of shocks of April-May 2009.

The chapter starts with a description of the geometric and structural characteristics of the buildings in the selected case study, surveyed in several occasions between 2009 and 2013, as discussed in 6.2. An analysis of the data collected during these inspections, providing a structural characterisation of the urban blocks and architectural assets, constituting the historic city centres of L'Aquila, is reported in section 6.3. This data constitutes the input for both FaMIVE and LOG-IDEAH tools as underlined in section 6.4 where an example of data collection on a building selected from the case study which information is required for each procedure.

In section 6.5, the buildings in the case study are classified according to structural features, while in section 6.6 their failure modes and damage levels observed on site by experts are illustrated and discussed.

In section 6.7, FaMIVE and LOG-IDEAH are applied and their output in terms of failure modes and damage levels are compared with the ones observed on site by experts.

This comparison is presented through two different validations, proposed to point out how both methods FaMIVE and LOG-IDEAH should be jointed in a hybrid method to assess the failure modes of masonry buildings.

The first validation is presented in section 6.8, where the estimated failure modes are compared with the failure modes observed on site by adopting two different measures, defined in section 3.4. The first one is the Precision defined as the proportion of estimated failure modes, which are correctly estimated and the second one is the Recall defined as the proportion of the observed failure modes that are correctly estimated.

Once these measures are calculated, the F1 score, introduced in section 3.4, is adopted to combine the results on the Precision and the Recall, and identify the capacity of prediction of the single method.

As discussed in section 3.4, the capacity of prediction of FaMIVE and LOG-IDEAH is also tested on two different random methods that generate 10000 sets of predictions. Both methods randomly associate one or more possible failure modes to an inspected façade. The first method assigns to all possible failure modes the same probability of being associated to a façade, while the second assigns to all possible failure modes, a probability of being associated to a façade that depends on the occurrence observed in the failure modes identified on site.

Based on these results, the hybrid approach is given by the results of FaMIVE and LOG-IDEAH that best match the failure modes observed on site by experts.

In section 6.11, a further classification of the inspected buildings is presented. This classification is performed by classifying buildings according to the failure modes and the vulnerability levels estimated by FaMIVE approach. Therefore, the second validation consists of comparing the damage levels estimated by FaMIVE with the damage levels observed on site and recorded in LOG-IDEAH.

The estimation of the damage levels obtained by using FaMIVE is carried out with the iterative approach described in sections 4.6 and 4.7. The results are illustrated by presenting first the capacity curves in section 6.10, and then showing their intersection

with the nonlinear acceleration-displacement spectrum derived from the abatement of the corresponding linear spectrum, as shown in section 6.11. The reduction of the linear spectrum is performed by using the ductility estimated with reference to the Equivalent Displacement (ED) method, described in section 4.6.2. This method is based on the assumption that the maximum displacement of an inelastic system is equal to the maximum displacement of an elastic system, characterised by the same mass and initial stiffness. The intersection between the capacity curves and the nonlinear spectrum provides the performance points, presented in section 6.12. Finally, the damage levels distribution is obtained by the intersection between the identified performance points in terms of displacement with the fragility curves, as shown in section 6.13.

Once the damage level distributions are estimated, these are compared with the damage level distributions recorded in LOG-IDEAH. This comparison is presented for building classes, defined with reference to the classifications introduced specifically for the case study of this work.

This has been done not only to validate the capacity of prediction of the proposed methods but also to identify the building classification that best represents the performance of the buildings observed on site, if possible. Results related to the comparison of the damage levels are presented in section 6.14.

Final remarks on the application and the capacity of the proposed hybrid method in predicting the events observed on site are discussed in section 6.14.

6.2 The historic city centre of L'Aquila and the seismic event of the 6th of April in 2009

On 6th of April in 2009 (01:32:40 UTC), the M 6.3 L'Aquila earthquake struck the Aterno Valley in the Abruzzo region, central Italy. The focal depth of the main event was about 9 km along the 15-18 km long NW-SE normal fault with about 45° dipping SW, matching the regional fault geometry in the Apennines (Pacor et al., 2011). The earthquake caused approximately 300 deaths, 1500 injuries and severe damage to over 60,000 buildings in 16 municipalities, including L'Aquila city centre (Alexander, 2010).

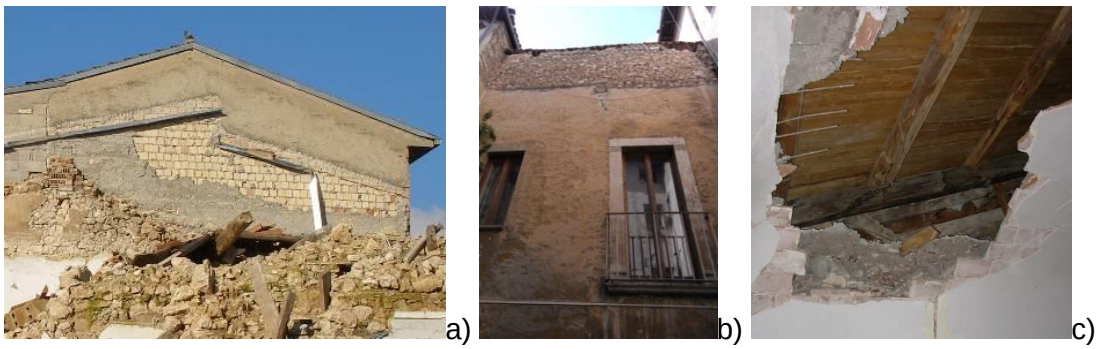

Figure 6-1: a) Building with a later addition, b) masonry building with a additional mezzanine, c) reinforced concrete screed added floor in the late 20th century to the bottom of the original timber floor (D'Ayala and Paganoni, 2011)

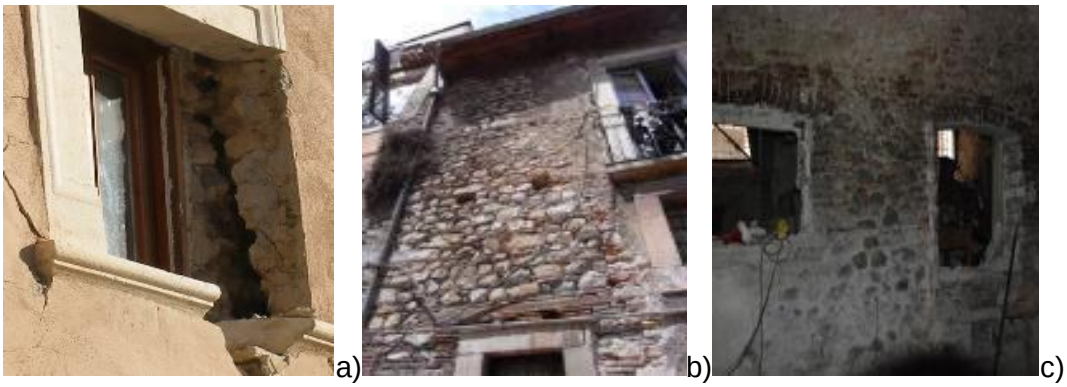

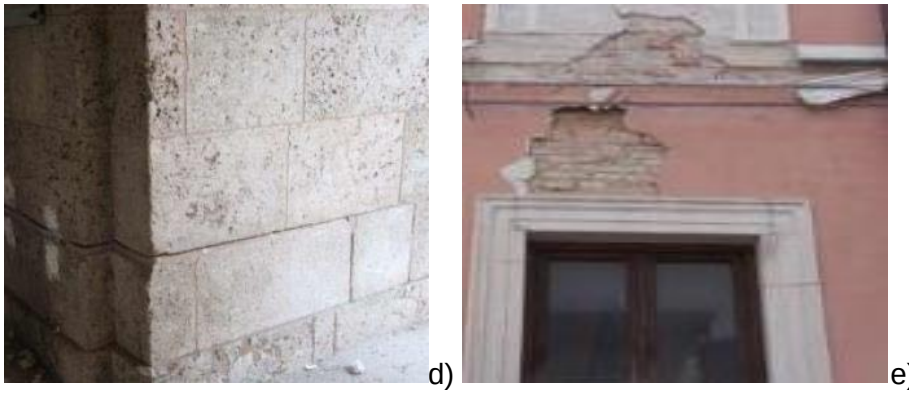

Figure 6-2: a) 'Muratura a sacco', b) roughly squared stone blocks mixed with bricks, c) rubble stone d) square stones and e) regular courses of fire brickworks

The city centre of L'Aquila is characterised by historic constructions mainly made in masonry, grouped in bulk-shaped urban blocks in a relatively regular street grid. The urban blocks are usually formed by four to eight buildings, arranged around small internal courtyards with variable dimensions depending on the size of the building and number of rooms.

The constructions generally have regular plan and regular elevations. In some buildings, the façades have irregular opening layouts due to alterations, extension or demolition of buildings, which can greatly diminish the integrity of a building, as discussed in section 4.2.

Almost 10% of the buildings are modified by the construction of additional stories, or mezzanines built above the original roof level, or by alterations carried out on the original floors, as illustrated in Figure 6-1a and Figure 6-1b. Most of the buildings are residential in use, and few have commercial, religious, or administrative functions.

Buildings in the same urban block differ in numbers of storeys that vary from one or two (for the oldest buildings) up to a maximum of five storeys (for the more recent constructions).

The area in plan can vary significantly according to the building use. Generally, the biggest constructions in plan are administrative or educational buildings while the residential or commercial ones have smaller plan.

The walls in a few cases appear to be solid but commonly are formed by two leaves of dressed stone poorly connected, and sometimes filled with rubble called "muratura a sacco" (Figure 6-2a).

a) b)

Figure 6-3: Classes of vault: a) barrel vault built with roughly shaped stone with a thickness of about 0.25 m, and b) shallow brickwork cross vault, with bricks laid in folio with overall thickness of 0.06 m (D'Ayala and Paganoni 2011)

The most common mortar observed in situ is lime, while the most common masonry fabric is a mixture of roughly squared stones courses alternating to fired bricks courses. A minority of the inspected buildings use rubble or square stones; or regular courses of fire brickwork (Figure 6-2b, c, d, e).

The original floor structures generally are brick or stone vaults at the ground floors and timber joist in the upper storey and roof. Following the 1703 earthquake, thin brick vaults were introduced in higher storeys, is some cases as false ceiling, in others as loadbearing structures. Only a minority of the buildings, altered in the 20th century, have jack arches with steel beams or reinforced concrete slab (Figure 6-3, Figure 6-4, and Figure 6-5).


a)

b)

Figure 6-4: a) Brickwork in folio vaults introduced after the 1703 earthquake as false ceilings, b) timber floors altered by the introduction of concrete screed in the late twentieth century (D'Ayala and Paganoni 2011)


a)

b)

Figure 6-5: a) Typical example of original floor in timber, b) collapse of a lightweight vault with steel beam

Most of the observed buildings have been rebuilt or repaired after the earthquakes of 1349, 1452 and 1703, which were particularly catastrophic events for the city. As it can be commonly observed in historic centres located in seismic prone areas, anchors are commonly adopted to improve the connections of the walls (Figure 6-10c). In the historic centre of L'Aquila the first anchors were made of timber (see Figure 6-6a) or, steel (see Figure 6-6 b and c).

The inspected buildings are also commonly restrained by quoins made of large squared stone blocks (Figure 6-7a and b). However, the efficacy of cut stone quoins might be limited, when the masonry fabric of the entire façade is very poor and internal walls are not well connected to the orthogonal façades. In a few cases, buildings' façades are restrained by a ring beam at the roof level (Figure 6-7c).

Generally, buildings are characterised by a good level of connections among walls and between walls and floors, as it is underlined by the observed damage levels reported in section 6.6. This is because a high number of buildings are strengthened and good quality materials are commonly adopted in the constructions. Houses that have bad performance are mainly characterised by slender walls, weak mortar, poor masonry and a lack of or ineffective restraining devices (Figure 6-6).

Figure 6-6: Traditional reinforcements: a) timber tie, b) wrought steel cross tie inserted in a quoin and c) 20th century steel tie with end plate (D'Ayala and Paganoni 2011)

Figure 6-7: a) and b) Examples of buidings with stone quoins (D'Ayala and Paganoni, 2011) and c) with ring beam at the roof level

6.3 Selection of the urban blocks

After a preliminary inspection of the historic city centre, investigations that are more detailed were carried out on the urban blocks highlighted in grey in the map of Figure 6-8. A total number of ninety buildings composes these urban blocks. The distribution

of their typical features is reported in Figure 6-9 and Figure 6-10, and described as follow.

More than 85% of the inspected buildings are low rise (two or three storeys) with their first storey being higher than the other ones, while the remaining inspected buildings are medium rise (four or five storeys). The typical storey height for the first level is between 3.5 m, and 4 m, whilst the others have a storey height between 3.0 m and 3.5 m.

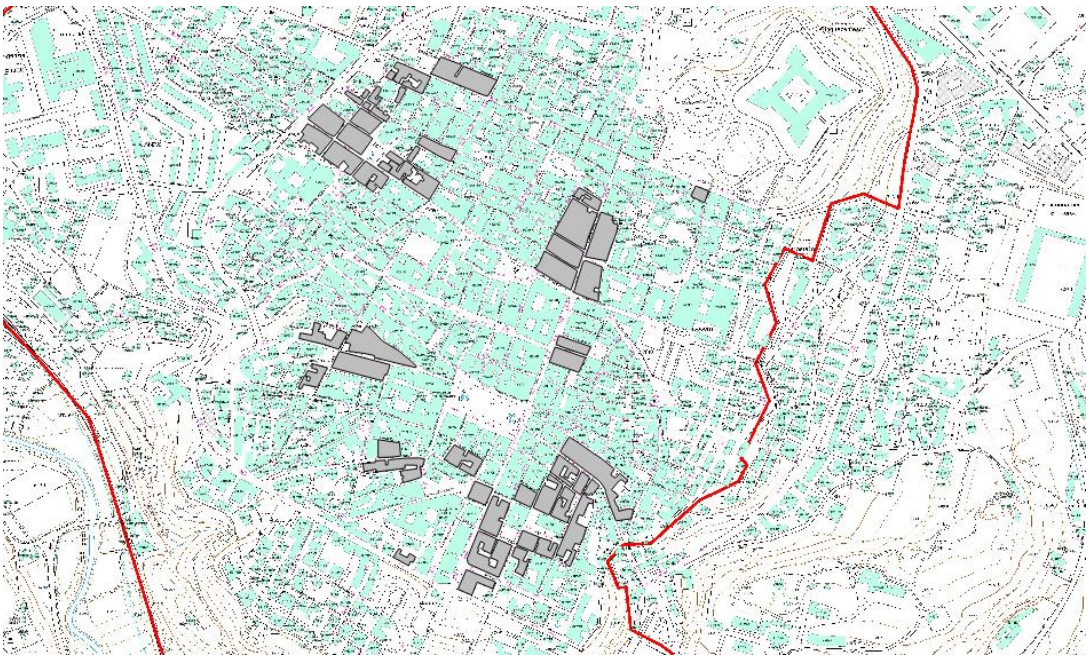

Figure 6-8: Identification of the urban blocks and façades inspected in the historic centre of L'Aquila. The red line points out the border of the historic al centre

This explains the total heights reported in Figure 6-9, and underlines the need of investigating how the rise effects on the building performance, (see section 6.5)

The foot print in most of the buildings have a limited dimension and a regular plan area, highlighted by a small percentage (~20%) of the inspected buildings having a foot print that is greater than 200 sqm. Therefore, the plan distribution is not a parameter that particularly affects the performance of the buildings considered in the specific case study.

The thicknesses of the walls have also been measured. The average of the thickness taken from the bottom to the top storey varies from a minimum of 0.30 m to a maximum of 1.5 m. Due to the high percentage (50%) of very thick walls, a good

seismic performance of most of the surveyed buildings is expected, since it is assumed for those buildings to have façades with good connections.

As expected from the discussion in the previous section, the most common mortar is lime observed in more than 90% of the inspected buildings, and only in a minority of the constructions the mortar is mud. For a few buildings (~2%), where the plaster did not allow inspection of the masonry fabric, the mortar has not been characterised.

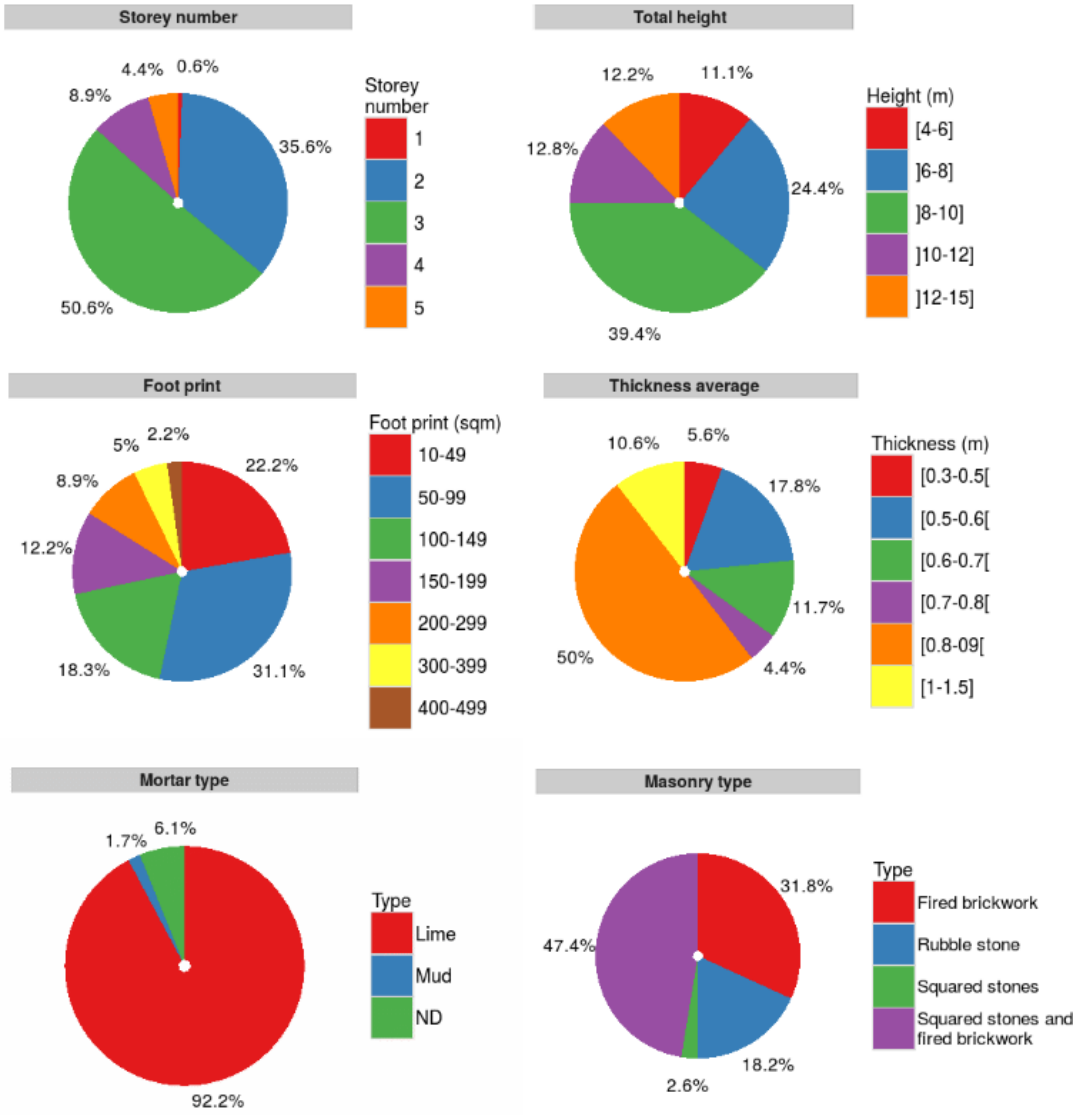

Figure 6-9: Distribution of storey number, height, plan area, wall thickness, mortar class and masonry class for the inspected buildings highlighted in Figure 6-8

These inspections have also confirmed that most of the buildings (~50%), are made of roughly squared stones together with fired brickwork. Buildings in stone masonry are also identified and cover a percentage of ~20% of the inspected houses. New

constructions are generally built by using fired-brickwork, as observed for ~30% of the houses surveyed on site. For the buildings with roughly constructional materials, a lower seismic capacity is expected compared to the ones achieved by houses with fired brickworks.

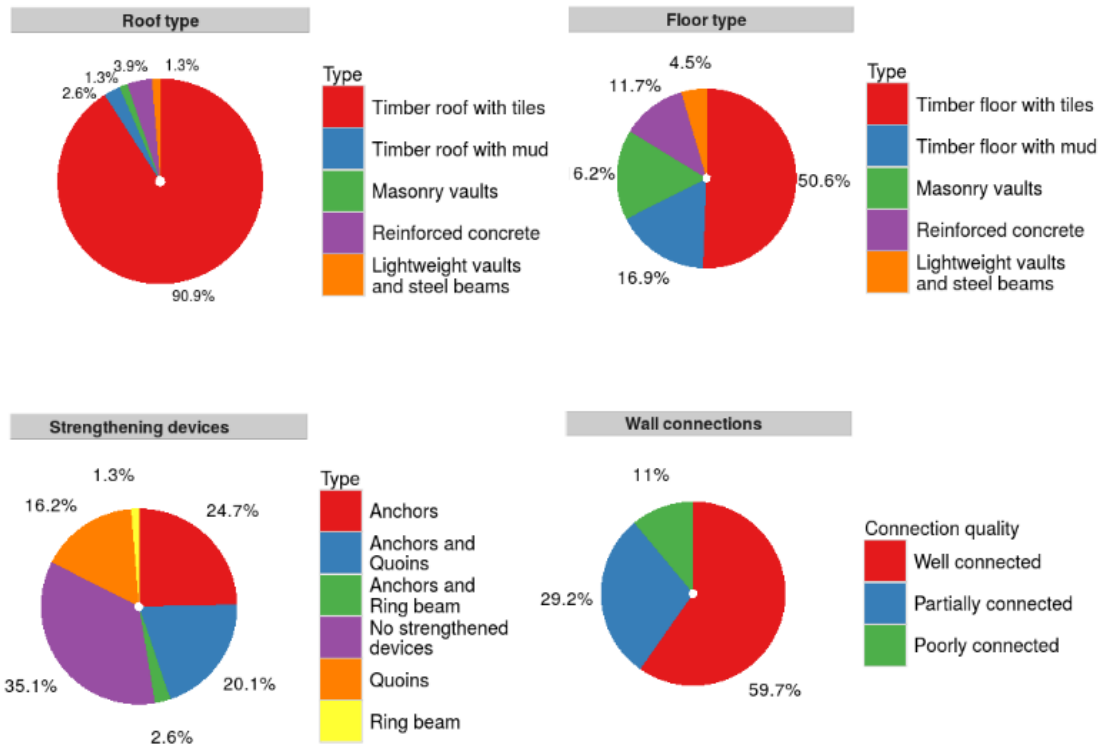

Figure 6-10: Distribution of roof class, floor class, strengthened devices, class of connections between walls of the inspected buildings highlighted in Figure 6-8

As discussed in the previous section, most of these buildings have timber floors (~70%) and only a minor percentage of the inspected houses have floors characterised by masonry vaults, or by lightweight vaults with steel beams. The percentage of the masonry constructions with reinforced concrete floors (~10%) are commonly new constructions or buildings where their original floors (generally in timber) were substituted with a concrete slabs that are adopted to increase the seismic performance of the inspected buildings.

Most of the buildings were constructed with strengthening devices, such as quoins for ~20% and anchors for ~25% of the inspected houses. Few examples of buildings (~1%) with ring beams have also been observed. For these houses, where the strengthening devices are efficient and improve the connections between walls and floors, failure modes due to overturning are likely to occur.

Finally, particular attention is given to the connections between walls, since deficiencies related to connections strongly influence the building performance, as discussed in chapter 4 and 5. A percentage of ~60% of the buildings have good connections either because they have been strengthened or have been properly constructed to resist seismic events.

Most of these buildings were surveyed on site and only a minority (10%) was inspected from photographs. For each building, at least two orthogonal elevations were inspected and the data was collected with the aid of the inspection form of FaMIVE, presented in section 4.31 and included in Appendix C and the web-platform of LOG-IDEAH, presented in section 5.12.

In the next section, an example is reported to illustrate how the building samples highlighted in Figure 6-8 have been inspected by using both methods FaMIVE and LOG-IDEAH.

6.4 Typical data collected on site by using FaMIVE and LOG-IDEAH

By way of an example, building 10.2 in Figure 6-11, taken from the area of study, is used to summarise the class of data collected as input for both methods. The pictures in Figure 6-11, taken on site, show the façades that have been inspected through visual inspection. Only external surveys are carried out.

The input data collected for FaMIVE are first stored at urban block level, by recording information related to its shape, and its number of buildings. For the building in question, it has a corner position in a bulk-shaped urban block, composed of six buildings.

Then the input data for FaMIVE is also collected at the building level by recording geometry in plan and elevation. The plan is a rectangular of 16m x 13m and the elevation has a total height of 9.5 m.

Data collected with FaMIVE

Urban data: bulk-shaped urban blocks, 8 buildings, corner position
Plan: rectangular shape (16 x 13) m
Height: 9.5 m
Opening layout: regular distribution of the openings
Floor and roof classes: timber beams
Number of internal bearing walls: 3 orthogonal to 10.2e and 2 orthogonal to 10.2n
Masonry class: stone and bricks
Mortar: lime
Presence of restraining elements: No
Vulnerable elements (presence of balcony, jetty, etc.): balconies

10.2e

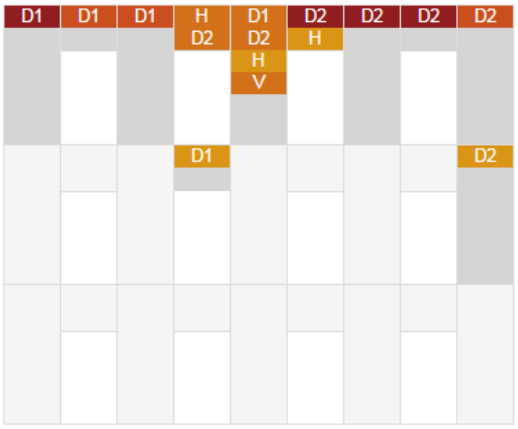

10.2n

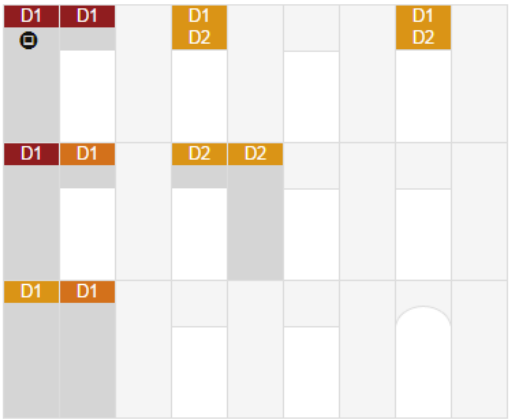

Data collected with LOG-IDEAH

LIGHT DAMAGE | SIG. DAMAGE | NEAR COLLAPSE | COLLAPSE | ARTISTIC ASSET | RESTRAINING INT.

For the legend of the damage classes refer to section 5.5

Figure 6-11: Data collected by using FaMIVE and LOG-IDEAH for building 10.2 assessed in L'Aquila city centre after the earthquake in 2009

After this general assessment, the survey becomes more detailed, as more information is recorded at the façade level. The opening layout and dimensions are recorded, as highlighted in Figure 4.15, by using tape or electronic laser measurement device. The façade 10.2e has four openings positioned regularly over three storeys. The opening size for the second and third storey is the same, slightly larger at the first storey. The opening layout at each storey is classified as E2 according to Figure 4-14a.

The façade 10.2n in Figure 6-11 has four openings at the second and third storey. These are positioned according to the opening layout E2 by referring to Figure 4-14a. The first storey has only three openings that are smaller than the ones at the upper storeys. These are positioned according to the opening layout E1R, in agreement with Figure 4-14a. The lateral piers at the edges of each storey of both façades are (N+) according to definitions provided in Figure 4-14b.

Following the definition of the geometry in elevation, roof/floors need to be characterised according to their class, as well as load bearing walls and their construction materials. For the inspected building, the floors and roof are made of timber beams, supported by the external façades, and two internal load bearing walls positioned along the two main orthogonal directions of the building. The construction material of the walls is of mixed composition since it is characterised by irregular stones and bricks, as the one in Figure 6-2. The mortar, as it is for most of the buildings in L'Aquila, is lime.

Presence of restraining elements such as anchors (Figure 6-6) or quoins (Figure 6-7) or presence of vulnerable elements such as porticoes, jetty or balconies, also need to be recorded. On these façades, balconies are identified and recorded.

The input data for LOG-IDEAH are also collected first at urban level by defining geometry of the urban blocks and the number of buildings in each block. Then the data is collected at building level, by defining its shape in plan and position of the façades that have been inspected. Finally, once the façades are sketched, as illustrated in section 5.12 the damage collection is carried out by recording location of the cracks, and severity, as defined in section 5.4 and section 5.5.

In Figure 6-11, the screenshots taken from the website of LOG-IDEAH illustrate the sketches representing the inspected façades. The cracks and their severity observed on site for both façades are directly recorded on these sketches. The nomenclature associated to the cracks and damage levels on the sketches has been defined in

section 5.4 and section 5.5. The façades are mainly damaged by diagonal cracks on their corners and horizontal cracks at the floor level. The damage severity goes from light damage to collapse.

6.5 Classification of the inspected façades based on the structural features observed on site

In this section, façades are classified according to their structural features, described in section 6.3. This has been carried out by using two existing classifications that have been slightly modified for the selected case study in this research. The need of classifying these façades according to their structural features rather than their occupancy or uses, derives from the necessity of adopting classifications suitable to classify and to record the variability in the geometric/structural features observed in historic houses, since these considerably affect the seismic behaviour, as discussed in section 6.2 and section 4.2.

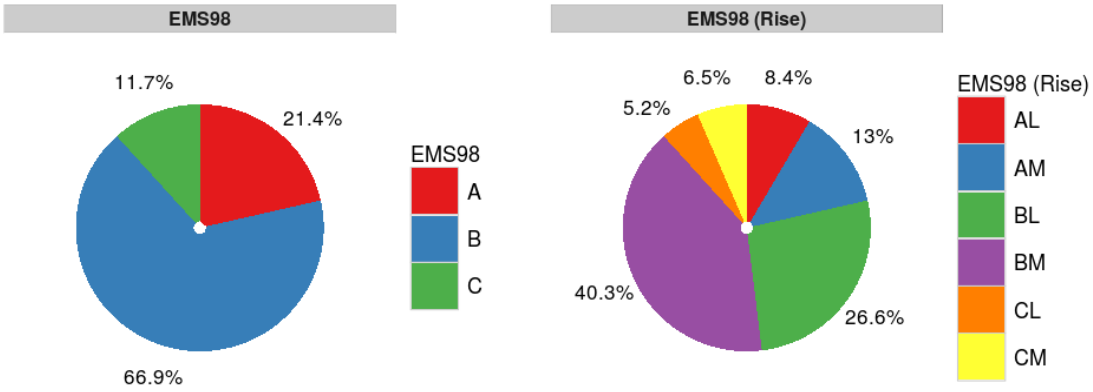

Figure 6-12: Building class distribution based on EMS'98 on the left (modified EMS'98 applied to the inspected façades) and EMS'98 (Rise) on the right (modified EMS'98 applied to the inspected façades by taking into accout their number of storeys)

The first classification considered for the selected case study is a modified version of the European Macroseismic Scale (modified EMS'98) introduced by Tertulliani et al. et al. (2011) while the second one is the PAGER classification (Jaiswal et al., 2011)

According to the modified EMS'98, buildings are classified according to their structural features in classes (or classes) associated to a vulnerability scales defined according to the guidelines of the modified EMS'98 (Tertulliani et al., 2011). In this work, the modified EMS'98 is favoured to the original version of EMS'98 (Grünthal,

1998, presented in section 3.2), since the modified classification can be better adapted to new case studies, by modifying existing building classes or including new ones, since it has a more flexible framework compared to the one that characterised the original EMS'98.

By using the modified EMS'98, the inspected façades in L'Aquila city centre are classified according to the following structural features: construction materials, floor classes, connection classes and presence of strengthening devices. This allows introducing three classes of buildings from (A) high to (C) low level of seismic vulnerability, as described below:

- Class A: buildings made of rubble stone, or mixed materials (squared stones and bricks), characterised by weak connections and timber horizontal structures or masonry vaults or lighweight vaults with steel beams;
- Class B: buildings made of square stone masonry or fired brickwork characterised by strong connections and timber horizontal structures or masonry vaults or lighweight vaults with steel beams. Presence of strengthening devices;
- Class C: buildings characterised by strong connections and reinforced concrete (RC) horizontal structures. Presence of strengthening devices.

The rise of the buildings can also be taken into consideration as an additional parameter to refine this classification. Therefore, these three classes are further subdivided in classes (L) Low (buildings with one and two storeys) and (M) Medium (buildings from three to five storeys) to take into account the rise of the inspected buildings and how this parameter affects the building performance.

The class distribution based on this classification is presented in Figure 6-12 as EMS'98 and EMS'98 (Rise).

As expected from the description introduced in section 6.2 of the historic city centre of L'Aquila, the most common building class is characterised by houses made of squares stones and fired brickwork walls, timber floors, and strong connections between floor and walls due to the presence of restraining elements or good construction techniques. Figure 6-12a and b also underline that only a minority of the inspected buildings have rigid diaphragm, by pointing out that only a minority of the inspected buildings has a reinforced concrete slab. These buildings are generally the

ones mentioned in section 6.2, whereby the original floors have been substituted with reinforced concrete floors. Class A, representing the houses with weak construction materials and weak connections covers only a limited portion of the inspected buildings.

The second building classification performed with reference the one introduced within PAGER project (Jaiswal et al. 2011), also subdivided buildings in classes according to their typical structural features. This classification available at http://pager.world-housing.net/ has a much wider geographic scope than the one proposed by the modified EMS'98, since buildings are catalogued according to the their geographic location, construction practice, local construction materials and floor classes observed in the specific region.

In the existing PAGER classification, some categories of buildings are still not very extended due to a lack of sufficient information about their structural system, and limited scientific information about their performance during seismic events. However, if new data is available or if a specific class that is not present in the PAGER classification is needed, the existing building classification can be continuously enriched with new building classes.

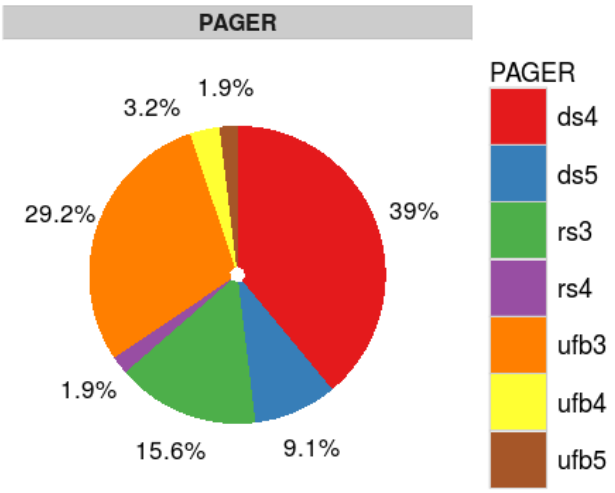

Figure 6-13: Building class distribution based on PAGER

By using the PAGER classification for the selected case study of this work, the following classes are identified and defined as follows:

- Class UFB3: Fired brickwork with timber horizontal structures;
- Class UFB4: Fired brickwork with vaults;

- Class UFB5: Fired brickwork with RC horizontal structures;
- Class DS4: Squared stones and fired brickwork with timber horizontal structures or vaults;
- Class DS5: Squared stones and fired brickwork with RC horizontal structures;
- Class RS3: Rubble stones with timber horizontal structures;
- Class RS4: Rubble stones with vaults or light vaults and steel beams.

Class DS5 is defined specifically for the case study of this work, while the other classes, although they are taken from the existing PAGER classification, have been slightly changed in their definition to encompass the inspected buildings.

The building class distribution (PAGER) of the seven classes defined above is shown in Figure 6-13. The most common building classes are the ones built with mixed materials and rubble stones, see Figure 6-2c. In particular, it can also be observed, as expected, that most of the buildings have original floors made of timber beams or vaults. The low percentage of buildings with reinforced concrete slabs, discussed previously, is confirmed in this classification. This floor class either is associated with brickworks (2%) or mixed materials (9%).

In Figure 6-14, the correlation between EMS'98 and PAGER classifications is illustrated. As expected, classes from A to C of the EMS'98 are correlated to the PAGER classes that are from buildings with the weakest materials and the most flexible floors to buildings with the strongest materials and the most rigid floors.

However, since the PAGER classification defines more classes of buildings, compared to the ones provided by EMS'98, it is expected that PAGER better takes into account the effect of the parameters impacting on the seismic vulnerability, and therefore it also has a higher capability to differentiate the performance of the single identified classes.

In the next section, the performance of the inspected buildings is illustrated and their failure modes are discussed from the point of view of the experts who have participated to the data collection of the selected case study for the current research project.

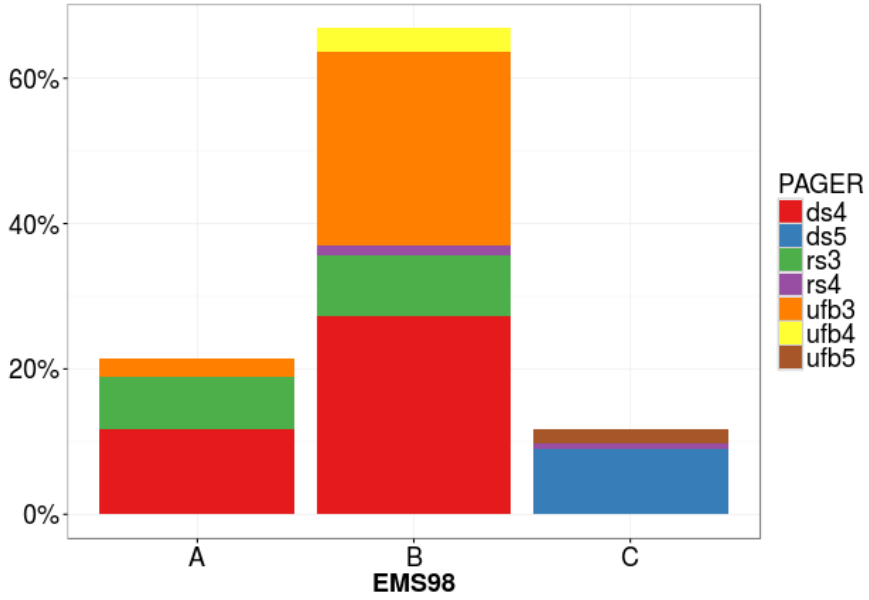

Figure 6-14: Correlation between EMS'98 and PAGER

6.6 Failure modes observed on site by experts

The failure modes of the buildings in the urban blocks of Figure 6-8 are identified by the author and other engineers who had used their own expert judgements and extensive experience in post-earthquake assessment to estimate the building performance.

These failure modes are not adopted as input of FaMIVE and LOG-IDEAH but they are only used to validate the results derived from the single methods and their union given in the proposed hybrid approach.

As introduced in chapter 4 and chapter 5, these failure modes can be classified according to four classes:

- No mechanism: façades with no damage;
- IP: in-plane failure modes;
- OOP: Out-of-plane;
- COMB: combined failure modes.

During the visual inspection, it has been observed that buildings in Figure 6-8, according to their deficiencies, and seismic damage can be associated to one or more possible failure modes, as showing in Figure 6-15 where the percentage of façades and related number of failure modes associated to each of them is illustrated.

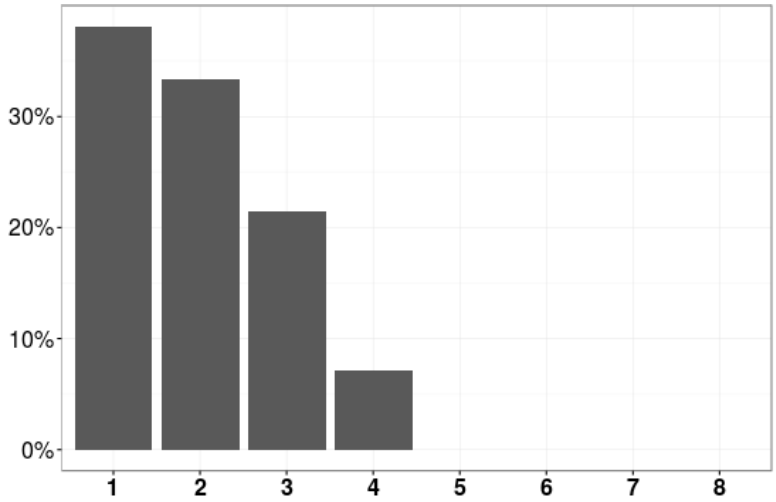

Figure 6-15: Occurrence in percentage of the number of failure modes observed for façade

Buildings (~40% in Figure 6-15) that fail for only one type of failure mode have generally a crack pattern that clearly underlines the causes of the type of failure mode whereby the building is failing. In these cases, since the surveyor is completely sure that what he is observing is the real failure mode of the inspected façade, these failure modes are defined as a *certain* event.

For the buildings in Figure 6-15, failing for more than one failure modes, these have either crack patterns that point out portions of the façade failing differently from each other, or same portions of façade failing for more failure modes. In these cases, more than one *certain* event is observed.

However, more than one failure modes are also associated to a façades, when buildings have several deficiencies, leading to a not straightforward identification of the failure modes. In this case, the different failure modes are associated to the same observed crack patterns and they are defined as *possible* events.

By mean of example, the building in Figure 6-16 illustrates that failure modes, apparently similar, in their crack pattern, are difficult to be excluded as possible solutions. This is underlined by the red diagonal crack that might be classified as H2.

However, the same red diagonal crack can also be associated to a partial development of an OOP, or a COMB, considering that the adjacent façades to the one with red cracks have not been inspected, and therefore there is no possibility to confirm if the crack patterns in blue are occurring. This example is very representative of the class of issues for those experts who carry out onsite inspection of the failure modes.


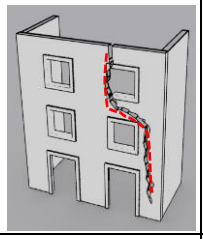
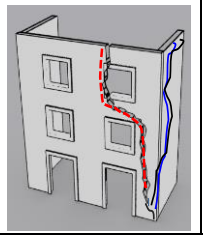
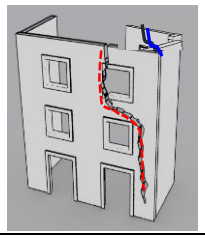
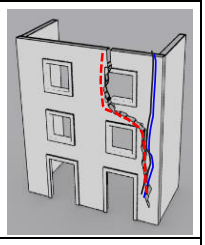

Diagonal cracks	IP	COMB		OOP
Light damage	H2	C	B1 or B2	D

Figure 6-16: Possible failure modes that can be associated to an observed crack pattern

The recognition of IP in class H2 (IP(H2)) in association with other failure modes is also confirmed in Figure 6-17, showing the distribution of this failure mode for the building sample of Figure 6-8, where for 60% of façades IP(H2) is always identified with at least one COMB of class B or C (COMB(B, C)) or at least one OOP of class D (OOP (D)). In this case when IP(H2) is identified together with COMB(B, C) and/or OOP(D), all of them are considered possible failure modes for the inspected building.

In Figure 6-17, it is also possible to observe that a minority of the inspected façades fail for IP(H2), or for IP(H2) together with "other" class introduced to define failure modes of classes A, E, F, G and H1, see Appendix B. In this case, IP(H2) is considered a *certain* failure mode for the inspected building.

It is also important to mention that in Figure 6-17, IP(H2) is never associated to both COMB(B,C) or OOP(D), since these two failure modes are mutually exclusive. This is because during the onsite observation, the quality of the materials, the level of structural detailing between façades and floors, and the presence of restraining elements can be assessed to verify if the lack of connections between walls is causing OOP(D), or if the lack of connections between walls and floors or ineffective restraining elements walls is causing COMB(B,C). Taking into account these considerations on *certain* and *possible* failure modes, Figure 6-18 shows in orange the failure mode distribution based on *certain* events and in grey the failure modes IP(H2), COMB(B,C), and OOP(D) defined as *possible* events with the reference to Figure 6-17.

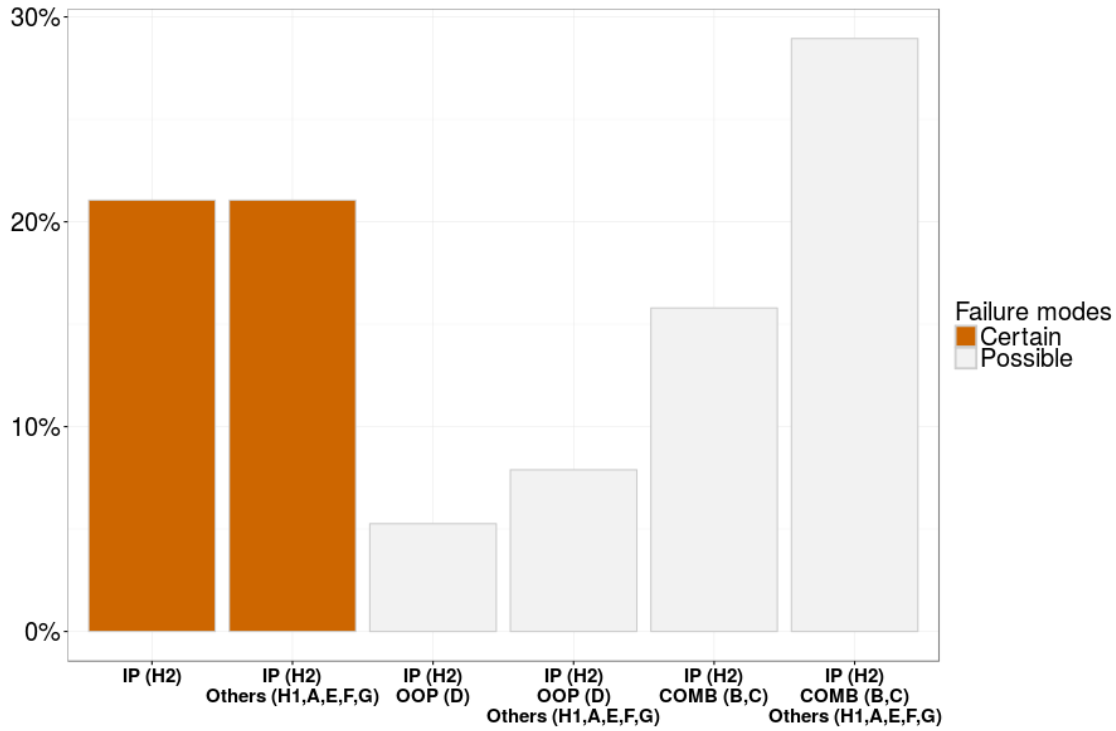

Figure 6-17: Occurrence in percentage of the in-plane failure modes IP(H2) observed on site in association with other failure modes

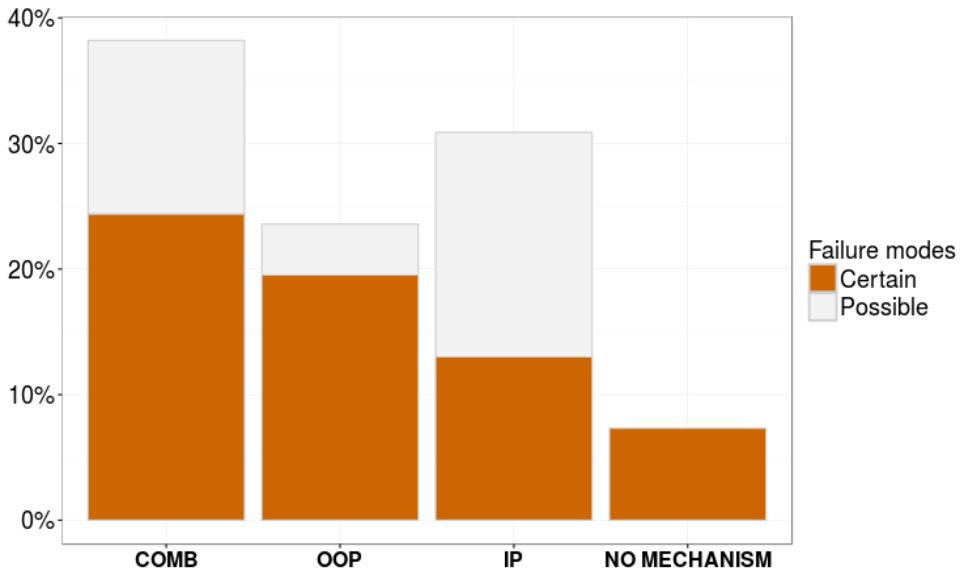

Figure 6-18: Occurrence in percentage of the failure modes observed on site

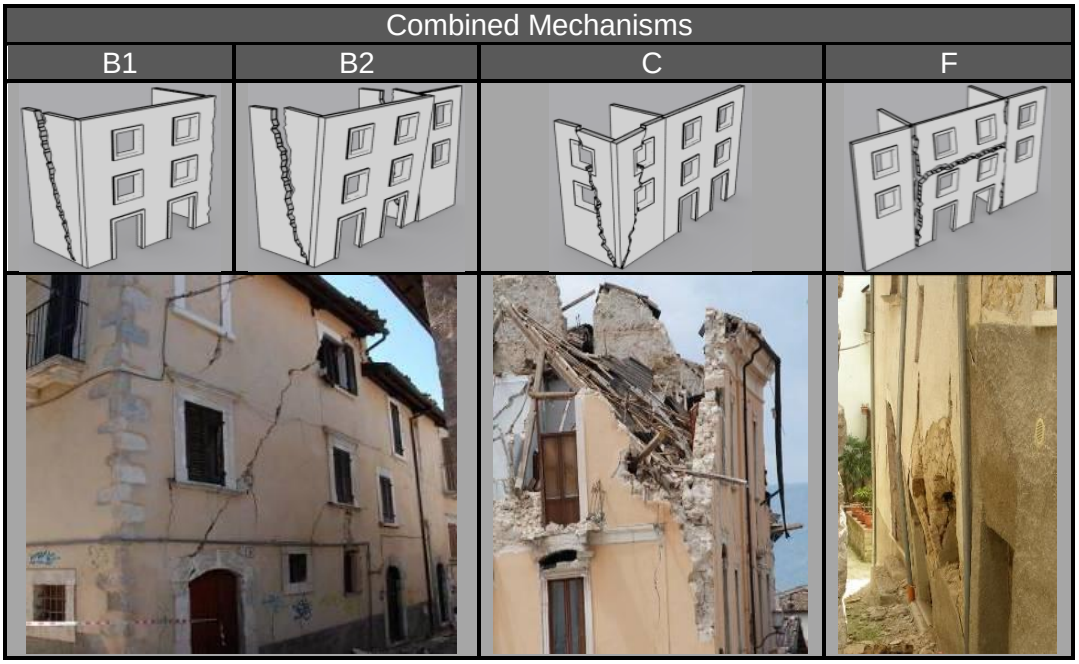

Figure 6-19: On site identification of the Combined Failure modes


a)

b)

Figure 6-20: Examples of failed steel cross-ties: a) material failure by tension of a timber tie; b) punching shear failure of the anchor plate through the masonry wall

In order to highlight how failure modes are distributed on the selected cases study according to expert judgements, the *possible* failure modes (in grey) are excluded from the following discussion that only refers to *certain* events (in orange).

Most of the observed buildings fail for COMB, since the majority of the inspected buildings have good connections or are strengthened, as discussed in section 6.3 and highlighted in Figure 6-10. The typical COMB observed for the selected buildings are reported in Figure 6-19, and they are classified in class B, C and F, with reference to section 4.2. As expected, the onsite investigations have underlined that buildings with good construction materials and good connections mainly tend to fail for B and C while

strengthened buildings with poor performance of ties or lack of capacity in the bearing walls (see Figure 6-20) tend to collapse for failure modes of class F.

The second most common observed failure modes is the OOP, as pointed out in Figure 6-18. Examples of these types of failure modes are reported in Figure 6-21: On site identification of the Out-of-plane failure modes and they are classified as A, E, D and G with reference to section 4.2. As expected, the onsite investigations have underlined that buildings with lack of connections between walls is the cause of the failure modes of class A and D, while aligned openings in the façade with poor connection of the spandrels' masonry to the piers' masonry, is the cause of the failure modes of class E.

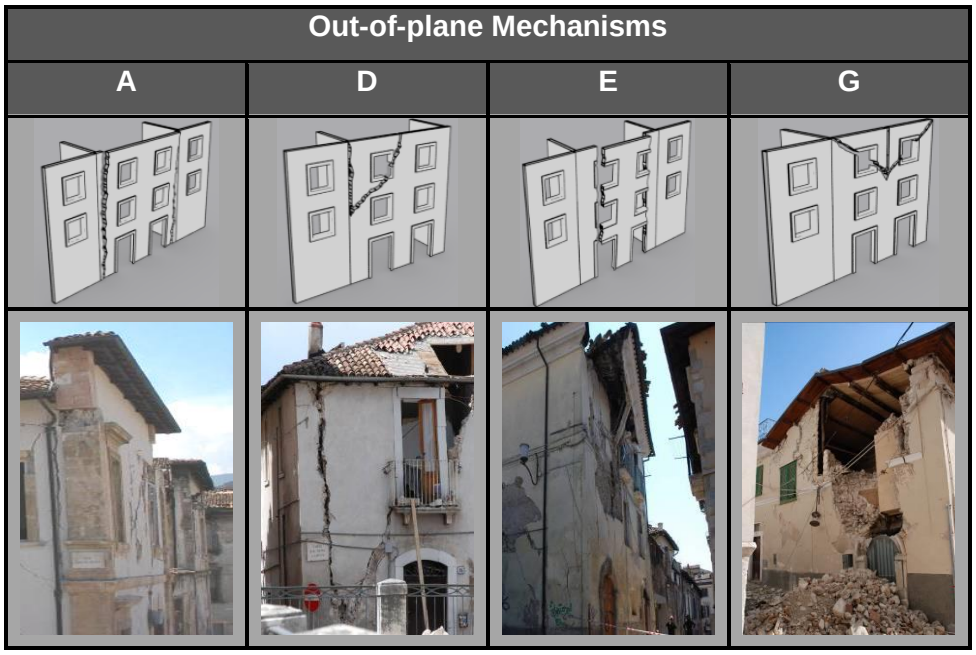

Figure 6-21: On site identification of the Out-of-plane failure modes

The onsite inspection has also confirmed that failure modes in class G are also very commonly observed either as a light damage limited to the top façade (Figure 6-22a) or complete collapse of the roof (Figure 6-22b). This type of failure modes is considered a very damaging failure mode in a building, only if this involves the collapse of at least half of the top storey. In this specific case, the failure mode G is taken into account in Figure 6-18, otherwise it is excluded.

Figure 6-22: a) Damage on the top of the façades and b) roof collapse due to thrusting action of the roof against the façades

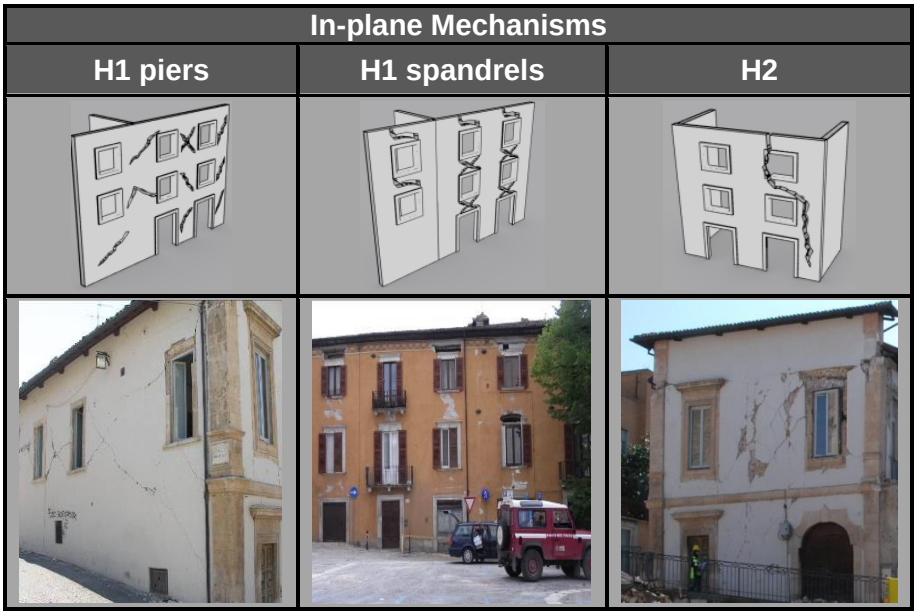

Figure 6-23: On site identification of the In-plane failure modes

Only a minor percentage of the inspected buildings fail for IP as reported in Figure 6-18. As discussed in section 4.2, the IP failure are represented by H2 and H1, see Figure 6-23. In particular, if H1 is a local damage of a single or few piers (H1 piers) or spandrels (H1 spandrels), this are excluded in Figure 6-18, since H1 is considered damaging for the inspected building only if this represents the failure mode of an entire façade or of only one storey (soft storey).

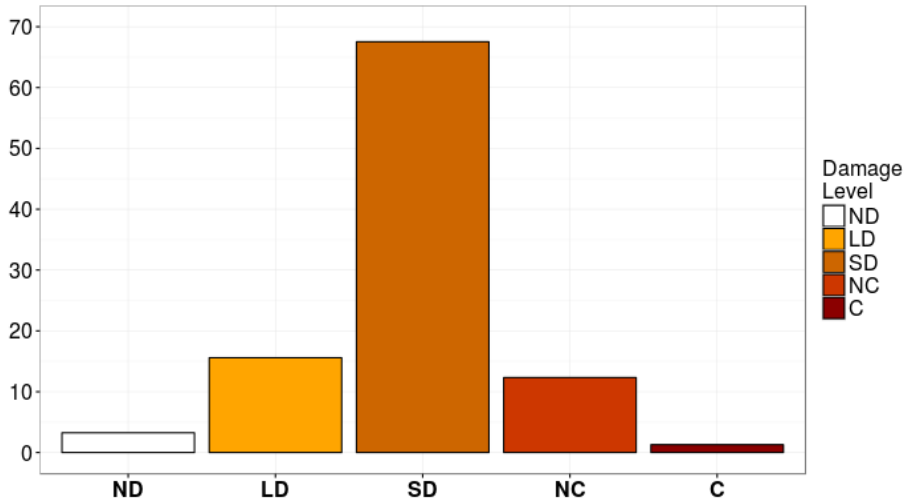

Figure 6-24: Occurrence in percentage of the damage level observed on site

The distribution of the damage levels is reported in Figure 6-24. This is classified according to five damage levels: ND: No Damage, LD: Light Damage; SD: Significant Damage; NC: Near Collapse; and C: Collapse, defined in section 4.5.

The number of total collapses observed in the selected urban blocks of Figure 6-8 was minor, while the proportions of partial collapses of the upper storeys were particularly high. In a minority of cases, total collapse of the façade was observed, and these were usually identified on buildings with substantial alterations or with additional storeys on the top of the original ones. Although the number of undamaged masonry buildings is very modest, the majority suffered either light damage or significant damage.

6.7 Analyses by using FaMIVE and LOG-IDEAH and discussion of the output

The input data is processed by using the analytical approach based on mechanics of FaMIVE and the knowledge based visual evaluation assessment of LOG-IDEAH. Their analyses aim at delivering output consisting of a list of the possible failure modes with their possibility level of occurrence and the distribution of the damage levels, as illustrated in chapter 4 for FaMIVE and chapter 5 for LOG-IDEAH.

In the sub-section 1.16.7.1, by way of example, FaMIVE and LOG-IDEAH are applied to a house located in the area of study. All failure modes predicted by both

methods are described and ranked according to their probability of occurrence estimated by using Table 4-1 and Table 5-6 for FaMIVE and LOG-IDEAH respectively.

Once these failure modes are identified for the inspected house, these solutions are compared with the failure modes observed on site to validate the capacity of prediction of both approaches with reference to the single house. This comparison leads to the formulation of solution selection criteria for the application of both methods at territorial scale, discussed in section 6.8 for FaMIVE and in section 6.14 for LOG-IDEAH.

6.7.1 Discussion of the type of results obtained by FaMIVE and LOG-IDEAH methods

Façades 10.2e and 10.2n of Figure 6-11 are analysed with FaMIVE and LOG-IDEAH after their damage severity, and failure modes have been identified on site as discussed in this section with reference to Figure 6-25.

A first interpretation of the crack pattern in terms of possible failure modes is presented in Figure 6-25. The cracks in blue on façade 10.2e represent the arch failure modes defined as G. This failure mode is caused by the punching effect of the roof that is spanning in the direction orthogonal to the façade 10.2e, as highlighted by the purlins circled in blue in the close up picture of Figure 6-26a. The cracks in purple on the façades 10.2e and 10.2.n respectively seem to underline that the walls might be failing due to H2.

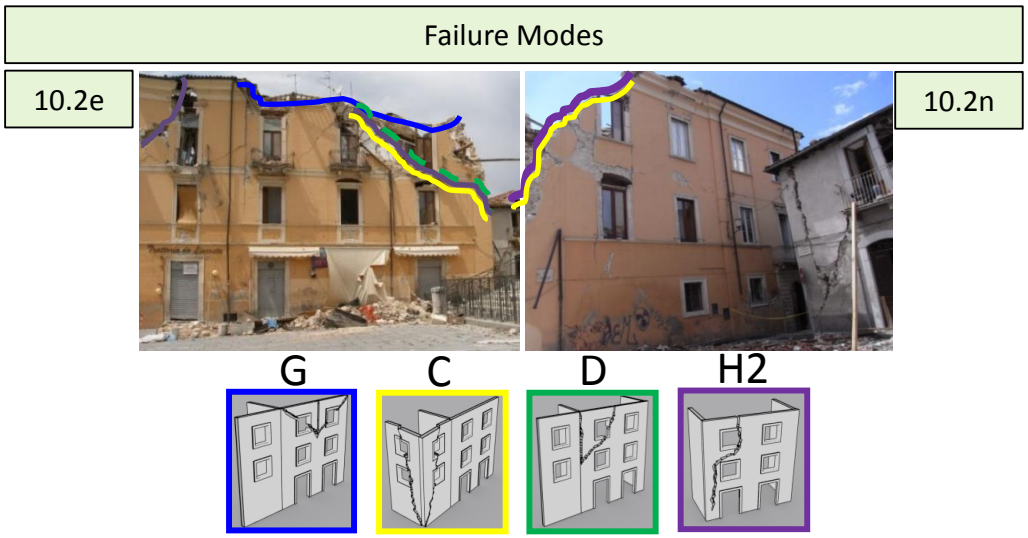

Figure 6-25:Failure modes oserved on site on the building 10.2

The diagonal cracks (in yellow) on the common corner of these façades might also be associated to a corner failure mode of class C. This type of failure mode, together with H2, generally occurs if the building is characterised by strong connections between adjacent walls, and between walls and floors or roof.

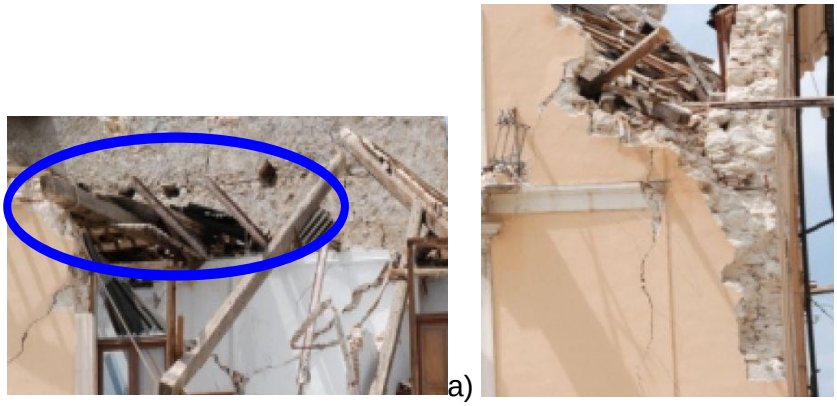
a) b)

Figure 6-26: Structural details of the building 10.2. a) Ortogonal purlins to the façade 10.2e, b) good construction materials observed from cracked corner of the building 10.2

The same diagonal cracks (also highlighted with a green dash line) might also point out that the cause of the failure mode is D, generally triggered by lack of connections between the two adjacent façades. However, this failure mode is excluded by looking carefully to this corner and its cracks in Figure 6-26b, since the roof is failing due to the loss of the top façades that are well connected, as highlighted by their construction material made of a very compact masonry.

Among the OOP, although G has the lowest value of λ, FaMIVE does not select this failure mode as the one leading to the highest vulnerability of the façade, since G only involves the failure of the spandrels on the top floor. However, although this failure mode is not the most vulnerable one, G is predicted as one of the possible solutions confirming what it is seen by observation on site.

FaMIVE also excludes the possibility that the other OOP failure modes are likely results, given their high collapse load factor and low vulnerability.

Among the COMB, although they are all considered possible, the failure mode C is the one with lowest λ and, therefore the one with the highest probability of occurrence among the estimated combined failure modes, as also shown by the value of vulnerability.

The failure mode with lowest λ involving the whole façade surfaces is H2.

Table 6-1: Collapse load factor multiplier and related vulnerability level associated to each possible failure mode computed by FaMIVE for the building 10.2

	OOP				COMB			IP		
Name façade	A	D	E	G	B1	B2	C	H1	H2	
10.2e	0.95	0.91	0.84	0.16	1.53	1.63	0.36	0.40	0.20	λ
	MEDIUM	LOW	MEDIUM	MEDIUM	LOW	LOW	HIGH	VERY HIGH	VERY HIGH	Vulnerability Level
10.2n	1.03	1.04	0.49	0.11	1.67	1.68	0.45	0.48	0.25	λ
	MEDIUM	LOW	MEDIUM	MEDIUM	LOW	LOW	HIGH	VERY HIGH	VERY HIGH	Vulnerability Level

In Table 6-1, the vulnerability level is defined as the product among I_{vuln} (vulnerability index), De (Damage extension) and factors that take into account the probability level of occurrence of a failure modes according to the boundary conditions defined for the inspected façades (see section 4.3 and Table 4-1 for details).

The highest vulnerability level is estimated for H2, that has lowest value of λ and the highest value of DE, since FaMIVE estimates that the entire façade is involved in the identified failure mode.

However, the highest occurrence identified in H2 with respect to other failure modes does not exclude the possibility that the failure mode C occurs. This suggests that if the failure mode with the second highest vulnerability level is considered together with the failure mode with the highest vulnerability level, FaMIVE increases its capacity of predicting the observed failure modes.

In Table 6-2 the results point out the predictions of the failure modes and related probability levels estimated by LOG-IDEAH for both façades, as discussed in section 5.9. All failure modes reported in Table 6-2 need to be referred to Appendix F.

LOG- IDEAH has also high capacity of capturing the failure modes observed on site, since failure modes G, H2 and the ones belonging to class C are estimated as the failure modes with the highest probability of occurrence. Therefore, this suggests that by selecting the failure modes with the highest probability of occurrence, LOG-IDEAH seems to capture the on site observations.

Table 6-2: Probability of occurrence level and damage levels identifeid for the possible failure modes captured by LOG-IDEAH for the building 10.2

		OOP		COMB					IP
		D-Left	D-Right	B1-Left	B1-Right	B2	C-Left	C-Right	H2
10.2e	Probability of occurrence level	LOW	LOW	LOW	VERY LOW	---		VERY HIGH	VERY HIGH
	Damage Level	NEAR COLLAPSE	COLLAPSE	COLLAPSE	COLLAPSE	---		COLLAPSE	COLLAPSE
10.2n	Probability of occurrence level	LOW		VERY LOW	LOW	VERY LOW	VERY HIGH		VERY HIGH
	Damage Level	COLLAPSE		COLLAPSE	COLLAPSE	COLLAPSE	COLLAPSE		COLLAPSE

In Table 6-2 other solutions are also reported with a lower possibility of occurrence, estimated by assuming the possible crack pattern on the façades that have not been inspected.

By analysing these failure modes with low probability of occurrence, the first is D that is predicted because the façades are only damaged by diagonal cracks but there is no evidence of the vertical ones, as discussed in Figure 6-25 by referring to the cracks highlighted in green.

The failure modes of class B are also identified as solution with a low probability level of occurrence. In this case, the low probability level of occurrence is not estimated from an incomplete development of a crack pattern, as it is for D, but is the consequence of an incomplete inspection considering that B2 requires the assessment of at least three façades in order to be identified.

However, although only two façades have been inspected in details, the close up picture of the building 10.2 in Figure 6-27 allows seeing façade 10.2w that was not inspected in the first instance during the onsite inspection. This façade 10.2w, only partially observed from this picture, with its cracks (in blue) together with the cracks (in red) on façade 10.2e might underline that failure mode B2 is identified. However the presence of the façade 10.2n and the absence of an evidence that 10.2n is failing in

overturning excludes that B2 or B1 are occurring and justifies why LOG-IDEAH predicts B2 or B1 as probable failure modes with only a low probability level of occurrence.

This result obtained from LOG-IDEAH and then confirmed through the observation is really important as it underlines the effectiveness of this tool in predicting the failure modes even when buildings have been only partially inspected.

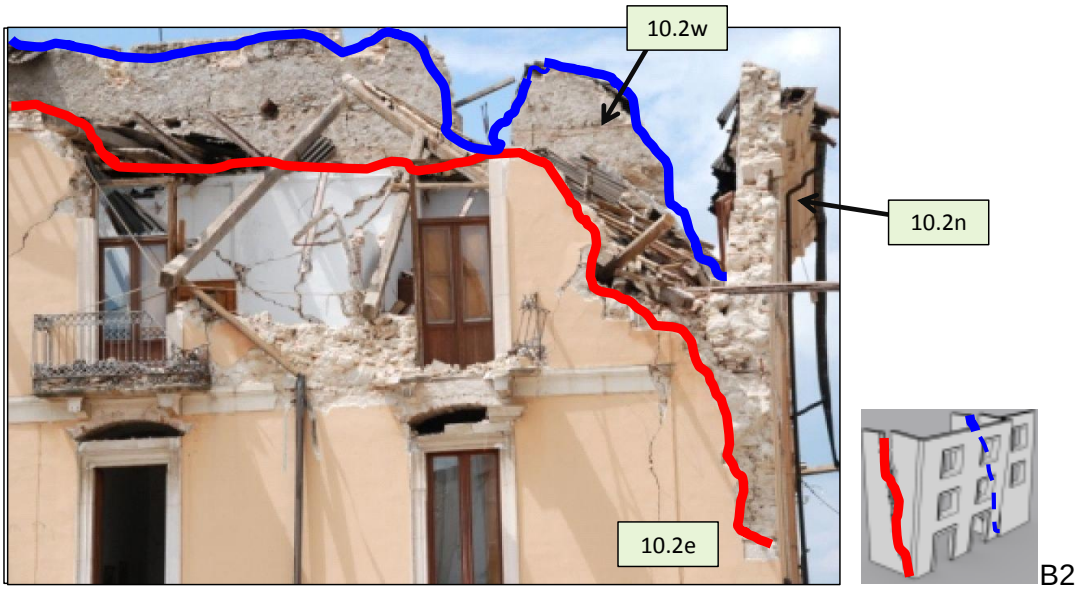

Figure 6-27: Identification of the failure mode B2 on the the building 10.2

On the other hand, in this specific case study, LOG-IDEAH is not capable to capture the failure mode G, although this has been estimated by both experts and FaMIVE. Such a lack of correlation derives from the rules defined in LOG-IDEAH suitable to capture G only if this failure mode has a clear crack pattern that shapes an arch, as illustrated in the logic tree in Appendix F. Therefore, since in this building the top right side of the façade 10.2e is completely collapsed, it is difficult to identify and to record the typical crack pattern that defines this type of failure mode.

In the next paragraph, both approaches are applied to the building blocks of Figure 6-8 by first ranking their output and then selecting different sets of results obtained by grouping the output according to different criteria based on the different probability level of occurrence associated to each estimated failure modes. The criteria of selection for these sets are described in details in the next section.

The damage levels identified by LOG-IDEAH correspond, by definition, to the damage levels observed on site, as discussed in section 5.10. On the other hand, since

FAMIVE estimates the damage for a mean value of performance of a building class, its validation against the damage levels observed on site is carried out at territorial scale as discussed in section 6.14.

6.8 Validation of the capacity of FaMIVE, LOG-IDEAH and the Hybrid method against the failure modes observed on site by experts

The validation of FaMIVE and LOG-IDEAH on the present case study is performed by using the approaches introduced in the methodology of section 3.4.

The approach FaMIVE is validated considering two different sets of results named FaMIVE_1 and FaMIVE_2. In FaMIVE_1, only one failure mode is selected for each façade, the one with the highest vulnerability level, while in FaMIVE_2, two failure modes are selected for each façade, the first and second with the highest vulnerability level, identified according to Table 4-1.

The software LOG-IDEAH is also validated considering two sets of results named LOG-IDEAH_1 and LOG-IDEAH_2. The sets are composed respectively by all failure modes with the highest and two highest probability levels of occurrence, identified according to Table 5-6.

Figure 6-28 shows the ratios between the total number of failure modes in each set of results and the total number of failure modes observed by experts. These ratios confirm that FaMIVE_1 provides the lowest number of predictions compared to the number of failure modes observed on site, while FaMIVE_2 and LOG-IDEAH_1 have a number of predicted failure modes that is comparable to the one observed onsite.

Figure 6-28 also shows the results of two hybrid sets (UNION_1 and UNION_2) obtained by joining the results of FaMIVE and LOG-IDEAH. In order to create the hybrid sets, LOG-IDEAH_1, that, as discussed below, best predicts the onsite observation, is joined first with FaMIVE_1 for UNION_1, and then with FaMIVE_2 for UNION_2. As expected, the union of the results of both methods show a number of estimates that is superior with respect to ones provided by the single method.

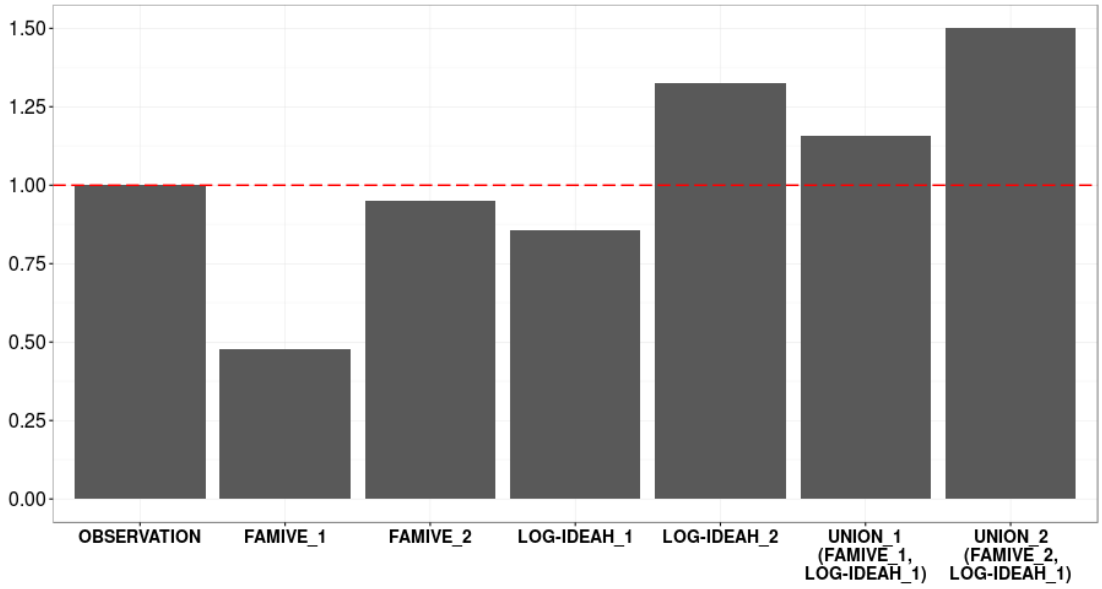

Figure 6-28: Ratio between total number of the failure modes provided by each set of resuts and total number of the observed failure modes. The set of results are obtained from FaMIVE, LOG-IDEAH and their union

The different number of failure modes estimated by each method is illustrated in Figure 6-29, showing the occurrence in percentage of the number of failure modes predicted for façade in each set of results.

As expected, the number of failure modes assigned for façade is one and two in FaMIVE_1 and FaMIVE_2 respectively and from minimum of one to a maximum of eight failure modes in LOG-IDEAH_1 and LOG-IDEAH_2.

The validation of all approaches on the basis of the failure modes observed on site is performed by computing Recall and Precision measures, defined in section 3.4, as shown in Figure 6-30.

As expected, in FaMIVE_1 the Recall that identifies the fraction of the observed failure modes that are predicted by the method is not very high compared to the other methods, because the number of results provided by FaMIVE_1 is considerably lower than the failure modes observed on site.

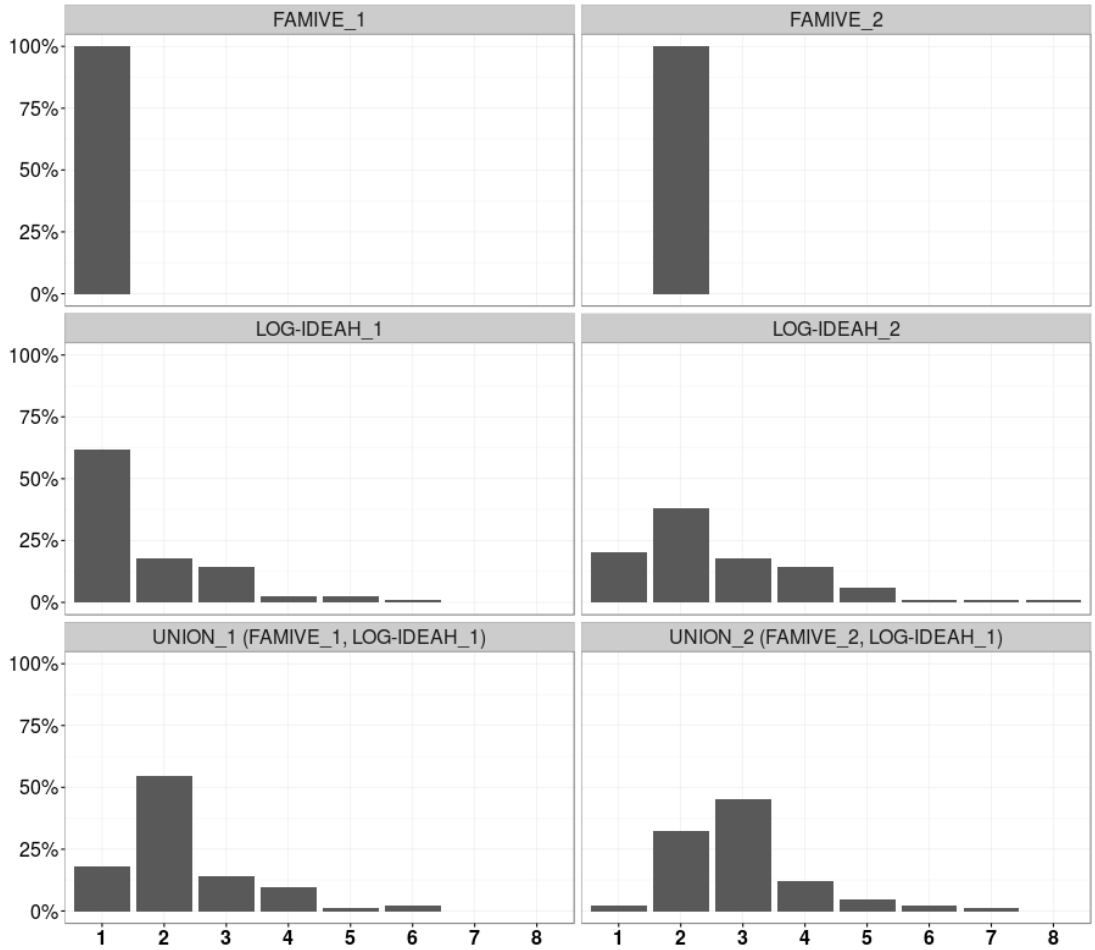

Figure 6-29: Occurrence in percentage of the number of failure modes predicted for façade by each set of resuts

This is confirmed by FaMIVE_2, where two predictions are provided for each façade and consequently the Recall increases significantly. However, both sets of FaMIVE have a Precision that is ~50% highlighting the good capacity of the method of predicting the failure modes observed on site. An interesting result is given by LOG-IDEAH_1. Although its number of predictions is lower than FaMIVE_2, its Recall is higher. Moreover, LOG-IDEAH_1 shows also the highest value of Precision, ~60%. Both the results underline the impressive capacity of prediction of LOG-IDEAH_1.

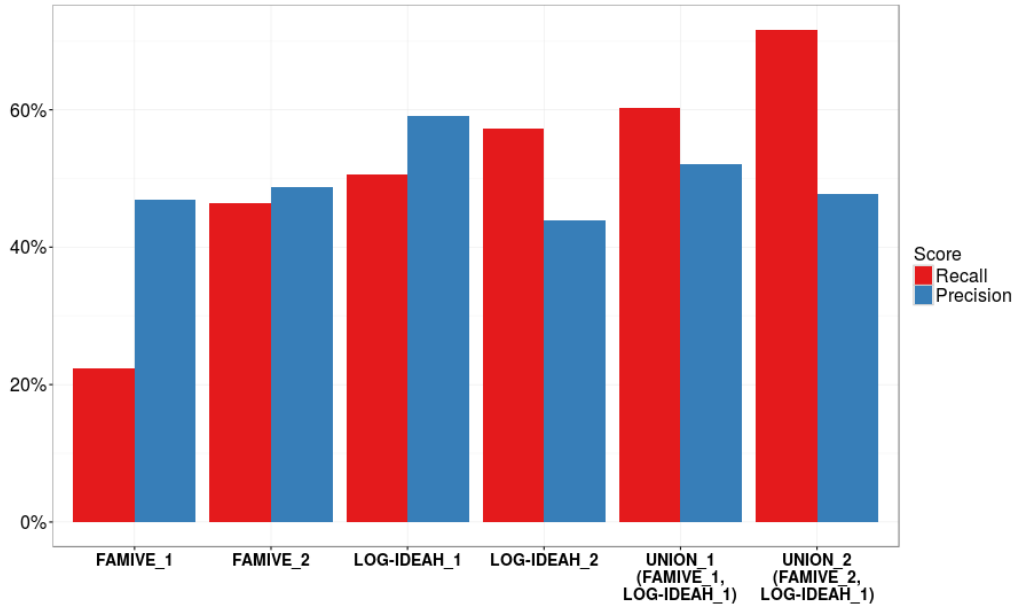

Figure 6-30: Recall and Precision estimated for the sets of results obtained by FaMIVE, and LOG-IDEAH. The results of the hybrid methods are also presented

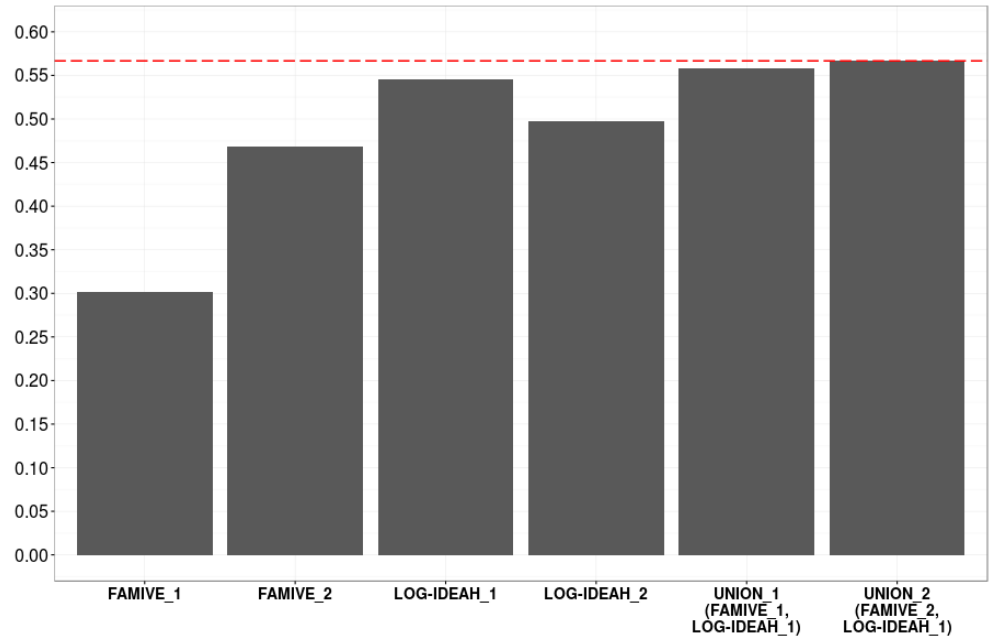

Figure 6-31: F-1 score estimated for the sets of results obtained by FaMIVE, and LOG-IDEAH. The results of the hybrid methods are also presented. The red dashed line shows the highest value of F-1 score obtained with the set of results UNION_2

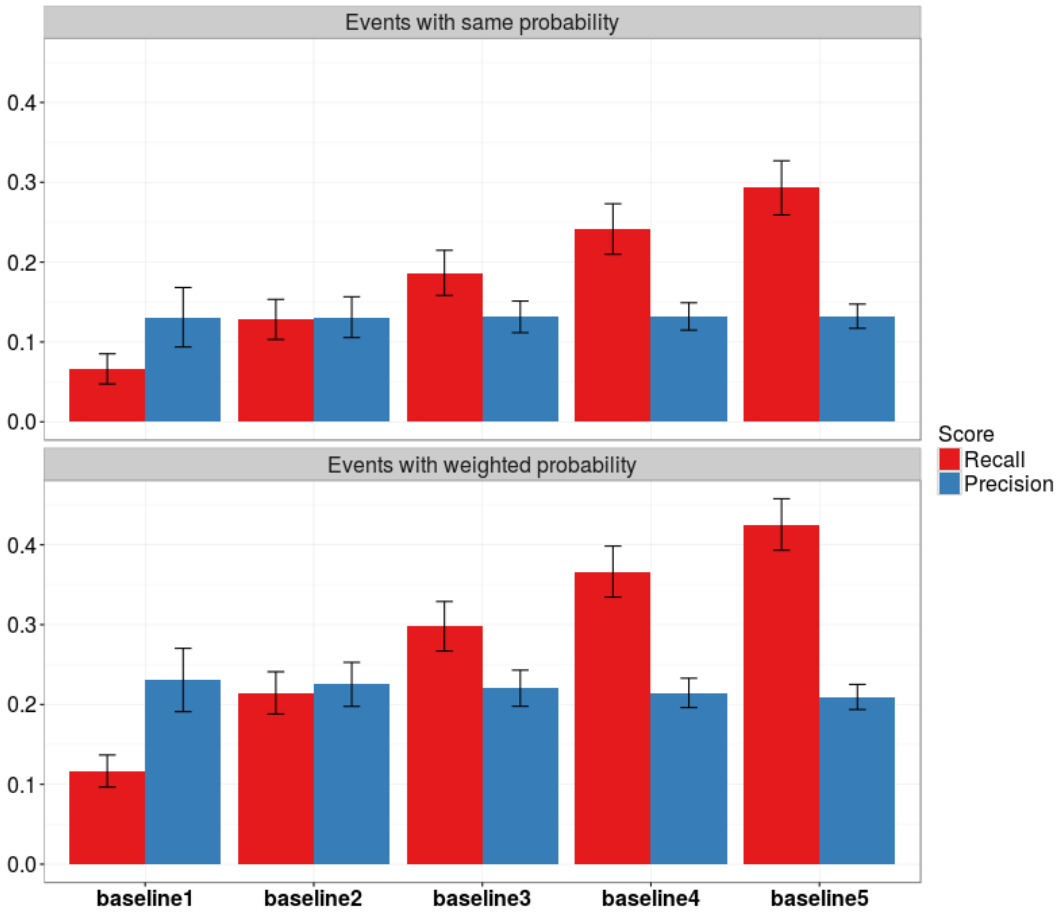

Figure 6-32: Recall and Precision of the random methods. In the first plot, the random method associated failure mode with the same probability of occurrence to each inspected façade. In the second plot, the random method associated failure mode with weighted probability of occurrence to each inspected façade. Baseline 1, Baseline 2, …, Baseline 5 refer to the number of failure modes associated to each inspected façades by each random method. The values denote means ± Stadard deviation.

The capacity of LOG-IDEAH to identify the failure modes with highest probability of occurrence among all possible ones is clearly underlined by the fact that although LOG-IDEAH_2 has a higher level of Recall with respect to LOG-IDEAH_1, as expected, it is also characterised by a consistent lower Precision value (~40%) than LOG-IDEAH_1 caused by the introduction of high number of False Positive (refer to chapter 3).

However, these results are not necessarily incorrect, since LOG_IDEAH often provides results that are difficult to be observed. Indeed, LOG_IDEAH estimates failure modes on both collected data and hypothesis on the crack patterns on façades that have not been inspected, as discussed in section 6.7.1, thereby introducing results that cannot be validated by the body of observations carried out.

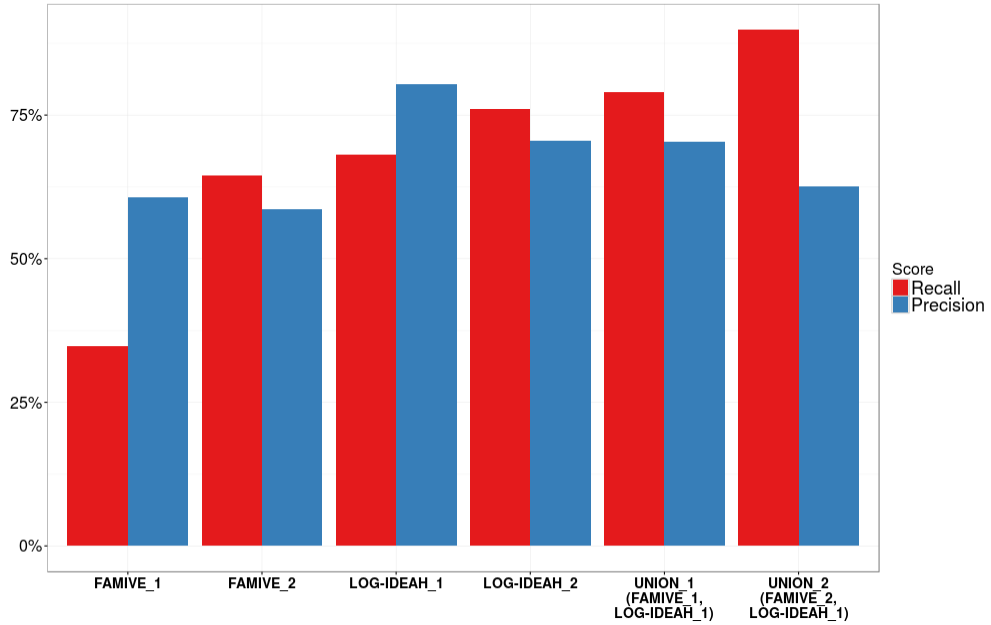

Figure 6-33: Recall and Precision estimated for the sets of results obtained by FaMIVE, and LOG-IDEAH, classyfing failure modes in COMB, OOP and IP. The results of the hybrid methods are also presented.

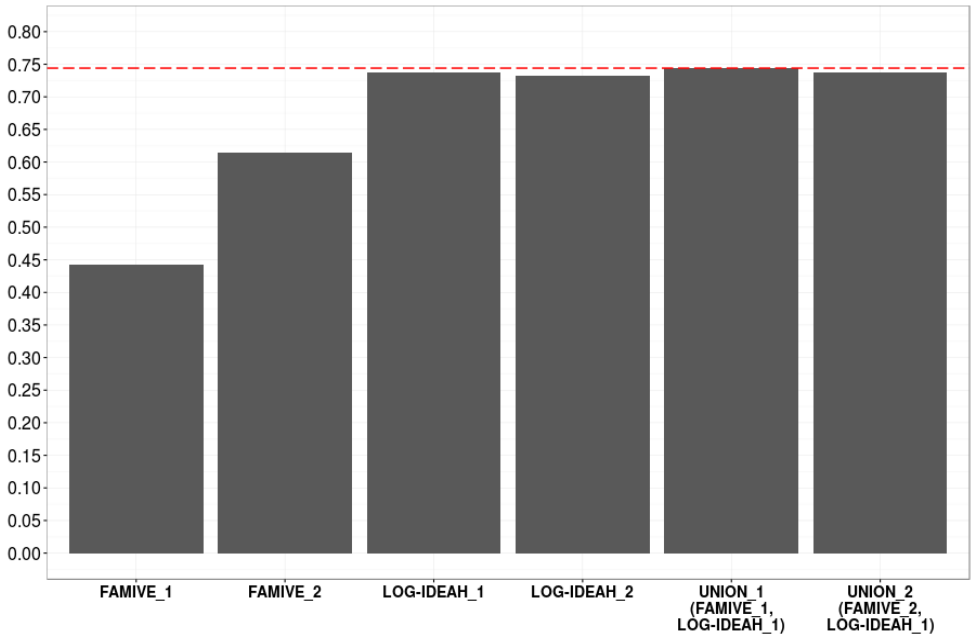

Figure 6-34: F-1 score estimated for the sets of results obtained by FaMIVE, and LOG-IDEAH, classyfing failure modes in COMB, OOP and IP. The results of the hybrid methods are also presented. The red dashed line shows the highest value of F-1 score obtained with the set of results UNION_1.

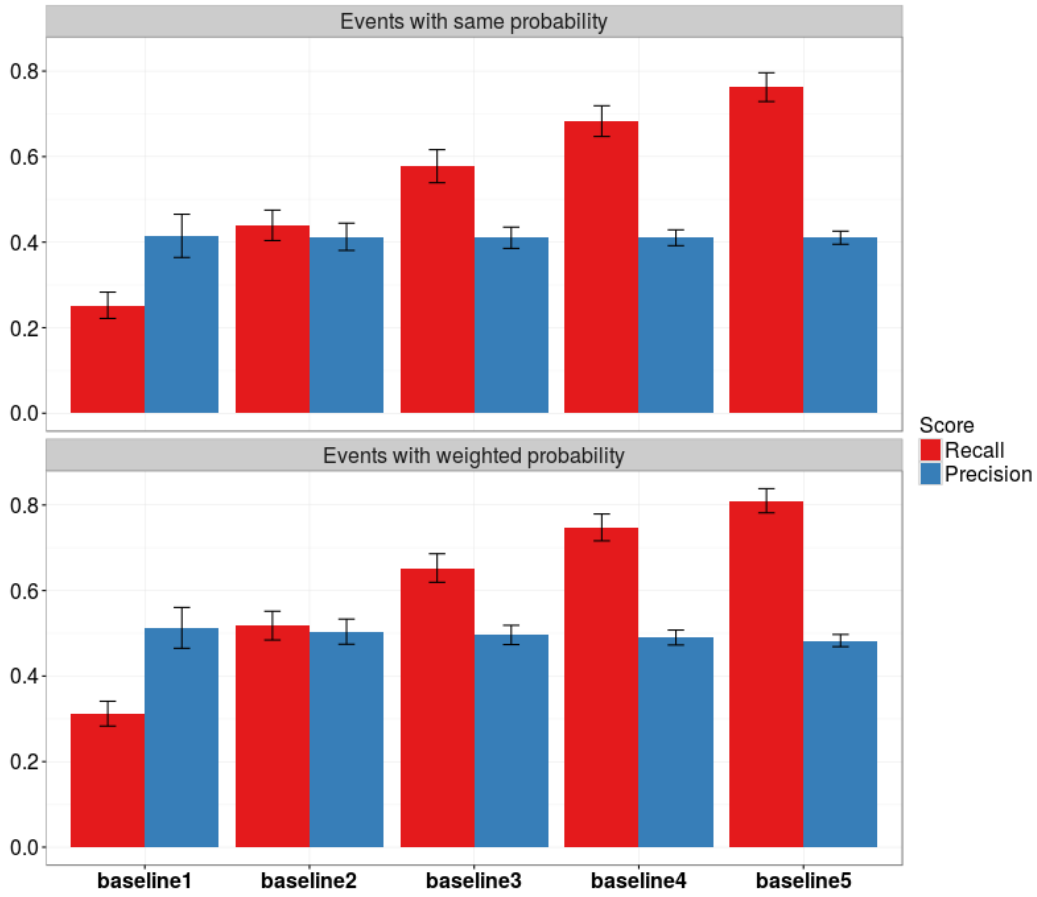

Figure 6-35: Recall and Precision of the random methods. In the first plot, the random method associated failure mode with the same probability of occurrence to each inspected façade. In the second plot, the random method associated failure mode with weighted probability of occurrence to each inspected façade. Baseline 1, Baseline 2, …, Baseline 5 refer to the number of failure modes associated to each inspected façades by each random method. The values denote means ± stadard deviation. Failure modes are classified in COMB, OOP and IP.

The best result is obtained by UNION_2 characterised by a Recall up to 70%, and a Precision that is comparable or higher than the ones estimated for the other methods. This underlines that the prediction of UNION_2 forecasts the highest number of observed events maintaining a good level of Precision.

This is confirmed by F1 scores introduced in section 3.4, and presented in Figure 6-31, where UNION_2 best predicts the observed failure modes, compared to the other methods. The strong capacity of prediction of the proposed approaches is also underlined by comparing their results with two random methods, introduced in section 3.4.

The first random method provides the same probability of occurrence to each possible failure mode, and then randomly associates these to each inspected façade (event with the same probability in Figure 6-32). The second one provides a probability of occurrence to each failure mode according to its frequency of occurrence observed on site and randomly associates this to each inspected façade (event with weighted probability in Figure 6-32).

Five sets of results are derived from each random method, whereby from one to five failure modes are associated to each inspected façade (from baseline 1 to baseline 5).

The comparison between Figure 6-32 and Figure 6-30 underlines that FaMIVE, LOG-IDEAH and the hybrid methods clearly have a higher performances, compared to the performances of the random methods.

Figure 6-33 shows the Precision and Recall of FaMIVE and LOG-IDEAH in predicting the observed failure modes that are classified according to COMB, OOP and IP failure modes. As expected, the results have a similar trend as the ones obtained in Figure 6-30. In this case, as observed in Figure 6-34, the set of results of LOG-IDEAH and UNION_1 have comparable performance.

The capacity of prediction of the proposed approaches is also underlined by comparing their results with two random methods introduced in section 3.4. By comparing the results of Precision and Recall in Figure 6-35 and Figure 6-33, it is clear that also classifying the failure modes in COMB, OOP, and IP, the performances of the random methods are lower than the performances of FaMIVE, LOG-IDEAH and of their union.

6.9 Classification of the inspected façades based on the failure modes and vulnerability levels estimated with FaMIVE

In this section, the inspected façades are classified according to the failure modes (COMB, OOP, and IP defined in chapter 4 and 5) estimated by FaMIVE, as the failure modes with the highest level of vulnerability, calculated as indicated in section 4.3. The estimated failure mode (FAILURE MODES) and vulnerability level (VULNERABILITY) distributions are shown in Figure 6-36.

These classifications based on the output of FaMIVE together with the classifications based on the structural features observed on site and presented in section 6.5 are considered in the next sections, where capacity curves are derived for each of the classes identified in the different classifications mentioned above.

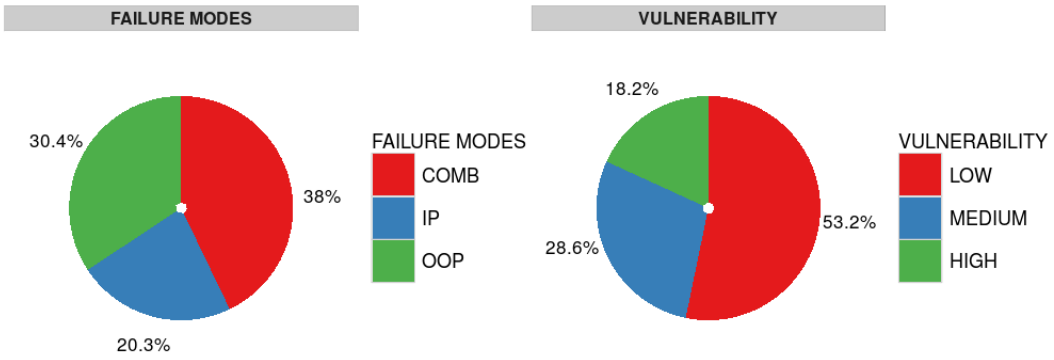

Figure 6-36: Building classification based on the estimated failure modes and related vulnerability

6.10 Estimation of the capacity curves

The capacity curves, as discussed in section 4.6.1 and graphically reported in Figure 4-26, are represented by branches that define the thresholds between the following damage states: LD: Light Damage, SD: Significant Damage, NC: Near Collapse, and C: Collapse, defined in section 4.5. The threshold points between damage states (expressed in terms of displacement and acceleration) are estimated for each inspected façade, and an average of these values is calculated for the building classes presented in section 6.5 and 6.9. This implies, as discussed in the previous section, that the capacity curves are derived for each building class identified in the following classifications: EMS'98, EMS'98 (Rise) and PAGER, based on the structural features observed on site, and FAILURE MODES, and VULNERABILITY estimated by FaMIVE.

In Figure 6-37 the capacity curves are presented for the building classes A, B and C of the modified EMS'98 classification (EMS'98), presented in Figure 6-12. Class C, composed of buildings with floors in RC, is the construction class with the highest shear capacity. However, this capacity is not much higher than the capacity estimated for the class B, which is represented by buildings with strong connections, provided by

good corner stones or anchors. As expected, class A, which is the weakest class, has the lowest shear capacity. In this classification, the highest ductility is observed for the strongest construction class C, while the lowest is for the weakest constructions, A.

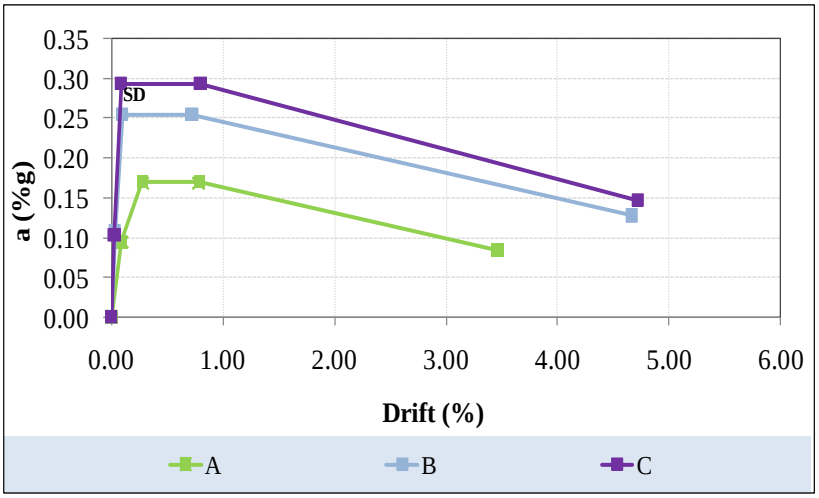

Figure 6-37: Capacity Curves for the building classes A, B and C (EMS'98 classification)

This trend is confirmed by Figure 6-38 for (EMS'98 (Rise)), where the classification of the modified EMS'98 has been refined by taking into account the rise of the buildings (L: LOW rise for bundling with 1 and 2 storeys and M: MEDIUM rise for bundling with 3 and 4 storeys).

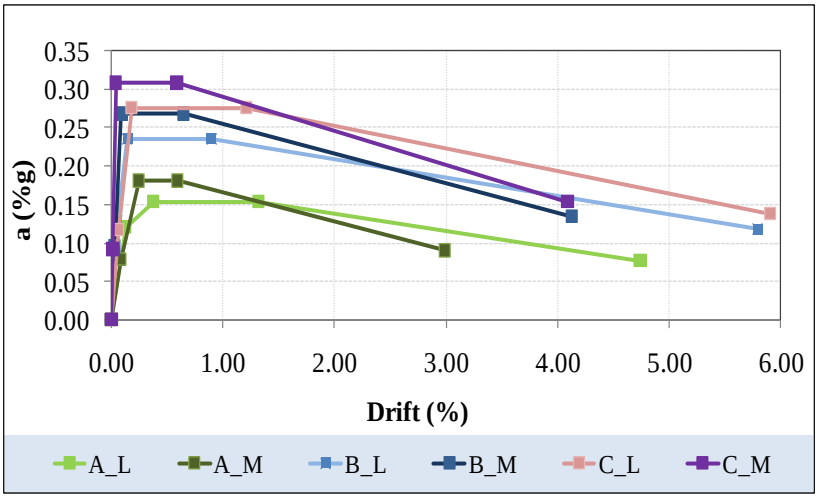

Figure 6-38: Capacity Curves for the building classes A-L, A-M, B-L, B-M, C-L and C-M (EMS'98 (Rise) classification)

Figure 6-39 shows the capacity curves of the inspected buildings classified according to the PAGER classes, presented in Figure 6-13. As expected, the

capacity curves of the buildings with brickwork (UFB) have a better response than both building categories (DS) made of mixed dressed stone masonry and (RS) made of rubble stones. The comparison also illustrates that the building response is affected not only by the construction material, but also by the class of horizontal structures. This is underlined by the capacity of the buildings with RC floor, that is highest among the other others, and it is followed first by buildings with vaults and then by buildings with timber floors.

It is also important to underline that the classes derived by the classification of buildings according to their common structural features do not necessarily group buildings with the same seismic response. This is because the common structural features as well as their irregularity affect the structural behaviour of the single building, and consequently the capacity of the single class.

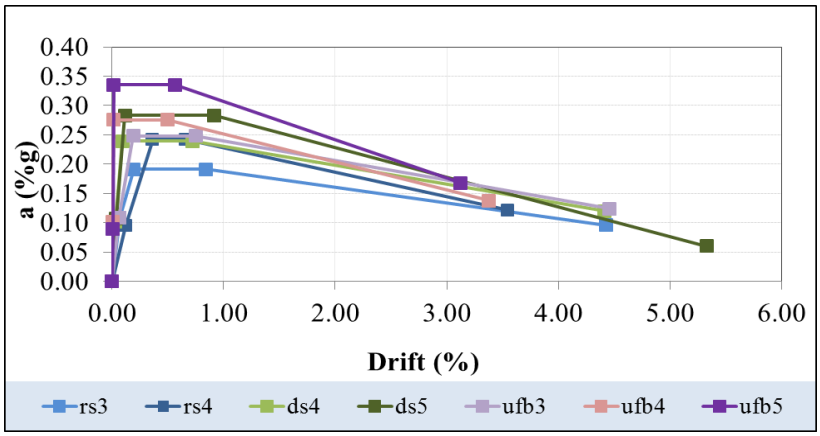

Figure 6-39: Capacity Curves for the building classes RS3, RS4, DS4, DS5, UFB3, UFB4 and UFB5 (PAGER classification)

In Figure 6-40, the capacity curves are derived for the façades classified according to the failure modes estimated as the most vulnerable ones by FAMIVE as reported in Figure 6-36, while in Figure 6-41, the capacity curves are derived by subdividing the previous classes COMB, IP and OP according to the height of the inspected façades.

Both sets of curves confirm that buildings failing in COMB have the highest capacity and ductility; the ones failing in OOP have the lowest shear capacity while the ones failing in IP have the most brittle collapse, confirmed by their lowest ductility, compared to the others.

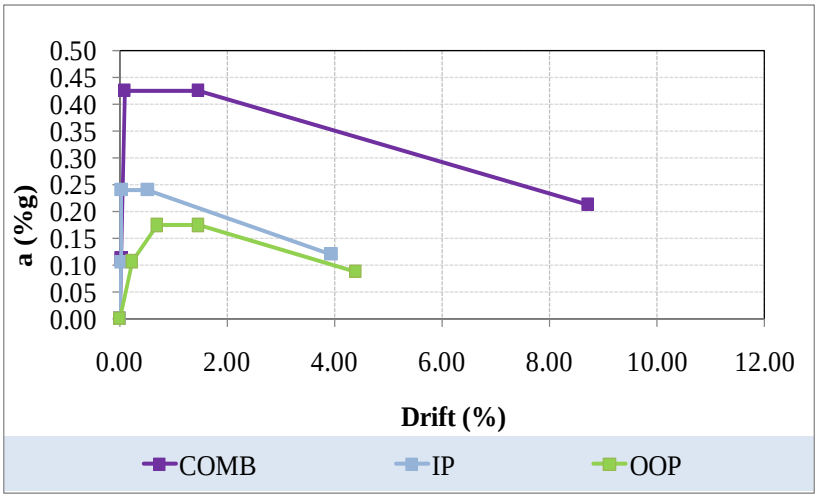

Figure 6-40: Capacity Curves for the building classes OOP, IP and COMB (FAILURE MODES classification)

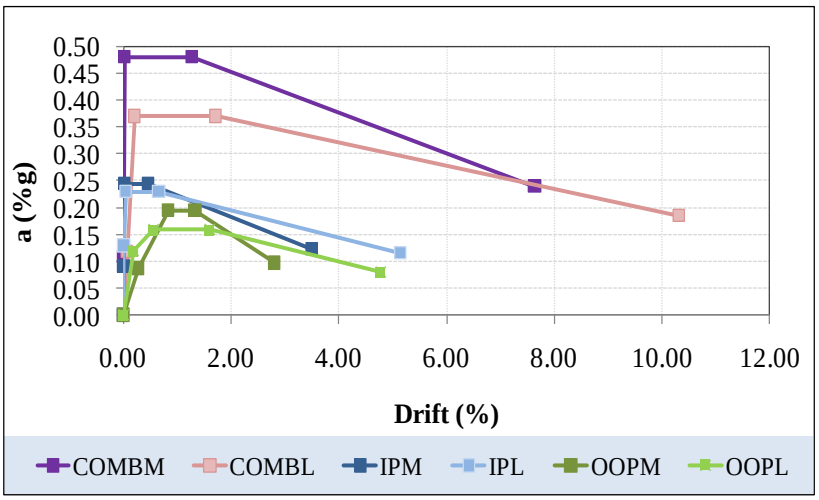

Figure 6-41: Capacity Curves for the building classes OOP-L, OOP-M, IP-L, IP–M, COMB-L and COMB-M (FAILURE MODES (Rise) classification)

Finally the capacity curves in Figure 6-42 are derived for groups of buildings classified according to the vulnerability classes determined with FaMIVE and their distribution presented in Figure 6-36.

This classification on the vulnerability levels, since it inherently gathers buildings with similar seismic response with respect to the other classifications considered in this section, defines capacity curves on classes of buildings with the same seismic response.

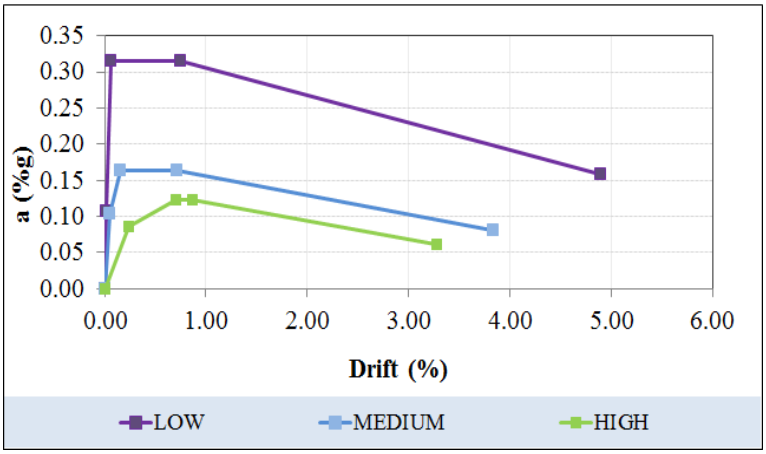

Figure 6-42: Capacity Curves for the building classes LOW, MEDIUM, and HIGH vulnerability (VULNERABILITY classification)

This is confirmed by the high value of capacity identified for the buildings failing for failure modes with the lowest vulnerability level, as this class is represented by constructions with good quality materials and strong connections or by houses strengthened by cross ties. A strong correlation between the vulnerability level associated to a failure and related building performance is also observed in the class of buildings failing for failure modes with the highest vulnerability. This class is mainly characterised by buildings with poor mechanical and structural features that have a low capacity.

Finally, the class with buildings failing for failure mode with medium vulnerability, as they are mainly composed of houses made of mixed roughly squared stones and brickwork, is also well represented by its stronger capacity than obtained for buildings with high vulnerability, and weaker than the one computed for buildings with low vulnerability.

6.11 Spectral acceleration

This section focuses on presenting the linear spectrum, adopted in the next paragraph to estimate the building performance with reference to N2 method (Fajfar et al. 2000) introduced in section 4.6.2 and section 4.6.3.

Fifty-eight of the approximately 300 digital strong-motion stations operated by the Italian Strong Motion Network and managed by the Department of Civil Protection of Italy recorded the main shock of L'Aquila in 2009 (Celebi et al. 2010). The

position of the ground motion stations and related records are available from the INGV archive (http://www.ingv.it/en/).

The linear spectrum in Figure 6-43 adopted for the present study has been downloaded from the strong ground motion station closest to the city, AQK (download of the corrected time histories from http://itaca.mi.ingv.it/ItacaNet/, last accessed 20/04/2010).

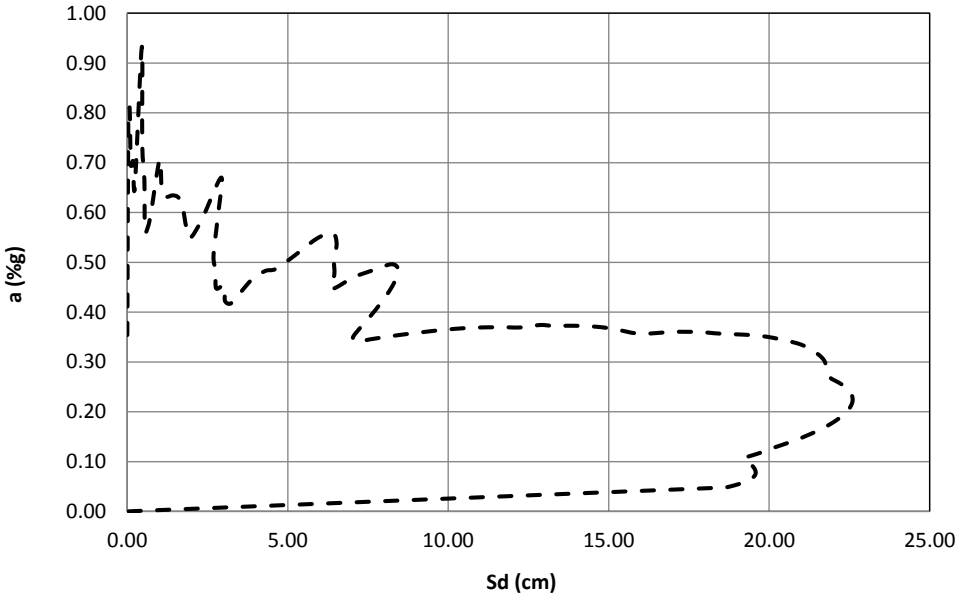

Figure 6-43: Linear Spectrum recorded from AQK ground motion station

6.12 Derivation of the performance points

The performance points, as discussed in section 4.6.2 and section 4.6.3 can be computed by using the iterative procedure integrated into the existing approach of FAMIVE based on the intersection between capacity curves and nonlinear spectral acceleration. In this section, such an intersection has been carried out between the capacity curves presented in section 6.10 and the nonlinear spectrum (NLSA) derived from the abatement of the linear spectrum (LSA) of section 6.11. The abatement of LSA, as discussed in section 4.6.2 and section 4.6.3, is performed through the value of ductility computed by equations (14) with reference to the (ED) approach.

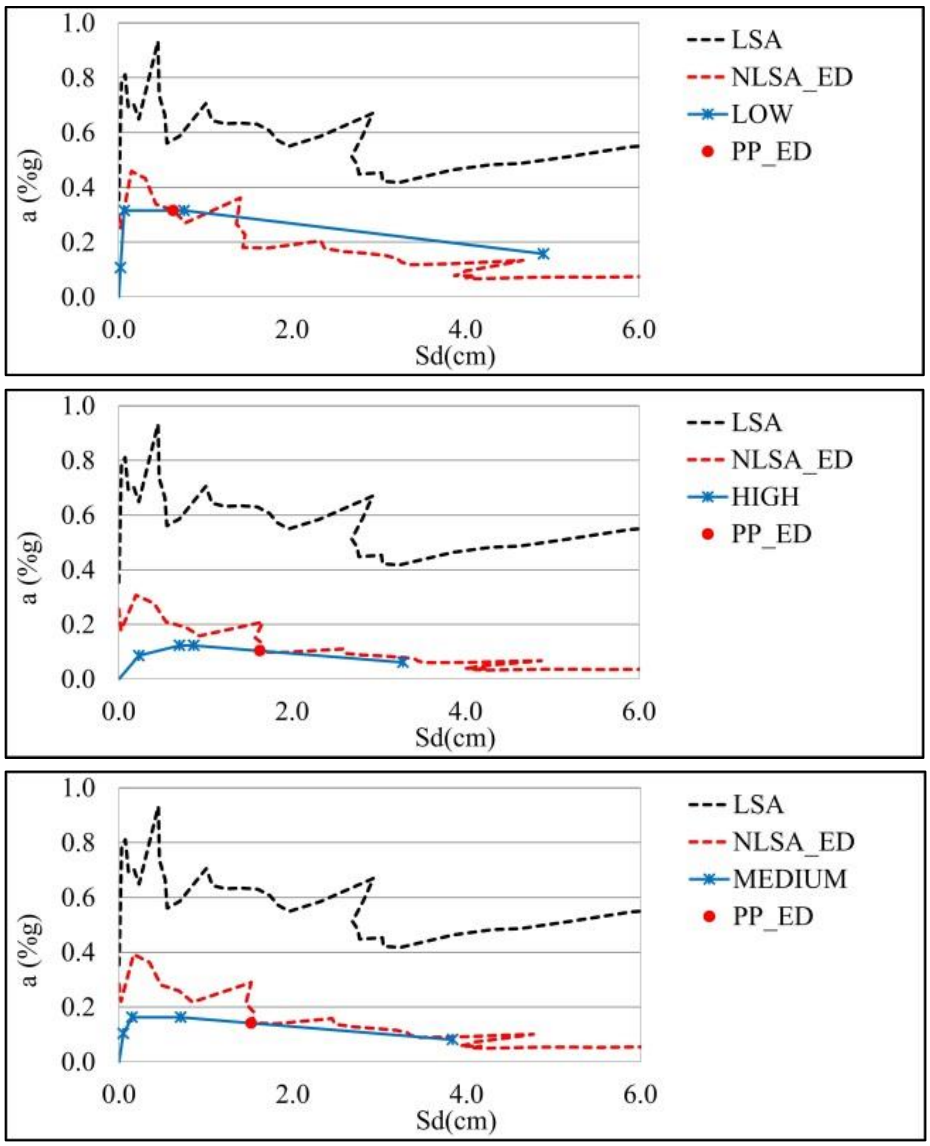

Figure 6-44: Performance points for classes Low, Medium, and High VULNERABILITY levels

By mean of illustration, Figure 6-44 shows the results derived from the application of this iterative approach to the inspected buildings classified in LOW, MEDIUM and HIGH VULNERABILITY. The intersection between the capacity curves (called with the name of the building classes of reference) and the nonlinear spectrum, named NLSA_ED is highlighted by the red dot, indicating the performance points (PP_ED).

As expected, the performance points derived for the inspected buildings classified according to their vulnerability level underline that the performance (performance point) of the LOW VULNERABILITY class is consistently better compared to the ones

estimated for the MEDIUM and HIGH VULNERABILITY classes that have comparable performance.

The iterative approach has been also applied to the classes belonging to EMS'98, EMS'98 rise, PAGER, FAILURE MODES, FAILURE MODES rise and VULNERABILITY, as reported in Appendix G, and the results are illustrated in Figure 6-45.

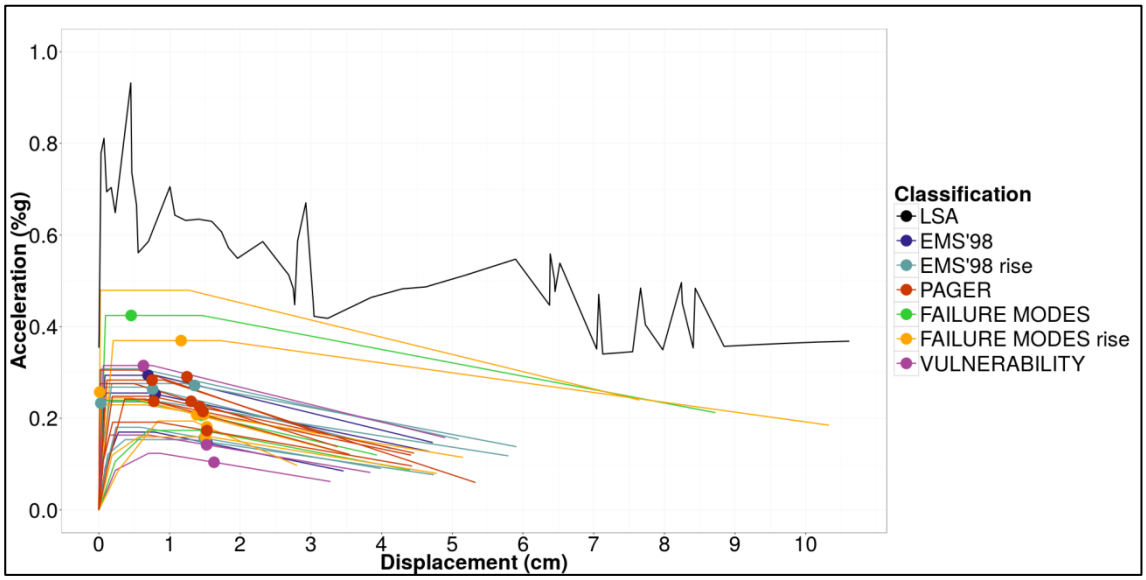

Figure 6-45: Performance points identified for the building classes belonging to EMS'98, EMS'98 rise, PAGER, FAILURE MODES, FAILURE MODES rise, and VULNERABILITY.

As expected from the observation most of the performance points identify a Significant Damage performance for most of the building classes, while the Near Collapse performance is generally evaluated for the weaker ones. The light damage is identified for classes with highest capacity, such as: CL, COMBL.

In the next section, the performance points in terms of displacement are used to identify the damage probability by intersecting those with the fragility curves derived for building classes.

6.13 Derivation of fragility curves and estimation of damage level distribution

The damage probability for the inspected buildings, as discussed in section 4.7, are computed by using the iterative procedure integrated into FaMIVE programme, based on the intersection between performance points in terms of displacement, and the

corresponding set of fragility functions computed for a given subset of buildings, according to the various classification criteria introduced in the previous sections.

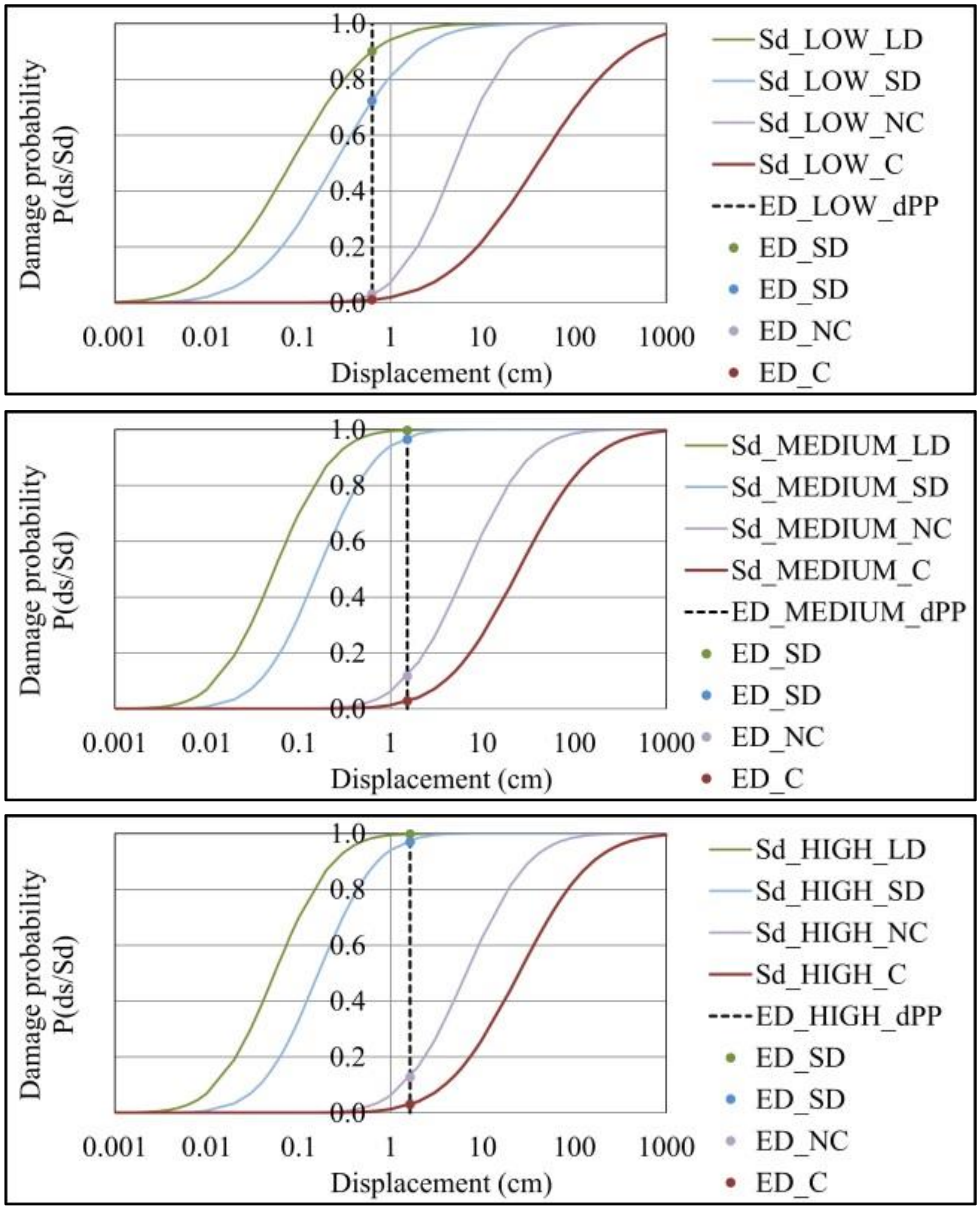

	equivalent displacement				
	NO DAMAGE	SLIGHT	MODERATE	EXTENSIVE	COMPLETE
HIGH	0%	3%	84%	10%	3%
MEDIUM	0%	3%	85%	9%	3%
LOW	10%	18%	69%	2%	1%

Figure 6-46: Damage probability for Low, Medium, and High VULNERABILITY levels

The performance points are taken from section 6.12 and the fragility curves are derived for building classes, as discussed in section 4.7, by computing the median and

standard deviation of the four damage states: LD: Light Damage, SD: Significant Damage, NC: Near Collapse and C: Collapse, defined in sections 4.5.

The intersection between fragility curves and performance points are illustrated in Appendix G.

By way of an example, Figure 6-4 shows the fragility curves and related damage probability (in term of percentage) derived with reference to buildings classified according to their vulnerability levels. These fragility curves, as all fragility curves in Appendix G, are characterised by a large distance between LD and SD derived from the long ductile plateau in the capacity curves estimated in section 6.10. These plots together with the other plots in Appendix G, underline that the intersection between the performance points (dashed black line) and fragility curves defined for the four damage states points out a high percentage of buildings failing for structural damage, in agreement with the observation carried out on site.

In the next section, the different damage probability derived by using the different classifications are validated against the damage levels observed on site with the scope of identifying the classification that have the greatest capacity of predicting damage scenarios due to earthquakes of given intensity.

6.14 Validation of damage levels

In this section, the comparison between:

- *observed damage levels*: damage severity recorded on site and stored in LOG-IDEAH and
- *estimated damage levels*: damage severity calculated by using the fragility functions derived for different grouping of the FaMIVE results in different classes.

is discussed and presented as follow.

As mentioned in previous sections, the inspected buildings have been classified according to EMS'98, EMS'98 (rise), and Pager classifications with reference to section 6.5, and Failure modes, Failure modes (rise) and Vulnerability levels with reference to section 6.9.

This implies that the comparison between *observed* and *estimated damage levels* is presented for all building classes identified in each classification mentioned above. The comparison is shown for the following damage levels: ND: No Damage, LD: Light Damage; SD: Significant Damage; NC: Near Collapse; and C: Collapse, as these are defined in chapter 4.

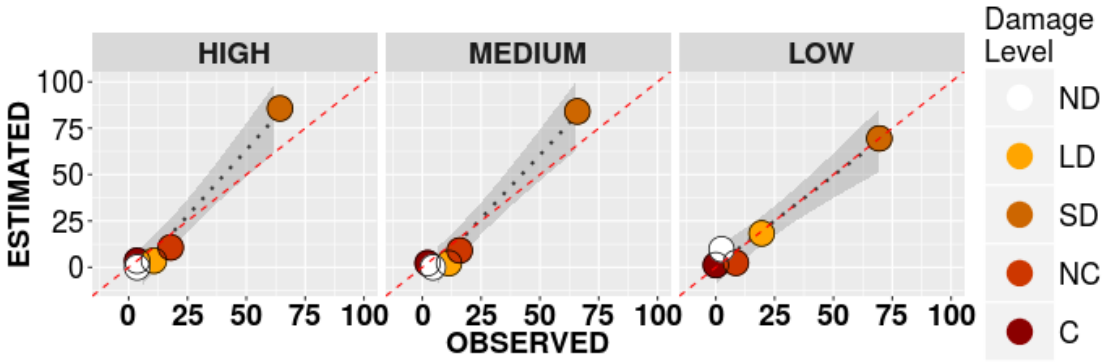

Figure 6-47: Correlation between the observed and estimated damage levels computed by ED approach. The percentage of estimated and observed damage levels are reported on the X and Y-axis. The black dashed line is calculated by a local polynomial regression fitting. The red dashed line represents the ideal correlation between the observed and estimated damage levels for HIGH, MEDIUM and LOW VULNERABILITY levels

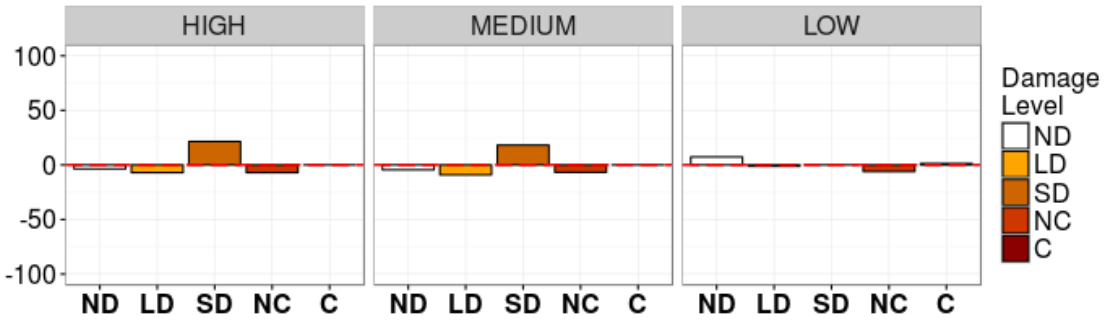

Figure 6-48: Difference in terms of percentage between observed and estimated damage levels computed by ED, for HIGH, MEDIUM and LOW VULNERABILITY levels

The *observed damage levels* in the area of study were already discussed in section 6.8 and their distribution for the single inspected façades is reported in Figure 6-24. The *observed damage level* distributions for building classes are directly introduced in the plots presented for the comparison.

For the *estimated damage level* distributions, these are introduced in section 6.13 as the damage probability distributions derived by the intersection between performance points and fragility curves, as presented in details in Appendix G.

The comparison between the *observed and estimated damage level* distributions for building classes are presented in Appendix H, and the most significant results derived from these comparison are discussed in this section.

The comparison between *observed damage levels* and *estimated damage levels* show a strong correlation. This has been particularly underlined when buildings are classified according to their level of vulnerability, as shown in Figure 6-47. These results confirm the observation of section 6.10, where it was already underlined that capacity curves derived for this classification reflect the expected capacity for these three classes: LOW, MEDIUM and HIGH vulnerability level.

The good correlation is also underlined in Figure 6-48, where the maximum differences in terms of percentage between the observed and estimated damage levels is ~ 25%, observed only for buildings with HIGH vulnerability level, characterised by a Severe Damage (SD) level.

The strong correlation between observed and estimated damage levels for the building classes belonging to the vulnerability classification is also highlighted by the value of Pvalue (<0.05) and Pearson correlation coefficient ρ (~1).

For more details of Pvalue and ρ calculated for all building classes, a table is presented at the end of Appendix H.

Conclusion

The methodology proposed in section 3.4 has been applied to the historic centre of L'Aquila, damaged by the earthquake of 2009 with the scope at identifying how FaMIVE and LOG-IDEAH can be jointed in a hybrid approach for the vulnerability assessment of historic city centres.

The union of both approaches have demonstrated to be suitable to analyse the performance of constructions characterised by irregularity in the geometry, mechanical properties, and structural features. This has been demonstrated through a validation approach used to join the results of both FaMIVE and LOG-IDEAH that best predict the onsite observation.

The validation has been performed by calculating two parameters: Recall, and Precision on the following sets of results:

- FaMIVE_1 and LOG-IDEAH_1, sets of results composed by failure modes with the highest probability of occurrence estimated by FaMIVE and LOG-IDEAH, respectively
- FaMIVE_2 and LOG-IDEAH_2, sets of results composed by failure modes with the two highest probability of occurrence estimated by FaMIVE and LOG-IDEAH, respectively

The validation based on the values obtained for Recall, Precision shows that:

- FaMIVE_2 (set of results with the two highest probability of occurrence) over performs FaMIVE_1 (set of results with the first highest probability of occurrence), while
- LOG-IDEAH_1 (set of results with the first highest probability of occurrence) performs better than LOG-IDEAH_2 (set of results with the two highest probability of occurrence).

Based on these considerations, the proposed hybrid set of results is named UNION_1, and it is given by the union of FaMIVE_2 and LOG-IDEAH_1, selected as the sets of results from FaMIVE and LOG-IDEAH that best predict the observed failure modes with relation to the estimated value of F1 score.

The second validation is performed to evaluate the correlation between the *observed damage levels* stored in LOG-IDEAH and the *estimated damage levels* derived by the iterative approach of FaMIVE.

The results are presented for building classes for the five levels of damage: ND: No Damage, LD: Light Damage; SD: Significant Damage; NC: Near Collapse; and C: Collapse, defined in chapter 4.

The comparison have underlined that there is a strong correlation between the *observed damage levels* and the *estimated damage levels.* This is particularly true, when the damage probability is estimated by classifying buildings according to their vulnerability levels.

7. CONCLUSIONS

7.1 Introduction

The development of the hybrid method in this research was driven by the awareness of a gap in the existing methods for the assessment of the seismic vulnerability of historic city centres. Indeed, although numerous numerical approaches for the estimation of the seismic performance of buildings are developed, only few of them focus on investigating the failure modes due to an earthquake. Furthermore, limited limited effort has been put to provide a tool based on visual inspection for understanding how buildings fail.

Such a gap stems from a number of issues, among which the challenge of identifying a procedure that outlines the knowledge and the expert judgement adopted to assess buildings on site by only using visual inspections.

Nowadays, in spite of codes providing approaches to assess deficiencies in buildings and methods to survey the damage severity after an earthquake, there is a lack of protocols and rules that guide surveyors on how buildings should be inspected to capture their possible failure modes.

The research project described in this dissertation strives to present a visual inspection tool for the identification of the failure modes of historic buildings and proves that the building behaviours of buildings is best evaluated by the joint application of an analytical method and a visual inspection tool into a hybrid approach for historic city centres.

7.2 Background and outcomes of the research project

Traditionally, historical city centres are built with masonry buildings, often characterised by very poor construction materials, lack of connections among structural

elements, irregularity in plan and elevations, and presence of ineffective strengthening devises. All these characteristics greatly affect the type of damage and the type of failure modes of buildings under seismic events.

To reduce the seismic vulnerability and loss of historic city centres, buildings need to be assessed to investigate their behaviour under seismic events with the scope at identifying their typical failure modes, and proposing approaches capable to predict the seismic vulnerability of buildings by taking into account their geometric/structural features, deficiencies and seismic damage.

The hybrid methodology proposed in this work is a post-earthquake assessment tool developed to investigate the correlation between structural features/deficiencies/seismic damage, mentioned above, and failure modes and to become a possible tool for the reduction of the seismic vulnerability based on strengthening strategies that take into account the failure modes to which buildings are most vulnerable.

Such a method is based on the use of two methods that investigate, respectively, the causes of the failure modes through an analytical approach and effects of the failure modes through a visual inspection.

The first method included in the hybrid approach is FaMIVE (Failure Mechanism Identification and Vulnerability Evaluation method) the best analytical method among the existing ones developed for the vulnerability assessment of masonry buildings. The new version of FaMIVE, developed in this work to assess the performances of irregular buildings, relies on mechanical approaches implemented to capture failure modes, by taking into account the structural features and deficiencies of buildings.

The second method included in the proposed hybrid methodology is the knowledge based LOG-IDEAH (LOGic trees for Identification of Damage due to Earthquakes for Architectural Heritage), that aims at investigating failure modes by the interpretation of seismic damage observed on site with rules based on engineering knowledge.

LOG-IDEAH is developed in this research to overcome the lacks of the existing guidelines and approaches that offer a limited support to the users wishing to investigate the failure modes by only using observation. Therefore, LOG-IDEAH is presented as a novel approach to bridge the gap between the failure modes and the

damage and cracks observed on a building, by providing logic trees and graphics to illustrate their correlation.

The data required as input for both approaches is stored on site simultaneously by using the inspection form of FaMIVE and the on line platform of LOG-IDEAH. The data is collected at the level of the single façade for FaMIVE, and at the level of the single building for LOG-IDEAH. The reliability of the collected data is also recorded as input in order to take into account if the collected data has been directly observed on site or assumed. The time required to collect the data for each method is approximately one hour that can be reduced by considering that buildings in the same urban block might have similar features.

The run of the single record is carried out in a few seconds for FaMIVE and LOG-IDEAH, respectively. Their results in terms of failure modes are comparable, and their union allows a better prediction of the failure modes observed on site, respect to the one that can be obtained by the single method.

In order to decide how the results from FaMIVE and LOG-IDEAH should be jointed, the validation of both approaches has been carried out on two different sets of results taken form the single method. The first sets of the results called FaMIVE_1 and LOG-IDEAH_1 are composed by failure modes with the highest probability of occurrence, as they have been taken from FaMIVE and LOG-IDEAH, respectively. The second sets, called FaMIVE_2 and LOG-IDEAH_2 of the results are composed by failure modes with the two highest probability of occurrence and they are, as they have been also taken from FaMIVE and LOG-IDEAH, respectively.

The validation has been carried out by calculating Precision and Recall on the single set of results against the failure modes observed on site. The results have shown that FaMIVE_2 and LOG-IDEAH_1 over performance FaMIVE_1 and LOG-IDEAH_2.

Therefore, the proposed hybrid set of results, named UNION_1, is given by the union of the failure modes belonging to FaMIVE_2 and LOG-IDEAH_1, selected as the sets of results from FaMIVE and LOG-IDEAH that best predict the observed failure modes and the hybrid method aims to overcome the limitation of other hybrid methods trying to complement results derived from different methods.

Furthermore, the FaMIVE method is also proposed to estimate damage probabilities through the intersection between the fragility curves and performance points, given by the intersections between capacity curves and non-linear spectra. Damage probabilities are estimated for building classes according to the structural features observed on site in the area of study, and the failure modes and vulnerability levels estimated by FaMIVE. The comparison between the damage probability estimated by FaMIVE and the damage observed on site has demonstrated a strong correlation in all building classes. In particular, this has been underlined when the comparison is between the observed and estimated damage levels for buildings classified according to their vulnerability levels.

7.3 Suggestion for future works

The validation process of the hybrid approach has given a number of promising results on masonry buildings made of the following materials: fired bricks, stones, rubbles and a mixed of the materials mentioned above. Moreover, the results have demonstrated that the approach is suitable to investigate the failure modes of irregular residential buildings in plan and in elevation, with and without courtyards, with deficiencies related to quality of materials, connections between walls, connections between walls and floors, and strengthening devices.

Furthermore, in order to implement this hybrid approach as a tool for the vulnerability reduction, the logic of this approach can be used to classify damaged buildings according to their (geometric and structures) features and identify possible correlation between these features and failure modes identified on the basis of their correlation with the observed cracks in relation to the rules of LOG-IDEAH. Therefore, this approach, if based on extended rules that also directly correlate features and failure modes, might become a tool for the vulnerability reduction that can provide strategies of interventions defined in relation to the specific features of the buildings and consequently in relation to the failure modes, to which buildings are most vulnerable.

Nevertheless, the hybrid method is yet not validated on buildings that are damaged not necessarily by seismic events but they are deteriorated by other causes such as: soil failure (e.g. liquefaction, settlements, landslides lack of maintenance) infiltrations,

corrosion, and presence of moisture or vegetation. Indeed, because of the numerous reasons that can raise the deterioration of a building and the extent of the specific research field, it was not feasible to explore the entire possible damage effecting building behaviour within the set timeframe.

Furthermore, this was not the goal set for this research either: the work carried out and described in the previous chapters aims to provide a tool to assess the typical failure modes of historic masonry buildings by investigating geometric and structural features and seismic deficiencies through an analytical method and by interpreting seismic crack patterns through a visual inspection tool.

Whilst this objective has been fulfilled, as discussed above, a number of challenges and open questions remain. Indeed, the results achieved so far prove that the hybrid approach is applicable specifically for residential masonry buildings whereby a set of failure modes are expected. In the same way, the expected failure modes catalogued for these classes of buildings might not include all the possibilities, since most of the these failure modes are identified after a seismic event in a complete condition of emergency, where the access to buildings is often denied and building inspections are frequently carried out from street.

Moreover, since the hybrid approach proposed in this research project, is developed to assess the seismic vulnerability at territorial scale, a particular attention should be given to failure modes that are caused by pounding of adjacent buildings, characterised by different heights, materials, and floor classes. Therefore, the further development of this approach can be achieved by identifying the parameters that mostly cause hammering between buildings, and the class of damage that highlights the occurrence of the typical failure modes due to the impact between buildings excited by a seismic event. Most importantly, by enriching the catalogue of the possible failure modes related to pounding, both specific analytical model based on mechanical approaches, for FaMIVE, and rules based on the interpretation of damage, for LOG-IDEAH can also be developed and integrated in the existing hybrid approach.

Further, for a variety of buildings made of geometric and structural features, different from the ones considered in this research, the proposed hybrid approach requires additional tuning and testing. However, in order to calibrate the hybrid approach on new building classes, an exact knowledge of how these buildings behave and respond to seismic events is required. Therefore, a supplementary challenge for

any future work regarding the proposed method for the seismic vulnerability assessment will be to enhance its capacity to predict failure modes for several building classes.

In order to achieve this, the creation of databases collating the most recurring geometry in plan and in elevation, opening layout, materials, floor classes, connections, typical seismic damage and severity is the first step to classify the existing buildings and identify their typical failure modes with the purpose to select an analytical method and a visual inspection tool that best predict the expected seismic response.

From an analytical point of view, approaches capable to assess the performance of buildings of different classes such as steel frames, reinforced concrete frames, etc. are numerous in both commercial and academic sectors. On the other hand, LOG-IDEAH can still be considered the approach to investigate failure modes by visual inspection, if this tool is integrated with rules adequate to capture the performance of the building classes under consideration, known their typical crack patterns and typical failure modes.

7.4 Final remarks

In conclusion, despite the limitation and the future challenges outlined above, this research has shown that the application of the proposed hybrid approach in the form of an innovative approach addresses the shortcoming of the procedure discussed in the previous sections, and offers substantive promise for future improvements and development in the field of the seismic vulnerability assessment at territorial scale.

APPENDIX A: INSPECTION FORM ASCI 41-13

TIER 1 CHECKLISTS

C Compliant
NC Non-Compliant
N/A Not Applicable
U Undefined

BASIC CHECKLIST

Very Low Seismicity Structural Components

C NC N/A U LOAD PATH: The structure shall contain a complete, well-defined load path, including structural elements and connections, that serves to transfer the inertial forces associated with the mass of all elements of the building to the foundation. (Commentary: Sec. A.2.1.1. Tier 2: Sec. 5.4.1.1)

C NC N/A U WALL ANCHORAGE: Exterior concrete or masonry walls that are dependent on the diaphragm for lateral support are anchored for out-of-plane forces at each diaphragm level with steel anchors, reinforcing dowels, or straps that are developed into the diaphragm. Connections shall have adequate strength to resist the connection force calculated in the Quick Check procedure of Section 4.5.3.7. (Commentary: Sec. A.5.1.1. Tier 2:

Sec. 5.7.1.1)

LIFE SAFETY BASIC CONFIGURATION CHECKLIST

Low Seismicity Building System *General*

C NC N/A U LOAD PATH: The structure shall contain a complete, well defined load path, including structural elements and connections, that serves to transfer the inertial forces associated with the mass of all elements of the building to the foundation. (Commentary: Sec. A.2.1.1. Tier 2: Sec. 5.4.1.1)

C NC N/A U ADJACENT BUILDINGS: The clear distance between the building being evaluated and any adjacent building is greater than 4% of the height of the shorter building. This statement shall not apply for the following building types: W1, W1a, and W2. (Commentary: Sec. A.2.1.2. Tier 2: Sec. 5.4.1.2)

C NC N/A U MEZZANINES: Interior mezzanine levels are braced independently from the main structure or are anchored to the seismic-force-resisting elements of the main structure. (Commentary: Sec. A.2.1.3. Tier 2: Sec. 5.4.1.3)

Building Configuration

C NC N/A U WEAK STORY: The sum of the shear strengths of the seismic-force-resisting system in any story in each direction is not less than 80% of the strength in the adjacent story above. (Commentary: Sec. A2.2.2. Tier 2: Sec. 5.4.2.1)

C NC N/A U SOFT STORY: The stiffness of the seismic-force-resisting system in any story is not less than 70% of the seismic-force-resisting system stiffness in an adjacent story above or less than 80% of the average seismic- force-resisting system stiffness of the three stories above. (Commentary: Sec. A.2.2.3. Tier 2: Sec. 5.4.2.2)

C NC N/A U VERTICAL IRREGULARITIES: All vertical elements in the seismic-force-resisting system are continuous to the foundation. (Commentary: Sec. A.2.2.4. Tier 2: Sec. 5.4.2.3)

C NC N/A U GEOMETRY: There are no changes in the net horizontal dimension of the seismic-force-resisting system of more than 30% in a story relative to adjacent stories, excluding one-story penthouses and mezzanines. (Commentary: Sec. A.2.2.5. Tier 2: Sec. 5.4.2.4)

C NC N/A U MASS: There is no change in effective mass more than 50% from one story to the next. Light roofs, penthouses, and mezzanines need not be considered. (Commentary: Sec. A.2.2.6. Tier 2: Sec. 5.4.2.5)

C NC N/A U TORSION: The estimated distance between the story center of mass and the story center of rigidity is less than 20% of the building width in either plan dimension. (Commentary: Sec. A.2.2.7. Tier 2: Sec. 5.4.2.6)

Moderate Seismicity: Complete the Following Items in Addition to the Items for Low Seismicity. Geologic Site Hazards

C NC N/A U LIQUEFACTION: Liquefaction-susceptible, saturated, loose granular soils that could jeopardize the building's seismic performance shall not exist in the foundation soils at depths within 50 ft under the building. (Commentary: Sec. A.6.1.1. Tier 2: 5.4.3.1)

C NC N/A U SLOPE FAILURE: The building site is sufficiently remote from potential earthquake-induced slope failures or rockfalls to be unaffected by such failures or is capable of accommodating any predicted movements without failure. (Commentary: Sec. A.6.1.2. Tier 2: 5.4.3.1)

C NC N/A U SURFACE FAULT RUPTURE: Surface fault rupture and surface displacement at the building site are not anticipated. (Commentary: Sec. A.6.1.3. Tier 2: 5.4.3.1)

High Seismicity: Complete the Following Items in Addition to the Items for Low and Moderate Seismicity. Foundation Configuration

C NC N/A U OVERTURNING: The ratio of the least horizontal dimension of the seismic-force-resisting system at the foundation level to the building height (base/height) is greater than 0.6S_a. (Commentary: Sec. A.6.2.1. Tier 2: Sec. 5.4.3.3)

C NC N/A U TIES BETWEEN FOUNDATION ELEMENTS: The foundation has ties adequate to resist seismic forces where footings, piles, and piers are not restrained by beams, slabs, or soils classified as Site Class A, B, or C. (Commentary: Sec. A.6.2.2. Tier 2: Sec. 5.4.3.4)

IMMEDIATE OCCUPANCY BASIC CONFIGURATION CHECKLIST

Very Low Seismicity Building System *General*

C NC N/A U LOAD PATH: The structure shall contain a complete, well-defined load path, including structural elements and connections, that serves to transfer the inertial forces associated with the mass of all elements of the building to the foundation. (Commentary: Sec. A.2.1.1. Tier 2: Sec. 5.4.1.1)

C NC N/A U ADJACENT BUILDINGS: The clear distance between the building being evaluated and any adjacent building is greater than 4% of the height of the shorter building. This statement need not apply for the following building types: W1, W1a, and W2. (Commentary: Sec. A.2.1.2. Tier 2: Sec. 5.4.1.2)

C NC N/A U MEZZANINES: Interior mezzanine levels are braced independently from the main structure or are anchored to the seismic-force-resisting elements of the main structure. (Commentary: Sec. A.2.1.3. Tier 2: Sec. 5.4.1.3)

Building Configuration

C NC N/A U WEAK STORY: The sum of the shear strengths of the seismic-force-resisting system in any story in each direction shall not be less than 80% of the strength in the adjacent story above. (Commentary: Sec. A.2.2.2. Tier 2: Sec. 5.4.2.1)

C NC N/A U SOFT STORY: The stiffness of the seismic-force-resisting system in any story shall not be less than 70% of the seismic-force-resisting system stiffness in an adjacent story above or less than 80% of the average seismic- force-resisting system stiffnessof the three stories above. (Commentary: Sec. A.2.2.3. Tier 2: Sec. 5.4.2.2)

C NC N/A U VERTICAL IRREGULARITIES: All vertical elements in the seismic-force-resisting system are continuous to the foundation. (Commentary: Sec. A.2.2.4. Tier 2: Sec. 5.4.2.3)

C NC N/A U GEOMETRY: There are no changes in the net horizontal dimension of the seismic-force-resisting system of more than 30% in a story relative

to adjacent stories, excluding one-story penthouses and mezzanines. (Commentary: Sec. A.2.2.5. Tier 2: Sec. 5.4.2.4)

C NC N/A U MASS: There is no change in effective mass more than 50% from one story to the next. Light roofs, penthouses, and mezzanines need not be considered. (Commentary: Sec. A.2.2.6. Tier 2: Sec. 5.4.2.5)

C NC N/A U TORSION: The estimated distance between the story center of mass and the story center of rigidity is less than 20% of the building width in either plan dimension. (Commentary: Sec. A.2.2.7. Tier 2: Sec. 5.4.2.6)

Low Seismicity: Complete the Following Items in Additionto the Items for Very Low Seismicity. Geologic Site Hazards

C NC N/A U LIQUEFACTION: Liquefaction-susceptible, saturated, loose granular soils that could jeopardize the building's seismic performance shall not exist in the foundation soils at depths within 50 ft under the building. (Commentary: Sec. A.6.1.1. Tier 2: 5.4.3.1)

C NC N/A U SLOPE FAILURE: The building site is sufficiently remote from potential earthquake-induced slope failures or rockfalls to be unaffected by such failures or is capable of accommodating any predicted movements without failure. (Commentary: Sec. A.6.1.2. Tier 2: 5.4.3.1)

C NC N/A U SURFACE FAULT RUPTURE: Surface fault rupture and surface displacement at the building site are not anticipated. (Commentary: Sec. A.6.1.3. Tier 2: 5.4.3.1)

Moderate and High Seismicity: Complete the Following Items in Addition to the Items for Low Seismicity. Foundation Configuration

C NC N/A U OVERTURNING: The ratio of the least horizontal dimension of the seismic-force-resisting system at the foundation level to the building height (base/height) is greater than 0.6S_a. (Commentary: Sec. A.6.2.1. Tier 2: Sec. 5.4.3.3)

C NC N/A U TIES BETWEEN FOUNDATION ELEMENTS: The foundation has ties adequate to resist seismic forces where footings, piles, and piers are not restrained by beams, slabs, or soils classified as Site Class A, B, or C. (Commentary: Sec. A.6.2.2. Tier 2: Sec. 5.4.3.4)

LS LIFE SAFETY STRUCTURAL CHECKLIST FOR BUILDING TYPES URM: UNREINFORCED MASONRY BEARING WALLS WITH FLEXIBLE DIAPHRAGMS AND URMA: UNREINFORCED MASONRY BEARING WALLS WITH STIFF DIAPHRAGMS

Low and Moderate Seismicity Seismic-Force-Resisting System

C NC N/A U REDUNDANCY: The number of lines of shear walls in each principal direction is greater than or equal to 2. (Commentary: Sec. A.3.2.1.1. Tier 2: Sec. 5.5.1.1)

C NC N/A U SHEAR STRESS CHECK: The shear stress in the unreinforced masonry shear walls, calculated using the Quick Check procedure of Section 4.5.3.3, is less than 30 lb/in.^{2} for clay units and 70 lb/in.^{2} for concrete units. (Commentary: Sec. A.3.2.5.1. Tier 2: Sec. 5.5.3.1.1)

Connections

C NC N/A U WALL ANCHORAGE: Exterior concrete or masonry walls that are dependent on the diaphragm for lateral support are anchored for out-of-plane forces at each diaphragm level with steel anchors, reinforcing dowels, or straps that are developed into the diaphragm. Connections shall have adequate strength to resist the connection force calculated in the Quick Check procedure of Section 4.5.3.7. (Commentary: Sec. A.5.1.1. Tier 2: Sec.

5.7.1.1)

C NC N/A U WOOD LEDGERS: The connection between the wall panels and the diaphragm does not induce cross-grain bending or tension in the wood ledgers. (Commentary: Sec. A.5.1.2. Tier 2: Sec. 5.7.1.3)

C NC N/A U TRANSFER TO SHEAR WALLS: Diaphragms are connected for transfer of seismic forces to the shear walls. (Commentary: Sec. A.5.2.1. Tier 2: Sec. 5.7.2)

C NC N/A U GIRDER–COLUMN CONNECTION: There is a positive connection using plates, connection hardware, or straps between the girder and the column support. (Commentary: Sec. A.5.4.1. Tier 2: Sec. 5.7.4.1)

High Seismicity: Complete the Following Items in Addition to the Items for Low and Moderate Seismicity. Seismic-Force-Resisting System

C NC N/A U PROPORTIONS: The height-to-thickness ratio of the shear walls at each story is less than the following (Commentary: Sec. A.3.2.5.2. Tier 2: Sec. 5.5.3.1.2):

Top story of multi-story building	9
First story of multi-story building	15
All other conditions	13

C NC N/A U MASONRY LAYUP: Filled collar joints of multi-wythe masonry walls have negligible voids. (Commentary: Sec. A.3.2.5.3. Tier 2: Sec. 5.5.3.4.1)

Diaphragms (Stiff or Flexible)

C NC N/A U OPENINGS AT SHEAR WALLS: Diaphragm openings immediately adjacent to the shear walls are less than 25% of the wall length. (Commentary: Sec. A.4.1.4. Tier 2: Sec. 5.6.1.3)

C NC N/A U OPENINGS AT EXTERIOR MASONRY SHEAR WALLS: Diaphragm openings immediately adjacent to exterior masonry shear walls are not greater than 8 ft long. (Commentary: Sec. A.4.1.6. Tier 2: Sec. 5.6.1.3)

Flexible Diaphragms

C NC N/A U CROSS TIES: There are continuous cross ties between diaphragm chords.

C NC N/A U STRAIGHT SHEATHING: All straight sheathed diaphragms have aspect ratios less than 2-to-1 in the

C NC N/A U SPANS: All wood diaphragms with spans greater than 24 ft consist of wood structural panels or diagonal

C U DIAGONALLY SHEATHED AND UNBLOCKED
N DIAPHRAGMS: All diagonally sheathed or unblocked wood
C structural panel diaphragms have horizontal spans less than
C U OTHER DIAPHRAGMS: The diaphragm does not consist of
N a system other than wood, metal deck, concrete, or

Connections

C U STIFFNESS OF WALL ANCHORS: Anchors of concrete or
N masonry walls to wood structural elements are installed taut
C and are stiff enough to limit the relative movement between
C U BEAM, GIRDER, AND TRUSS SUPPORTS: Beams,
N girders, and trusses supported by unreinforced masonry
C walls or pilasters have independent secondary columns for

IO IMMEDIATE OCCUPANCY STRUCTURAL CHECKLIST FOR BUILDING TYPES URM: UNREINFORCED MASONRY BEARING WALLS WITH FLEXIBLE DIAPHRAGMS AND URMA: UNREINFORCED MASONRY BEARING WALLS WITH STIFF DIAPHRAGMS

Very Low Seismicity

Seismic-Force-Resisting System

C NC N/A U REDUNDANCY: The number of lines of shear walls in each principal direction is greater than or equal to 2. (Commentary: Sec. A.3.2.1.1. Tier 2: Sec. 5.5.1.1)

C NC N/A U SHEAR STRESS CHECK: The shear stress in the unreinforced masonry shear walls, calculated using the Quick Check procedure of Section 4.5.3.3, is less than 30 lb/in.^{2} for clay units and 70 lb/in.^{2} for concrete units. (Commentary: Sec. A.3.2.5.1. Tier 2: Sec. 5.5.3.1.1)

Connections

C NC N/A U WALL ANCHORAGE: Exterior concrete or masonry walls that are dependent on the diaphragm for lateral support are anchored for out-of-plane forces at each diaphragm level with steel anchors, reinforcing dowels, or straps that are developed into the diaphragm. Connections shall have adequate strength to resist the connection force calculated in the Quick Check procedure of Section 4.5.3.7. (Commentary: Sec. A.5.1.1. Tier 2: Sec.

5.7.1.1)

C NC N/A U WOOD LEDGERS: The connection between the wall panels and the diaphragm does not induce cross-grain bending or tension in the wood ledgers. (Commentary: Sec. A.5.1.2. Tier 2: Sec. 5.7.1.3)

C NC N/A U TRANSFER TO SHEAR WALLS: Diaphragms are connected for transfer of seismic forces to the shear walls. (Commentary: Sec. A.5.2.1. Tier 2: Sec. 5.7.2)

C NC N/A U GIRDER–COLUMN CONNECTION: There is a positive connection using plates, connection hardware, or straps between the girder and the column support. (Commentary: Sec. A.5.4.1. Tier 2: Sec. 5.7.4.1)

Foundation System

C NC N/A U DEEP FOUNDATIONS: Piles and piers are capable of transferring the lateral forces between the structure and the soil. (Commentary: Sec. A.6.2.3.)

C NC N/A U SLOPING SITES: The difference in foundation embedment depth from one side of the building to another shall not exceed one story high. (Commentary: Sec. A.6.2.4)

Low, Moderate, and High Seismicity: Complete the Following Items in Addition to the Items for Very Low Seismicity. Seismic-Force-Resisting System

C NC N/A U PROPORTIONS: The height-to-thickness ratio of the shear walls at each story is less than the following (Commentary: Sec. A.3.2.5.2. Tier 2: Sec. 5.5.3.1.2):

Top story of multi-story building	9
First story of multi-story building	15
All other conditions	13

C NC N/A U MASONRY LAYUP: Filled collar joints of multi-wythe masonry walls have negligible voids. (Commentary: Sec. A.3.2.5.3. Tier 2: Sec. 5.5.3.4.1)

Diaphragms (Stiff or Flexible)

C NC N/A U OPENINGS AT SHEAR WALLS: Diaphragm openings immediately adjacent to the shear walls are less than 15% of the wall length. (Commentary: Sec. A.4.1.4. Tier 2: Sec. 5.6.1.3)

C NC N/A U OPENINGS AT EXTERIOR MASONRY SHEAR WALLS: Diaphragm openings immediately adjacent to exterior masonry shear walls are be greater than 4 ft long. (Commentary: Sec. A.4.1.6. Tier 2: Sec. 5.6.1.3)

C NC N/A U PLAN IRREGULARITIES: There is tensile capacity to develop the strength of the diaphragm at reentrant corners or other locations of plan irregularities. (Commentary: Sec. A.4.1.7. Tier 2: Sec. 5.6.1.4)

C NC N/A U DIAPHRAGM REINFORCEMENT AT OPENINGS: There is reinforcing around all diaphragm openings larger than 50% of the building width in either major plan dimension. (Commentary: Sec. A.4.1.8. Tier 2: Sec. 5.6.1.5)

Flexible Diaphragms

C NC N/A U CROSS TIES: There are continuous cross ties between diaphragm chords. (Commentary: Sec. A.4.1.2. Tier 2: Sec. 5.6.1.2)

C NC N/A U STRAIGHT SHEATHING: All straight sheathed diaphragms have aspect ratios less than 1-to-1 in the direction being considered. (Commentary: Sec. A.4.2.1. Tier 2: Sec. 5.6.2)

C NC N/A U SPANS: All wood diaphragms with spans greater than 12 ft consist of wood structural panels or diagonal sheathing. (Commentary: Sec. A.4.2.2. Tier 2: Sec. 5.6.2)

C NC N/A U DIAGONALLY SHEATHED AND UNBLOCKED DIAPHRAGMS: All diagonally sheathed or unblocked wood structural panel diaphragms have horizontal spans less than 30 ft and aspect ratios less than or equal to 3-to-1. (Commentary: Sec. A.4.2.3. Tier 2: Sec. 5.6.2)

C NC N/A U NONCONCRETE FILLED DIAPHRAGMS: Untopped metal deck diaphragms or metal deck diaphragms with fill other than concrete shall consist of horizontal spans of less than 40 ft and have aspect ratios less than 4-to-1. (Commentary: Sec. A.4.3.1. and Tier 2: Sec.

C NC N/A U OTHER DIAPHRAGMS: The diaphragm does not consist of a system other than wood, metal deck, concrete, or horizontal bracing. (Commentary: Sec. A.4.7.1. Tier 2: Sec. 5.6.5)

Connections

C NC N/A U STIFFNESS OF WALL ANCHORS: Anchors of concrete or masonry walls to wood structural elements are installed taut and are stiff enough to limit the relative movement between the wall and the diaphragm to no greater than 1/8 in. before engagement of the anchors. (Commentary: Sec. A.5.1.4. Tier 2: Sec. 5.7.1.2)

C NC N/A U BEAM, GIRDER, AND TRUSS SUPPORTS: Beams, girders, and trusses supported by unreinforced masonry walls or pilasters have independent secondary columns for support of vertical loads. (Commentary: Sec.

A.5.4.5. Tier 2: Sec. 5.7.4.4)

NONSTRUCTURAL CHECKLIST

Life Safety Systems

C NC N/A U LS-LMH; PR-LMH. FIRE SUPPRESSION PIPING: Fire suppression piping is anchored and braced in accordance with NFPA-13.

C NC N/A U LS-LMH; PR-LMH. FLEXIBLE COUPLINGS: Fire suppression piping has flexible couplings in accordance with NFPA-13. (Commentary:

C NC N/A U LS-LMH; PR-LMH. EMERGENCY POWER: Equipment used to power or control life safety systems is anchored or braced. (Commentary:

C NC N/A U LS-LMH; PR-LMH. STAIR AND SMOKE DUCTS: Stair pressurization and smoke control ducts are braced and have flexible connections at

C NC N/A U LS-MH; PR-MH. SPRINKLER CEILING CLEARANCE: Penetrations through panelized ceilings for fire suppression devices provide clearances in accordance with NFPA-13. (Commentary: Sec.

C NC N/A U LS-not required; PR-LMH. EMERGENCY LIGHTING: Emergency and egress lighting equipment is anchored or braced. (Commentary: Sec.

Hazardous Materials

C NC N/A U LS-LMH; PR-LMH. HAZARDOUS MATERIAL EQUIPMENT: Equipment mounted on vibration isolators and containing hazardous material is equipped with restraints or snubbers. (Commentary: Sec.

C NC N/A U LS-LMH; PR-LMH. HAZARDOUS MATERIAL STORAGE: Breakable containers that hold hazardous material, including gas cylinders, are restrained by latched doors, shelf lips, wires, or other methods.

C NC N/A U LS-MH; PR-MH. HAZARDOUS MATERIAL DISTRIBUTION: Piping or ductwork conveying hazardous materials is braced or otherwise protected from damage that would allow hazardous material release.

C NC N/A U LS-MH; PR-MH. SHUT-OFF VALVES: Piping containing hazardous material, including natural gas, has shut- off valves or other devices to

C NC N/A U LS-LMH; PR-LMH. FLEXIBLE COUPLINGS: Hazardous material ductwork and piping, including natural gas piping, has flexible

C NC N/A U LS-MH; PR-MH. PIPING OR DUCTS CROSSING SEISMIC JOINTS: Piping or ductwork carrying hazardous material that either crosses seismic joints or isolation planes or is connected to independent structures has couplings or other details to accommodate the relative

Partitions

C NC N/A U LS-LMH; PR-LMH. UNREINFORCED MASONRY: Unreinforced masonry or hollow-clay tile partitions are braced at a spacing of at most 10 ft in Low or Moderate Seismicity, or at most 6 ft in High Seismicity. (Commentary: Sec. A.7.1.1. Tier 2: Sec. 13.6.2)

C NC N/A U LS-LMH; PR-LMH. HEAVY PARTITIONS SUPPORTED BY CEILINGS: The tops of masonry or hollow- clay tile partitions are not laterally supported by an integrated ceiling system. (Commentary: Sec. A.7.2.1. Tier 2: Sec. 13.6.2)

C NC N/A U LS-MH; PR-MH. DRIFT: Rigid cementitious partitions are detailed to accommodate the following drift ratios: in steel moment frame, concrete moment frame, and wood frame buildings, 0.02; in other buildings, 0.005. (Commentary A.7.1.2 Tier 2: Sec. 13.6.2)

C NC N/A U LS-not required; PR-MH. LIGHT PARTITIONS SUPPORTED BY CEILINGS: The tops of gypsum board partitions are not laterally supported by an integrated ceiling system. (Commentary: Sec. A.7.2.1.

C NC N/A U LS-not required; PR-MH. STRUCTURAL SEPARATIONS: Partitions that cross structural separations have seismic or control joints.

C NC N/A U LS-not required; PR-MH. TOPS: The tops of ceiling-high framed or panelized partitions have lateral bracing to the structure at a spacing

Ceilings

C NC N/A U LS-MH; PR-LMH. SUSPENDED LATH AND PLASTER: Suspended lath and plaster ceilings have attachments that resist seismic forces for every 12 ft^2 of area. (Commentary: Sec. A.7.2.3. Tier 2: Sec. 13.6.4)

C NC N/A U LS-MH; PR-LMH. SUSPENDED GYPSUM BOARD: Suspended gypsum board ceilings have attachments that resist seismic forces for every 12 ft^2 of area. (Commentary: Sec. A.7.2.3. Tier 2: Sec. 13.6.4)

C NC N/A U LS-not required; PR-MH. INTEGRATED CEILINGS: Integrated suspended ceilings with continuous areas greater than 144 ft^2, and ceilings of smaller areas that are not surrounded by restraining partitions, are laterally restrained at a spacing no greater than 12 ft with members attached to the structure above. Each restraint location has a minimum of four diagonal wires and compression struts, or diagonal members capable of resisting compression. (Commentary: Sec. A.7.2.2. Tier 2: Sec. 13.6.4)

C NC N/A U LS-not required; PR-MH. EDGE CLEARANCE: The free edges of integrated suspended ceilings with continuous areas greater than 144 ft^2 have clearances from the enclosing wall or partition of at least the following: in Moderate Seismicity, 1/2 in.; in High Seismicity, 3/4 in. (Commentary: Sec. A.7.2.4. Tier 2: Sec. 13.6.4)

C NC N/A U LS-not required; PR-MH. CONTINUITY ACROSS STRUCTURE JOINTS: The ceiling system does not cross any seismic joint and is not attached to multiple independent structures. (Commentary: Sec. A.7.2.5. Tier 2: Sec. 13.6.4)

C NC N/A U LS-not required; PR-H. EDGE SUPPORT: The free edges of integrated suspended ceilings with continuous areas greater than 144 ft^2 are supported by closure angles or channels not less than 2 in. wide. (Commentary: Sec. A.7.2.6. Tier 2: Sec. 13.6.4)

C NC N/A U LS-not required; PR-H. SEISMIC JOINTS: Acoustical tile or lay-in panel ceilings have seismic separation joints such that each continuous portion of the ceiling is no more than 2500 ft^2 and has a ratio of long-to-short dimension no more than 4-to-1. (Commentary: Sec. A.7.2.7. Tier 2: 13.6.4)

Light Fixtures

C NC N/A U LS-MH; PR-MH. INDEPENDENT SUPPORT: Light fixtures that weigh more per square foot than the ceiling they penetrate are supported independent of the grid ceiling suspension system by a minimum of two wires at diagonally opposite corners of each fixture. (Commentary: Sec. A.7.3.2. Tier 2: Sec. 13.6.4 and 13.7.9)

C NC N/A U LS-not required; PR-H. PENDANT SUPPORTS: Light fixtures on pendant supports are attached at a spacing equal to or less than 6 ft and, if rigidly supported, are free to move with the structure to which they are attached without damaging adjoining components. (Commentary: A.7.3.3. Tier 2: Sec. 13.7.9)

C NC N/A U LS-not required; PR-H. LENS COVERS: Lens covers on light fixtures are attached with safety devices. (Commentary: Sec. A.7.3.4. Tier 2: Sec. 13.7.9)

Cladding and Glazing

C NC N/A U LS-MH; PR-MH. CLADDING ANCHORS: Cladding components weighing more than 10 lb/ft^2 are mechanically anchored to the structure at a spacing equal to or less than the following: for Life Safety in Moderate

Seismicity, 6 ft; for Life Safety in High Seismicity and for Position Retention in any seismicity, 4 ft. (Commentary: Sec. A.7.4.1. Tier 2: Sec. 13.6.1)

C NC N/A U LS-MH; PR-MH. CLADDING ISOLATION: For steel or concrete moment frame buildings, panel connections are detailed to accommodate a story drift ratio of at least the following: for Life Safety in Moderate Seismicity, 0.01; for Life Safety in High Seismicity and for Position Retention in any seismicity, 0.02. (Commentary: Sec.

A.7.4.3. Tier 2: Section 13.6.1)

C NC N/A U LS-MH; PR-MH. MULTI-STORY PANELS: For multi-story panels attached at more than one floor level, panel connections are detailed to accommodate a story drift ratio of at least the following: for Life Safety in Moderate Seismicity, 0.01; for Life Safety in High Seismicity and for Position Retention in any seismicty,

0.02. (Commentary: Sec. A.7.4.4. Tier 2: Sec. 13.6.1)

C NC N/A U LS-MH; PR-MH. PANEL CONNECTIONS: Cladding panels are anchored out-of-plane with a minimum number of connections for each wall panel, as follows: for Life Safety in Moderate Seismicity, 2 connections; for Life Safety in High Seismicity and for Position Retention in any seismicity, 4 connections. (Commentary: Sec. A.7.4.5. Tier 2: Sec. 13.6.1.4)

C NC N/A U LS-MH; PR-MH. BEARING CONNECTIONS: Where bearing connections are used, there is a minimum of two bearing connections for each cladding panel. (Commentary: Sec. A.7.4.6. Tier 2: Sec. 13.6.1.4)

C NC N/A U LS-MH; PR-MH. INSERTS: Where concrete cladding components use inserts, the inserts have positive anchorage or are anchored to reinforcing steel. (Commentary: Sec. A.7.4.7. Tier 2: Sec. 13.6.1.4)

C NC N/A U LS-MH; PR-MH. OVERHEAD GLAZING: Glazing panes of any size in curtain walls and individual interior or exterior panes over 16 ft^2 in area are laminated annealed or laminated heat-strengthened glass and are detailed to remain in the frame when cracked. (Commentary: Sec. A.7.4.8: Tier 2: Sec. 13.6.1.5)

Masonry Veneer

C NC N/A U LS-LMH; PR-LMH. TIES: Masonry veneer is connected to the backup with corrosion-resistant ties. There is a minimum of one tie for every 2-2/3 ft^2, and the ties have spacing no greater than the following: for Life Safety in Low or Moderate Seismicity, 36 in.; for Life Safety in High Seismicity and for Position Retention in any seismicity, 24 in. (Commentary: Sec. A.7.5.1. Tier 2: Sec. 13.6.1.2)

C NC N/A U LS-LMH; PR-LMH. SHELF ANGLES: Masonry veneer is supported by shelf angles or other elements at each floor above the ground floor. (Commentary: Sec. A.7.5.2. Tier 2: Sec. 13.6.1.2)

C NC N/A U LS-LMH; PR-LMH. WEAKENED PLANES: Masonry veneer is anchored to the backup adjacent to weakened planes, such as at the locations of flashing. (Commentary: Sec. A.7.5.3. Tier 2: Sec. 13.6.1.2)

C NC N/A U LS-LMH; PR-LMH. UNREINFORCED MASONRY BACKUP: There is no unreinforced masonry backup. (Commentary: Sec. A.7.7.2. Tier 2: Section 13.6.1.1 and 13.6.1.2)

C NC N/A U LS-MH; PR-MH. STUD TRACKS: For veneer with metal stud backup, stud tracks are fastened to the structure at a spacing equal to or less than 24 in. on center. (Commentary: Sec. A.7.6.1. Tier 2: Section

13.6.1.1 and 13.6.1.2)

C NC N/A U LS-MH; PR-MH. ANCHORAGE: For veneer with concrete block or masonry backup, the backup is positively anchored to the structure at a horizontal spacing equal to or less than 4 ft along the floors and roof. (Commentary: Sec. A.7.7.1. Tier 2: Section 13.6.1.1 and 13.6.1.2)

C NC N/A U LS-not required; PR-MH. WEEP HOLES: In veneer anchored to stud walls, the veneer has functioning weep holes and base flashing. (Commentary: Sec. A.7.5.6. Tier 2: Section 13.6.1.2)

C NC N/A U LS-not required; PR-MH. OPENINGS: For veneer with metal stud backup, steel studs frame window and door openings. (Commentary: Sec. A.7.6.2. Tier 2: Sec. 13.6.1.1 and 13.6.1.2)

Parapets, Cornices, Ornamentation, and Appendages

C NC N/A U LS-LMH; PR-LMH. URM PARAPETS OR CORNICES: Laterally unsupported unreinforced masonry parapets or cornices have height-to-thickness ratios no greater than the following: for Life Safety in Low or Moderate Seismicity, 2.5; for Life Safety in High Seismicity and for Position Retention in any seismicity, 1.5. (Commentary: Sec. A.7.8.1. Tier 2: Sec. 13.6.5)

C NC N/A U LS-LMH; PR-LMH. CANOPIES: Canopies at building exits are anchored to the structure at a spacing no greater than the following: for Life Safety in Low or Moderate Seismicity, 10 ft; for Life Safety in High Seismicity and for Position Retention in any seismicity, 6 ft. (Commentary: Sec. A.7.8.2. Tier 2: Sec. 13.6.6)

C NC N/A U LS-MH; PR-LMH. CONCRETE PARAPETS: Concrete parapets with height-to-thickness ratios greater than

2.5 have vertical reinforcement. (Commentary: Sec. A.7.8.3. Tier 2: Sec. 13.6.5)

C NC N/A U LS-MH; PR-LMH. APPENDAGES: Cornices, parapets, signs, and other ornamentation or appendages that extend above the highest point of anchorage to the structure or cantilever from components are reinforced and anchored to the structural system at a spacing equal to or less than 6 ft. This checklist item does not apply to parapets or cornices covered by other checklist items. (Commentary: Sec. A.7.8.4. Tier 2: Sec. 13.6.6)

Masonry Chimneys

C NC N/A U LS-LMH; PR-LMH. URM CHIMNEYS: Unreinforced masonry chimneys extend above the roof surface no more than the following: for Life Safety in Low or Moderate Seismicity, 3 times the least dimension of the chimney; for Life Safety in High Seismicity and for Position Retention in any seismicity, 2 times the least dimension of the chimney. (Commentary: Sec. A.7.9.1. Tier 2: 13.6.7)

C NC N/A U LS-LMH; PR-LMH. ANCHORAGE: Masonry chimneys are anchored at each floor level, at the topmost ceiling level, and at the roof. (Commentary: Sec. A.7.9.2. Tier 2: 13.6.7)

Stairs

C NC N/A U LS-LMH; PR-LMH. STAIR ENCLOSURES: Hollow-clay tile or unreinforced masonry walls around stair enclosures are restrained out-of-plane and have height-to-thickness ratios not greater than the following: for Life Safety in Low or Moderate Seismicity, 15-to-1; for Life Safety in High Seismicity and for Position Retention in any seismicity, 12-to-1. (Commentary: Sec. A.7.10.1. Tier 2: Sec. 13.6.2 and 13.6.8)

C NC N/A U LS-LMH; PR-LMH. STAIR DETAILS: In moment frame structures, the connection between the stairs and the structure does not rely on shallow anchors in concrete. Alternatively, the stair details are capable of accommodating the drift calculated using the Quick Check procedure of Section 4.5.3.1 without including any lateral stiffness contribution from the stairs. (Commentary: Sec. A.7.10.2. Tier 2: 13.6.8)

Contents and Furnishings

C NC N/A U LS-MH; PR-MH. INDUSTRIAL STORAGE RACKS: Industrial storage racks or pallet racks more than 12 ft high meet the requirements of ANSI/MH 16.1 as modified by ASCE 7 Chapter 15. (Commentary: Sec.

C NC N/A U LS-H; PR-MH. TALL NARROW CONTENTS: Contents more than 6 ft high with a height-to-depth or height- to-width ratio greater than 3-to-1 are anchored to the structure or to each other. (Commentary: Sec. A.7.11.2. Tier 2: Sec. 13.8.2)

C NC N/A U LS-H; PR-H. FALL-PRONE CONTENTS: Equipment, stored items, or other contents weighing more than

20 lb whose center of mass is more than 4 ft above the adjacent floor level are braced or otherwise restrained. (Commentary: Sec. A.7.11.3

C NC N/A U LS-not required; PR-MH. ACCESS FLOORS: Access floors more than 9 in. high are braced. (Commentary: Sec. A.7.11.4. Tier 2: Sec. 13.8.3)

C NC N/A U LS-not required; PR-MH. EQUIPMENT ON ACCESS FLOORS: Equipment and other contents supported by access floor systems are anchored or braced to the structure independent of the access floor. (Commentary: Sec. A.7.11.5. Tier 2: Sec. 13.7.7 and 13.8.3)

C NC N/A U LS-not required; PR-H. SUSPENDED CONTENTS: Items suspended without lateral bracing are free to swing from or move with the structure from which they are suspended without damaging themselves or adjoining components. (Commentary. A.7.11.6. Tier 2: Sec. 13.8.2)

Mechanical and Electrical Equipment

C NC N/A U LS-H; PR-H. FALL-PRONE EQUIPMENT: Equipment weighing more than 20 lb whose center of mass is more than 4 ft above the adjacent floor level, and which is not in-line equipment, is braced. (Commentary:

A.7.12.4. Tier 2: 13.7.1 and 13.7.7)

C NC N/A U LS-H; PR-H. IN-LINE EQUIPMENT: Equipment installed in-line with a duct or piping system, with an operating weight more than 75 lb, is supported and laterally braced independent of the duct or piping system. (Commentary: Sec. A.7.12.5. Tier 2: Sec. 13.7.1)

C NC N/A U LS-H; PR-MH. TALL NARROW EQUIPMENT: Equipment more than 6 ft high with a height-to-depth or height-to-width ratio greater than 3-to-1 is anchored to the floor slab or adjacent structural walls. (Commentary: Sec. A.7.12.6. Tier 2: Sec. 13.7.1 and 13.7.7)

C NC N/A U LS-not required; PR-MH. MECHANICAL DOORS: Mechanically operated doors are detailed to operate at a story drift ratio of 0.01. (Commentary: Sec. A.7.12.7. Tier 2: Sec. 13.6.9)

C NC N/A U LS-not required; PR-H. SUSPENDED EQUIPMENT: Equipment suspended without lateral bracing is free to swing from or move with the structure from which it is suspended without damaging itself or adjoining components. (Commentary: Sec. A.7.12.8. Tier 2: Sec. 13.7.1 and 13.7.7)

C NC N/A U LS-not required; PR-H. VIBRATION ISOLATORS: Equipment mounted on vibration isolators is equipped with horizontal restraints or snubbers and with vertical restraints to resist overturning. (Commentary: Sec.

A.7.12.9. Tier 2: Sec. 13.7.1)

C NC N/A U LS-not required; PR-H. HEAVY EQUIPMENT: Floor-supported or platform-supported equipment weighing more than 400 lb is anchored to the structure. (Commentary: Sec. A.7.12.10. Tier 2: 13.7.1 and 13.7.7)

C NC N/A U LS-not required; PR-H. ELECTRICAL EQUIPMENT: Electrical equipment is laterally braced to the structure. (Commentary: Sec. A.7.12.11. Tier 2: 13.7.7)

C NC N/A U LS-not required; PR-H. CONDUIT COUPLINGS: Conduit greater than 2.5 in. trade size that is attached to panels, cabinets, or other equipment and is subject to relative seismic displacement has flexible couplings or connections. (Commentary: Sec. A.7.12.12. Tier 2: 13.7.8)

Piping

C NC N/A U LS-not required; PR-H. FLEXIBLE COUPLINGS: Fluid and gas piping has flexible couplings. (Commentary: Sec. A.7.13.2. Tier 2: Sec. 13.7.3 and 13.7.5)

C NC N/A U LS-not required; PR-H. FLUID AND GAS PIPING: Fluid and gas piping is anchored and braced to the structure to limit spills or leaks. (Commentary: Sec. A.7.13.4. Tier 2: Sec. 13.7.3 and 13.7.5)

C NC N/A U LS-not required; PR-H. C-CLAMPS: One-sided C-clamps that support piping larger than 2.5 in. in diameter are restrained. (Commentary: Sec. A.7.13.5. Tier 2: Sec. 13.7.3 and 13.7.5)

C NC N/A U LS-not required; PR-H. PIPING CROSSING SEISMIC JOINTS: Piping that crosses seismic joints or isolation planes or is connected to independent structures has couplings or other details to accommodate the relative seismic displacements. (Commentary: Sec.

Ducts

C NC N/A U LS-not required; PR-H. DUCT BRACING: Rectangular ductwork larger than 6 ft^2 in cross-sectional area and round ducts larger than 28 in. in diameter are braced. The maximum spacing of transverse bracing does not exceed 30 ft. The maximum spacing of longitudinal bracing does not exceed 60 ft. (Commentary: Sec.

A.7.14.2. Tier 2: Sec. 13.7.6)

C NC N/A U LS-not required; PR-H. DUCT SUPPORT: Ducts are not supported by piping or electrical conduit. (Commentary: Sec. A.7.14.3. Tier 2: Sec. 13.7.6)

C NC N/A U LS-not required; PR-H. DUCTS CROSSING SEISMIC JOINTS: Ducts that cross seismic joints or isolation planes or are connected to independent structures have couplings or other details to accommodate the relative seismic displacements. (Commentary: Sec. A.7.14.5. Tier 2: Sec. 13.7.6)

Elevators

C NC N/A U LS-H; PR-H. RETAINER GUARDS: Sheaves and drums have cable retainer guards. (Commentary: Sec.

A.7.16.1. Tier 2: 13.8.6)

C NC N/A U LS-H; PR-H. RETAINER PLATE: A retainer plate is present at the top and bottom of both car and counterweight. (Commentary: Sec. A.7.16.2. Tier 2: 13.8.6)

C NC N/A U LS-not required; PR-H. ELEVATOR EQUIPMENT: Equipment, piping, and other components that are part of the elevator system are anchored. (Commentary: Sec. A.7.16.3. Tier 2: 13.8.6)

C NC N/A U LS-not required; PR-H. SEISMIC SWITCH: Elevators capable of operating at speeds of 150 ft/min or faster are equipped with seismic switches that meet the requirements of ASME A17.1 or have trigger levels set to 20% of the acceleration of gravity at the base of the structure and 50% of the acceleration of gravity in other locations. (Commentary: Sec. A.7.16.4. Tier 2: 13.8.6)

C NC N/A U LS-not required; PR-H. SHAFT WALLS: Elevator shaft walls are anchored and reinforced to prevent toppling into the shaft during strong shaking. (Commentary: Sec. A.7.16.5. Tier 2: 13.8.6)

C NC N/A U LS-not required; PR-H. COUNTERWEIGHT RAILS: All counterweight rails and divider beams are sized in accordance with ASME A17.1. (Commentary: Sec. A.7.16.6. Tier 2: 13.8.6)

C NC N/A U LS-not required; PR-H. BRACKETS: The brackets that tie the car rails and the counterweight rail to the structure are sized in accordance with ASME A17.1. (Commentary: Sec. A.7.16.7. Tier 2: 13.8.6)

C NC N/A U LS-not required; PR-H. SPREADER BRACKET: Spreader brackets are not used to resist seismic forces. (Commentary: Sec. A.7.16.8. Tier 2: 13.8.6)

C NC N/A U LS-not required; PR-H. GO-SLOW ELEVATORS: The building has a go-slow elevator system. (Commentary: Sec. A.7.16.9. Tier 2: 13.8.6)

APPENDIX B: LIST OF THE FAILURE MODES ESTIMATED BY FAMIVE

Combined Mechanisms			
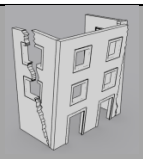 B1: façade overturning with one side wall	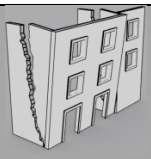 B2: façade overturning with two sides wall	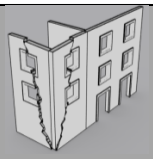 C: overturning with diagonal cracks involving corners	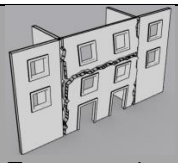 F: overturning constrained by ring beams or ties
In Plane Mechanisms			
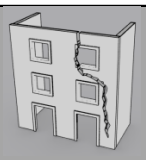 H1: diagonal cracks on piers and spandrels	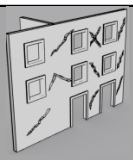 H2 (piers): diagonal and X cracks on piers	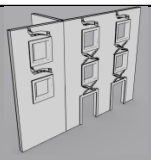 H2 (spandrels): diagonal and X cracks on spandrels	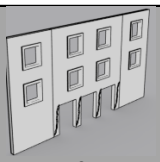 M1: soft storey due to shear	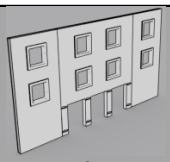 M2: soft storey due to shear due to bending
Out of Plane Mechanisms			
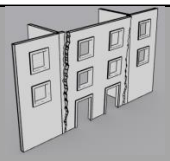 A:façade overturning with vertical cracks	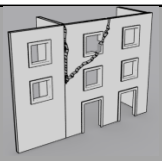 D: façade overturning with diagonal cracks	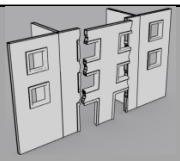 E: façade overturning with cracks at spandrels	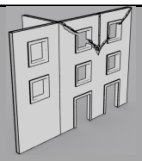 G: façade overturning with diagonal cracks

APPENDIX C: INSPECTION FORM OF FAMIVE

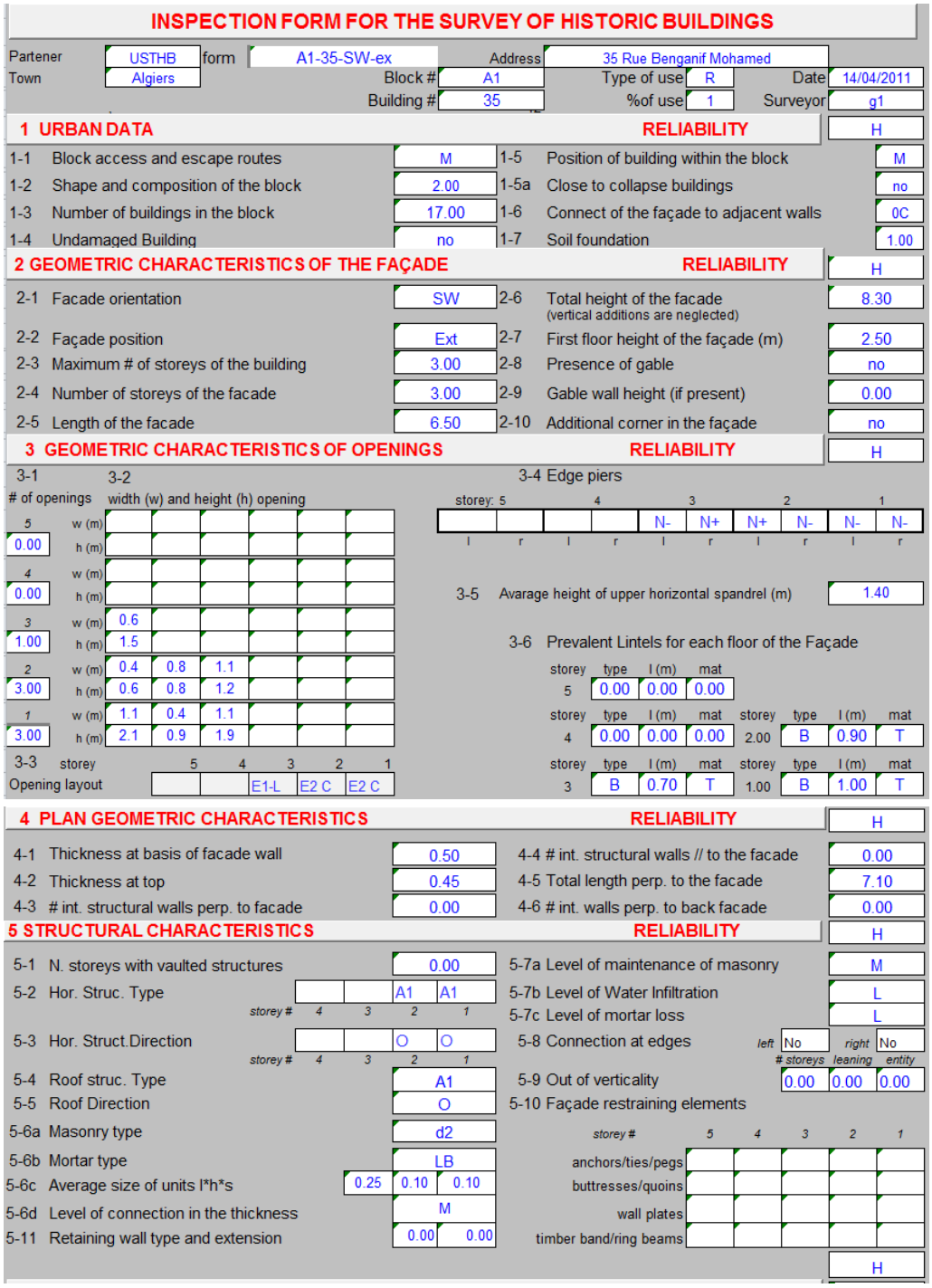

INSPECTION FORM FOR THE SURVEY OF HISTORIC BUILDINGS

Partener: USTHB — form: A1-35-SW-ex — Address: 35 Rue Benganif Mohamed
Town: Algiers — Block #: A1 — Type of use: R — Date: 14/04/2011
Building #: 35 — %of use: 1 — Surveyor: g1

1 URBAN DATA — RELIABILITY: H

1-1	Block access and escape routes	M	1-5	Position of building within the block	M
1-2	Shape and composition of the block	2.00	1-5a	Close to collapse buildings	no
1-3	Number of buildings in the block	17.00	1-6	Connect of the façade to adjacent walls	0C
1-4	Undamaged Building	no	1-7	Soil foundation	1.00

2 GEOMETRIC CHARACTERISTICS OF THE FAÇADE — RELIABILITY: H

2-1	Facade orientation	SW	2-6	Total height of the facade (vertical additions are neglected)	8.30
2-2	Façade position	Ext	2-7	First floor height of the façade (m)	2.50
2-3	Maximum # of storeys of the building	3.00	2-8	Presence of gable	no
2-4	Number of storeys of the facade	3.00	2-9	Gable wall height (if present)	0.00
2-5	Length of the facade	6.50	2-10	Additional corner in the façade	no

3 GEOMETRIC CHARACTERISTICS OF OPENINGS — RELIABILITY: H

3-1 # of openings / 3-2 width (w) and height (h) opening

storey						
5	0.00	w (m)						
		h (m)						
4	0.00	w (m)						
		h (m)						
3	1.00	w (m)	0.6					
		h (m)	1.5					
2	3.00	w (m)	0.4	0.8	1.1			
		h (m)	0.6	0.8	1.2			
1	3.00	w (m)	1.1	0.4	1.1			
		h (m)	2.1	0.9	1.9			

3-3 Opening layout

storey	5	4	3	2	1
			E1-L	E2 C	E2 C

3-4 Edge piers

storey:	5		4		3		2		1	
					N-	N+	N+	N-	N-	N-
	l	r	l	r	l	r	l	r	l	r

3-5 Avarage height of upper horizontal spandrel (m): 1.40

3-6 Prevalent Lintels for each floor of the Façade

storey	type	l (m)	mat	storey	type	l (m)	mat
5	0.00	0.00	0.00				
4	0.00	0.00	0.00	2.00	B	0.90	T
3	B	0.70	T	1.00	B	1.00	T

4 PLAN GEOMETRIC CHARACTERISTICS — RELIABILITY: H

4-1	Thickness at basis of facade wall	0.50	4-4	# int. structural walls // to the facade	0.00
4-2	Thickness at top	0.45	4-5	Total length perp. to the facade	7.10
4-3	# int. structural walls perp. to facade	0.00	4-6	# int. walls perp. to back facade	0.00

5 STRUCTURAL CHARACTERISTICS — RELIABILITY: H

5-1	N. storeys with vaulted structures	0.00	5-7a	Level of maintenance of masonry	M
5-2	Hor. Struc. Type (storey # 4 3 2 1)	A1 A1	5-7b	Level of Water Infiltration	L
			5-7c	Level of mortar loss	L
5-3	Hor. Struct.Direction (storey # 4 3 2 1)	O O	5-8	Connection at edges (left / right)	No / No
5-4	Roof struc. Type	A1	5-9	Out of verticality (# storeys / leaning / entity)	0.00 / 0.00 / 0.00
5-5	Roof Direction	O	5-10	Façade restraining elements	
5-6a	Masonry type	d2			
5-6b	Mortar type	LB			
5-6c	Average size of units l*h*s	0.25 / 0.10 / 0.10			
5-6d	Level of connection in the thickness	M			
5-11	Retaining wall type and extension	0.00 / 0.00			

storey #	5	4	3	2	1
anchors/ties/pegs					
buttresses/quoins					
wall plates					
timber band/ring beams					

H

6 FURTHER VULNERABILITY ELEMENTS — RELIABILITY: 0.00

6-1a # floor (vertical addition): 0.00

6-2 Vertical addition/parapet: L 3.00, h 3.00, t 0.40

6-4 Chimney flue within the façade wall:

6.6 Settlement: element 0.00, entity 0.00, position 0.00

6-5 Roof overhanging: depth 0.00, # struts 0.00

6.9 Porticoes:

	depth	Lp	# pillars
1	0.00	0.00	0.00
2	0.00	0.00	0.00
3	0.00	0.00	0.00
4	0.00	0.00	0.00
5	0.00	0.00	0.00

6-7 Jetty/ Oriel/ balcony/CBU: D 0.45, L 6.50, t 0.50, # storeys 2.00, # struts 15.00

6.8 Sabat: D 0.00, L 0.00, # storeys 0.00

6-10 Vaulted structures

	storey	span	rise	t	type	spring-h	profile	support	supp-w	supp-d
top level										
bottom levels										

7 DAMAGE LEVEL AND MECHANISMS IDENTIFICATIONS — RELIABILITY: H

7-1 Mechanisms identification

Class	Type	D. level
A		
B1		
B2		
C		
D		
E	TOTAL	2
F		
G		
H		
I		
H2		
M		
L		
Other kind of damage or failure not identified		

7-2 Crack pattern description per storey

Horizontal cracks	
Vertical cracks	TOTAL
Corner cracks	
Diagonal cracks	TOTAL
Masonry failure	
roof collapse	
floor collapse	

7-3 Damage extention on the facade (%): 50%

Sketches

Notes

Film number:

Pictures numbers:

APPENDIX D: CORRELATION BETWEEN STRUCTURAL ELEMENTS AND CULTURAL ASSETS

(Ref: D'Ayala D, Novelli V (2010) Deliverable D5 from PERPETUATE project)

A1: Carved or plastically decorated vertical structural assets	 Carved stone columns in the Mosque of Delhi (India).	Piers, Columns and Pillars
B1: Assets connected to vertical structural elements	 Mural paintings in Cappella Sistina in Rome (Italy)	
C1: Assets jutting out from vertical structural elements	 Carved wooden corbels in a historic building in Venice (Italy).	

Figure D-1: Correlation between vertical structural elements and cultural assets

A2: Carved or plastically decorated horizontal structural assets	 Tikse gompa in Ladakh (India).	Spandrels, Lintels, and Beams
B2: Assets connected to horizontal structural elements	 Moulded plasters in a historic building in Rome (Italy)	
C2: Assets jutting out from vertical structural elements	 Gargoyles in Notre Dame cathedral in Paris (France).	

Figure D-2: Correlation between horizontal structural elements and cultural assets

A3: Carved structural arched structural elements	 Septimius Severus arch in Rome (Italy).	Arches
B3: assets connected to the intrados of arched structural elements	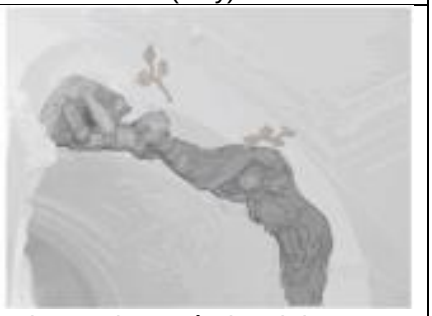 Plasters in Gesù church in Rome (Italy)	
C3: Assets jutting out from arched structural elements	 Meaux Cathedral Gargoyle Lion	

Figure D-3: Correlation between arched structural elements and cultural assets

APPENDIX E: LOGIC TREES

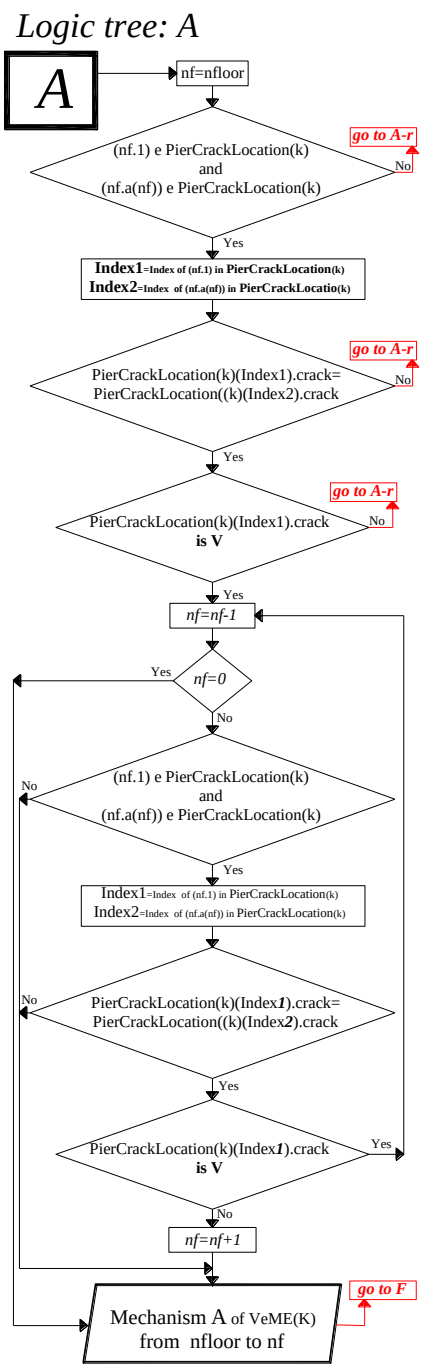

Note: Logic tree A

This LT checks the crack pattern on the VeME in blue in order to verify if the mechanism A is verified.

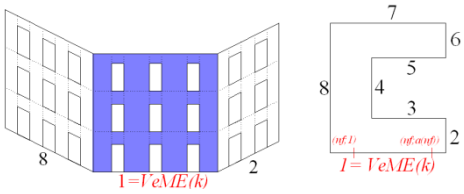

LT checks:

Check if the vertical cracks in red on the yellow piers at the edges of the VeME are occurring at the top floor (condition 1)

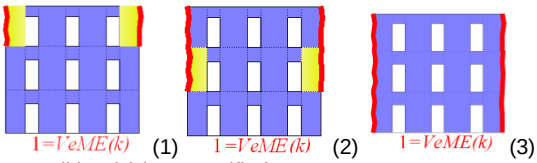

If the condition (1) is not verified go to A-r.

In case the conditions (1) is verified go to lower level and check the number of floors for which the vertical cracks in red on the yellow piers at the edges of the VeME are occurring (condition 2).

If for a generic nf floor, the crack descriptions is not identified the Mechanism A is occurring from the Top Floor to the nf+1 floor (shown a)

If the crack pattern is identified from the top to the bottom floor of the VeME in blue the Mechanism A is occurring and involves the entire façade, (shown b).

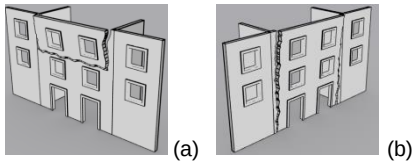

Identified the Mechanism A, go to F

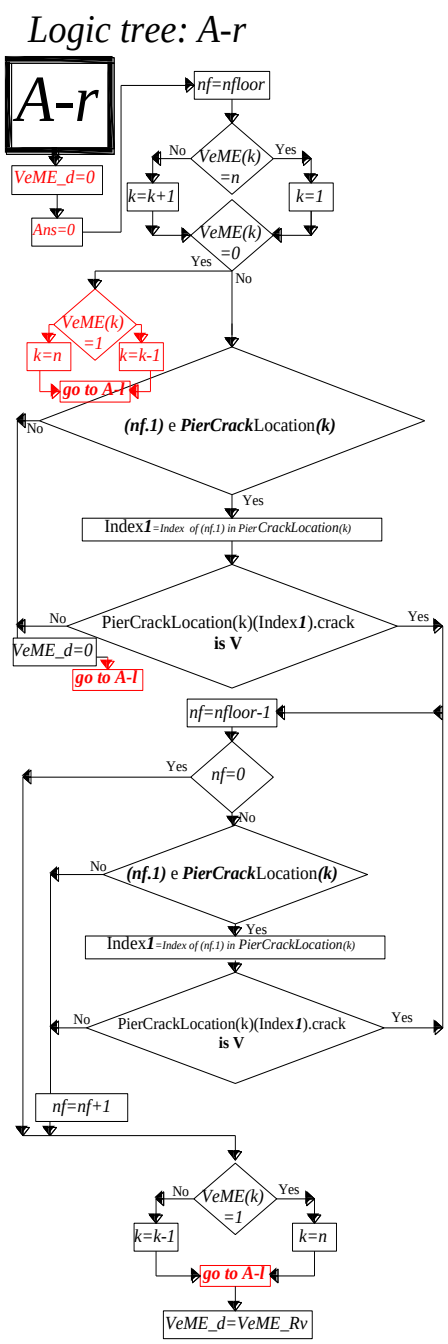

Note: Logic tree A-r

In order to identify the mechanism A2 on the VeME in red, the crack pattern described by the LTs A-r and A-l require to be verified. The LT A-r checks the damage on VeME_R (initially a variable VeME_d which indicates the damaged façade s is set equal to 0, in order to remember that no damage on the façade s has been identified yet).

LT checks:

Check if any data is available for VeME_R. If no data is available for VeME_R, go to A-l.

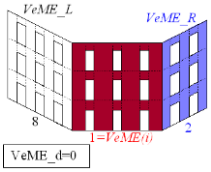

In case data is available for VeME_R, check if the Vertical crack in red on the yellow pier is identified at the top floor of VeME_R, (condition1).

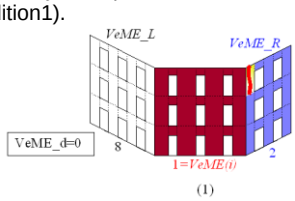

(1)

If the condition (1) is not verified, go to A-l .

In case the condition (1) is verified go to the lower level and check if the Vertical crack in red on the yellow pier of VeME_R is occurring. (condition 2)

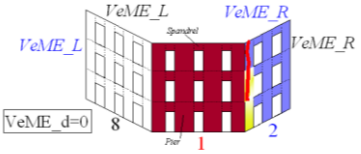

(2)

Such a crack description requires to be checked from the top to the bottom level of VeME_R. In case for a generic nf floor the mentioned crack description is not identified the crack pattern is occurring from the top floor to the nf+1 floor of VeME_R otherwise it is occurring from the top floor to the bottom floor.

Identified the crack pattern on VeME-R (condition 3), set VeME_d=VeME_Rv, (this indicates that vertical crack pattern has been identified on VeME-R) and go to A-l.

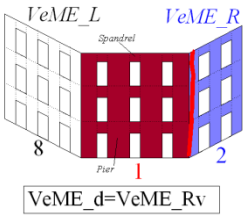

(3)

Logic tree: A-l

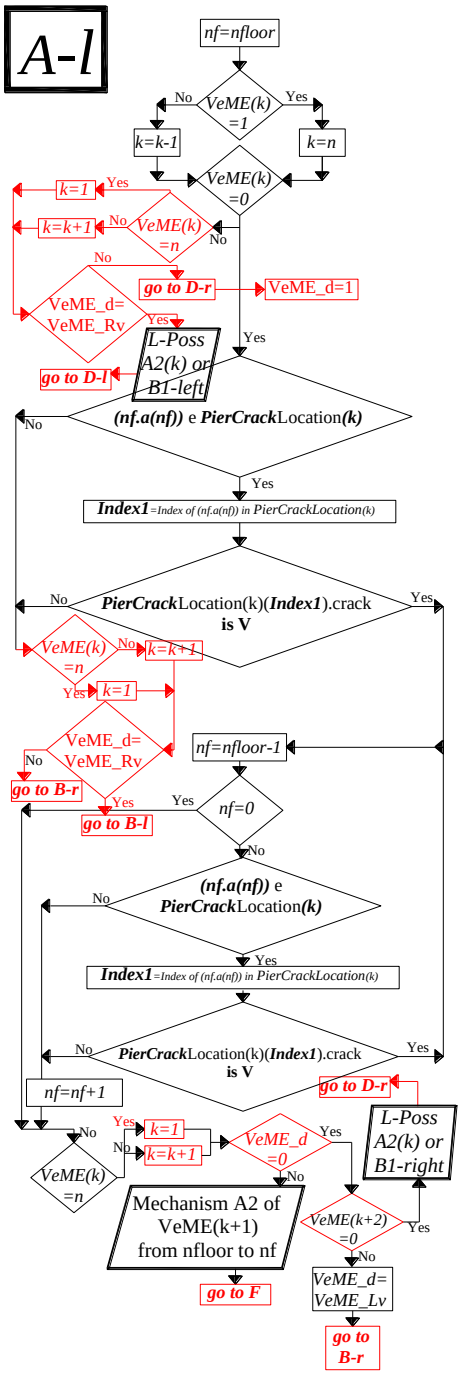

Note: Logic tree A-l

It might be possible to enter in this LT in two conditions: VeME_R is not damaged (VeME_d=0) or VeME_R is damaged according the crack pattern identified by A-r (VeMe_d=VeME_Rv).

The LT A-l verifies the crack pattern on VeME_L in blue.

LT Checks:

Check the data on VeME_L, if no data is available for VeME_L, for (VeME_d=0) go to B-r while for (VeMe_d=VeME_Rv); Mechanism A2 or B1-left with low possibility is identified and Mechanism D-Left requires to be checked on VeME_R.

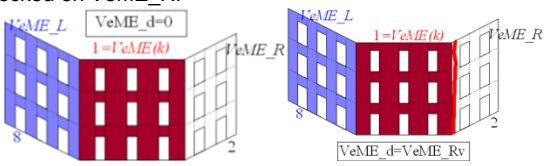

If data is available for VeME_L, check if the vertical crack in red on the yellow pier is identified at the top floor of VeME_L. If this condition (1) is not verified, for (VeME_d=0) go to B-r while for (VeMe_d=VeME_Rv); go to B-l

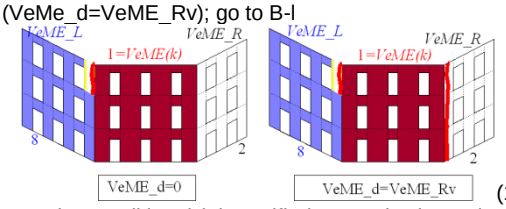

(1)

In case the condition (1) is verified go to the lower level and check if the vertical crack in red on the yellow pier of VeME_L is occurring. (condition 2)

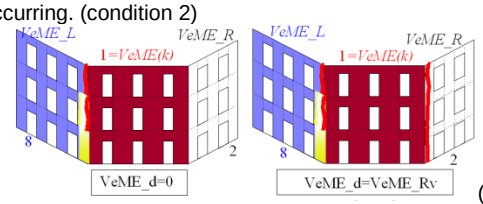

(2)

Such a crack description requires to be checked from the top to the bottom level of VeME_L.

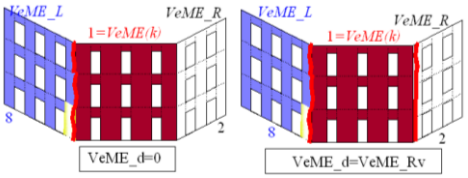

(3)

In case (VeME_d=VeME_Rv) if the condition (2) is verified partial Mechanism A2 is identified on VeME in red (or shown b) while if the condition (3) is verified total Mechanism A2 is identified on VeME in red (or shown a).

In case (VeMe_d=0) and the condition (2) or (3) is verified if for VeME_R no data is available Mechanism A2 or B1-Righr with Low Possibility is identified on VeME in red and the Mechanism D-Right requires to be verified on VeME_L, while for VeME_R data is available, go to B-r and set (VeMe_d=VeME_Lv).

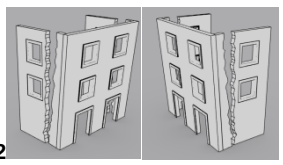

A2

Identified the Mechanism A2, go to F

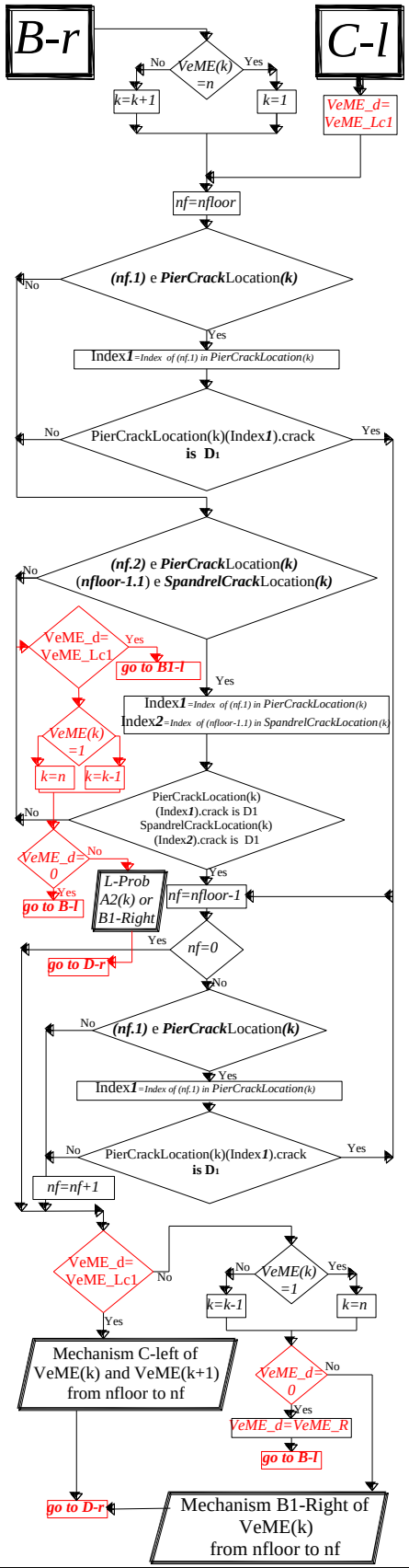

Note: Logic tree B-r (1/2)

This LT is used to identify two similar crack patterns which are checked on different façades. In case this LT has been achieved by passing through B-r, the checks are performed for VeME_R, while if this has been achieved through C-l the checks are performed on VeME in red.

The present note will only discuss about the checks carried out by starting this LT from B-r, indeed for C-l another note will be reported latterly.

The required conditions in order to begin the present LT from B-r are the following: VeME_R and VeME_L are not damaged according the crack identifiable with A-l and A-r (VeME_d=0) or VeME_L is damaged according a vertical crack pattern identified by A-l (VeMe_d=VeME_Lv).

In case (VeME_d=0), the crack pattern described by B-r and B-l require to be verified, in order to identify the mechanism B2 on VeME in red.

In case (VeMe_d=VeME_Lv), the crack pattern described by B-r requires to be verified, in order to identify the mechanism B1-Right on VeME in red. The Logic tree B-r checks the damage on VeME_R.

LT Checks:

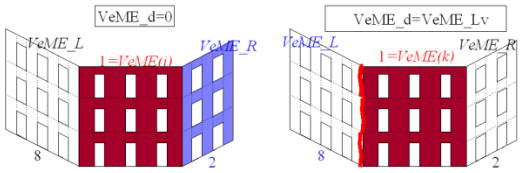

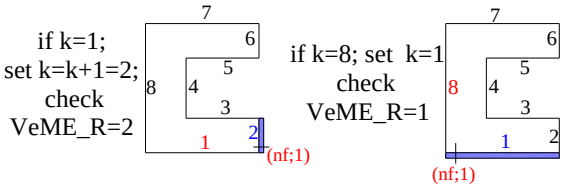

Check if the diagonal crack in red on the yellow pier is identified at the top floor of VeME_R, (condition 1)

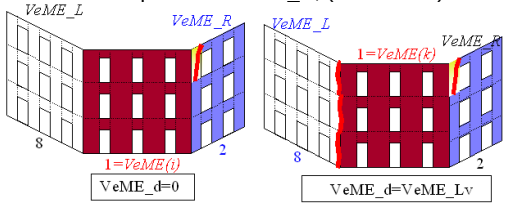

(1)

If the condition (1) is not verified check if the diagonal cracks in blue on the pier and spandrel in yellow of VeME_R are occurring. (condition 2)

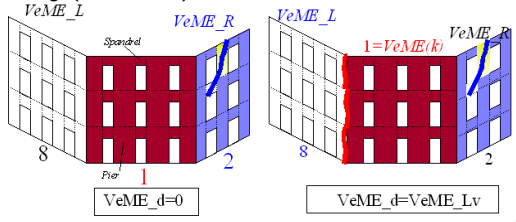

(2)

Note: Logic tree B-r (2/2)

if both conditions are not verified in case (VeME_d=0), go to B-l, in case (VeMe_d=VeME_Lv), Mechanism A2 or B1-Right with low probability is identified on VeME I red and Mechanism D-Right requires to be checked on VeME_L

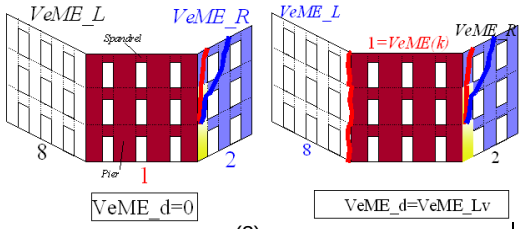

(3)

In case one of the two crack description is verified go to the lower level and check if the diagonal crack in red or blue on the yellow piers of VeME_R is occurring. (condition 3)

The last crack description requires to be checked up to the bottom level of the VeME_R.

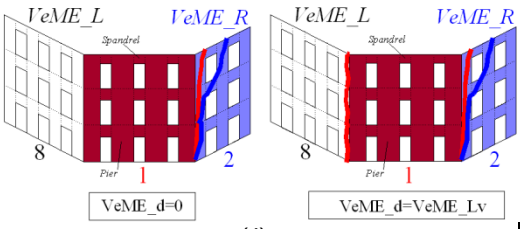

(4)

In case for a generic nf floor the mentioned crack description is not identified the crack pattern is occurring from the top floor to the nf+1 floor of VeME_R otherwise it is occurring from the top floor to the bottom floor.

If for all the floors the crack pattern specified in this logic tree is identified on VeME_R, set VeME_d=VeME_R and go to B-l.

Identified the crack pattern on VeME-R (condition 4),

in case VeME_d=0, set VeME_d=VeME_R, (this indicates that crack pattern described by B-r has been identified on VeME-R) and go to B-l,

while in case VeME_d= VeME_Lv the Mechamism B1-Right is occurring on VeME in red. Identified the Mechanism B1-Right, go to D-r

B1-Right 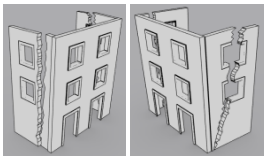

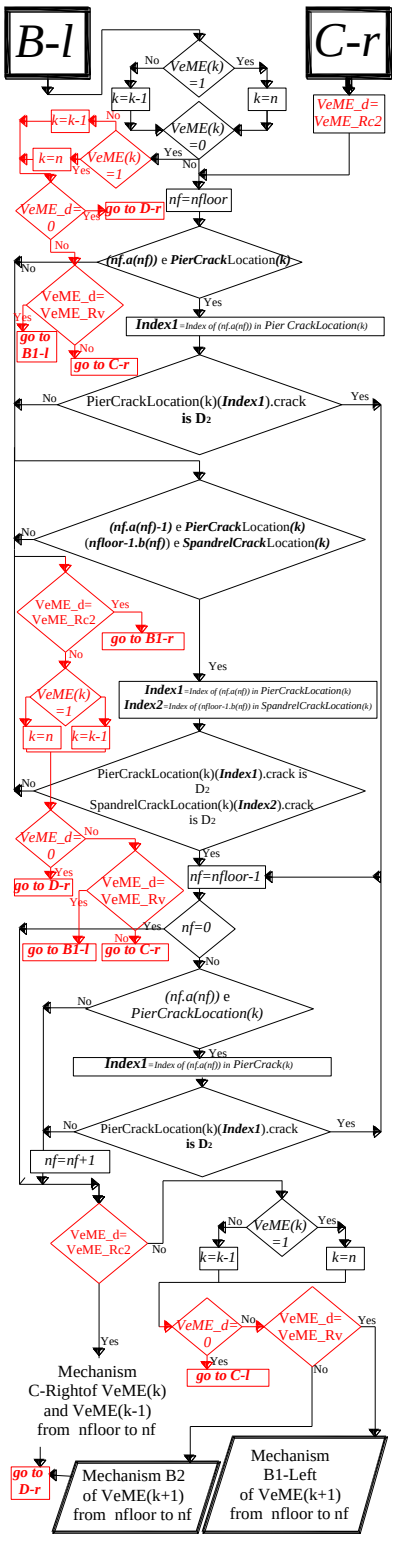

Note: Logic tree B-l (1/2)

This LT is used to identify two similar crack patterns which are checked on different façades. In case this LT has been achieved by passing through B-l, the checks are performed for VeME_L, while if this has been achieved through C-r the checks are performed for VeME in red.

The present note will only discuss about the checks carried out by starting this LT from B-l, indeed for C-r another note will be reported latterly.

The required conditions in order to begin the present LT from B-l are the following: VeME_R and VeME_L are not damaged according to the crack identifiable with A-l (for VeME_L) A-r and B-r (VeME_d=0) or VeME_R is damaged according to the vertical crack pattern identified by A-l (VeME_d=VeME_Rv) or VeME_R is damaged according to the crack pattern identified by B-r (VeME_d=VeME_R)

In case (VeME_d=0), the crack pattern described by B-l requires to be verified, in order to identify the mechanisms with low possibility of occurrence.

In case (VeME_d=VeME_Rv), the crack pattern described by B-l requires to be verified, in order to identify the mechanism B1-Left on VeME in red.

In case (VeME_d=VeME_R), the crack pattern described by B-l requires to be verified, in order to identify the mechanism B2 on VeME in red.

The Logic tree B-r checks the damage on VeME_L.

LT Checks:

if k=1; set k=8 check VeME_L=8

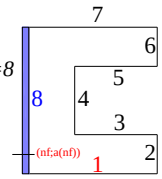

if k=8; set k=k-1=7; check VeME_L=7

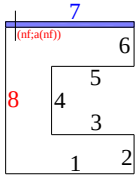

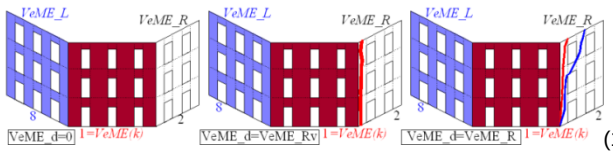

(1)

Check if the diagonal crack in red on the yellow pier is identified at the top floor of VeME_L, (condition 2)

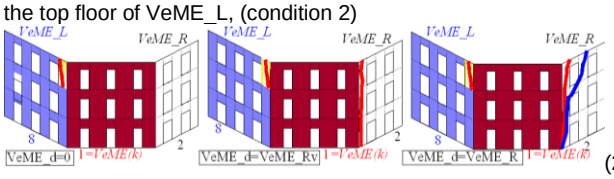

(2)

If the condition (1) is not verified check if the diagonal cracks in blue on the pier and spandrel in yellow of VeME_L are occurring. (condition 3)

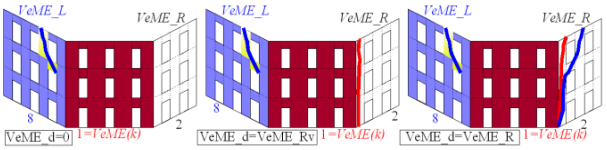

(3)

Note: Logic tree B-l (2/2)
if both conditions are not verified

in case (VeME_d=0), go to D-r,

in case (VeMe_d=VeME_Rv), Mechanism A2 or B1-Left with low probability is identified on VeME in red and Mechanism D-Left requires to be checked on VeME_R,

in case (VeMe_d=VeME_R), go to C-l

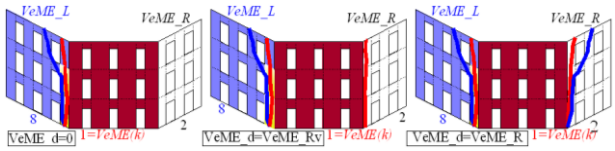

(4)

In case one of the two crack description (in red or blue) is verified, go to the lower level and check if the diagonal crack in red or blue on the yellow piers of VeME_L is occurring. (condition 4)

The last crack description requires to be checked up to the bottom level of the VeME_L.

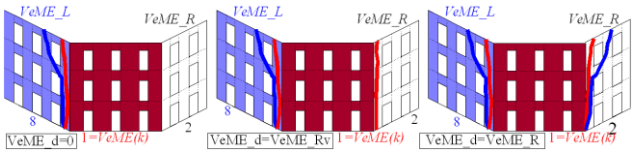

(5)

If the condition (4) is verified partial Mechanisms are identified while if the condition (5) is verified total Mechanisms are identified)
Therefore,

if (VeMe_d= VeMe_Rv), Mechanism B1-Left is occurring on VeME in red

if (VeMe_d= VeMe_R), Mechanism B2 is occurring on VeME in red.

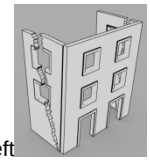
B1-Left
(VeMe_d= VeMe_Rv)

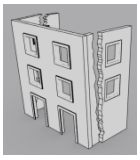

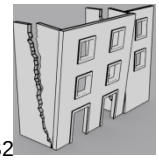
B2
(VeMe_d= VeMe_R)

Identified such mechanisms go to D-r.

In case (VeMe_d=0), go to C-l.

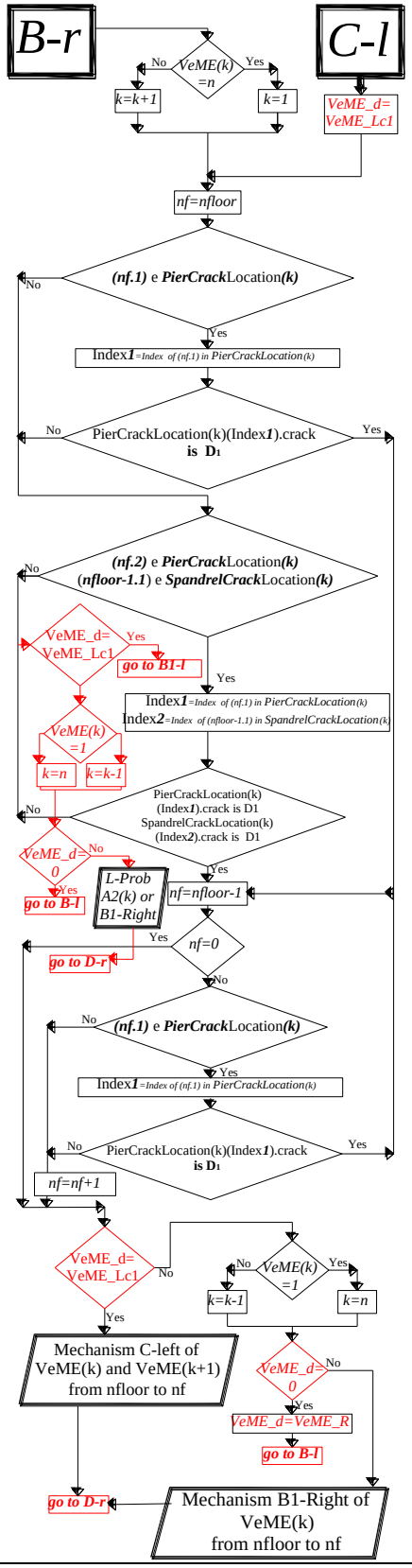

Note: Logic tree C-l

The LT on the left is the same which has been shown for B-r previously; indeed as it has been explained before this LT has been developed in order to identify two similar crack patterns which are checked on different façades.

The present note will discuss about the checks on VeME in red carried out by starting this LT from C-l.

The required condition in order to begin the present LT from C-l is the following: VeME_L is damaged according to the crack pattern identified by B-L and VeME_R is not damaged according to the crack pattern identifiable by A-r and B-r (VeMe_d=VeME_Lc1)

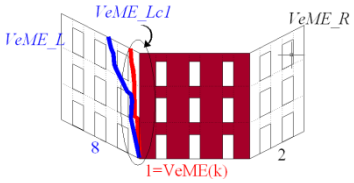

LT Checks:

Check if the diagonal crack in red on the yellow pier is identified at the top floor of VeME (condition 1).

If the condition (1) is not verified check if the diagonal cracks in blue on the pier and spandrel in yellow of VeME are occurring (condition 2)

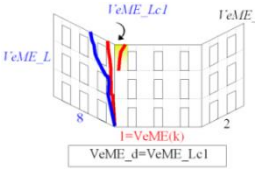

(1)

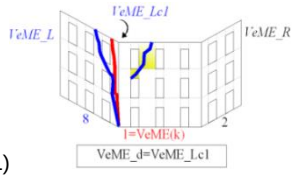

(2)

If both conditions are not verified go to B1-l.

In case one of the two crack descriptions is verified go to the lower level and check if a diagonal crack on the yellow pier of VeME is occurring. (Condition 3). The last crack description requires to be checked up to the bottom level of the VeME.

In case for a generic nf floor the mentioned crack description is not identified the crack pattern is occurring from the top floor to the nf+1 floor of VeME otherwise it is occurring from the top floor to the bottom floor.

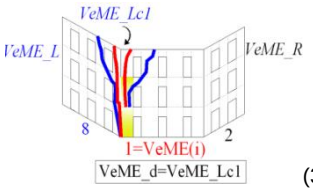

(3)

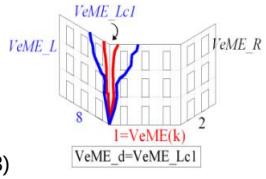

(4)

If the condition (3) is verified partial Mechanism C-Left is identified while if the condition (4) is verified total Mechanism C- Left is identified.

C-Left 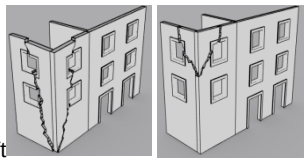

Identified the mechanism go to D-r

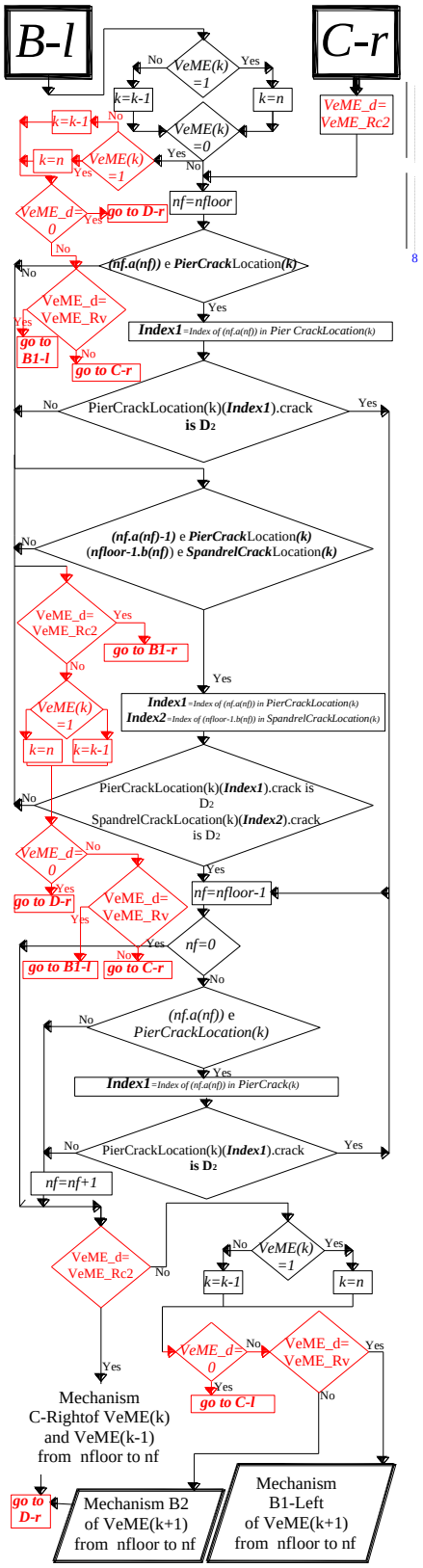

Note: Logic tree C-r

The LT on the left is the same which has been shown for B-l previously; indeed as it has been explained before this LT has been developed in order to identify two similar crack patterns which are checked on different façade.

The present note will discuss about the checks on VeME in red carried out by starting this LT from C-r.

The required condition in order to begin the present LT from C-r is the following: VeME_R is damaged according to the crack pattern identified by B-r and VeME_L is not damaged according to the crack pattern identifiable by A-l and B-l (VeMe_d=VeME_Rc2)

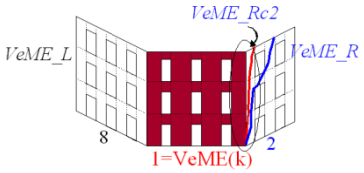

LT Checks:

Check if the diagonal crack in red on the yellow pier is identified at the top floor of VeME (condition 1).

If the condition (1) is not verified check if the diagonal cracks in blue on the pier and spandrel in yellow of VeME are occurring (condition 2)

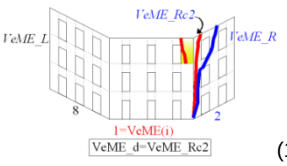

(1)

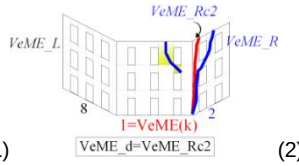

(2)

If both conditions are not verified go to B1-r.

In case one of the two crack descriptions is verified go to the lower level and check if a diagonal crack on the yellow pier of VeME is occurring. (Condition 3). The last crack description requires to be checked up to the bottom level of the VeME.

In case for a generic nf floor the mentioned crack description is not identified the crack pattern is occurring from the top floor to the nf+1 floor of VeME otherwise it is occurring from the top floor to the bottom floor.

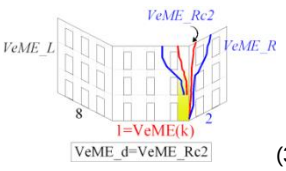

(3)

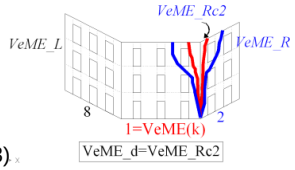

(4)

If the condition (3) is verified partial Mechanism C-Right is identified while if the condition (4) is verified total Mechanism C-Right is identified.

C-Right 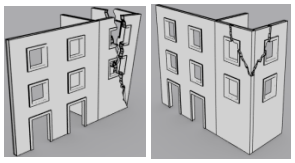

Identified the mechanism go to D-r

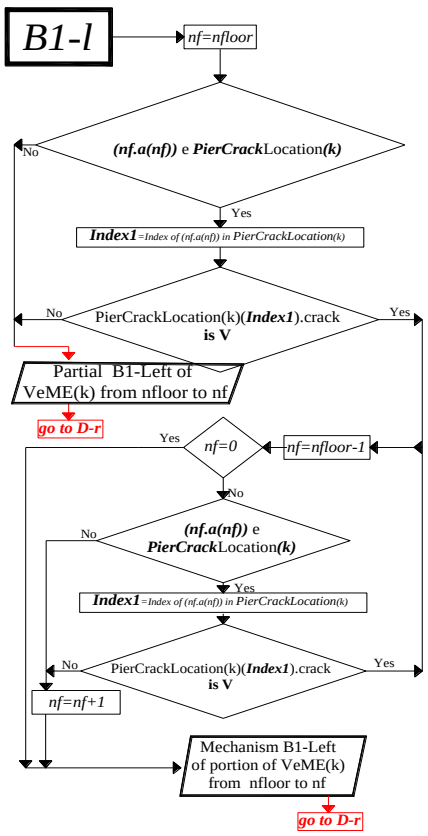

Note: Logic tree B1-l

This LT checks the crack pattern on the VeME in red in order to verify if the mechanism B1-left is occurring, when the blue or red crack patterns on the VeME_L has been already identified by using the B-l.

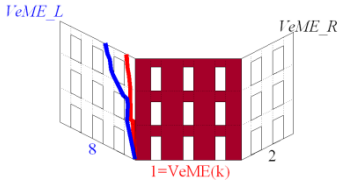

LT checks:

Check if Vertical crack in red on the yellow pier of the VeME is occurring at the top floor (condition 1). If the condition (1) is not verified go to D-r.

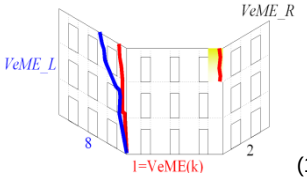

(1)

In case the conditions (1) is verified go to lower level and check if the Vertical crack in red on the yellow piers of the VeME is occurring (condition 2).

Check if the last condition is verified from the top to the bottom level of the VeME (condition 3).

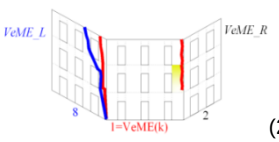

(2)

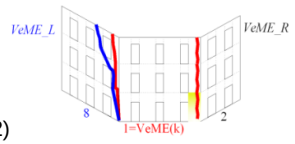

(3)

If the condition 3 is verified the Mechanism B1-left is occurring.

B1-left 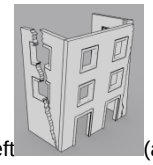 (a) 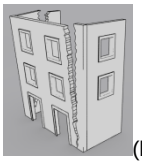 (b)

Identified the Mechanism B1-Left, go to F

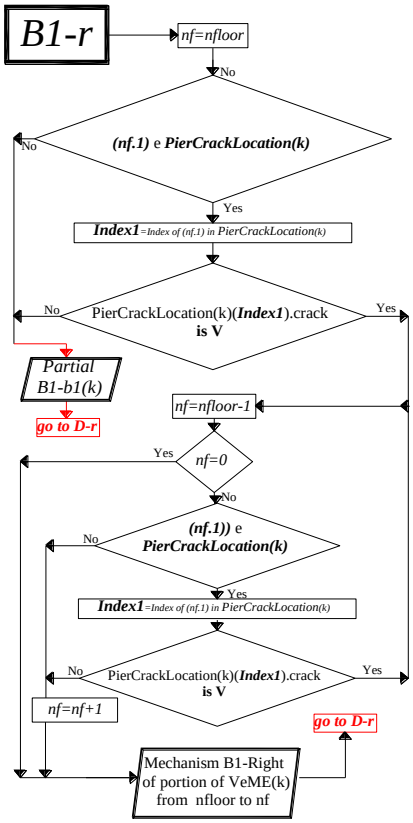

Note: Logic tree B1-r

This LT checks the crack pattern on the VeME in red in order to verify if the mechanism B1-right is occurring, when the blue or red crack patterns on the VeME_R has been already identified by using the B-r.

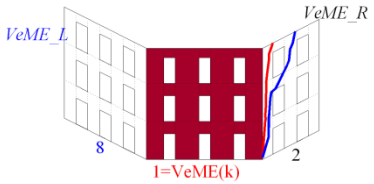

LT checks:

Check if the Vertical crack in red on the yellow pier of the VeME is occurring at the top floor (condition 1)

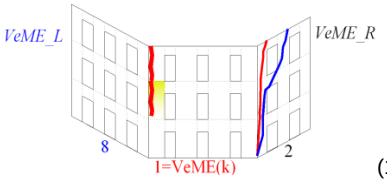

(1)

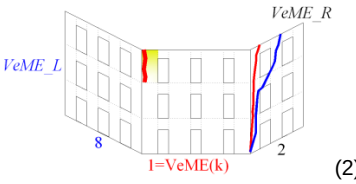

(2)

If the condition (1) is not verified go to D-r.

In case the conditions (1) is verified go to lower level and check if the Vertical crack in red on the yellow piers of the VeME is occurring (condition 2). Check if the last condition is verified from the top to the bottom level of the VeME (condition 3)

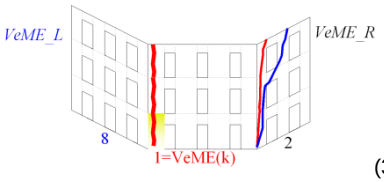

(3)

B1-right 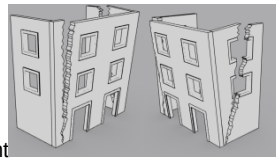

If the condition 3 is occurring the Mechanism B1-Right is verified.

Identified the Mechanism B1-Right, go to F

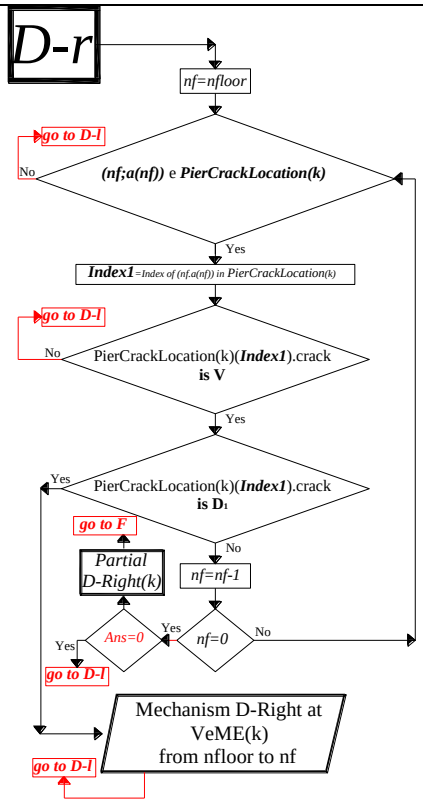

Note: Logic tree D-r

This LT checks the crack pattern on the VeME in blue in order to verify on this façade if the mechanism D-Right is occurring

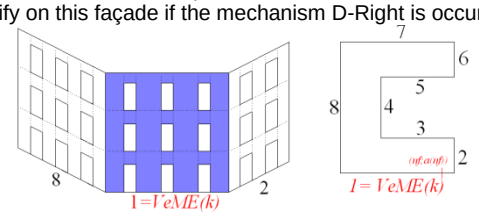

LT checks:

Check if both vertical and diagonal cracks in red on the yellow pier (condition 1) of the VeME are occurring at the top floor. In case this condition is verified, D-Right is identified on VeME, otherwise check the same condition from the lower level to the bottom level of the same façade. In case this crack description is identified at nf floor, verify that all piers from the upper level (nf+1) to the top level have a vertical crack, (condition 2). In case this condition is verified, D-Right has been recognised and go to check D-Left, otherwise go to D-Left

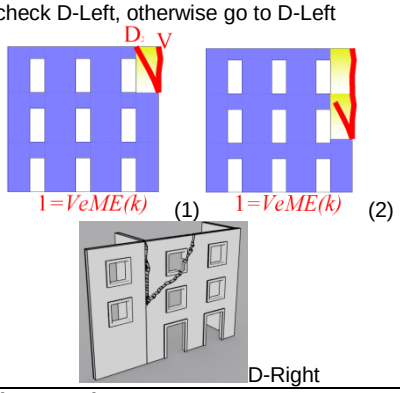

D-Right

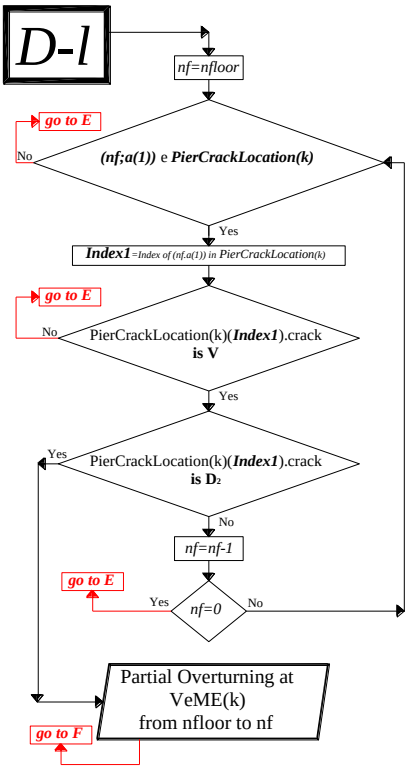

Note: Logic tree D-l

This LT checks the crack pattern on the VeME in blue in order to verify if the mechanism D-Left is verified

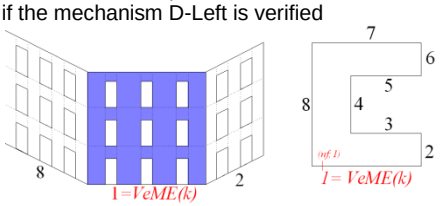

LT checks:

Check if both vertical and diagonal cracks in red on the yellow pier (condition 1) of the VeME are occurring at the top floor. In case this condition is verified, D-Left is identified on VeME, otherwise check the same condition from the lower level to the bottom level of the same façade. In case this crack description is identified at a generic nf floor, verify that all piers from the upper level (nf+1) to the top level have a vertical crack, (condition 2). In case this condition is verified, D-Left is recognised and go to check F, otherwise go to E

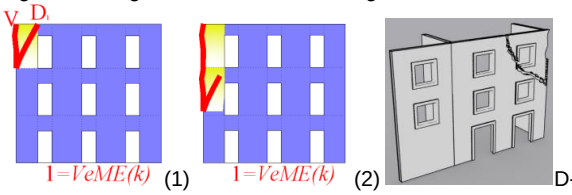

D-Left

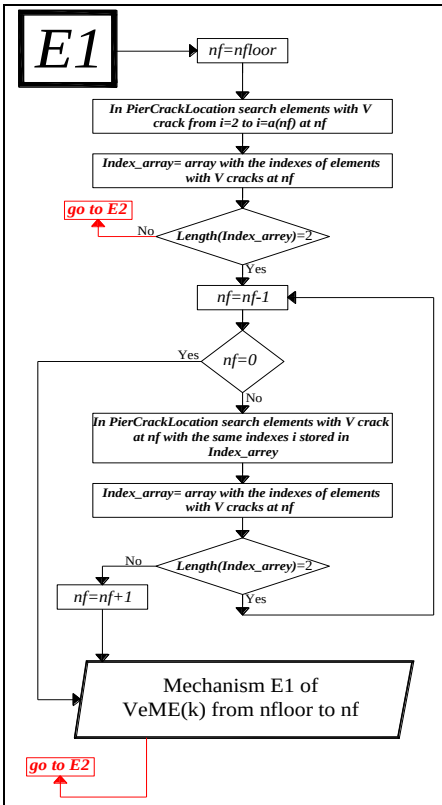

Note: Logic tree E-1

This LT checks the crack pattern on the VeME in blue in order to verify if the mechanism E1 is occurring.

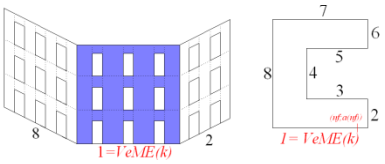

LT checks:

Check if the vertical cracks in red on the yellow piers of the VeME are occurring at the top floor (condition 1). If the condition (1) is not verified go to E2. In case the condition (1) is verified go to lower level and check if the vertical cracks in red are occurring up to the bottom level (condition 2 and 3). In case this is verified E1 is recognised and E2 can be checked, otherwise go directly to E2

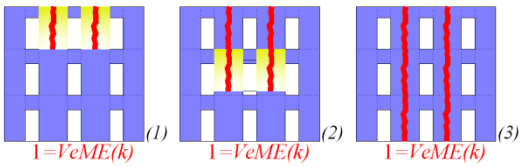

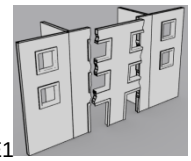

E1

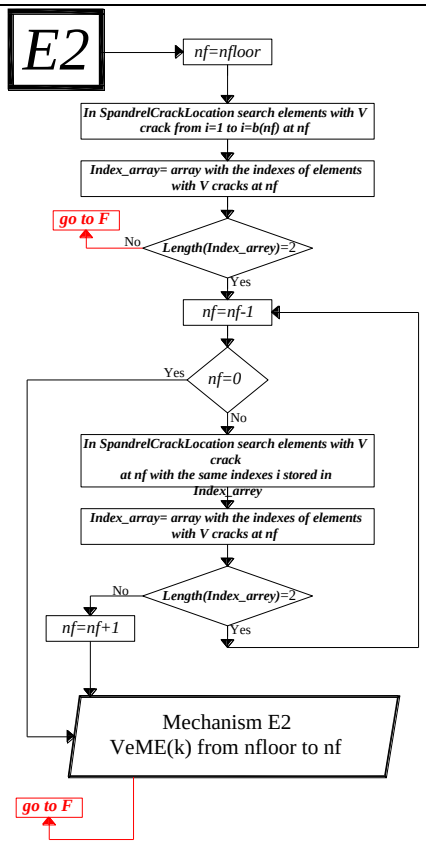

Note: Logic tree E-2

This LT checks the crack pattern on the VeME in blue in order to verify if the mechanism E2 is occurring.

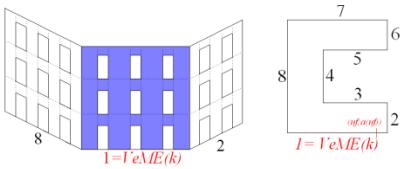

LT checks:

Check if the vertical cracks in red on the yellow spandrels of the VeME are occurring at the top floor (condition 1). If the condition (1) is not verified go to F. In case the condition (1) is verified go to lower level and check if the vertical cracks in red are occurring up to the bottom level (condition 2 and 3). In case this is verified E1 is recognised and F can be checked, otherwise go directly to F

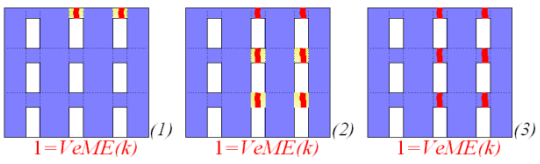

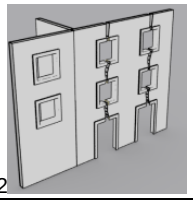

E2

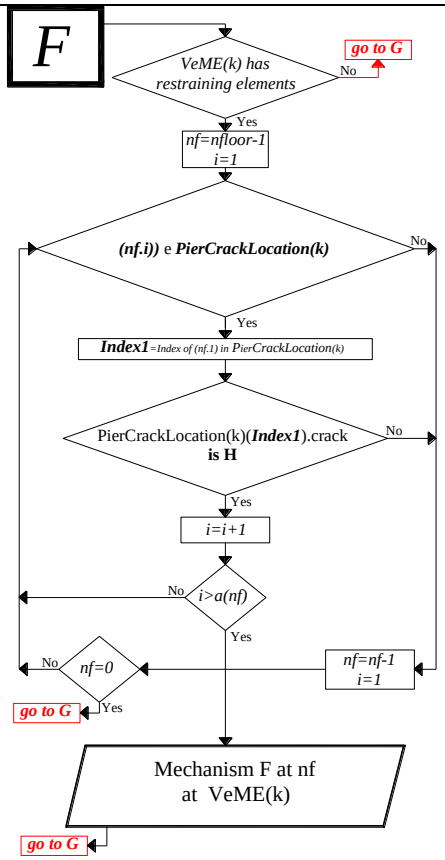

Note: Logic tree F

This LT checks the crack pattern of VeME which describes the Mechanism F, in case there are any restraining elements on the inspected façade.

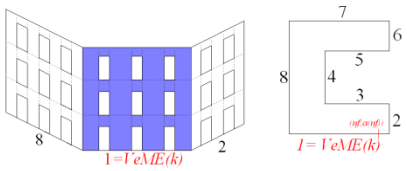

LT checks:

Check from the top floor to the bottom if the first pier on the left has a horizontal crack. In case this occurs for a generic floor check if all the piers at that level have a horizontal crack (Condition 1, 2, 3). If this is verified the Mechanism F is occurring on VeME and mechanism H1 can be checked otherwise go directly to check H1.

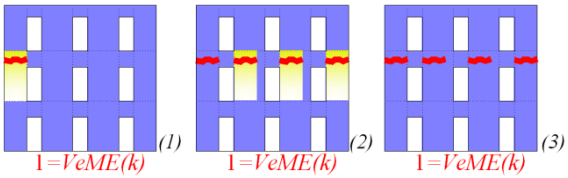

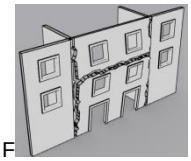

F

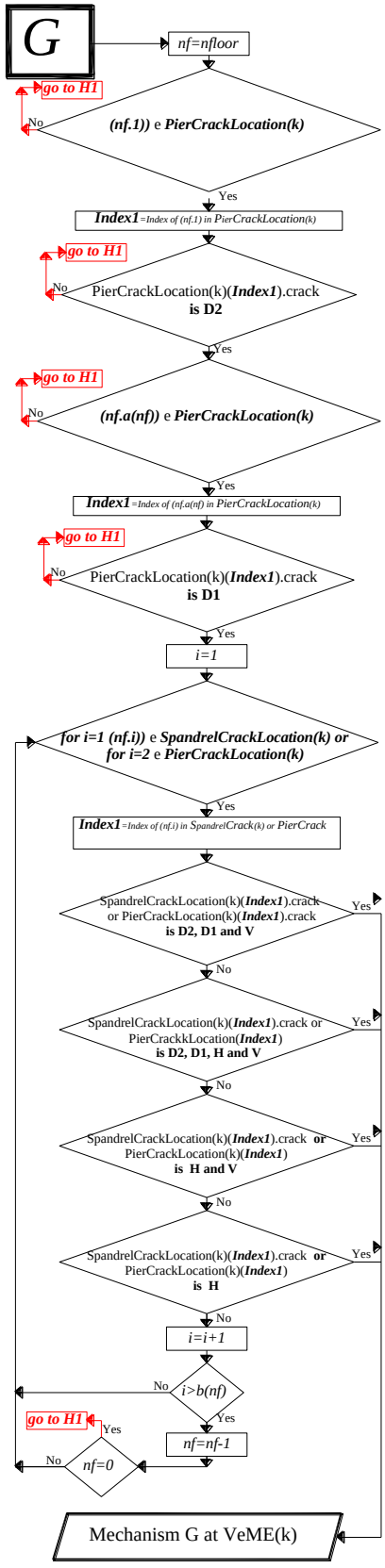

Note: Logic tree G (1/2)

This LT verifies if the crack pattern of VeME which describes the Mechanism G is occurring.

LT checks:

Check if the diagonal crack is occurring on the yellow pier at top floor of the façade , (condition 1).

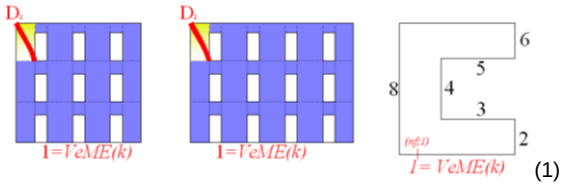

(1)

In case this is not occurring, H1 requires to be checked, otherwise verify if the pier in yellow in (condition 2) has a diagonal crack.

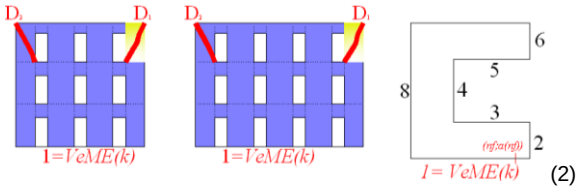

(2)

If this is not verified H1 requires to be checked, otherwise go to the lower level and verify if the crack description (2 diagonal cracks and 1 vertical crack) of the pier or of the spandrel in the condition 3 is occurring

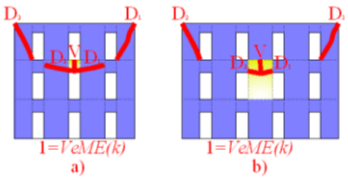

(3)

If this is not verified, check if the crack description (2 diagonal cracks, 1 vertical crack and 1 horizontal crack) of the pier or the spandrel in the condition 4 is occurring, otherwise the mechanism G is identified on the VeME in blue.

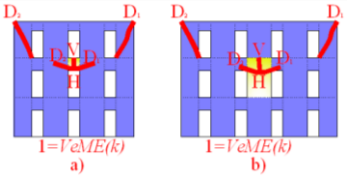

(4)

If this is not verified, check if the crack description (1 vertical crack and 1 horizontal crack) of the pier or the spandrel in the condition 5 is occurring, otherwise the mechanism G is identified on the VeME in blue.

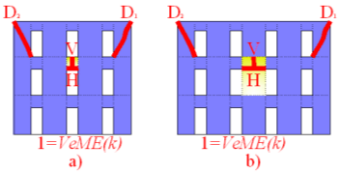

(5)

Note: Logic tree G (2/2)

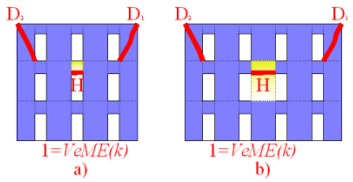

(6)

If this is not verified, check if the crack description (1 horizontal crack) of the pier or the spandrel in the condition 6 is occuring, otherwise the mechanism G is identified on the VeME in blue. If this is not verified, go to check H1.

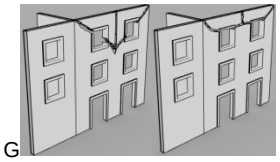

G

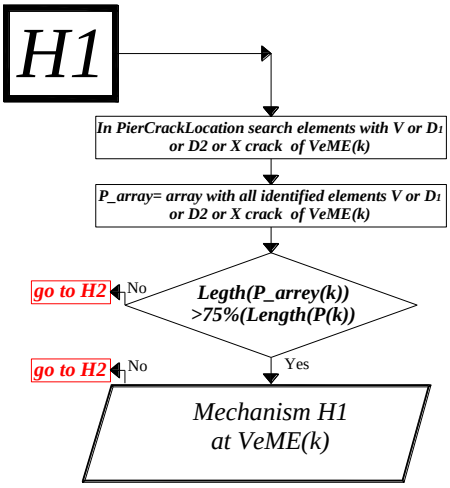

Note: Logic tree H1

This LT verifies if the crack pattern of VeME which describes the Mechanism H1 is occurring.

LT checks:

Check if the 75% of the total number of the piers of the inspected façade has a diagonal or vertical or X cracks. If this is verified the Mechanism H1 has been identified otherwise go to H2

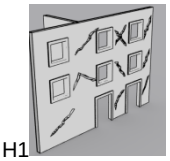

H1

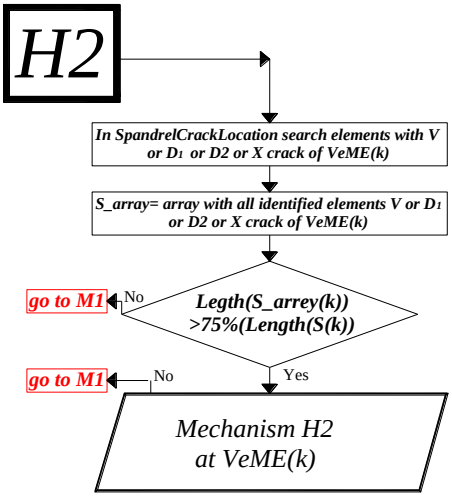

Note: Logic tree H2

This LT verifies if the crack pattern of VeME which describes the Mechanism H2 is occurring.

LT checks:

Check if the 75% of the total number of the spandrel of the façade has a diagonal or vertical or X crack. If this is verified the Mechanism H2 has been identified otherwise go to M1

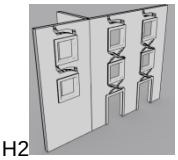

H2

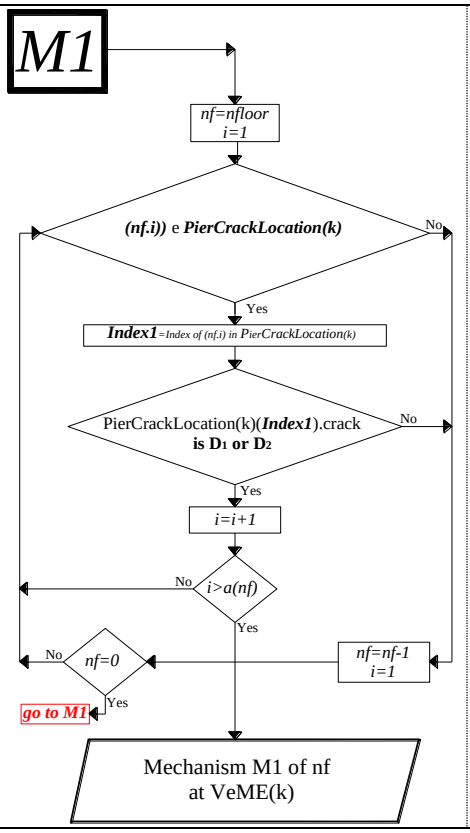

Note: Logic tree M1

This LT verifies if the crack pattern of VeME which describes the Mechanism M1 is occurring.

LT checks:

Check if there is at least a floor in which all the pillars have a diagonal crack. If this is verified M1is occurring, otherwise go to check M2

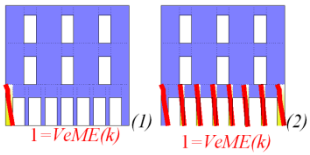

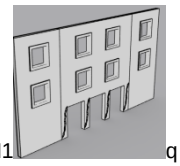

M1 q

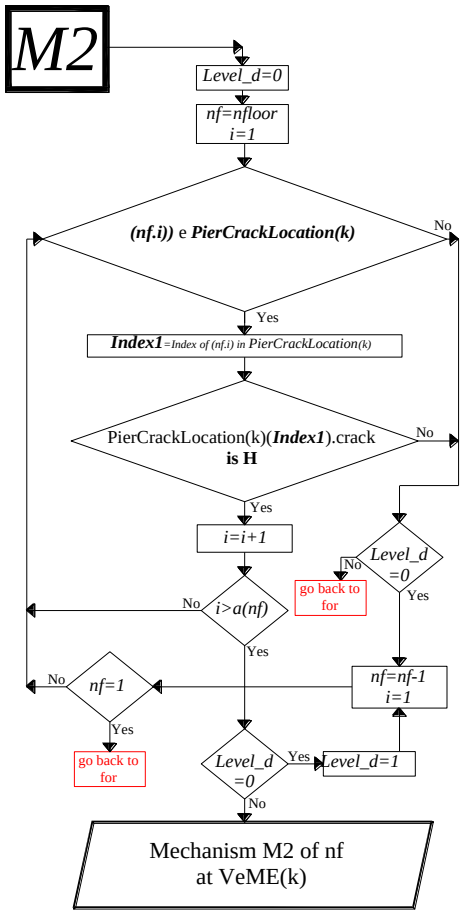

Note: Logic tree M2

This LT verifies if the crack pattern of VeME which describes the Mechanism M2 is occurring.

LT checks:

Check if there is at least a floor in which all the pillars have a horizontal crack at their top and bottom. If this is verified M2 is occurring.

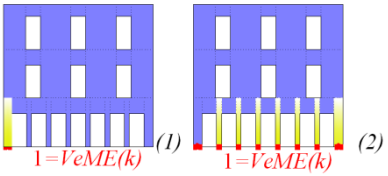

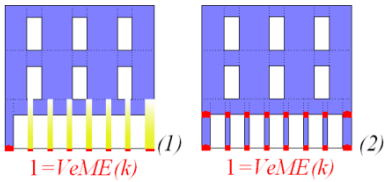

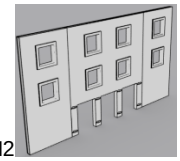
M2

APPENDIX F: LIST OF THE FAILURE MODES ESTIMATED BY LOG-IDEAH

OUT-OF-PLANE Failure Modes	
A1	D-Left or D-Right (left or right corner of the VeME)
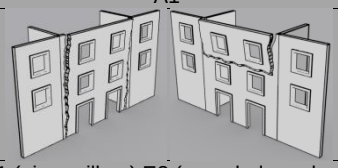	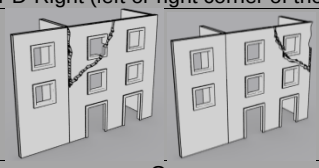
E1 (piers-pillars) E2 (spandrels-arches)	G
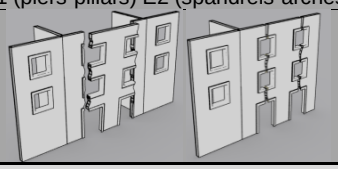	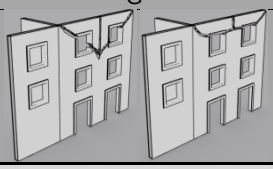
COMBINED Failure modes	
A2 (vertical Cracks)	B2 (diagonal cracks)
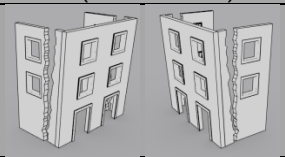	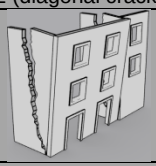
B1-Left	B1-Right
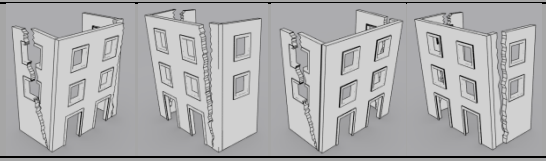	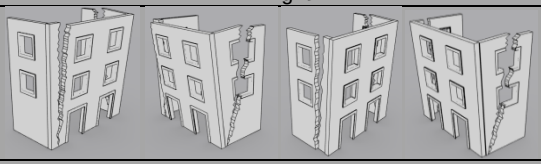
C-Left C-Right (left or right corner of the VeME)	F
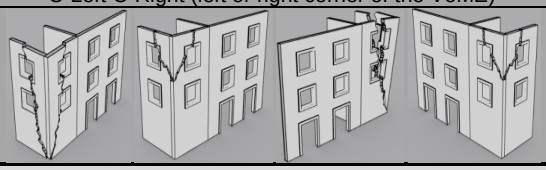	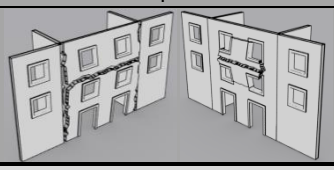
IN-PLANE Failure modes	
H1 (piers); H1 (spandrels) H2 (piers and spandrels)	M1 M2
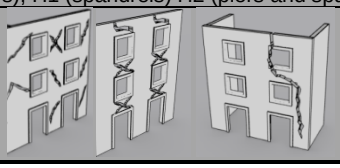	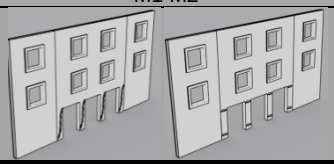

APPENDIX G: PERFORMANCE POINTS AND DERIVATION OF THE DAMAGE PROBABILITY

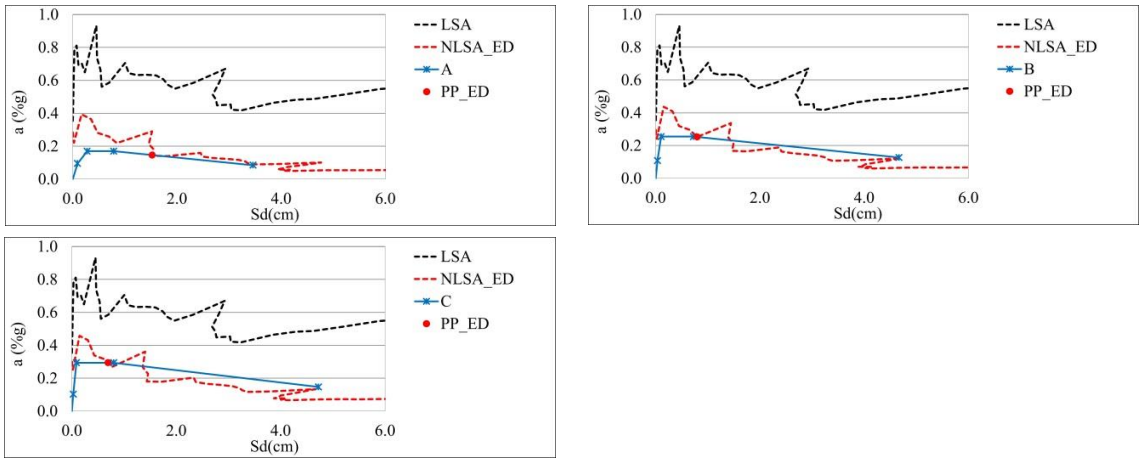

Figure G-1a: Performance points for classes: A, B and C (modified EMS'98).

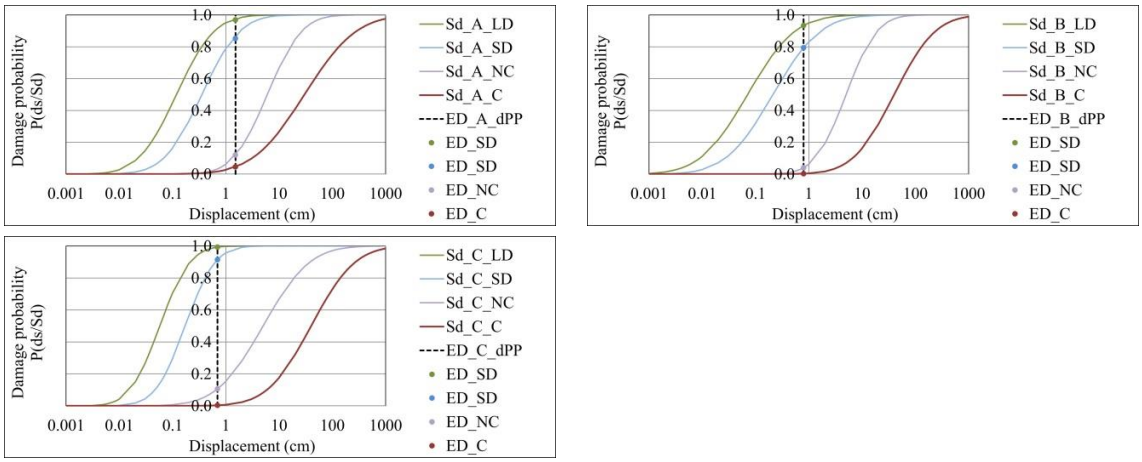

Figure G-1b: Damage probability for classes: A, B and C (modified EMS'98).

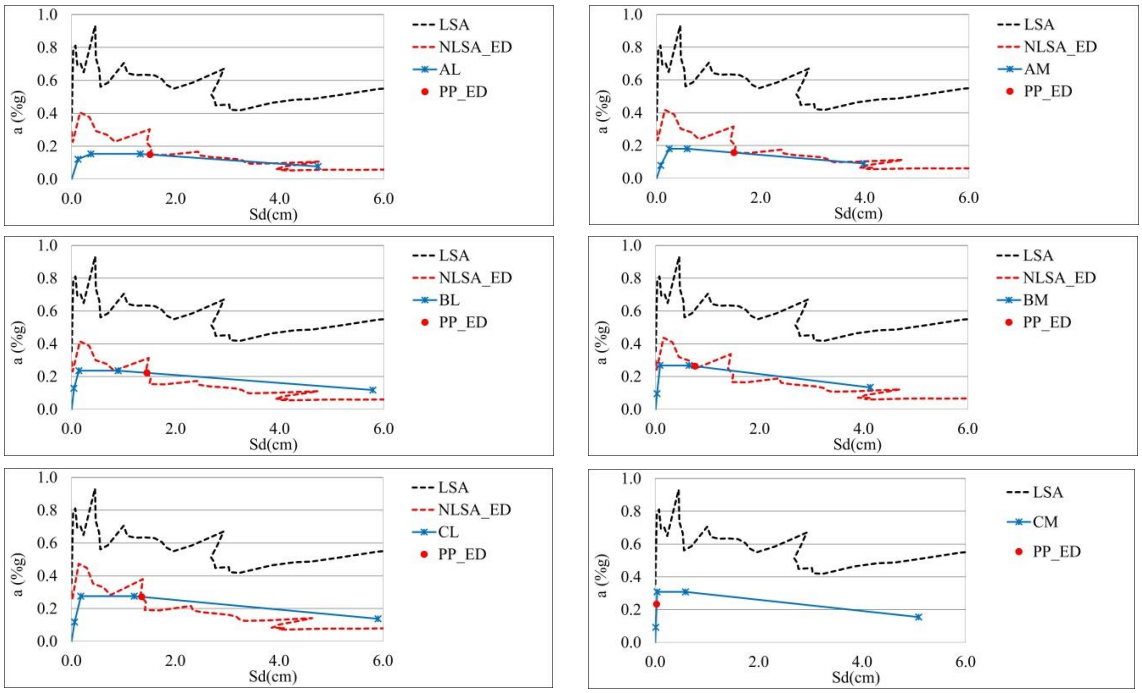

Figure G-2a: : Performance points for classes: AL, AM, BL, BM, CL, and CM (modified EMS'98)

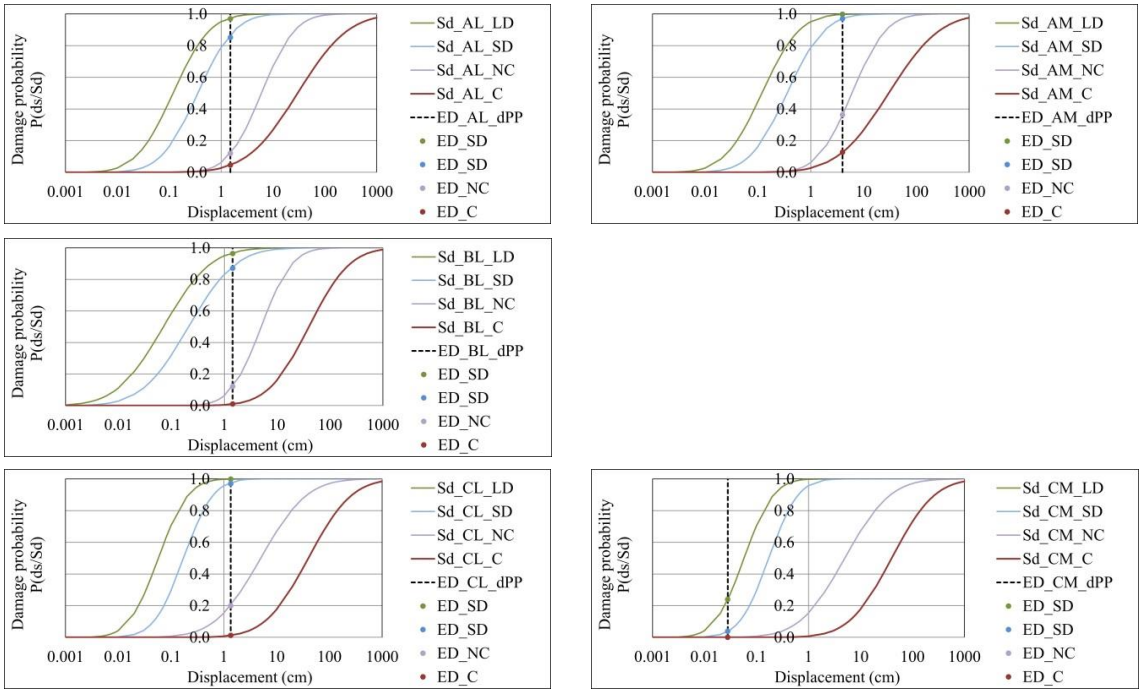

Figure G-2b: Damage probability for classes: AL, AM, BL, BM, CL, and CM (modified EMS'98)

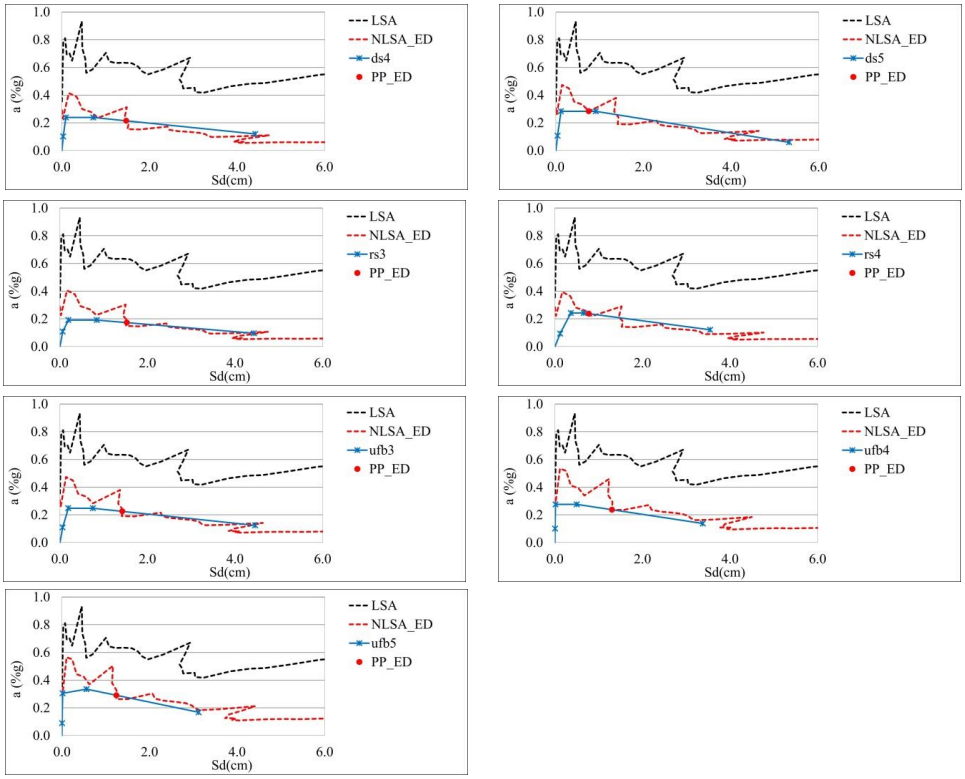

Figure G-3a: Performance points for classes rs3, rs4, ds4, ds5, ufb3, ufb4 and ufb5 (PAGER classification)

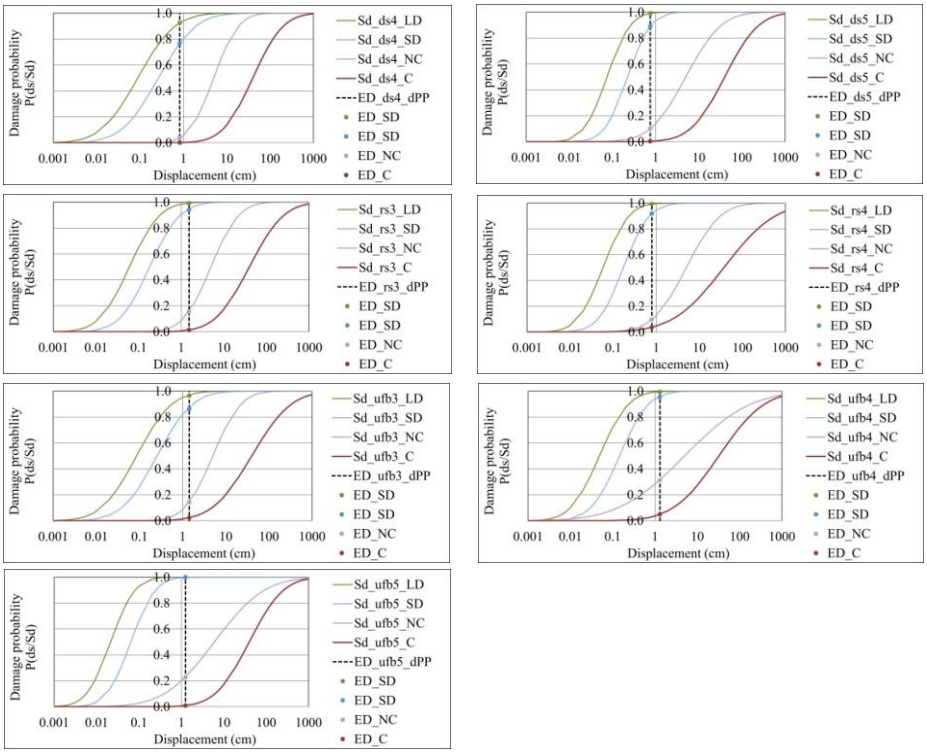

Figure G-3b: Damage probability for classes rs3, rs4, ds4, ds5, ufb3, ufb4 and ufb5 (PAGER classification)

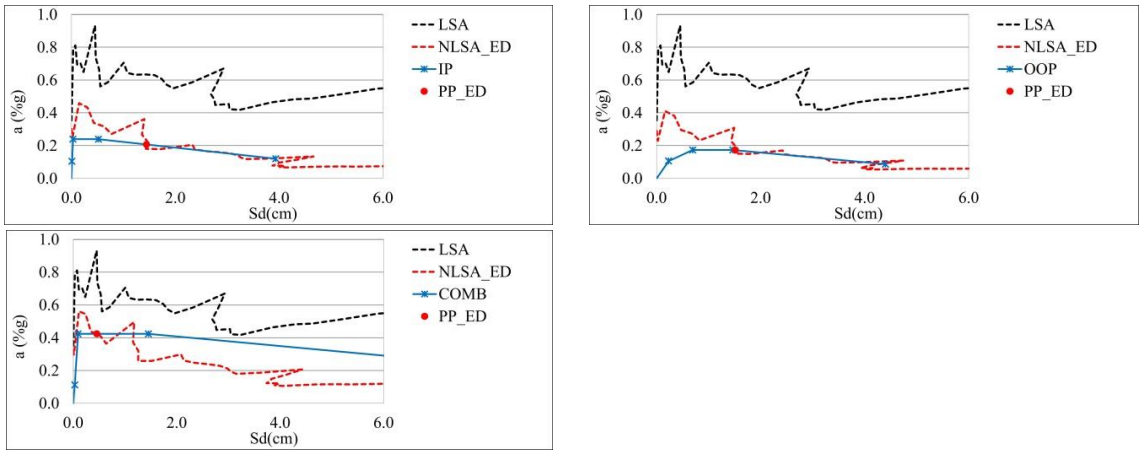

Figure G-4a: Performance points for classes OOP, IP, and COMB

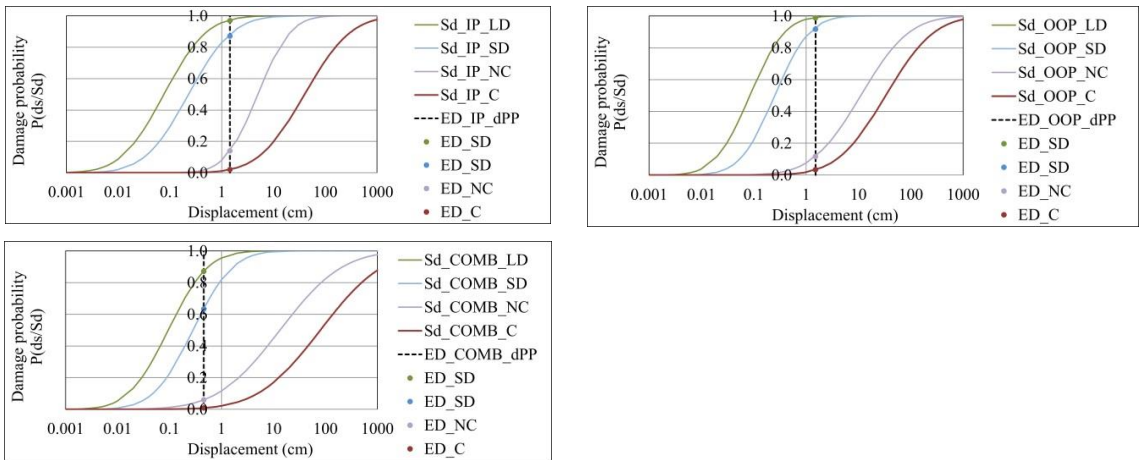

Figure G-4b: Damage probability for classes OOP, IP, and COMB

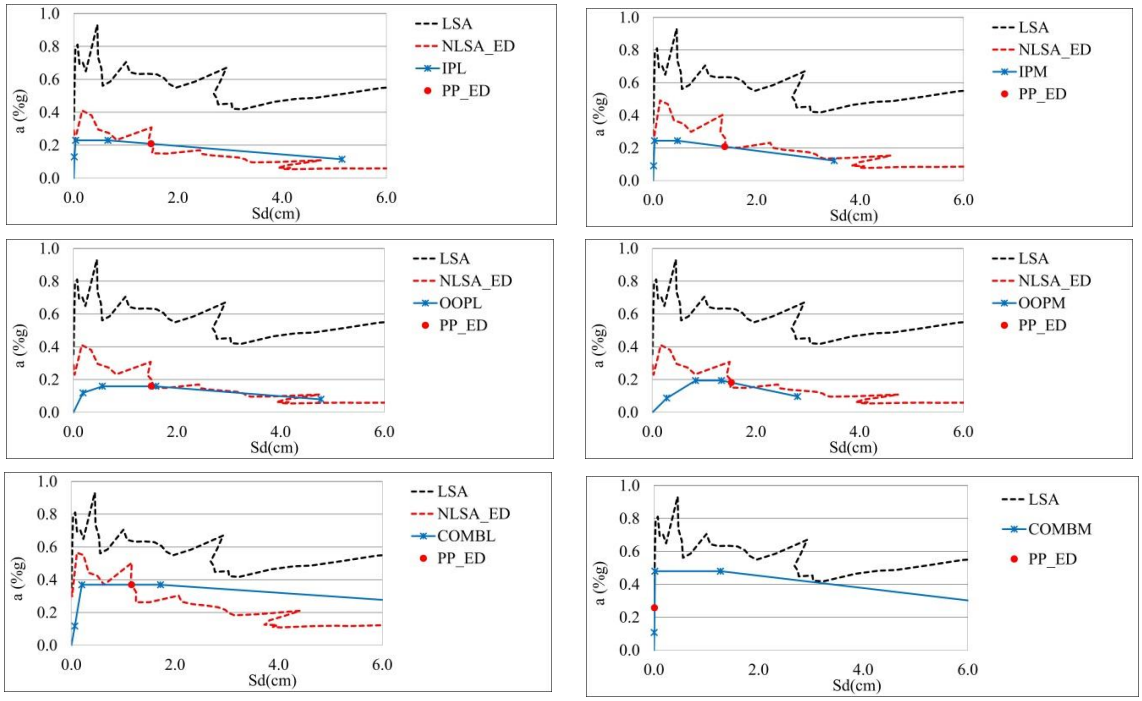

Figure G-5a: Performance points for classes OOPL, OOPM, IPL, IPM, COMBL, and COMBM

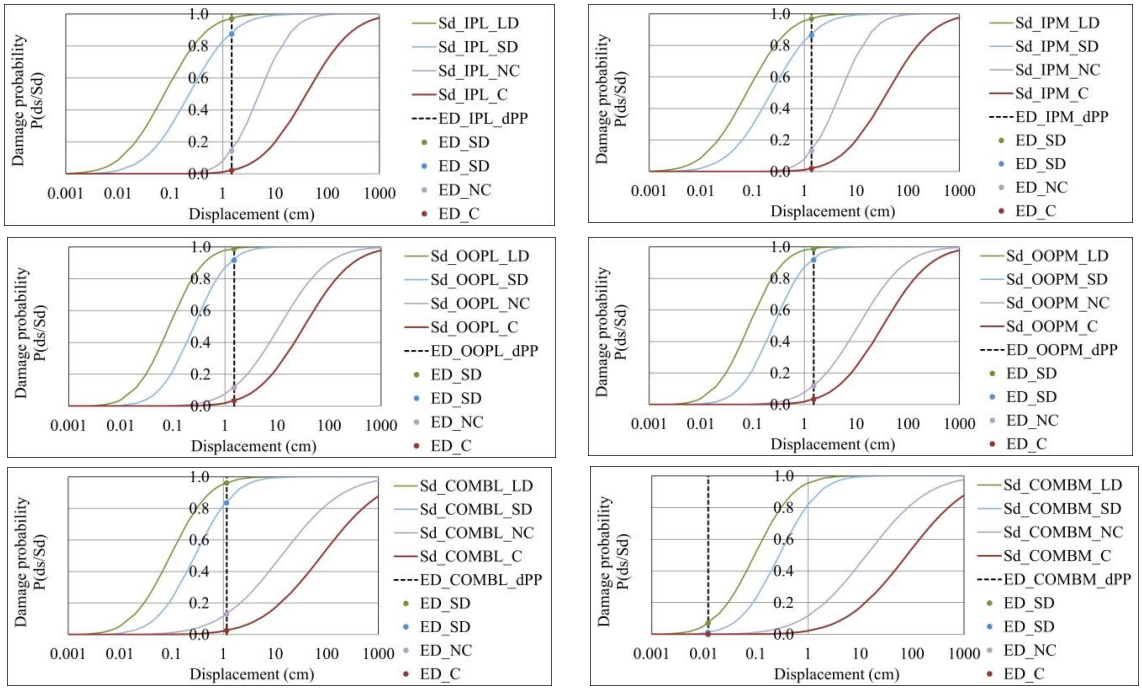

Figure G-5b: Damage probability for classes OOPL, OOPM, IPL, IPM, COMBL, and COMBM

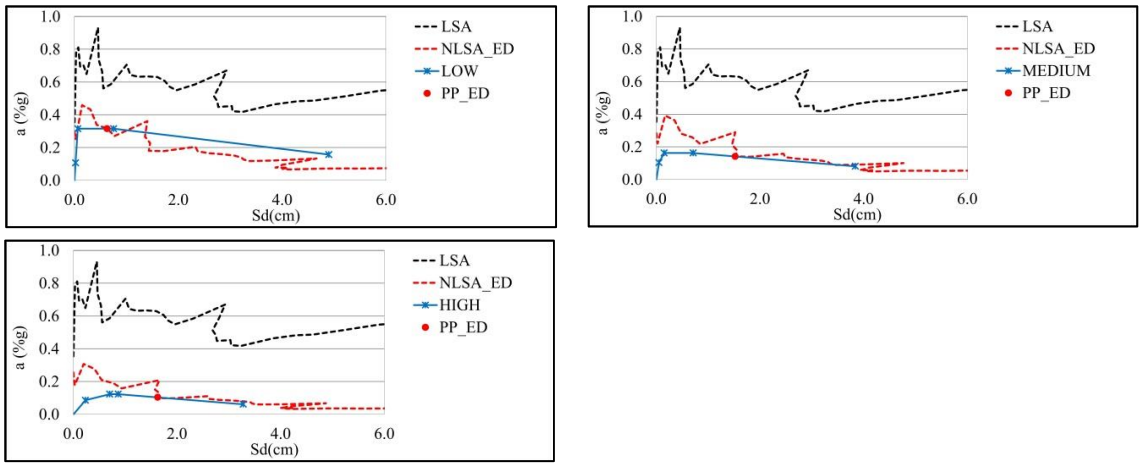

Figure G-6a: Performance points for classes Low, Medium, and High

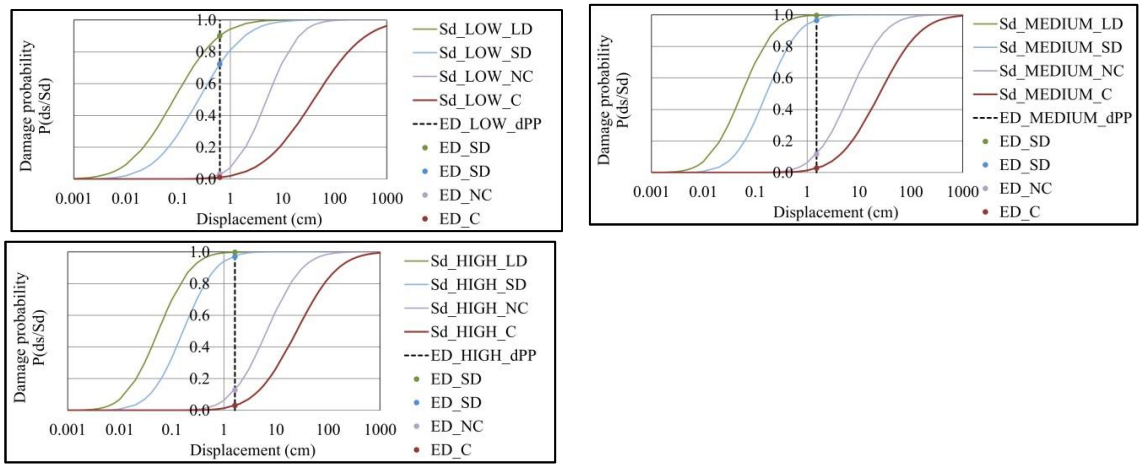

Figure G-6b: Damage probability for classes Low, Medium, and High

APPENDIX H: COMPARISON BETWEEN OBSERVED DAMAGE LEVELS AND ESTIMATED DAMAGE LEVELS

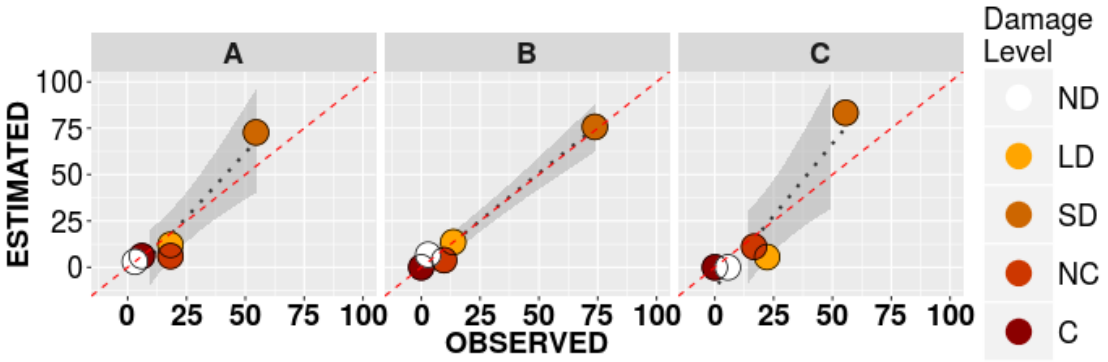

Figure H-1: Correlation between the observed and estimated damage levels computed by ED approach. The percentage of estimated and observed damage levels are reported on the X and Y-axis. The black dashed line is calculated by a local polynomial regression fitting. The red dashed line represents the ideal correlation between the observed and estimated damage levels for classes A, B and C (modified EMS'98).

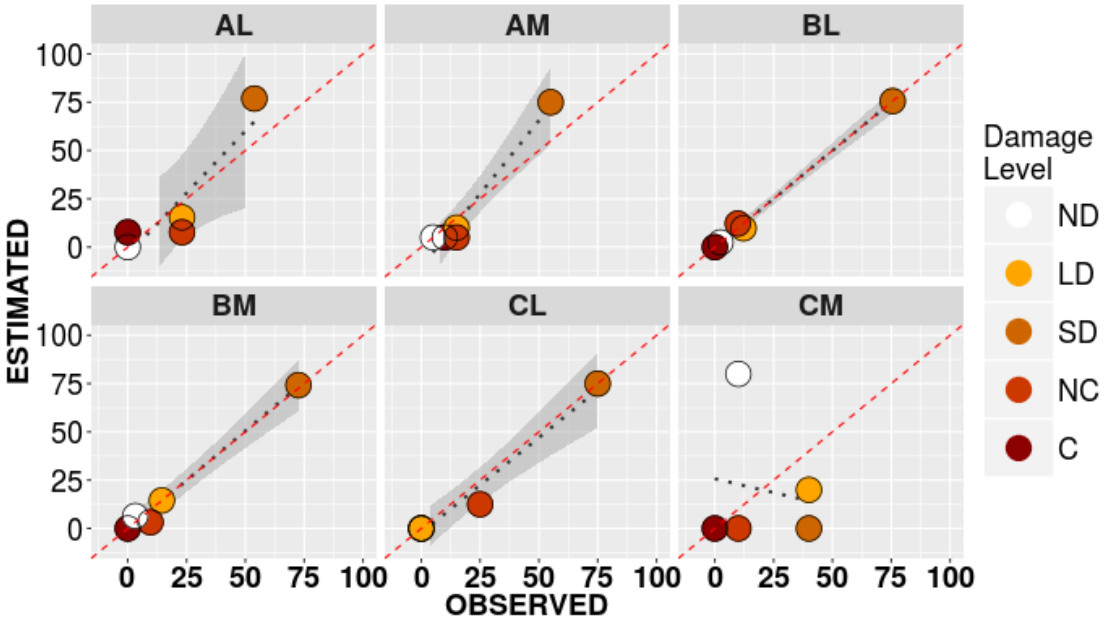

Figure H-2: Correlation between the observed and estimated damage levels computed by ED approach. The percentage of estimated and observed damage levels are reported on the X and Y-axis. The black dashed line is calculated by a local polynomial regression fitting. The red dashed line represents the ideal correlation between the observed and estimated damage levels for classes AL, AM, BL, BM, CL and CM (modified EMS'98).

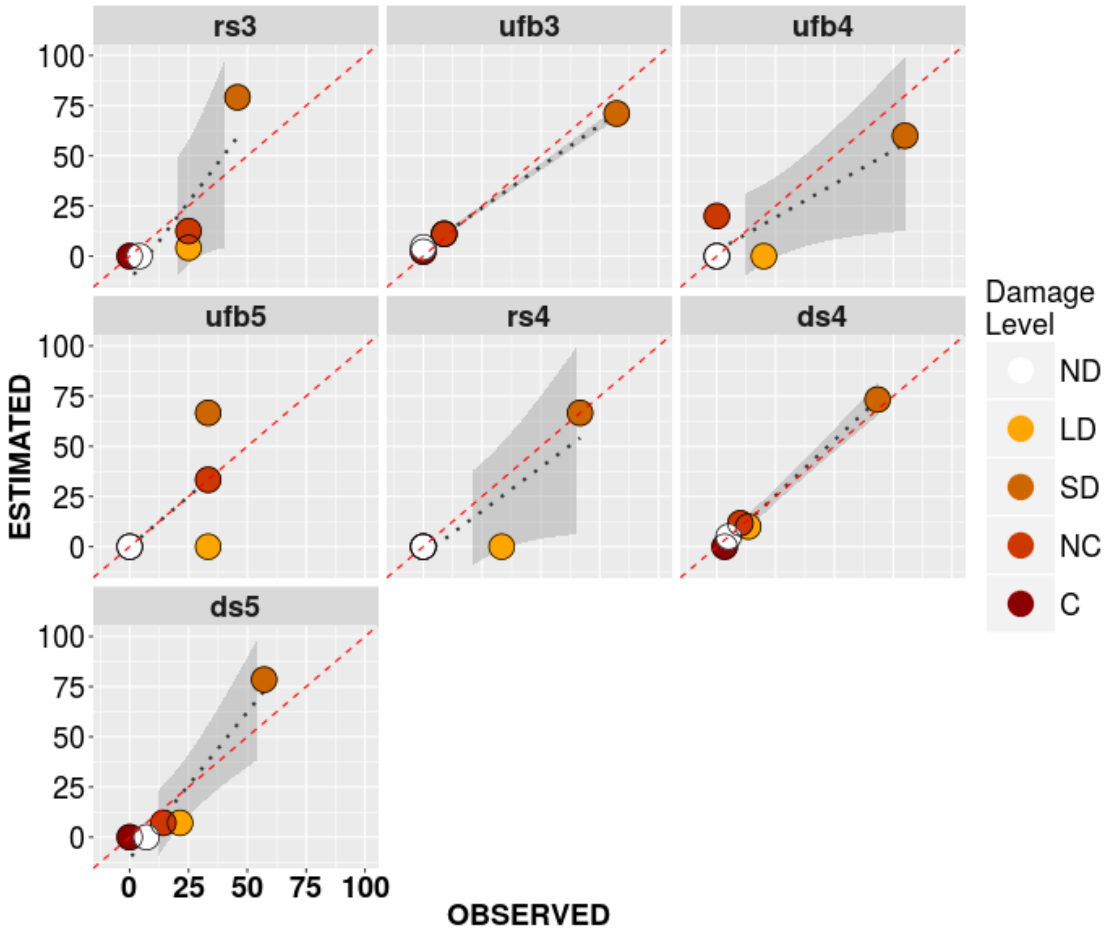

Figure H-3: Correlation between the observed and estimated damage levels computed by ED approach. The percentage of estimated and observed damage levels are reported on the X and Y-axis. The black dashed line is calculated by a local polynomial regression fitting. The red dashed line represents the ideal correlation between the observed and estimated damage levels for classes: rs3, rs4, ds4, ds5, ufb3, ufb4 and ufb5

(PAGER classification)

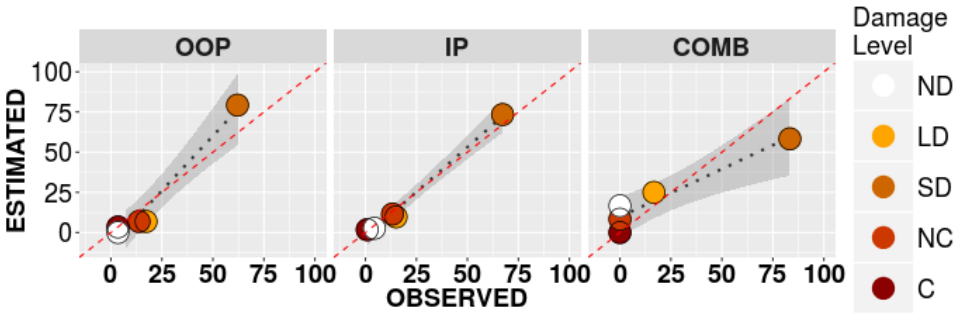

Figure H-4: Correlation between the observed and estimated damage levels computed by ED approach. The percentage of estimated and observed damage levels are reported on the X and Y-axis. The black dashed line is calculated by a local polynomial regression fitting. The red dashed line represents the ideal correlation between the observed and estimated damage levels for classes: OOP, IP, COMB (PAGER classification)

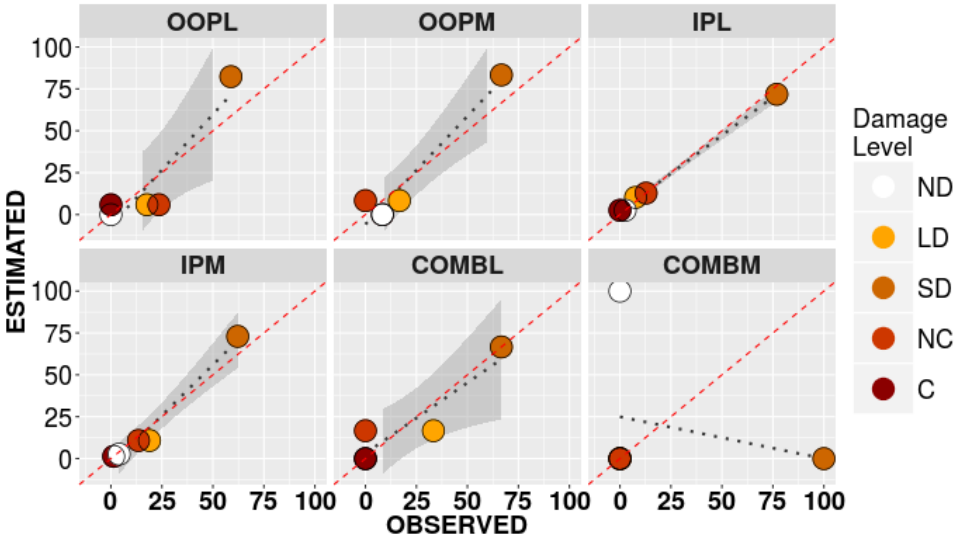

Figure H-5: Correlation between the observed and estimated damage levels computed by ED approach. The percentage of estimated and observed damage levels are reported on the X and Y-axis. The black dashed line is calculated by a local polynomial regression fitting. The red dashed line represents the ideal correlation between the observed and estimated damage levels for classes: OOPL, OOPM, IPL, IPM, IPM, COMBL, and COMBM

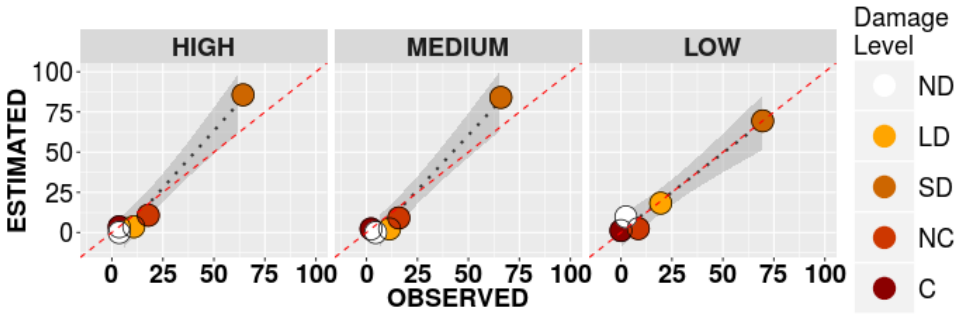

Figure H-6: Correlation between the observed and estimated damage levels computed by ED approach. The percentage of estimated and observed damage levels are reported on the X and Y-axis. The black dashed line is calculated by a local polynomial regression fitting. The red dashed line represents the ideal correlation between the observed and estimated damage levels for classes: HIGH, MEDIUM and LOW VULNERABILITY,.

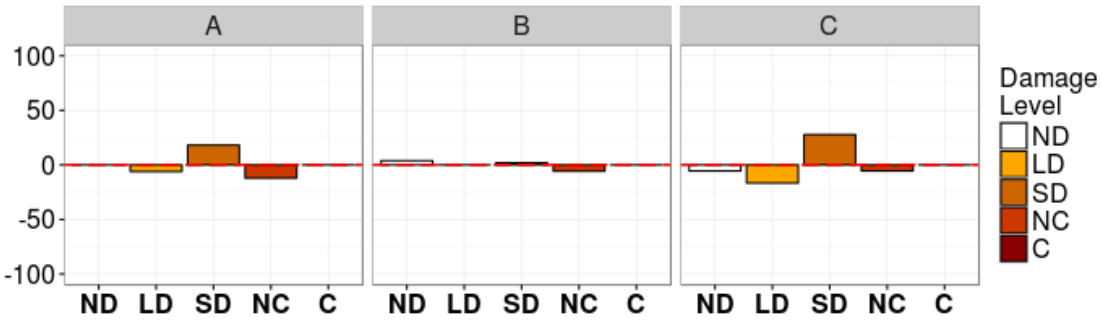

Figure H-7: Difference in terms of percentage between observed and estimated damage levels computed by ED, for classes A, B, and C

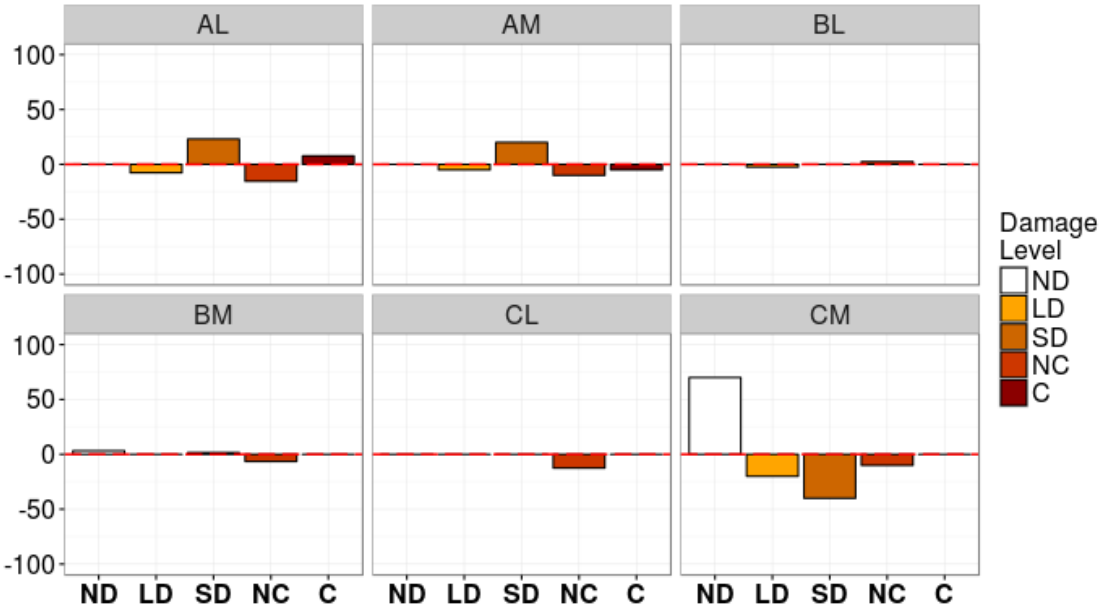

Figure H-8: Difference in terms of percentage between observed and estimated damage levels computed by ED, for classes AL, AM, BL, BM, CL and CM

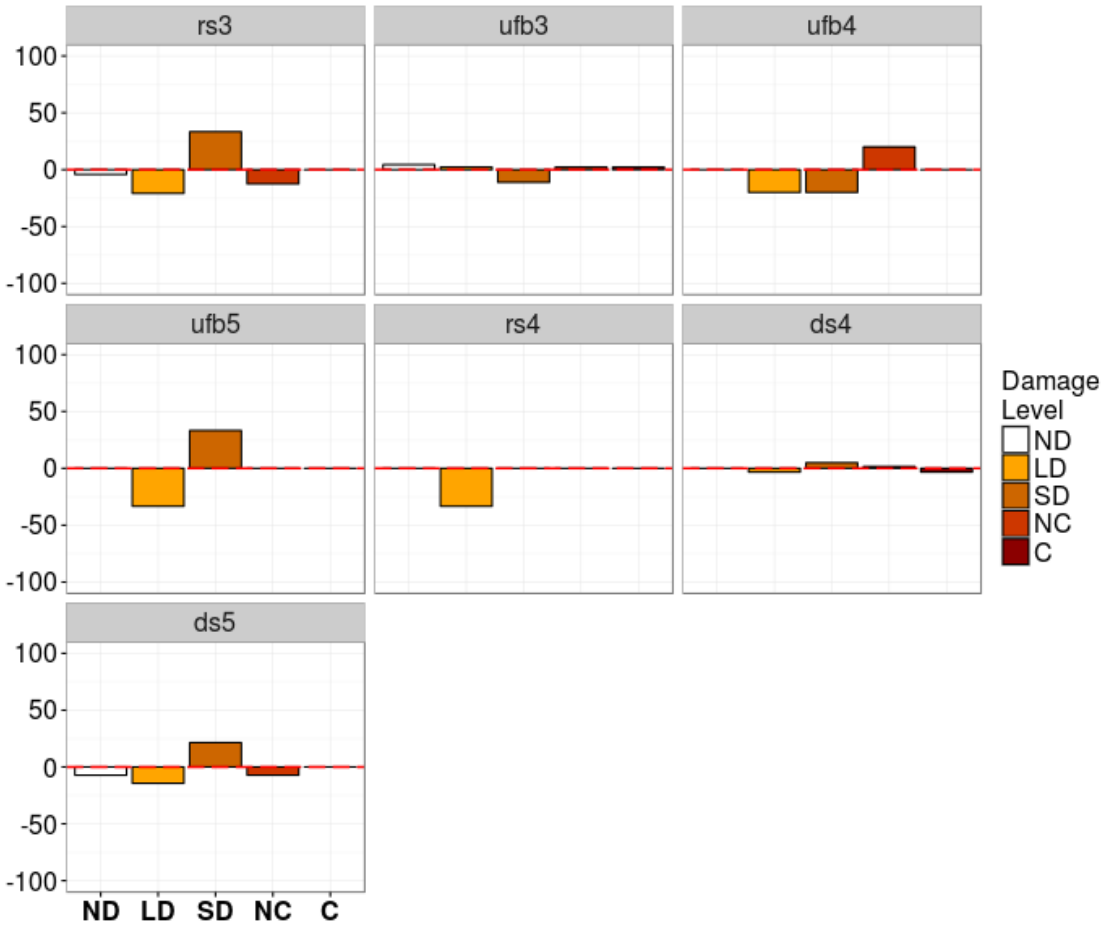

Figure H-9: Difference in terms of percentage between observed and estimated damage levels computed by ED, for classes rs3, rs4, ds4, ds5, ufb3, ufb4 and ufb5 (PAGER classification)

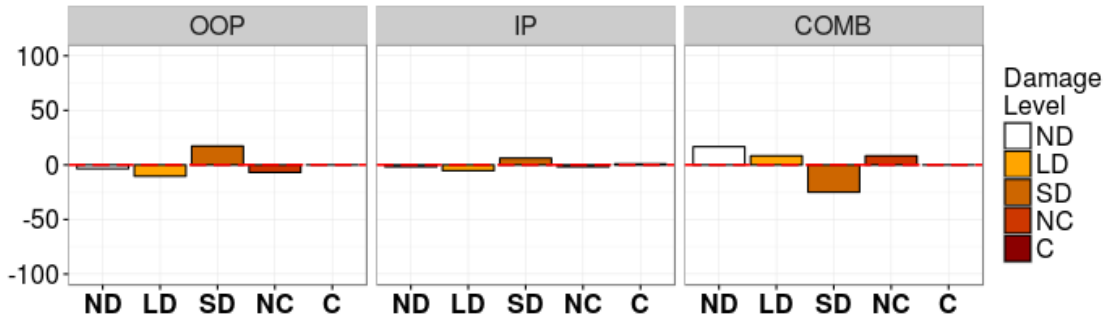

Figure H-10: Difference in terms of percentage between observed and estimated damage levels computed by ED, for classes OOP, IP, and COMB

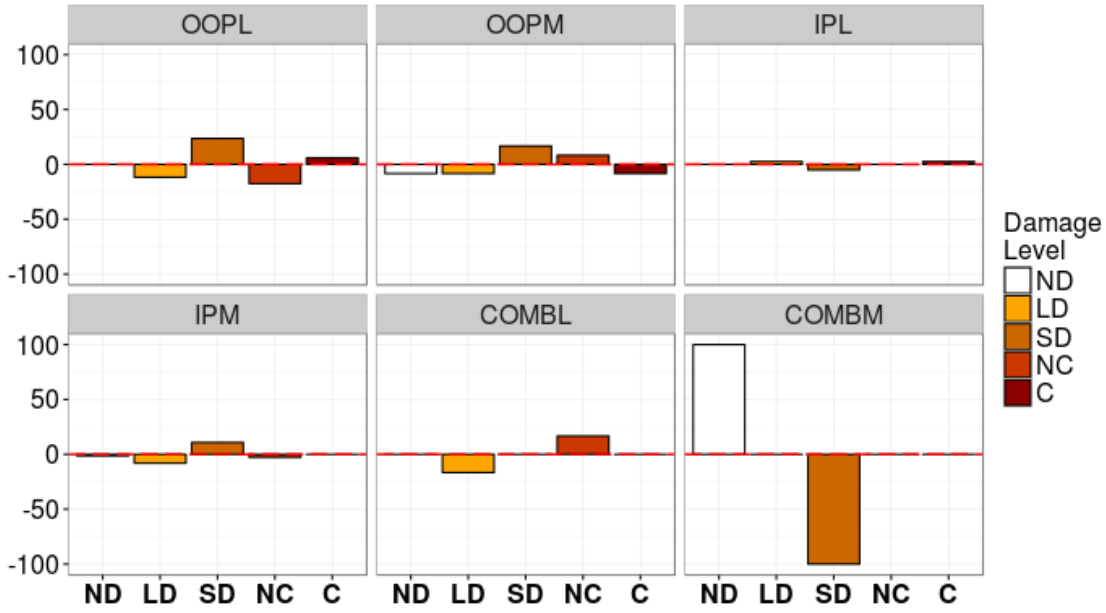

Figure H-11: Difference in terms of percentage between observed and estimated damage levels computed by ED, for classes OOPL, OOPM, IPL, IPM, COMB and COMBL

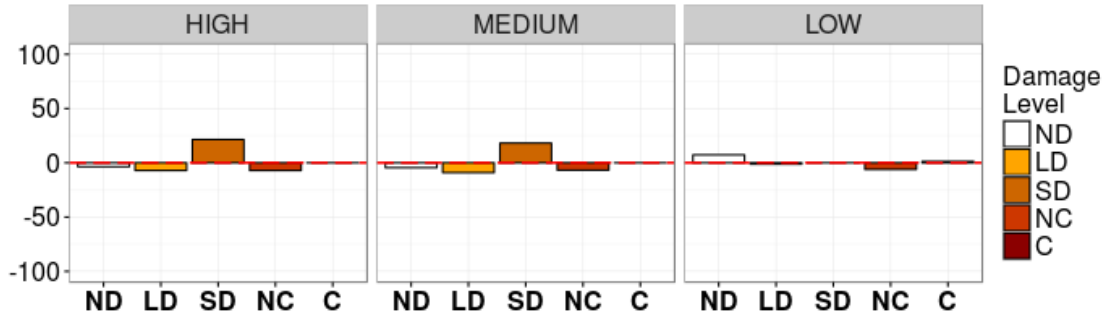

Figure H-12: Difference in terms of percentage between observed and estimated damage levels computed by ED, for classes HIGH, MEDIUM LOW VULNERABILITY

Classification	Building class	P-value	ρ
EMS'98	B	0.00060	0.99367
EMS'98	A	0.00844	0.96318
EMS'98	C	0.01461	0.94680
EMS'98 (rise)	BL	0.00007	0.99850
EMS'98 (rise)	BM	0.00066	0.99326
EMS'98 (rise)	CL	0.00214	0.98529
EMS'98 (rise)	AM	0.00255	0.98347
EMS'98 (rise)	AL	0.03487	0.90459
EMS'98 (rise)	CM	0.80432	-0.15430
Failure modes	IP	0.00036	0.99552
Failure modes	OOP	0.00266	0.98298
Failure modes	COMB	0.01099	0.95604
Failure modes (rise)	IPL	0.00003	0.99919
Failure modes (rise)	IPM	0.00158	0.98796
Failure modes (rise)	OOPM	0.00660	0.96874
Failure modes (rise)	COMBL	0.02756	0.91856
Failure modes (rise)	OOPL	0.02900	0.91572
Failure modes (rise)	COMBM	0.68504	-0.25000
Pager	ufb3	0.00001	0.99960
Pager	ds4	0.00016	0.99735
Pager	ds5	0.00881	0.96210
Pager	ufb4	0.04563	0.88561
Pager	rs4	0.05205	0.87500
Pager	rs3	0.06943	0.84809
Pager	ufb5	0.27223	0.61237
Vulnerability	MEDIUM	0.00125	0.98970
Vulnerability	HIGH	0.00133	0.98931
Vulnerability	LOW	0.00204	0.98572

Figure H-13: P-value and Pearson corralation coefficinet (ρ) for building classes

REFERENCES

Abbas N., Calderini C., Cattari S., Lagomarsino S., Rossi M. Ginanni Corradini R., Marghella G., Piovanello V. (2010/) Deliverable 4 Classification of the cultural heritage assets and description of the limit states and identification of damage measures. Perpetuate project (http://www.perpetuate.eu/wp-content/uploads/Deliverable-D4_def1.pdf)

Abhari R.. Anderson J., Arnold W., Canavero F. Data Mining. (2011) Concepets, Models, Methods, and Algorithms A JOHN WILEY & SONS, INC., PUBLICATION, IEEE PRESS.

Abrams, D. P. (1992, July). Strength and behavior of unreinforced masonry elements. In Proceedings of Tenth World Conference on Earthquake Engineering (pp. 3475-3480).

Adeli, H. (2001). Neural networks in civil engineering: 1989–2000. Computer-Aided Civil and Infrastructure Engineering, 16(2), 126-142.

Aldemir, T. (2013). A survey of dynamic methodologies for probabilistic safety assessment of nuclear power plants. Annals of Nuclear Energy, 52, 113-124.

Angeletti, E., Canepa, C., Martinetti, G., & Venturello, P. (1988). Silica gel functionalized with amino groups as a new catalyst for Knoevenagel condensation under heterogeneous catalysis conditions. Tetrahedron letters, 29(18), 2261-2264.

Alexander, D. E. (2010). The L'Aquila earthquake of 6 April 2009 and Italian Government policy on disaster response. Journal of Natural Resources Policy Research, 2(4), 325-342.

Areitio, M. G. (1990, July). The natural evolution step for the CAT: The Expert System. In Computer Aided Training in Science and Technology, Proceedings of the International Conference on Computer Aided Training in Science and Technology (pp. 9-13). Barcelona.

Askan A., and Yucemen, M.S. (2010) Probabilistic methods for the estimation of potential seismic damage: Application to reinforced concrete buildings in Turkey, Structural Safety, Vol. 32, Issue 4, pp. 262-271

Antoniou, G., & Van Harmelen, F. (2004). A semantic web primer. MIT press.

ASCE 41-13 (2013) Seismic rehabilitation of existing buildings (ASCE/SEI 41-13). Virginia: American Society of Civil Engineers Reston;.

ASCE. (2005). “Minimum disign loads for building and other structures.” ASCE 7–05, New York.

(ATC), 1997. NEHRP Commentary on the Guidelines for the Seismic Rehabilitation of Buildings, prepared for the Building Seismic Safety Council, published by the Federal Emergency Management Agency, FEMA 274, Washington, D.C.

ATC-40, (1996). Seismic evaluation and retrofit of concrete buildings. Relatório n SSC 96 01, Applied Technology Council, ATC 40. Redwood City, Califórnia.

ATC-33 (1995). Guidelines for the seismic rehabilitation of Buildigns – 50% Draft, Applied Technology Council., Redwood City, Claifornia

ATC-20 (1989) Procedures for Post-Earthquake Safety Evaluation of Buildings, ATC-20, Redwood City, CA.

ATC-21-1 (1988), “Rapid Visual Screening of Buildings for Potential Seismic Hazards: Supporting Documentation”, Applied Technology Council, Redwood city, CA, USA.

ATC-20i (2003): Applied Technology Council, Users manual: Mobile postearthquake building safety evaluation data acquisition system (Version 1.0), ATC-20i. Redwood City, California.

ATC-20 (1989): Applied Technology Council. Procedures for post-earthquake safety evaluation of buildings, Redwood City, CA.

Baggio C., Bernardini A., Colozza R., Corazza L., Della Bella M., Di Pasquale G., Dolce M., Goretti A., Martinelli A. (2009); "Manuale per la compilazione della scheda di 1° livello di rilevamento danno, pronto intervento e agibilità per edifici ordinari nell’emergenza post-sismica (AeDES)", Editrice Italiani nel Mondo srl - Roma

Baral, C. (2003).Knowledge Representation, Reasoning, and Declarative Problem Solving.Cambridge University Press, Cambridge, England.

Barbat, A.H Pujades L. G. Lantada N., Moreno R. (2008): ‘‘Seismic damage evaluation in urban areas using a capacity spectrum based method: Application to Barcelona’’ Soil Dynamics and Earthquake Engineering 28 (10–11) 851–865]

Barbat, A.H., Yépez Moya, F. and Canas, J.A. (1996); “Damage Scenarios Simulation for Seismic Risk Assessment in Urban Zones”, Earthquake Spectra, Vol. 12, No. 3, pp. 371-394.

Bendimerad, F., (2001) Loss Estimation: A Powerful Tool for Risk Assessment and Mitigation, Soil Dynamics and Earthquake Engineering”, Elsevier, No:21, p:467-472

Bernardini A., Gori R, Modena C. (1990); “An application of coupled analytical models and experiential knowledge for seismic vulnerability analyses of masonry buildings”; In A. Koridze (ed) Engineering Aspects of Earthquake Phenomena, Vol. 3: 161-180. Oxon: Omega Scientific, 1990

Benedetti, D. and Petrini, V. (1984); “Sulla Vulnerabilità Di Edifici in Muratura: Proposta Di Un Metodo Di Valutazione”, L’industria delle Costruzioni, Vol. 149, No. 1, pp. 66-74.

Benedetti, D., Benzoni, G. and Parisi, M. A. (1988),“Seismic vulnerability and risk evaluation for old urban nuclei” Earthquake Engineering & Structural Dynamics 16: 183–201. doi: 10.1002/eqe.4290160203

Bernardini A., Lagomarsino S.; (2008), "The seismic vulnerability of architectural heritage"; Proceedings of the Institution of Civil Engineers; Structures & Buildings; Vol.161, SB4;August; pp. 171-181

Bernardini, A., Giovinazzi, S., Lagomarsino, S., & Parodi, S. (2007). The vulnerability assessment of current buildings by a macroseismic approach derived from the EMS-98 scale.

Berrais, A. (2005). A knowledge-based expert system for earthquake resistant design of reinforced concrete buildings. Expert Systems with Applications, 28(3), 519-530.

Berrais, A., & Watson, A. S. (1993). Expert systems for seismic engineering: the state-of-the-art. Engineering Structures, 15(3), 146-154.

Bertero, R. D. (1995). Inelastic torsion for preliminary seismic design. Journal of Structural Engineering, 121(8), 1183-1189.

Borri, A., & Castori, G. (2004). Influence of bonding defects in masonry vaults and arches strengthened at their intrados with FRP. Proc. Mechanics of masonry structures strengthened with FRP-materials, 7-16.

Borzi, B., Pinho, R., & Crowley, H. (2008). Simplified pushover-based vulnerability analysis for large-scale assessment of RC buildings. Engineering Structures, 30(3), 804-820.

Bothara JK, Dhakal RP, Mander JB (2010) Seismic performance of an unreinforced masonry building: An experimental investigation. Earthq Eng Struct D 39(1):45-68

Braga F.; Dolce M.; Liberatore D (1982); "A statistical study on damaged buildings and ensuing review of the MSK -76 SCALE", Proceedings of the 7th European Conference on Earthquake Engineering, Athens, Greece

Bray, T., Paoli, J., Sperberg-McQueen, C. M., Maler, E., & Yergeau, F. (1998). Extensible markup language (XML). World Wide Web Consortium Recommendation REC-xml-19980210. http://www. w3. org/TR/1998/REC-xml-19980210, 16, 16.

Brunner, D., Lemoine, G., & Bruzzone, L. (2010). Earthquake damage assessment of buildings using VHR optical and SAR imagery. IEEE Transactions on Geoscience and Remote Sensing, 48(5), 2403-2420.

BSSC, NEHRP (1997) guidelines for the seismic rehabilitation of buildings, FEMA-273, developed by ATC for FEMA,Washington, D.C., 1997

Cadei M., Lazzari M., Salvaneschi P. (1990). Safety management of civil structures using knowledge based systems. In Proceedings of the third international conference on Industrial and engineering applications of artificial intelligence and expert systems - Volume 2 (IEA/AIE '90)

Cardona, O. D. (2004). The need for rethinking the concepts of vulnerability and risk from a holistic perspective: a necessary review and criticism for effective risk management. Mapping vulnerability: Disasters, development and people, 17.

Calderini, C., Cattari, S., & Lagomarsino, S. (2009). In-plane strength of unreinforced masonry piers. Earthquake Engineering & Structural Dynamics, 38(2), 243-267.

Calvi G. M., Pinho R., Magenes G., Bommer J.J., Restrepo-Vélez L.F. and Crowley H. (2006); Development of seismic vulnerability assessment methodologies over the past 30 years G.M. ISET Journal of Earthquake Technology, Paper No. 472, Vol. 43, No. 3, September 2006, pp. 75-104

Calvi, G. M., Kingsley, G. R., & Magenes, G. (1996). Testing of masonry structures for seismic assessment. Earthquake Spectra, 12(1), 145-162.

Carocci C. F. (2011) "Small centres damaged by 2009 L'Aquila earthquake: on site analyses of historic masonry clusters" BulletinEarthquake Engineering DOI 10.1007/s10518-011-9284-0

Carocci C. F. (2001) "Guidelines for the safety and preservation of historic centres in seismic areas" Historic Constructions, P.B. Lourenço, P. Roca (Eds.), Guimarães, p. 145- 165

Carreño, M. L., Cardona, O. D., & Barbat, A. H. (2012). New methodology for urban seismic risk assessment from a holistic perspective. Bulletin of earthquake engineering, 10(2), 547-565.

Carreño, M. L., Cardona, O. D., & Barbat, A. H. (2007). Urban seismic risk evaluation: a holistic approach. Natural Hazards, 40(1), 137-172.

Carreno M.L.,Cardona O. D and Barbat A. H. (2004). Expert system feor building damage evaluation If of earthquake. 13th World Conference on Earthquake Engineering Vancouver, B.C., Canada, August 1-6, 2004, Paper No. 3047

Casapulla, C., & D'Ayala, D. (2006). In-plane collapse behaviour of masonry walls with frictional resistances and openings. New Delhi: Structural Analysis of Historic Constructions.

CSSC (1999). California Seismic Safety Commission. www.seismic.gov

CBC, (2010), Title 24, California Code of Regulations, Part 2 – California Building Code, California Building Standards Commission, Sacramento, California.

CEN (2005) EN 1998-3:2005/AC:2010 Eurocode 8: design of structures for earthquake resistance – part 3: assessment and retrofitting of buildings. European Committee for Standardisation, Brussels, Belgium

CEN (2002) . Application and Use of Eurocodes. CONSTRUCT 01/483. Direction General Enterprises, Commission Europeenne, Brussels, 2002.

CEN (1994) . Eurocode 8, Design Provisions for Earthquake Resistance of Structures, European Prestandard ENV 1998. Comite Europeen de Normalisation, Brussels, 1994.

CEN (2004) . Eurocode 8, Design of Structures for Earthquake Resistance— Part 1: general rules, seismic actions and rules for buildings. EN 1998-1: 2004. Comite Europeen de Normalisation, Brussels, 2004.

CEN (1996) EN 1996-1-1 :2005 (E) Eurocode 6: design of masonry structures. General rules and rules for building. European Committee for Standardisation, Brussels, Belgium

Chandler, A. M. and Nelson, T. K. L. (2001), “Performance-Based Design in Earthquake Engineering: A Multi-Disciplinary Review,” Engineering Structures, Vol. 23, pp. 1525-1543.

Charter, V. (1964). International charter for the conservation and restoration of monuments and sites. In Second international congress of architects and technicians of historic monuments.

Charter, A. (1931). The Athens Charter for the restoration of historic monuments. In Ist International Congress of Architects and Technicians of Historic Monuments, Athens, October.

Chevallier, Arnaud (2016). Strategic Thinking in Complex Problem Solving. Oxford, UK, Oxford University Press. p.47

Chen, C. S., Cheng, M. Y., & Wu, Y. W. (2012). Seismic assessment of school buildings in Taiwan using the evolutionary support vector machine inference system. Expert Systems with Applications, 39(4), 4102-4110.

Chopra, A. K., & Goel, R. K. (1999). Capacity-demand-diagram methods based on inelastic design spectrum. Earthquake spectra, 15(4), 637-656.

Coburn, A.W., Spence, R.J.S., Pomonis, A., (1994). Vulnerability and Risk Assessment, second ed. UNDP Disaster Management Training Programme.

D'ayala, D., & Lagomarsino, S. (2015). Performance-based assessment of cultural heritage assets: outcomes of the European FP7 PERPETUATE project. Bulletin of Earthquake Engineering, 13(1), 5.

D’ayala, D., Meslem, A., Vamvatsikos, D., Porter, K., Rossetto, T., Crowley, H., & Silva, V. (2014). Guidelines for Analytical Vulnerability Assessment of low/mid-rise Buildings: Methodology. Vulnerability Global Component Project.

D’Ayala, D. Novelli V. (2013). Seismic vulnerability Assessment of masonry Structures. Encyclopaedia of Earthquake Engineering (pp. 334-365).

D’Ayala D., Novelli V., De Vos M., Padget J (2012) Deliverable 30: Freeware software with the implementation of the vulnerability models. Perpetuate project (http://www.perpetuate.eu/wp-content/uploads/D301.pdf)

D’Ayala D, Novelli V (2012) Deliverable 27: Formulation of vulnerability models including the survey form to collect the data required by the adopted models. Perpetuate project (http://www.perpetuate.eu/wp-content/uploads/Deliverable-D27.pdf)

D'Ayala D., Paganoni S. (2011) “Assessment and analysis of damage in L’Aquila historic city centre after 6th April 2009” Bulletin of Earthquake Engineering, Vol.9, Number 1, pp. 81-104

D’Ayala D, Novelli V (2010) Deliverable D5: Abacus of the most common seismic damage. Perpetuate project (http://www.perpetuate.eu/wp-content/uploads/Deliverable-D5.pdf)

D’ayala, D. F. (2005). Force and displacement based vulnerability assessment for traditional buildings. Bulletin of Earthquake Engineering, 3(3), 235-265.

D'Ayala D, and Speranza E. (2003) "Definition of Failure modes and Seismic Vulnerability of Historic Masonry Buildings." Earthquake Spectra Vol.19, August, pp. 479-509

D Ayala, D; (1999) Correlation of seismic damage between classes of buildings: churches and houses. In: Bernardini, A, (ed.) International Workshop on Measures of Damage to Masonry Buildings. (41 - 58). Balkema: Rotterdam.

D'Ayala, D., Spence, R., Oliveira, C., & Pomonis, A. (1997). Earthquake loss estimation for Europe's historic town centres. Earthquake Spectra, 13(4), 773-793.

De Natale, G., Madariaga, R., Scarpa, R., & Zollo, A. (1987). Source parameter analysis from strong motion records of the Friuli, Italy, earthquake sequence (1976-1977). Bulletin of the Seismological Society of America, 77(4), 1127-1146.

Di Pasquale, G., Orsini, G. and Romeo, R.W. (2005). "New Developments in Seismic Risk Assessment in Italy", Bulletin of Earthquake Engineering, Vol. 3, No. 1, pp. 101-128

De Stefano, M., & Pintucchi, B. (2008). A review of research on seismic behaviour of irregular building structures since 2002. Bulletin of Earthquake Engineering, 6(2), 285-308.

Dolce, M., Masi, A., Marino, M. and Vona, M. (2003)."Earthquake Damage Scenarios of the Building Stock of Potenza (Southern Italy) Including Site Effects", Bulletin of Earthquake Engineering, Vol. 1, No. 1, pp. 115-140.

Doherty KT, Griffith MC, Lam N, Wilson, J. (2002) "Displacement-based Seismic Analysis for Out-of plane Bending of Unreinforced Masonry Walls".Earthquake Engineering and Structural Dynamics, 31: 833-850.

Dokas, I. M. (2005, September). Developing Web Sites For Web Based Expert Systems: A Web Engineering Approach. In ITEE (pp. 202-217).

D.P.C.M. 23 February 2006 (G.U. 7.3.2006, n. 55).

Dovers, SR, Handmer, JW.(1995). "Ignorance, the precautionary principle, and sustainability" Ambio Stockholm [AMBIO]. Vol. 24, no. 2, pp. 92-97.

Erdik, M., Sesetyan, K., Demircioglu, M., Hancilar, U., Zulfikar, C., Cakti, E., ... & Harmandar, E. (2010). Rapid earthquake hazard and loss assessment for Euro-Mediterranean region. Acta Geophysica, 58(5), 855-892.

Erdik, M., Aydinoglu, N., Fahjan, Y., Sesetyan, K., Demircioglu, M., Siyahi, B., ... & Yuzugullu, O. (2003). Earthquake risk assessment for Istanbul metropolitan area. Earthquake Engineering and Engineering Vibration, 2(1), 1-23.

Erdik, M. (Ed.) (2003) "Earthquake Risk Assessment for The Istanbul Metropolitan Area", Final Report. Bogazici University.

Fajfar, P., Dolšek, M., Marušić, D., & Stratan, A. (2006). Pre-and post-test mathematical modelling of a plan-asymmetric reinforced concrete frame building. Earthquake engineering & structural dynamics, 35(11), 1359-1379.

Fajfar, P. (2000). A nonlinear analysis method for performance-based seismic design. Earthquake spectra, 16(3), 573-592.

Fajfar, P. (1999) Capacity spectrum method based on inelastic demand spectra." Earthquake engineering and structural dynamics 28.9 979-994.

Fajfar, P., Vidic, T., & Fischinger, M. (1989). Seismic demand in medium-and long-period structures. Earthquake Engineering & Structural Dynamics, 18(8), 1133-1144.

Fajfar, P, and Gašperšič P.. (1996) The N2 method for the seismic damage analysis of RC buildings." Earthquake Engineering & Structural Dynamics 25.1. 31-46.

Fajfar, P., Vidic, T., & Fischinger, M. (1989). Seismic demand in medium-and long-period structures. Earthquake Engineering & Structural Dynamics, 18(8), 1133-1144.

FEMA P-154. (2015) Rapid Visual Screening of Buildings for Potential Seismic Hazards: A Handbook (third ed.)Federal Emergency Management Agency, Washington DC, USA (January)

FEMA 440, (2005), Improvements of Nonlinear Static Seismic Analysis Procedures, Federal Emergency Management Agency, Washington, D.C.

FEMA (2003). HAZUS-MH MR1: Technical Manual, Federal Emergency Management Agency, Washington, D.C

FEMA 356, (2000), Prestandard and Commentary for the Seismic Rehabilitation of Buildings, Federal Emergency Management Agency, Washington, D.C.

FEMA (1999) Federal Emergency Management Agency. In: HAZUS 99 Earthquake Loss Estimation Methodology, User Manual. Federal Emergency Management Agency, Washington, DC, United States 314 pp

FEMA 273, (1997), Guidelines to the Seismic Rehabilitation of Existing Buildings, Federal Emergency Management Agency, Washington, D.C.

Formisano, A. (2012). Seismic behaviour and retrofitting of the Poggio Picenze Historical Centre damaged by the L'Aquila earthquake. In Proceedings of the eleventh international conference on computational structures technology, Civil-Comp Press, Stirlingshire, UK, Paper (Vol. 199).

Formisano, A., Florio, G., Landolfo, R., & Mazzolani, F. M. (2015). Numerical calibration of an easy method for seismic behaviour assessment on large scale of masonry building aggregates. *Advances in Engineering Software*, *80*, 116-138.

Formisano A., Mazzolani F.M, Florio G., Landolfo R. (2010a) "A quick methodology for seismic vulnerability assessment of historic masonry clusters" Urban Habitat Constructions under Catastrophic Events – Mazzolani (Ed) 2010 Taylor & Francis Group, London, ISBN 978-0-415-60685-1

Formisano A., Mazzolani F.M, Florio G., Landolfo R., Indirli M. (2010b) "Seismic vulnerability analysis of historic centres: A GIS application in Torre del Greco" Urban Habitat Constructions under Catastrophic Events (Proceedings) – Mazzolani (Ed).2010 Taylor & Francis Group, London, ISBN 978-0-415-60685-1

Freeman, S. A. (1998). The capacity spectrum method as a tool for seismic design. In Proceedings of the 11th European conference on earthquake engineering (pp. 6-11).

Freeman, W. J. (1975). Mass action in the nervous system.

Galarreta, J. F., Kerle, N., & Gerke, M. (2015). UAV-based urban structural damage assessment using object-based image analysis and semantic reasoning. *Natural Hazards and Earth System Sciences*, *15*(6), 1087.

Gebser, M., Kaufmann, B., Neumann, A., & Schaub, T. (2007, May). clasp: A conflict-driven answer set solver. In International Conference on Logic Programming and Nonmonotonic Reasoning (pp. 260-265). Springer Berlin Heidelberg.

Gelfond, M. and Lifschitz, V. (1988).The stable model semantics for logic programming.In Proceedings of the 5th International Conference and Symposium on Logic Programming. MIT Press, 1070{1080

Gelfond, M. and Lifschitz, V. (1991).Classical negation in logic programs and disjunctive databases.New Generation Computing 9, 3-4, 365, 386.

Gerke, M., & Kerle, N. (2011). Automatic structural seismic damage assessment with airborne oblique Pictometry© imagery. Photogrammetric Engineering & Remote Sensing, 77(9), 885-898.

Gehl, P., Douglas, J., Rossetto, T., Macabuag, J., Nassirpour, A., Minas, S. and Duffour, P. (2014) 'Investigating the use of record-to-record variability in static capacity spectrum approaches', Proceedings of the 2nd International Conference on Vulnerability and Risk Analysis and Management (ICVRAM2014) & 6th International Symposium on Uncertainty Modelling and Analysis (ISUMA2014), Liverpool, UK.

Giardini, D., Grünthal, G., Shedlock, K. M. and Zhang, P. (1999) The GSHAP Global Seismic Hazard Map. Annali di Geofisica 42 (6), 1225-1228.

Ginge, A., & Murugesan, S. (2001). „Web Engineering: An Introduction", Multimedia.

Giovinazzi, S. and Lagomarsino, S.(2004);"A Macroseismic Method for the Vulnerability Assessment of Buildings", Proceedings of the 13th World Conference on Earthquake Engineering, Mediterranean", Proceedings of CNR-Gruppo Nazionale per la Difesa dai Terremoti, Roma, Italy.Vancouver, Canada, Paper No. 896

Giovinazzi, S., & Lagomarsino, S. (2005). Fuzzy-random approach for a seismic vulnerability model. Proc. of ICOSSAR 2005.

Giovinazzi S, Lagomarsino S. (2002); "Seismic Risk Analysis: a method for the vulnerability assessment of built-up ares", Genoa, (Italy)

Giovinazzi, S. and Lagomarsino, S. (2001);"Una Metodologia per L'analisi Di Vulnerabilità Sismica Del Costruito",Proceedings of the X Congresso Nazionale on L'Ingegneria Sismica in Italia Potenza-Matera, Italy, Paper No. 121

Giuffè, A. (editor) (1993a), Sicurezza e conservazione dei centri storici – Il caso Ortigia, Ed. Laterza (In Italian).

Giuffrè A. (1993b) “Sicurezza e conservazione dei centri storici. Il caso Ortigia.” Bari: Laterza, 1993. Valluzzi MR, Cardani G, Binda L, Modena C. “Analysis of the seismic vulnerability of masonrybuildings in historic centres and intervention proposals”, Proceedings of the 6th Int. Symp. on the Conservation of Monuments in the Mediterranean Basin, Lisbon, Portugal, 7-10 April 2004 (6 pp., to appear).

Gomes G., Vincente H., Macedo J., Alves V., Neves J. (2013) A Logic Programming Approach to the Conservation of buildings based on an extension of the Eindhoven classification model. Polibits (48) ISSN. 1870-9044; pp. 31-38

Gómez-Pérez, A., & Benjamins, R. (1999). Overview of knowledge sharing and reuse components: Ontologies and problem-solving methods. IJCAI and the Scandinavian AI Societies. CEUR Workshop Proceedings.

Goretti A., Di Pasquale G. (2002) “An overview of Post-Earthquake Damage Assessment in Italy” Eeri Invitational Workshop, An Action plan to develop earthquake damage and loss data protocols, California.

GNDT.“Rischio sismico di edifici pubblici-Parte I Aspetti metodologici”. Consiglio Nazionale delle Richerche - Gruppo Nazionale per la Difesa dai Terremoti, Roma, 1993. (In Italian)

Griffith MC, Magenes G, Melis G, Picchi L. (2003) Evaluation of out-of-plane stability of unreinforced masonry walls subjected to seismic excitation”. Journal on Earthquake Engineering, Special Issue; 1(7): 141-169.

Grünthal, G. (editor) (1998). “Cahiers du Centre Européen de Géodynamique et de Séismologie: Volume 15 – European Macroseismic Scale 1998”, European Center for Geodynamics and Seismology, Luxembourg.

Han J., Kamber M., Pei J. (2012) Dara Mining. Concepts and Techniques. Third edition Morgan Kaufmann is an imprint of Elsevier

Hancilar, U., Tuzun, C., Yenidogan, C., & Erdik, M. (2010). ELER software- a new tool for urban earthquake loss assessment. Natural Hazards and Earth System Sciences,10(12), 2677-2696.

Hassanzadeha R, Nedović-Budića Z, Alavi Razavib A, Norouzzadehb M, Hodhodkianb H (2012) Interactive approach for GIS-based earthquake scenario development and resource estimation (Karmania hazard model). Comput Geosc, volume 51, February 2013, pp 324–338

ING-GNDT (2001): Catalogo Strumentale dei TerremotiItaliani dal 1981 al 1996, Version 1.0 (CD-ROM)

IBC (2003) The International Building Code. International Code Council, Virginia, USA

ICB (2000) International Conference of Building Officials. Guidelines for the Seismic Retrofit of Existing Buildings. (2000). www.iccsafe.org

ICOMOS/ISCARSAH Committee (2005) Recommendations for the analysis, conservation and structural restoration of architectural heritage. See www.icomos.org

Kappos, A. J., & Panagopoulos, G. (2010). Fragility curves for reinforced concrete buildings in Greece. Structure and Infrastructure Engineering, 6(1-2), 39-53.

Kappos, A.J.' Panagopoulos, G., Penelis, G.G. (2008) "Development of a seismic damage and loss scenario for contemporary and historic buildings in Thessaloniki, Greece" Soil Dynamics and Earthquake EngineeringVolume 28, Issue 10-11, October 2008, Pages 836-850

Kappos, A. J., Panagopoulos, G., Panagiotopoulos, C., & Penelis, G. (2006). A hybrid method for the vulnerability assessment of R/C and URM buildings. Bulletin of Earthquake Engineering, 4(4), 391-413.

Kappos, A. J., Penelis, G. G., & Drakopoulos, C. G. (2002). Evaluation of simplified models for lateral load analysis of unreinforced masonry buildings. Journal of structural Engineering, 128(7), 890-897.

Kappos, A.J., Stylianidis, K.C. and Pitilakis, K. (1998) "Development of Seismic Risk Scenarios Based on a Hybrid Method of Vulnerability Assessment", Natural Hazards, Vol. 17, No. 2, pp. 177-192

Karantoni, F. V., & Bouckovalas, G. (1997). Description and analysis of building damage due to Pyrgos, Greece earthquake. Soil Dynamics and Earthquake Engineering, 16(2), 141-150.

Kerle, N. (2010). Satellite-based damage mapping following the 2006 Indonesia earthquake—How accurate was it?. International Journal of Applied Earth Observation and Geoinformation, 12(6), 466-476.

Kerle, N., Heuel, S., & Pfeifer, N. (2008). Real-time data collection and information generation using airborne sensors (pp. 43-74). Taylor & Francis/Balkema: Leiden, The Netherlands.

Kircher, C. A., Nassar, A. A., Kustu, O., & Holmes, W. T. (1997). Development of building damage functions for earthquake loss estimation. Earthquake spectra, 13(4), 663-682.

Krishnamurthy, J., Venkatesa Kumar, N., Jayaraman, V., & Manivel, M. (1996). An approach to demarcate ground water potential zones through remote sensing and a geographical information system. International Journal of Remote Sensing, 17(10), 1867-1884.

Kuhn, M. R., & Inan, M. I. (1989). Early integration of computational methods in the engineering curriculum. In Computer Utilization in Structural Engineering: (pp. 399-407). ASCE.

Jaiswal, K., & Wald, D. J. (2013). Strategies for rapid global earthquake impact estimation: the Prompt Assessment of Global Earthquakes for Response (PAGER) system.

Jaiswal, K. S., Wald, D. J., Earle, P. S., Porter, K. A., & Hearne, M. (2011). Earthquake casualty models within the USGS Prompt Assessment of Global

Earthquakes for Response (PAGER) system. In Human Casualties in Earthquakes (pp. 83-94). Springer Netherlands.

Jalayer, F. and Cornell, C. A. (2009) 'Alternative nonlinear demand estimation methods for probability-based seismic assessments', Earthquake Engineering and Structural Dynamics, 38(8), pp.951-972.

Jaramillo, N., Carreño, M. L., & Lantada, N. (2016). Evaluation of social context integrated into the study of seismic risk for urban areas. International journal of disaster risk reduction, 17, 185-198.

JBDPA, (2001) Japan Building Disaster Prevention Association Standard for Seismic Evaluation of Existing Reinforced Concrete Buildings , (English version, 1st edition), Tokyo, Japan.

Lagomarsino, S., & Cattari, S. (2015). PERPETUATE guidelines for seismic performance-based assessment of cultural heritage masonry structures. Bulletin of Earthquake Engineering, 13(1), 13-47.

Lagomarsino, S., Penna, A., Galasco, A., & Cattari, S. (2013). TREMURI program: an equivalent frame model for the nonlinear seismic analysis of masonry buildings. *Engineering Structures*, *56*, 1787-1799.

Lagomarsino S, Modaressi H, Pitilakis K, Bosjlikov V, Calderini C, D'Ayala D, Benouar D, Cattari S (2010) PERPETUATE project: the proposal of a performance-based approach to earthquake protection of cultural heritage. Adv Mater Res 133–134:1119–1124. doi:10.2495/STR110581

Lagomarsino S.; (2006), "On the vulnerability assessment of monumental buildings"; Bullettin of Earthquake Engineering; Vol.4, 25 August;pp. 445-463

Lagomarsino S. Giovinazzi S. (2006) "Macroseismic and mechanical models for the vulnerability and damage assessment of current buildings"; Bulletin of Earthquake Engineering.4, 25 August: pp. 415-443

Lagomarsino S., Cattari S., Pagnini L., Parodi S (2010); "Probabilistic seismic damage scenario by mechanical models: the case study of Sulmona (Italy)", Proc. of 14th European Conference on Earthquake Engineering, Ohrid, Republic of Macedonia; September

Lang K. (2002) "Seismic vulnerability of existing buildings"; Institute of Structural Engineering (IBK), ETH Zurich, Report No. 273, vdf Hochschulverlag, Zurich,

Lang, K. and Bachmann, H. (2004) "On the seismic vulnerability of existing buildings: a case study of the city of Basel". Earthquake Spectra 20(1), 43–66.

Leão, B. F., & Rocha, A. F. (1990). Proposed methodology for knowledge acquisition: a study on congenital heart disease diagnosis. Methods of Information in Medicine, 29(1), 30-40.

Lehane, M. S., & Moore, C. J. (1996). Applying case-based reasoning in bridge design. Information Processing in Civil and Structural Engineering, 1-5.

Lourenço, P. B., & Roque, J. A. (2006). Simplified indexes for the seismic vulnerability of ancient masonry buildings. Construction and Building Materials, 20(4), 200-208.

Lourenco P. B,.Roque J.A (2005), "Simplified indexes for the seismic vulnerability of ancient masonry buildings "; Construction and Building MATERIALS, Octoberpp. 200-208

Lu, P., Chen, S., & Zheng, Y. (2012). Artificial intelligence in civil engineering. Mathematical Problems in Engineering, 2012.

Magliulo, P., Di Lisio, A., Russo, F., & Zelano, A. (2008). Geomorphology and landslide susceptibility assessment using GIS and bivariate statistics: a case study in southern Italy. Natural Hazards, 47(3), 411-435.

Maimon, O., & Rokach, L. (2005). Decomposition methodology for knowledge discovery and data mining. In Data Mining and Knowledge Discovery Handbook (pp. 981-1003). Springer US.

Maio, R., Vicente, R., Formisano, A., & Varum, H. (2015). Seismic vulnerability of building aggregates through hybrid and indirect assessment techniques. Bulletin of Earthquake Engineering, 13(10), 2995-3014.

Maruyama, Y., Tashiro, A. & Yamazaki, F. (2014). Detection of collapsed buildings due to earthquakes using a digital surface model constructed from aerial images, Journal of Earthquake and Tsunami, 8(1), 1450003,World Scientific Publishing Company, DOI: 10.1142/S1793431114500031.

Medvedev, G. I., & Merbs, B. P. (1964). The Place of the Culture of Verkholenskaia Gora in the Archaeological Sequence of the Baikal Region. *American Antiquity*, 461-466.

Melchor-Lucero O. and Ferregut C. (1995).Toward an expert system for damage assessment of structural concrete elements. Artificial Intelligence for Engineering Design, Analysis and Manufacturing, 9 pp. 401–418

Metternicht, G., Hurni, L., & Gogu, R. (2005). Remote sensing of landslides: An analysis of the potential contribution to geo-spatial systems for hazard assessment in mountainous environments. Remote sensing of Environment, 98(2), 284-303.

Minas, S., Galasso, C. and Rossetto, T. (2014) 'Preliminary investigation on selectingoptimal intensity measures for simplified fragility analysis of mid-rise RC buildings',15th European Conference on Earthquake Engineering (2ECEES), Istanbul, Turkey

Miranda, E., Akkar, D. S., & Ruiz-Garcia, J. (2002). ATC-55: Summary of Evaluation of Current Nonlinear Static Procedures-SDOF Studies. *Applied Technology Council*.

Molina, S., Lang, D. H., & Lindholm, C. D. (2010). SELENA–An open-source tool for seismic risk and loss assessment using a logic tree computation procedure. Computers & Geosciences, 36(3), 257-269.

Moradi, M., Delavar, M. R., & Moshiri, B. (2015). A GIS-based multi-criteria decision-making approach for seismic vulnerability assessment using quantifier-guided OWA operator: a case study of Tehran, Iran. Annals of GIS, 21(3), 209-222.

Munoz, J. J., Bonet, J., Huerta, A., & Peraire, J. (2009). Upper and lower bounds in limit analysis: adaptive meshing strategies and discontinuous loading. International Journal for Numerical Methods in Engineering, 77(4), 471-501.

Natke, H. G., & Yao, J. T. P. (1993). Detection and Location of Damage Causing Non-linear System Behavior. In Safety Evaluation Based on Identification Approaches Related to Time-Variant and Nonlinear Structures (pp. 188-203). Vieweg+ Teubner Verlag.

Nasiri (2012) Structural Assessment and Retrofit Design for Golestan Historical Masonry Dam. 3rd National Conference on Earthquake & Structure

NIBS (1997) National Institute of Building Science. Earthquake Loss Estimation Methodology. HAZUS97: Technical Manual. Report prepared for the Federal Emergency Management Agency. (Washington D.C. NIBS)

Nofal, M., & Fouad, K. M. (2014). Developing Web-Based Semantic Expert Systems Based Semantic Expert Systems Based Semantic Expert Systems.

Novelli VI, D'Ayala D (2015) LOG-IDEAH: LOGic trees for identification of damage due to earthquakes for architectural heritage. Bulletin of Earthquake Engineering. DOI 10.1007/s10518-014-9622-0.

Novelli V., D'Ayala D., Makhloufi N., Zekagh A., Benouar D. (2015). A procedure for the identification of the seismic vulnerability at territorial scale. Application to the Casbah of Algiers. Bullettin of Earthquake Engineering; DOI 10.1007/s10518-014-9666-1.

Novelli V. I., D'Ayala D. (2012) Assessment of the most damaged historic centres of the Region Emilia Romagna due to the earthquake of the 20th and 29th of May 2012. Ingegneria Sismica.

Novelli, V., De Vos, M., Padget, J. and D'Ayala, D., (2012). LOG-IDEAH : ASP for architectonic asset preservation. In: Dovier, A. and Santos Costa, V., eds. Technical Communications of the 28th International Conference on Logic Programming (ICLP'12). Dagstuhl: Schloss Dagstuhl-Leibniz-Zentrum fuer Informatik, pp. 393-403.

NRCC. 1993. Guidelines for seismic evaluation of existing buildings. Institute for Research in Construction, National Research Council of Canada (NRC), Ottawa, Ont.

NTC (2008). Norme tecniche per le Costruzioni, D.M. 14.1.2008 (Italian Building Code, in Italian).

OES, (1995) : California Office of Emergency Services "Vision 2000:Performance Based Seismic Engineering of Buildings", Prepared by Structural Engineers Association of California, Sacramento, CA 1995.

Ogawa H. and Fu K. S., (1985).An inexact inference for damage assessment of existing structures.Int.J. Man-Machine Studies, vol. 22, pp. 295–306, 1985.

Olivera C.S., Mota de Sa., Ferreira M.A. (2005); "Application of two different vulnerability methodologies to asset seismic scenarios in Lisbon", Proceedings of the 250th Anniversary 1755 Lisbon Earthquake, Lisbon, Portugal

Olivera C.S, Ferreira M.A., Mota de SA. F. (2004);"Seismic vulnerability of buildings and impact analysis elements for mitigation policies", Proceedings of the Eleventh Italian Conference on Earthquake Engineering, Genoa, Italy

OPCM 3274 (2003). Primi elementi in material di criteri generali per la classificazione sismica del territorio nazionale e di normative tecniche per le costruzioni in zona sismica. Gazzetta Ufficiale 105: S.O. 72, (in Italian)

OPCM 3431 (2005). Ulteriori modifiche ed integrazioni all'OPCM 3274, recante «Primi elementi in materia di criteri generali per la classificazione sismica del territorio nazionale e di normative tecniche per le costruzioni in zona sismica». Gazzetta Ufficiale 107: S.O. 85, (in Italian)

O.P.C.M n. 3753, Gazzetta Ufficiale, 7th April 2009, n. 81. (2) (in Italian).

Orsini, G. (1999). A model for buildings' vulnerability assessment using the parameterless scale of seismic intensity (PSI). Earthquake Spectra, 15(3), 463-483.

Paquette, J., & Bruneau, M. (2003). Pseudo-dynamic testing of unreinforced masonry building with flexible diaphragm. Journal of structural engineering, 129(6), 708-716.

Parisi, F., & Augenti, N. (2013). Earthquake damages to cultural heritage constructions and simplified assessment of artworks. Engineering Failure Analysis, 34, 735-760.

Pereira AS (2009) The opportunity of a disaster: the economic impact of the 1755 Lisbon earthquake, Journal of Economic History 69(2):466,2009

Pitilakis, K., Crowley, H., & Kaynia, A. M. (2014). SYNER-G: typology definition and fragility functions for physical elements at seismic risk. Geotechnical, Geological and Earthquake Engineering, 27.

Porter, K. A., Farokhnia, K., Cho, I. H., Grant, D., Jaiswal, K., Wald, D., & Noh, H. (2012, September). Global vulnerability estimation methods for the global earthquake model. In 15th World Conference on Earthquake Engineering, Lisbon, Portugal (pp. 24-28).

Raphael, B., & Smith, I. (1998). Finding the right model for bridge diagnosis. In Artificial intelligence in structural engineering (pp. 308-319). Springer Berlin Heidelberg.

Reinhorn, A. M., & Calvi, G. M. (1997). Inelastic Analysis Techniques in. on Seismic Evaluation and Retrofit, 103.

Rossetto, T., Ioannou, I., & Grant, D. N. (2013). Existing empirical fragility and vulnerability relationships: compendium and guide for selection. Pavia, Italy: GEM Foundation.

Saiidi, M., & Sozen, M. A. (1981). Simple nonlinear seismic analysis of R/C structures. Journal of the Structural Division, 107(5), 937-953.

Pacor, F., Paolucci, R., Luzi, L., Sabetta, F., Spinelli, A., Gorini, A., ... & Dolce, M. (2011). Overview of the Italian strong motion database ITACA 1.0. Bulletin of Earthquake Engineering, 9(6), 1723-1739.

Pitilakis, K., Crowley, H., & Kaynia, A. M. (2014). SYNER-G: typology definition and fragility functions for physical elements at seismic risk. Geotechnical, Geological and Earthquake Engineering, 27.

Ramos L. F., Lourenco P. B (2004), "Modelling and vulnerability of historic city centre in seismic areas: a case study in Lisbon"; Engineering structures, April, pp. 1295-1310

Restrepo-Vélez LF, Magenes G. (2004) A mechanics-based procedure for the seismic risk assessment of masonry buildings at urban scale. Proceedings of the XI Convegno Nazionale ANIDIS, Genova.

Rossetto, T., Ioannou, I., Grant, D. N., & Maqsood, T. (2014). Guidelines for empirical vulnerability assessment (Vol. 6, p. 3). GEM Technical Report 2014-X, GEM Foundation, Pavia,. www. globalquakemodel. org GEM Technical Report 2010-X.

Rossetto, T., Gehl, P., Minas, S., Nassirpour, S., Macabuag, J., Duffour, P. and Douglas, J. (2014). 'Sensitivity analysis of different capacity approaches to assumptions in the modeling, capacity and demand representations'. ASCE-ICVRAM-ISUMA conference, Liverpool, UK.

Rota, M., Penna, A. and Strobbia, C. (2006). “Typological Fragility Curves from Italian Earthquake Damage Data”, Proceedings of the First European Conference on Earthquake Engineering and Seismology, Geneva, Switzerland, Paper No. 386

Sabetta, F., Goretti, A. and Lucantoni, A. (1998). “Empirical Fragility Curves from Damage Surveys and Estimated Strong Ground Motion”, Proceedings of the 11th European Conference on Earthquake Engineering, Paris, France, pp. 1-11.

Salgado-Gálvez, M. A., Romero, D. Z., Velásquez, C. A., Carreño, M. L., Cardona, O. D., & Barbat, A. H. (2016). Urban seismic risk index for Medellín, Colombia, based on probabilistic loss and casualties estimations. Natural Hazards, 80(3), 1995-2021.

Spence, R., Coburn, A.W. and Pomonis, A.(1992);"Correlation of Ground Motion with Building Damage: The Definition of a New Damage-Based Seismic Intensity Scale", Proceedings of the Tenth World Conference on Earthquake Engineering, Madrid, Spain, Vol. 1, pp. 551-556

Staab, S. & Studer, R. (2013). Handbook on Ontologies. Springer Berlin Heidelberg. https://books.google.co.uk/books?id=uTwDCAAAQBAJ

Tertulliani, A., Arcoraci, L., Berardi, M., Bernardini, F., Camassi, R., Castellano, C., .. & Rossi, A. (2011). An application of EMS’98 in a medium-sized city: the case of L’Aquila (Central Italy) after the April 6, 2009 Mw 6.3 earthquake. Bulletin of Earthquake Engineering, 9(1), 67-80.

Tesfamariam, S., Sadiq, R., & Najjaran, H. (2010). Decision making under uncertainty—An example for seismic risk management. Risk analysis, 30(1), 78-94.

Tomazevic, M. (1978). The computer program POR. Report ZRMK.

Tomaževič, M. (1999); "Earthquake-resistant design of masonry buildings”, Imperial College Press, London

UNDRO (1980) Natural disasters and vulnerability analysis. Report of Expert Group Meeting. (Geneva:United Nations).

UNDP/UNIDO (1985), “Post-Earthquake Damage Evaluation and Strength Assessment of Buildings under Seismic Conditions”, Volume 4, Vienna

Uschold, M., & Gruninger, M. (1996). Ontologies: Principles, methods and applications. The knowledge engineering review, 11(02), 93-136.

Van Heijst, G., Schreiber, A. T., & Wielinga, B. J. (1997). Using explicit ontologies in KBS development. International journal of human-computer studies, 46(2-3), 183-292.

Vahdat, K., Smith, N. J., & Amiri, G. (2014). Developing a Knowledge Based Expert System (KBES) for Seismic Risk Management. In Vulnerability, Uncertainty, and Risk: Quantification, Mitigation, and Management (pp. 1746-1755).

Vamvatsikos, D. and Cornell, C.A. (2002) 'Incremental Dynamic Analysis', Earthquake Engineering and Structural Dynamics, 31(3), pp.491-514.

Vatan M., Arun G. (2010) “Monument Damage Hazards and Rehabilitation Technologies” 8th International Symposium on the Conservation of Monuments in the Mediterranean Basin, Patras, Greece.

Vicente; C. Oliveira; T.M. Ferreira; H. Rodrigues; A.A. Costa (2014) Chap. 4: Seismic Structural Assessment of Existing Building at Urban Level. In: "Lisbon in Motion Workshop: Risk assessment, rehabilitation and urban plan". Alexandre A. Costa, Mónica Amaral Ferreira, Alexandra Carvalho, Cristina Oliveira, Isabel Lopes and Rui Carrilho Gomes (Eds.). SPES. Book ISBN: 978-989-20-5085-0. pp.39-48.

Voigt, S., Kemper, T., Riedlinger, T., Kiefl, R., Scholte, K., & Mehl, H. (2007). Satellite image analysis for disaster and crisis-management support. IEEE transactions on geoscience and remote sensing, 45(6), 1520-1528.

Watson, I. (1998). Applying case-based reasoning: techniques for enterprise systems. Morgan Kaufmann Publishers Inc..

Whitman R.V.; Reed JW; Hong ST(1973);"Earthquake damage probability matrices", Proceedings of the 5th World Conference on Earthquake Engineering

Whitman R.V.(1973);"Damage probability Matrices for Prototype Buildings ", Research Report R73-57, Cambridge, Massachuesetts

Wielanda M, Pittorea M, Parolaia S, Zschaua J, Moldobekovb B, Begalievc U (2012) Estimating building inventory for rapid seismic vulnerability assessment: Towards an integrated approach based on multi-source imaging. Soil Dyn Earthq Eng, volume 36, May 2012, pp 70–83

Yi, T., Moon, F. L., Leon, R. T., & Kahn, L. F. (2006). Lateral load tests on a two-story unreinforced masonry building. Journal of Structural Engineering, 132(5), 643-652.

Zhang, Y., & Kerle, N. (2008). Satellite remote sensing for near-real time data collection (Vol. 6, pp. 75-102). Taylor & Francis Group: London, UK.

Zobin, V.M., Cruz-Bravo, A. A., Venture-Ramirez (2010) Microzonation of seismic risk in a low-rise Latin American city, based on the macroseismic evaluation of the vulnerability of residential buildings; Colima city, Mexico, Natural Hazards Earth System Science, Vol. 10, pp. 1347-1358.